UiT The Arctic University of Norway

Faculty of Health Sciences

Department of Medical Biology

Evolutionary genomics of cowpox virus and recombination *in vitro* between a naturally occurring cowpox virus and a vaccinia virus vectored influenza vaccine

Diana Karina Diaz Cánova

A dissertation for the degree of Philosophiae Doctor (PhD)

April 2023

A dissertation for the degree of Philosophiae Doctor

Evolutionary genomics of cowpox virus and recombination *in vitro* between a naturally occurring cowpox virus and a vaccinia virus vectored influenza vaccine

Diana Karina Diaz Cánova

Molecular Inflammation Research Group
Department of Medical Biology
Faculty of Heath Sciences
UiT- The Artic University of Norway

April 2023

To my grandmother, Josefa N. Mendoza Zavala vda. de Diaz.

Acknowledgements

This PhD project was performed at the Molecular Inflammation Research Group (MIRG), Department of Medical Biology, Faculty of Health Sciences, the Artic University of Norway-UiT.

First and foremost, I would like to express my profound gratitude to my two wonderful supervisors, Ugo Moens and Malachy Okeke. I am infinitely grateful for all the support, patience and encouragement that you gave me during this journey that was not an easy one, but we succeeded!

Thank you Ugo, for always having the door to your office open so I could run to you when I had a problem or a silly question to ask. You were always there for me despite your busy schedule. I really appreciate your kind words of encouragement in our meetings that made me realize how much I have achieved and learnt. I am really impressed by how efficient you are. When I asked for a document, five minutes later you were knocking at my office door with the signed document!

Malachy, despite you not being here in Tromsø, I could always count on you! The distance was not a problem and you managed to supervise well me during these years. Even when something went wrong in my experiments you could guide me from Nigeria. Thanks for allowing me to contact you anytime. You were always available and ready to answer my questions. Sometimes I thought you would get mad because of my millions of questions, but you did not! You were always so kind and patient.

Both of you, Ugo and Malachy, were the right match. You complemented each other and made a great team! Thanks for having me as your PhD student, for sharing all your knowledge with me and believing in me.

I would like to thank Andreas Nitsche for giving me the opportunity to visit the Robert Koch Institute in Berlin. The research stay in your institute was a cornerstone in my PhD. Also, I want to give my infinite gratitude to Annika Brinkmann for introducing me to this new world called "bioinformatics". I really appreciate your patience during those two weeks in Berlin. Without you I would not have been able to analyze all my sequencing data.

I want to thank Carla Mavian. I am so grateful that we worked together, and you shared your knowledge in BEAST to me.

I want to thank Rolf Andersen from the Orakelet, you were just a star! When I had a problem with the server or any programs, you were always there helping me, providing solutions and you made my PhD life much easier by introducing me to the UiT server. Thanks a lot!!

Juan Daniel Montenegro thanks for being so patient and helping me with my bioinformatics troubles. You taught me new bioinformatics programs that are now part of the methodology used in my articles ¡Eres un capo!

Thanks to the past members of the Molecular Inflammation Research Group (Conny, Kashif, Aelita, Baldur, Dag, Marianne, Maria and Gianina) for creating a nice atmosphere in the lab. A special thanks to my lovely and sweet friend Connyzita, thanks for all the love, hugs and chocolates. I miss your priceless hugs!

I would like to thanks to the Old and New “Lab-gang” of the 9th floor (Adri, Clement, Jessin, Ekaterina, Ahmed, Bishnu, Srijana, Jeanette, Jalal, Maria, Gaute, Kjersti, Mushtaq, Hermoine, Theresa, Bhupender, Dorotha, Jonathan, Ken, Martin, Erick and Mikal), Almudena and Swapnil for the delicious common lunches, parties, coffee/cake breaks, laughs, talks, etc. Thanks for all the nice memories.

Clementine, thanks for being a wonderful friend, for being by my side in the most difficult moments. I could always count on you. You were like a big brother always advising me when I needed it most. Also, thanks for all the amazing memories (our trips, parties, birthday dinners, burgers, laughs, etc.), you just made my PhD journey and my life much lighter and easier, thank you from the bottom of my heart!

Adri, thanks a lot for being the big sister that I needed in Norway. Despite you moving to Oslo, you always called me, checked on me, advised me and supported me when I needed it the most, thanks, thanks, thanks!! You don’t know how much I treasure you! I love you, my Adri!. My dear friend Jessin, thanks for sharing your bioinformatics knowledge with me and helping me when I was going crazy with the bioinformatics programs. Also, thanks for spoiling me with your delicious Indian food.

I also want to thank my lovely ladies (Alejandra, Karla and Angie) that made my life in Tromsø very pleasant with their great sense of humor and warm company. Sometimes life is not easy, but you showed me that women are extremely strong, brave, and courageous and can overcome any obstacle in life. Alejandra (Margothcita), thanks for the wonderful gift that you gave me (my cute Godson Sander) and for pampering me when I really needed it, you made me feel at home.

Thanks to my lovely family, especially to my beloved dad, grandmother and my sister Susan, for their endless love, always believing in me and cheering me up. Grandma thanks for always supporting me to pursue my dreams and keeping me in your prayers. If it was not for you, I could not be writing these words ¡Te amo con todo mi ser!

Above all, I want to thank God for being with me and guiding me during this journey and blessing me with wonderful people around me.

¡Gracias totales!

D.K.D.C

Table of Contents

LIST OF ABBREVIATIONS

AKMV	Ahkmeta virus
AKPV	Alaskapox virus
ATI	A-type inclusion
BPXV	Buffalopox virus
BHK	Baby hamster kidney
BI	Bayesian inference
CAM	Chorioallantoic membrane
CDS	Coding sequence
CEF	Chicken embryo fibroblast
CEV	Cell-associated enveloped virus
CHO	Chinese hamster ovary
ChPV	Chordopoxvirinae
CMLV	Camelpox virus
CNPV	Canarypox virus
CPXV	Cowpox virus
CrmB	Cytokine response modifier B
CrmD	Cytokine response modifier D
CVA	Chorioallantois VACV Ankara
dsDNA	double-stranded DNA
ECTV	Ectromelia virus
EEV	Extracellular enveloped virus
ER	Endoplasmic reticulum
ERA	Environmental risk assessment
EU	European Union
GATU	Genome Annotation Transfer Utility
GMO	Genetically modified organism
HA	Hemagglutinin
HPD	High posterior density interval
HSPV	Horsepox virus
ICTV	International Committee on Taxonomy of Viruses
IEV	Intracellular enveloped virus
IMV	Intracellular mature virus
ITR	Inverted terminal repeat
IV	Immature virus
IVN	Immature virus with nucleoid
LSDV	lumpy skin disease virus
MAFFT	Multiple Alignment Fast Fourier Transform
ML	Maximum Likelihood
moi	Multiplicity of infection
MPXV	Monkeypox virus
MVA	Modified Vaccinia virus Ankara
MVA-HANP	MVA vectored influenza vaccine
NGS	Next-generation sequencing
NP	Nucleoprotein
OPXV	Orthopoxvirus
ORF	Open reading frame
ppi	Post primary infection
RCNV	Raccoonpox virus

RDP	Recombination detect program
RSV	Respiratory Syncytial virus
SKPV	Skunkpox virus
TATV	Taterapox virus
TGS	Third generation sequencing
tMRCA	Time to the most recent common ancestor
UK	United Kingdom
VACV	Vaccinia virus
VARV	Variola virus
VOCs	Viral Orthologous Clusters database
VPXV	Volepox virus
WHO	World health organization

LIST OF FIGURES

LIST OF TABLES

LIST OF PAPERS

Paper I

Diaz-Cánova, D., Moens, U. L., Brinkmann, A., Nitsche, A., and Okeke, M. I. (2022). Genomic Sequencing and Analysis of a Novel Human Cowpox Virus With Mosaic Sequences From North America and Old World Orthopoxvirus. *Front. Microbiol.* 13. doi:10.3389/FMICB.2022.868887

Paper II

Diaz-Cánova, D., Mavian, C., Brinkmann, A., Nitsche, A., Moens, U., and Okeke, M. I. (2022). Genomic Sequencing and Phylogenomics of Cowpox Virus. *Viruses 2022, Vol. 14, Page 2134* 14, 2134. doi:10.3390/V14102134.

Paper III

Diaz-Cánova, D., Brinkmann, A., Nitsche, A., Moens, U., and Okeke, M. I. Whole genome sequencing of recombinant viruses obtained from co-infection and superinfection of Vero cells with Modified Vaccinia virus Ankara vectored influenza vaccine and a naturally occurring *Cowpox virus.* Manuscript

SUMMARY

Modified vaccinia virus Ankara (MVA) is a promising orthopoxvirus (OPXV) vector vaccine candidate due to its host range restriction and good safety profile as a smallpox vaccine. It has been widely tested in clinical trials as a recombinant vector for vaccination against infectious diseases and cancers in humans and animals. Furthermore, it is being used as smallpox and Mpox vaccine. However, the extensive use of MVA and MVA vectored vaccines have the potential for MVA or MVA vectored vaccine to recombine with naturally circulating OPXV. *Cowpox virus* (CPXV) as a close relative of MVA is a potential candidate for recombination. Hence, the genetic diversity and evolution of CPXV was assessed in this work, as well as recombination *in vitro* between a naturally occurring CPXV and MVA vectored vaccine in cells in which MVA multiplies poorly. CPXV is classified as a single species; however, we demonstrated that CPXV might be an assemblage of several species based on its high genetic diversity, lack of monophyly, and close phylogenetic relationship with other OPXV. CPXV strains were separated into five major clusters rather than one monophyletic cluster. Furthermore, we described a new, distinct cluster closely related to *Ectromelia virus* (ECTV) and *Abatino macacapox virus* (Abatino) named "ECTV-Abatino-like CPXV". Additionally, we showed evidence that a Norwegian CPXV isolate was a natural occurring recombinant CPXV that might have emerged following multiple recombination events between different OPXV species from the Old World and North America. Under *in vitro* conditions, the progeny viruses obtained from co-infection and superinfection of Vero cells with MVA-HANP and CPXV-No-F1 had mosaic genomes and displayed parental and non-parental plaque phenotypes. Furthermore, some progeny viruses contained the transgene from MVA-HANP and regained genes that were deleted or fragmented in MVA-HANP. Overall, these findings will contribute to the environmental risk assessment of MVA and MVA vectored vaccines and to the improvement of the biosafety of MVA vectored vaccines.

1. INTRODUCTION

1.1 Poxvirus

Poxviridae is a family of large double-stranded DNA (dsDNA) viruses [1]. The family is divided into two subfamilies based on its host range: *Chordopoxvirinae (ChPV)*, viruses that infect vertebrates, and *Entomopoxvirinae*, viruses that infect insects. There are four and eighteen genera within *Entomopoxvirinae* and *Chordopoxvirinae*, respectively (https://ictv.global/taxonomy). Among *Chordopoxvirinae*, only species of the genera *Orthopoxvirus*, *Parapoxvirus*, *Molluscipoxvirus*, and *Yatapoxvirus* are known to cause human infections [2]. The best characterized genus within vertebrate poxviruses is *Orthopoxvirus* (OPXV). Some OPXV including *Variola virus* (VARV), *Vaccinia virus* (VACV)-like, *Cowpox virus* (CPXV), *Monkeypox virus* (MPXV), and *Camelpox virus* (CMLV) can cause human diseases [3]. The genus *Orthopoxvirus* includes twelve species. According to their endemism, OPXV are divided into the New World and the Old World OPXV. The Old World or African-Eurasian OPXV group contains: CPXV, VACV, MPXV, VARV, CMLV, *Taterapox virus* (TATV) and *Ectromelia virus* (ECTV). The New world OPXV group comprises three species that are endemic to North America: *Raccoonpox virus* (RCNV), *Volepox virus* (*VPXV*) and *Skunkpox virus* (SKPV) [4]. Recently, three novel OPXV species have been discovered in different locations: *Abatino macacapox virus* (Abatino) in Italy, *Ahkmeta virus* (AKMV) in Georgia and *Alaskapox virus* (AKPV) in the United States [5–7], although AKPV is still not formally classified as an OPXV species.

1.2 Orthopoxvirus

1.2.1 *Variola virus*

VARV is the most notorious OPXV, as it is the causative of smallpox. VARV has humans as an exclusive host and no animal reservoirs have been found [8]. Smallpox is a highly contagious airborne disease with high mortality rates (15-45%) [9,10] that caused around 300-500 million deaths world-wide in the 20th century [11]. The term "variola" for smallpox was derived from the latin word *various* (meaning spotted) or from *varus* (meaning pimples) [12], and refers to the pustules that appears on the body and face. Later, the term "small pockes" (pocke means sac) was used to differentiate it from syphilis, "great pockes" [13]. The first historical record of smallpox was in Egypt from the mummy of Ramses V, who died 1157 BC [14]. From Egypt, the disease started to spread to other parts of the world. One of the first methods to mitigate smallpox was variolation, which consisted in the inoculation of smallpox pus or scabs into the skin (Indian method) or in intranasal insufflation of dried smallpox scabs (Chinese method) to a healthy person [15]. It was an effective method to prevent smallpox, but the mortality rate was approximately 2% [9,10]. After 1798, variolation was gradually replaced by a safer procedure called vaccination [10]. Compared to variolation, vaccination gave the same protection, but with less severe symptoms. In 1959, the World Health organization (WHO) launched a Global

Smallpox Eradication Program with the aim to eradicate smallpox [10]. From 1959 to 1977, the WHO organized vaccination campaigns world-wide. The last natural smallpox case was recorded in 1977 [16], and in 1980 the WHO formally declared the eradication of smallpox, and the routine smallpox vaccination ceased [17].

Prior to the eradication of smallpox, there were multiple VARV strains that were circulating. However, there were two main variants: *variola major* with a mortality rate of 20-45% (which is the most common cause of death related to smallpox) and *variola minor* or *alastrim*, characterized by a much lower mortality rate (1-2%) [9,10]. The latter variant was common in Western Africa and America and appeared in the end of the 19th century [10]. After smallpox eradication, the WHO decided that all VARV stocks should be destroyed or deposited in two international centers in the State Research Center of Virology and Biotechnology in Russia and the Center for Disease Control and Prevention in the United States [18]. Those are the only two WHO-approved centers that can conduct research on VARV. The WHO had planned to destroy all VARV stocks but given the potential for a bioterrorist attack, the destruction has been postponed for a few years until the development of new antiviral agents against smallpox and until the committee decides the best options for global public health [19] .

1.2.2 *Cowpox virus*

CPXV is a zoonotic OPXV that is the causative agent of the disease cowpox. Historically, cowpox has been associated with the first vaccine used by the English physician Edward Jenner who established a safer method called "vaccination" to protect against smallpox in 1798. He had heard the folk tale that anyone who contracted cowpox could not catch smallpox [20]. Based on this belief, in 1796, he inoculated the boy James Phipps with cowpox pustules from the hand of the milkmaid Sara Nelmes. Some weeks after, Jenner infected the boy with smallpox pus and the boy did not develop the disease. After this finding, he repeated the same procedure with other children and concluded that vaccination offers a full protection against smallpox [21,22]. Jenner called the pustular material "*variolae vaccinae*" (smallpox of the cow) to make reference to the cow (latin word *vacca*) [23,24] and later the "*variolae vaccinae*" was referred to as vaccine [25]. However, until now, there is still uncertainty about the nature of the virus that Jenner used as a first vaccine. Probably he might have used VACV or *Horsepox virus* (HSPV) [22,26–28]. In 1798, Jenner published his discovery, which was the basis for vaccination and immunology [22]. Although vaccination had been first used by Benjamin Jesty 22 years before Jenner [29,30], there is no evidence that Jenner knew about Jesty's vaccinations [29]. Thus, the credits for developing vaccination were given to Jenner [29,30].

CPXV is endemic of Eurasia, mainly in Europe [31–37]. CPXV has the broadest host range among OPXV [3,38], which is thought to be associated with its high number of host range genes [39,40]. Its natural reservoir hosts are probably wild rodents such as bank voles (*Myodes glareolus*), common voles (*Microtus arvalis*) and field voles (*Microtus agrestis*) [31,41,42]. CPXV infects many non-reservoir species such as felines, monkeys, dogs, alpacas, rats, cats and horses [36,42–47]. CPXV even causes spillover infections from infected animals to humans [34,48–59]. Most human

CPXV cases were caused by contact with infected cats [49,59,60]. In humans, the disease is usually self-limiting with pox lesions and mild symptoms, but it can lead to fatal infections, especially in immune-compromised individuals [61–63]. The first zoonotic case was reported in the Netherlands in 1985, in which a woman was infected with CPXV from a domestic cat [64]. In the last decades, multiple lethal and non-lethal CPXV outbreaks in animals have been reported as well as human cases of CPXV infections [42,61–63,65–67]. In the Fennoscandian region, CPXV infections in humans and felines have been reported (CPXV-No-H1, CPXV-No-H2, CPXV-Swe-H1, CPXV-Swe-H2, CPXV-No-F1 and CPXV-No-F2) [45 45,68–72]. Interestingly, one of these Fennoscandian CPXV isolates, CPXV-No-H2, was a peculiar CPXV strain [71]. The phylogenetic analysis using the *p4c* gene revealed that CPXV-No-H2 was clustered separate from the other CPXV isolates. This was evidence of the genetic diversity among CPXV isolates. Other studies have also revealed that CPXV is genetically heterogeneous [70,72–78].

The traditional nomenclature used in poxvirus taxonomy, that is naming the virus after the host from which it was isolated, brought confusion in the classification of cowpox. For instance, cows are susceptible to both CPXV and VACV. Jenner described cowpox as a disease characterized by pustules on the nipples and utters of cows that were infected from horses [22]. Later, Downie defined CPXV as strains that were isolated from the spontaneous disease in cattle or from human lesions caused by directly infection from that source. Additionally, he described some biological properties of CPXV such as the presence of A-type inclusion bodies (ATI) and red hemorrhagic pocks on the chorioallantoic membrane (CAM) of chicken eggs after infection [79]. Since then, the classification of CPXV has been based on host specificity and the two main criteria described by Downie. As a consequence, several viruses have been classified as CPXV [80–83]. The classification of CPXV is still a matter of debate. It has been proposed that CPXV is not one single species and it may contain more than one species [70,72,73,75,76,84].

1.2.3 *Vaccinia virus*

VACV has been used as a vaccine against smallpox in the 20th century [79]. Although it is still not clear when VACV started to be used, it is thought that at some point during 19th century cowpox was swapped for VACV [10]. However, recent evidence showed that old smallpox vaccines were more similar to HSPV [22,26–28], which is more closely related to VACV than to CPXV. Therefore, it has been suspected that Jenner may have used a HSPV-like virus instead of CPXV [26,85,86].

The exact origin of VACV is still unknown as well as its natural reservoir, even though VACV is the most studied OPXV. Since VACV strains have been attenuated in the laboratory, it was thought that VACV strains were unable to establish an infection in nature [3]. However, VACV-like infections have been reported in multiple species (such as cat, cattle, buffaloes and rabbit) and in different places throughout the world [3,47,87–93]. VACV and VACV-like have a broad host range [3,94] and are considered endemic in South America and Asia [94].

There are several variants of VACV-like that have been described such as HSPV, Buffalopox virus (BPXV) and Brazilian VACV-like [3,47,87]. BPXV outbreaks have occurred in several countries, affecting mainly buffaloes but also humans [89,95,96]. In South America, multiple outbreaks of VACV-like infections have been recorded, especially in Brazil [3,97–99]. Brazilian VACV-like strains were mainly isolated from cattle and humans, although they have been detected in other animals [3,100–102]. It is likely that Brazilian VACV-like derived from a spillback of a vaccine strain to wild hosts rather than being natural VACV populations circulating in an unknown reservoir [3,85,103]. VACV-like infections in humans were associated with infected animals (zoonotic transmission) [104,105]. Although human-to-human transmission (interhuman transmission) has also been reported [106,107].

Several VACV strains have been used to develop smallpox vaccines. There are four major types of VACV vaccines: first-, second-, third- and fourth-generation vaccines [108,109]. The first-generation vaccines were live vaccines produced in live animals and were used during the Global Smallpox Eradication campaign [10,110]. Many VACV strains were used to develop first-generation vaccines, for instance the New York City Board of Health (NYCBH) strain was used in the USA, the Temple of Heaven (Tian Tan) strain was used in China and the Lister strain was used in Africa, Asia, Europe and the USA [10,109,111]. Nonetheless, these vaccines were not recommended due to safety problems. The second-generation vaccines were produced in tissue culture with good manufacturing practices [109]. However, like first generation vaccines, they may still cause severe side effects [109,112]. The poor safety profile of VACV second-generation vaccines led to the third-generation vaccines. These vaccines are live but attenuated VACV that maintained their immunogenicity and protection against smallpox [108]. The attenuation was obtained after multiple passages of the parental virus in cell cultures, which generated random mutations in its genome [109]. Several attenuated VACV strains have been developed such as modified Vaccinia virus Ankara (MVA) and Lister-16m8 (LC16m8) [113,114]. In the fourth-generation vaccines, the attenuation is achieved using genetic engineering. The genomes of the fourth-VACV strains are manipulated by, for example, inserting, deleting or interrupting specific genes [109]. An example of these vaccines is NYVACV [115]. Moreover, subunit-based vaccines are included within the fourth-generation vaccines [116,117]. Recombinant DNA technology has played an important role in the development of VACV-based vaccines. The ability of incorporate foreign DNA (up to 25kb) into the VACV genome [118] opened the opportunity of using VACV as viral vector against other diseases.

Modified Vaccinia virus Ankara

MVA was originally developed in the 1970s as a smallpox vaccine. MVA is an attenuated VACV strain derived from Chorioallantois VACV Ankara (CVA). CVA was passaged more than 500 times in primary chicken embryo fibroblasts (CEF) to be attenuated. After 516 passages, an attenuated virus was obtained and CVA was renamed MVA [119]. Upon more than 570 passages, the CVA genome had suffered six major deletions as well as minor deletions, insertions and point mutations (Figure 1). As a result, the CVA genome was reduced by around 13%, from 208 kbp (CVA) to 178 kbp (MVA) [120–122]. The mutations led to the deletion, fragmentation and disruption of multiple genes in MVA responsible for evasion of the host

immune response and regulating the viral host range, such as the *K1L*, *C12L* and *C16L* genes [122,123]. Although the six major deletions took place in genomic regions of CVA where truncated or fragmented genes pre-existed (e.g. *A39R* and *A55R* gene). The small mutations affected 122 of the 195 genes in MVA [122]. It is presumed that the genetic modifications render MVA incapable to multiply in most mammalian and human cells [121,124,125].

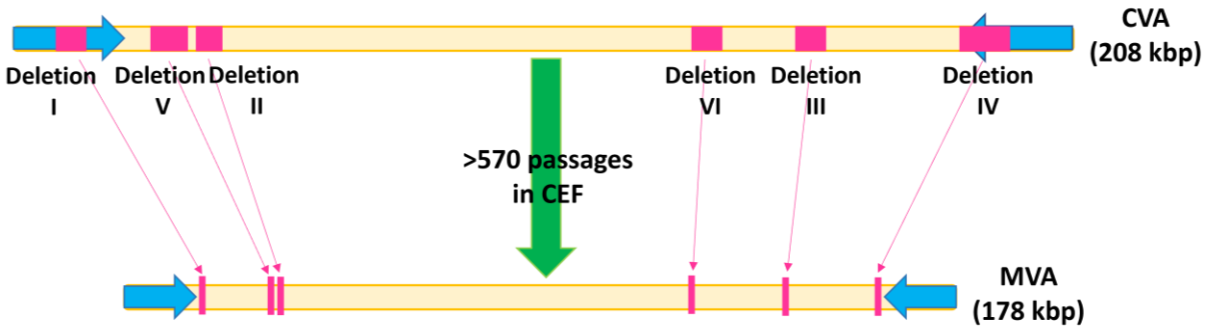

Figure 1. Schematic representation of the CVA and MVA genomes. The pink boxes represent the deleted regions in the CVA genome. The blue arrows represent ITR.

MVA was administrated to over 120,000 people in Germany when smallpox was not endemic in the country. Among those vaccinated were children, immunocompromised individuals and elderly people. The vaccines showed mild or moderate adverse effects, such as local reaction (redness) and fever [114,126–128]. MVA-BN has been authorized for use as a smallpox vaccine in Europe (with the trade name Imvanex), Canada (with the trade name Imvamune) and in USA (with the trade name Jynneos) [129,130]. Furthermore, it has been approved as a Mpox vaccine [131]. MVA-BN is derived from the MVA-584 strain, following six rounds of plaque purification. It has a more restricted host range than other MVA strains [132]. Due to its excellent safety profile, attenuation *in vivo*, immunogenicity *in vivo*, and the ability to incorporate and express foreign DNA with correct post-translational modification, MVA is one of the promising viral vectors for development of recombinant vaccines and gene delivery [133,134]. MVA has been used to develop recombinant vaccines against numerous diseases, both in humans and animals, and cancers. The development of vaccines using MVA vectors are in different phases of clinical trials, including MVA vaccines against HIV [135,136], Ebola [137–140], respiratory syncytial virus [141], Middle East Respiratory Syndrome [142], cytomegalovirus [143], influenza [144,145], tuberculosis [146] and malaria [147–149].

1.2.4 *Monkeypox virus*

Mpox is a zoonotic disease caused by MPXV. The virus causes mild symptoms but in immunosuppressed patients, individuals with pre-existing medical conditions, elderly people and young children the disease can be more severe with fatal outcomes [150–153]. Similar to smallpox, Mpox is more often lethal in children than in adults [151,154,155]. Mpox is endemic in

West and Central Africa [156]. MPXV strains are divided into Clade I (formerly Central African clade) and Clade II (formerly West African clade) [157]. The Clade I has a higher fatality rate (10.6%) than the Clade II (3.6%) [158]. There are two routes of MPXV transmission: (1) from animal to human (zoonotic) and (2) from human to human (interhuman), which includes mother-to-child (vertical transmission) [153,155,158].

MPXV was first identified in captive monkeys in Denmark in 1958 [159]. Natural infections of MPXV have been detected in other mammalian species [160]. Although there is no definitive reservoir of MPXV, it is presumed that African rodents are the reservoir [160]. The first human Mpox case was reported in the Democratic Republic of Congo in 1970 [161]. After this, human cases of Mpox have been reported in endemic countries [160,162,163]. From 2013 to 2021, sporadic non-endemic cases imported from endemic countries were reported in the USA, Singapore, Israel and the United Kingdom (UK) [164–168]. It is thought that those MPXV outbreaks were spillovers from animals to humans [157,169]. In May 2022, the global Mpox outbreak started in the UK [170], and since then 86,724cases have been confirmed in 110 countries [171].

1.2.5 *Ectromelia virus*

ECTV is the causative agent of mousepox, a lethal, acute exanthematous disease of laboratory mouse colonies [172,173]. The natural reservoir of ECTV is likely wild mice. One ECTV strain was isolated from wild mice in Germany [174]. ECTV has a very narrow host range, its host is the mouse. However, human cases of ECTV infection have been reported in China and one case in fox [175–177]. The first ECTV strain (ECTV-Hampstead) was discovered in a laboratory mouse colony in Hampstead, the UK [173]. After that, several outbreaks occurred in Europe, Japan, China and the USA [174,178,179]. ECTV-Hampstead was the progenitor of the outbreaks in Europe. It is thought that ECTV-Hampstead was also responsible for the outbreaks in Russia, Japan and the USA (from the 1980s) [174]. The ECTV outbreaks in the USA caused high mortality in laboratory mice and losses of millions of dollars [180]. Mousepox was a serious threat to laboratory mice, but it has been eliminated due to increased health surveillance and improvements in animal facilities [180]. However, mousepox is still relevant as it is the best small animal model of smallpox. In addition, it has been used in studies of OPXV infection and pathogenesis [172,181,181,182]. Compared to CPXV, ECTV produces white lesions on chorioallantoic membrane (CAM) of chicken eggs and V^- ATI phenotype. However, ECTV-Hampstead produced the wild type V^+ ATI and the atypical $V^{+/}$ ATI. Furthermore, it contained a complete *p4c* gene. Whereas the other ECTV strains contained a truncated *p4c* gene and produced V^- ATI [174,183].

1.2.6 *Alaskapox virus*

AKPV has not been classified as OPXV, but it has been suggested that it represents a novel OPXV. AKPV was isolated from a patient in Alaska, the USA. The distribution of AKPV is unknown as well the infection source of the patient. It has been speculated that either the patient was in contact with fomites brought from abroad or the virus was circulating in small mammals,

like other OPXV, in the areas close to the residence of the patient. The sampling of small mammals and the fomites tested negative for OPXV, although the sampling was limited [7,184].

1.3 Virus structure

Poxviruses are ovoid or brick-shaped viruses (220-450 nm x 140-260 nm) [185]. The virions are composed of three main substructures: viral core, one or two lateral bodies and the viral membrane(s) (Figure 2) [186–188]. The core contains the dsDNA genome, structural proteins and enzymes needed for the transcription of early viral genes [189–191]. The core is encased by a core wall that has a biconcave shape [186]. The core wall is composed of two layers: the inner layer or "smooth layer", formed by A3; and the outer layer or "palisade layer", formed by A10 and A4 [192]. The lateral bodies reside on the concave regions of the core [187,193]. They are proteinaceous structures that carry host modulatory proteins such as the phosphoprotein F17R, the phosphatase H1 and a glutaredoxin-2 (G4L) [193]. The virus is surrounded by one lipoprotein bilayer membrane and one additional outer membrane (envelope) [194].

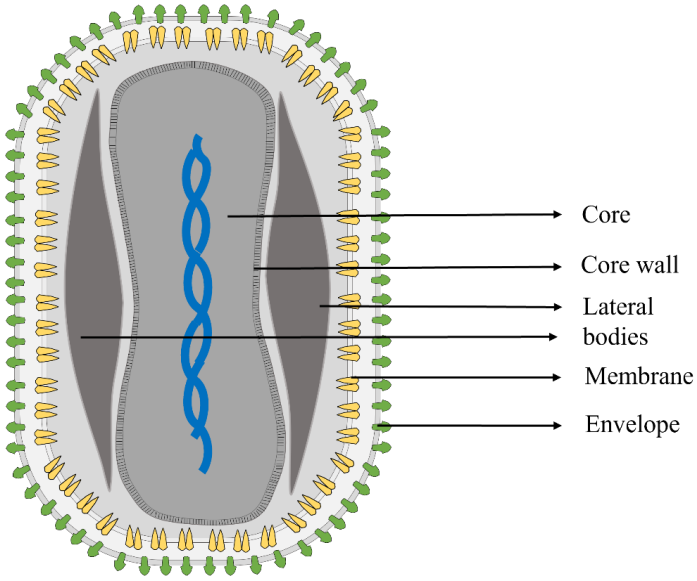

Figure 2. Schematic diagram of *Vaccinia virus* structure.

1.3.1 Genome organization

The genome of poxviruses is a double strand DNA that varies in length from 122 kbp, in *Cetacean poxvirus* of OPXV genus [195], to 360 kbp, in *Canarypox virus* (CNPV) of the *Avipoxvirus* genus [196]. Poxvirus genomes contain from approximately 133 genes (in Yatapoxvirus and Parapoxvirus) to 328 genes (in CNPV) [196]. Their genome consists of the central region and two variable regions at the termini. The end of the variable region contains inverted terminal regions (ITR). ITR are identical sequences in inverse direction at the opposite end with hairpin loops that join the two DNA strands [1]. ITR are variable in size between species. and can contain genes that are present in diploid copies in the genome or not contain genes, as in VARV [197–199].

The central region of the genome is highly conserved between the poxviruses, sharing similar gene location (synteny) and genome organization [84,198]. In this region, there are 49, 90 and 109 genes that are conserved among poxviruses, chordopoxviruses and OPXV, respectively [198,200–202]. The conserved genes are involved in essential functions such as DNA replication, transcription, and virion assembly [84,200,202]. In contrast, the variable regions comprise genes that encode proteins involved in the interaction with the host including host range, immunomodulation and pathogenicity. These genes are termed as "non-conserved genes" or "accessory genes" [8,198,200,201]. Compared to the conserved genes, those genes are more divergent and not highly conserved between poxviruses [198,202,203]. Furthermore, those genes have more variability in gene length than the genes in the central region [198]. Thus, the main differences in the genome of OPXV species are in the terminal variable genomic regions [204].

1.4 Viral cycle

The prototype of the OPXV is VACV. Thus, the viral cycle is described with reference to VACV. The complete viral cycle of VACV occurs in the cytoplasm of the host cell [1] (Figure 3).

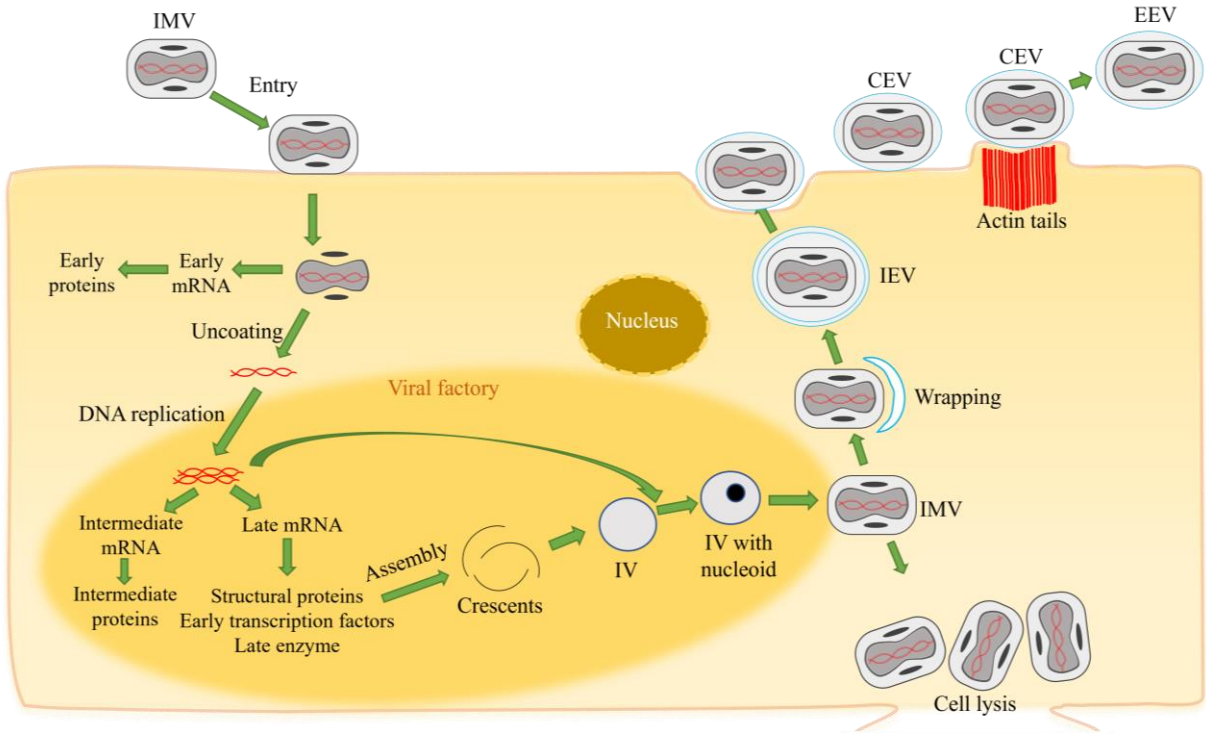

Figure 3. Schematic overview of the *Vaccinia virus* life cycle. IV, immature virion; IVN, immature virion with nucleoid; IMV, intracellular mature virion; IEV, intracellular enveloped virus; CEV, cell-associated enveloped virus; EEV, extracellular enveloped virus.

1.4.1 Virus entry and uncoating

The viral cycle starts with the viral entry (binding and fusion) (Figure 3). VACV attaches to the cell through the interaction of glycosaminoglycans and viral membrane proteins. There are at least 15 proteins involved in the viral entry: four proteins used for binding to the cell (D8, A27 and H3 and A26) and eleven required for viral fusion (A16L, A21L, A28L, F9, G3L, G9R, H2, J5, L1R, L5R and O3L) [205]. The last ones are called the entry-fusion complex (EFC). The virion entry occurs either through macropinocytosis or direct fusion of the viral membrane with the cell membrane [1,206].

Upon entry, the core and the lateral bodies are released in the cytoplasm [205]. The lateral bodies are dissociated from the core and disassembled [207]. The core is released in the cytoplasm and transported by microtubules close to the endoplasmic reticulum or perinuclear region of the cytoplasm [208–210], followed by the transcription of early viral genes [211]. The expression of early genes does not require *de novo* protein synthesis because the viral particles contain their own transcription machinery [1,212]. More than 100 genes are transcribed inside the viral core [213] and the early mRNAs are detected within 20 min post infection [214,215]. The transcripts are extruded from the core and translated in the cytosol. The core is uncoated and the viral genome is released to the cytoplasm (Figure 3) [211].

When the cell is infected with VACV, superinfection can be prevented by the interaction of A56 and K2 proteins on the membrane of the infected cell with the A16-G9 subcomplex of EFC of subsequent viruses, which blocks the viral entry after membrane fusion [216,217]. The mechanism by which viruses prevents superinfection with a second virus is called superinfection exclusion. There is another mechanism of superinfection exclusion that does not require the A56 or K2 proteins and prevents the viral fusion of the superinfecting virion and the infected cells, but this mechanism is not completely elucidated, yet [218].

1.4.2 Viral DNA replication

After the genome has been released, viral DNA replication starts, followed by the expression of intermediate and late genes [211]. The viral genome in the cytoplasm is surrounded by membranes derived from the rough endoplasmic reticulum (ER), forming a “virus factory” or “replication factories” in the cytoplasm (Figure 3) [187,219,220]. It has been proposed that the ER membranes might protect the viral genome from cellular recognition and degradation. Viral DNA replication occurs in the viral factories [211]. Each viral factory is derived from one viral particle [208,221]. Since the cell DNA machinery is located in the nucleus, VACV produces its own viral DNA replication machinery before viral DNA synthesis. The early viral proteins that mediate the viral DNA replication are: B1, I3, H5, G5, A50, E9, A20, D4 and D5 [221–232].

Transcription and translation of intermediate and late proteins also take places in the viral factories as well as the viral assembly [233]. The activation of intermediate and late genes requires viral DNA replication [234] as the newly replicated DNA serves as a template for the transcription of these genes [235]. Most intermediate and late mRNAs are detected at 100 min post infection

[214,234]. The intermediate viral genes encode DNA binding and packaging proteins, core-associated proteins and late transcription factors [213], whereas the late viral genes encode structural proteins, the viral RNA transcription machinery, early gene transcription factors and proteins involved in morphogenesis and entry [236,237].

1.4.3 Virus assembly and egress

The viral assembly occur in the viral factories (Figure 3) [238]. During the morphogenesis VACV produces four types of virions: intracellular mature virion (IMV), intracellular enveloped virus (IEV), cell-associated enveloped virus (CEV) and extracellular enveloped virus (EEV) [239]. IMV has a single lipid bilayer membrane compared to CEV and EEV that contain one additional membrane (envelope), derived from either endosomes or trans-golgi [240,241]. The virion morphogenesis begins with the formation of viral crescents, which are open membranes derived from the ER [242]. The crescent grows until it forms a spherical immature virion (IV). Before it closes the viral genome is packaged into IV. These IV are called IV with nucleoid (IVN). Then IVN matures to intracellular mature virion (IMV) (Figure 3) [243].

IMVs are released from the viral factory. The majority of IMV stay inside the cell until cell lysis. In species such as CPXV, ECTV and AKPV, IMV are occluded within a dense protein matrix in the cytoplasm called ATI bodies [79,174,184]. Three phenotypes of ATI exist: IMV are inside the ATI matrix (V^+), ATI with no IMV inside or on its surface (V^-) and IMV are only in the periphery of ATI ($V^{+/}$) [244,245]. The *atip*, *p4c* and *A27L* genes are involved in the production of the wild type V^+ ATI [246–248]. The other IMV are transported from the viral factories to the site of wrapping on microtubules. IMV are wrapped by a double membrane derived from either endosomes or trans-golgi [240,241], resulting in intracellular enveloped virus (IEV). The double membrane contains nine proteins (A33, A34, A36, A56, B5, E2, F12, F13 and K2). The deletion of any of these proteins, except for A56 and K2, causes a small plaque phenotype [1]. The deletion or mutation of A56 or K2 causes the formation of syncytia (fusion of infected cells) [249 250–253].

The transportation of the IEV to the cell surface and egression needs three proteins A36, F12 and E2 [254,255]. A36 and F12 are only present on the outer membrane of the IEV [256]. IEV is moved to the cell surface and its outer membrane fuses with the cell membrane, exposing the virion on the cell membrane [239]. Upon fusion A36 is accumulated in cell membrane [257] . The viral particle has one lesser membrane and if it is retained on the surface is called cell-associated enveloped virus (CEV). When CEV is released from the cell, it is known as extracellular enveloped virus (EEV) [239]. CEV is important for cell-to-cell spread [239,258]. A33, A34 and B5 proteins are required for efficient cell-to-cell spread [259–261]. These proteins are associated with the formation of comet-shaped plaques [259,262,263]. When EEV reaches an infected cell, the infected cell expressing A33 and A36 on the membrane to repel the superinfecting EEV. A33 and A36 induce actin tails to spread EEV to neighboring cells [264]. This is another form of superinfection exclusion.

1.5 Viral tropism

The poxvirus tropism can be classified in three levels: cell tropism, tissue tropism and host tropism [265]. The cell tropism refers to the ability of the virus to infect cell cultures. Based on this ability, cells can be defined as permissive, semi-permissive and non-permissive. The tissue and host tropism are the ability of the virus to infect tissue and host species, respectively [265]. The initiation of the viral cycle for many viruses begins with the binding to the cell. Thus, it is considered that the viral binding has an important role in cell and tissue tropism [265]. However, several poxviruses can successfully enter to non-permissive cells [266–269], as it has been observed for MVA [119]. This indicates that cell tropism is affected by other downstream events [8,270]. The cell tropism depends on the ability of the virus to manipulate the intracellular antiviral pathways that is activated upon viral entry, the ability of the cell to provide complementing host factors needed for the viral multiplication [8,271,272] as well as the presence/absence of antiviral genes [272]. In the poxviral genome, within the non-conserved genes, there are genes involved in the modulation of the host antiviral response. These genes are defined as virulence genes [8,38]. Within the virulence genes, the ones that are required for the successful multiplication of poxviruses in a set of cultured cells are referred to as "host range genes" [8,38]. The host range genes encode proteins called host range factors that target antiviral and anti-inflammatory host pathways [38] and influence the virus tropism [8]. In poxvirus, 38 host range gene homologs have been identified and are classified in 12 gene families [38,39,271]. The most studied host range genes are *E3L* and *K3L* [38].

VACV can productively multiply in most mammalian and avian cells, but not in Chinese hamster ovary (CHO) cells [273]. The insertion of the CPXV Chinese hamster ovary host range gene (*CP77*) permitted VACV to multiply in CHO cells [274]. The first host range genes identified in VACV that are required for multiplication in human cells were *K1L* and *C7L* [275–277]. It has been shown that the deletion of *K1L* and *C7L* in VACV leads to abortive infection in human cells, pig kidney cells and rabbit kidney RK13 cells [275–278]. The multiplication deficient in human and pig kidney cells is overcome by the insertion of either *K1L*, *C7L* or *CP77* gene, whereas multiplication in rabbit kidney cells is restored by the insertion of either *K1L* or *CP77* gene, but not the *C7L* gene [273,277,278]. Other host range genes have been identified in VACV, *E3L* and *C12L* (encoding serine protease inhibitor-1, SPI-1). The *E3L* gene is required to grow VACV in Vero cells and human HeLa cells, but not in rabbit RK-13 cells, hamster BHK cells and CEF cells [279–281]. *C12L* is needed for VACV multiplication in human A549 cells [282,283].

MVA has a restricted host range and is unable to productively infect human and most mammalian cells [121,124,284]. However, MVA still multiplies in human cells such as osteosarcoma TK−143B cells [123,124,132,284,285]. Furthermore, it has been observed that MVA strains differ in their ability to multiply in different human cell lines [132]. MVA also multiplies efficiently in some non-human mammalian cell lines such as baby hamster kidney (BHK-21) cells (Table 1) [121,124,284–288].

Table 1. Cell lines susceptibility to MVA

Cell lines	Species	Multiplication of MVA strains								
		MVA[a]	MVA-II/85	MVA-VR1508	MVA-BN	MVA-B	MVA-572	MVA-1721	MVA-574	MVA-LZ
MDCK	Canine; kidney	SP							NP	
Ederm	Equine; skin								NP	
RO5R	Fruit bat Egyptian			P						
RO5T	Fruit bat Egyptian			P						
RO6E	Fruit bat Egyptian			P						
CHL	Hamster Chinese; lung	NP								
CHO	Hamster Chinese; ovaries	NP		NP						
BHK-21	Hamster Syrian; kidney	P		P	P	P				P
HEK-293	Human; kidney	NP		NP	NP	NP	NP	P		SP
HeLa	Human; cervix	NP	SP		NP	NP	NP	P	NP	SP
SW839	Human; kidney	NP								
TK-143B	Human; bone	P	SP		NP		NP	P		
MRC-5	Human; lung		NP		NP	NP			NP	
FS-2	Human; skin		NP							
Caco-2	Human; colorectal			NP						
FHs74int	Human; esophagus			NP						
Hutu-80	Human; small intestine			NP						
A549	Human; lung			SP						
HaCaT	Human; skin				NP		SP	P		
HRT18	Human; colon								NP	
Hep-2	Human; larynx								NP	
SK 29 MEL 1	Human; skin									NP
LC5	Human; lung									NP
85 HG 66	Human; brain									NP
U138	Human; brain									NP
C8166	Human; blood (T-cell)									NP
HUT 78	Human; blood (T-cell)									NP
SY9287	Human; blood (B-cell)									NP
MA104	Monkey; kidney								P	
MIB	Monkey; blood (B-cell)									NP
BSC-1	Monkey African Green; kidney	SP								
CV1	Monkey African Green; kidney	SP,P								P
Vero	Monkey African Green; kidney	SP		SP	SP	SP			SP	
FRhK-4	Monkey Rhesus; kidney	NP								
Balb3t3	Mouse; embryonal fibroblast		NP			NP				

NMULI	Mouse; glandular epithelial			SP						
AG101	Mouse; skin				NP		NP	NP		
DBT	Mouse; brain								NP	
PK(15)	Pig; kidney	NP		NP						
BEL	Pig; lung								SP	
MDBK	Pig; kidney								NP	
RK13	Rabbit; kidney	NP		NP					NP	
RAB-9	Rabbit; skin	NP								
SIRC	Rabbit; cornea	NP								
IEC-6	Rabbit; small intestine			P		SP				
H4IIE	Rat; liver			NP						

P: permissive, SP: semi-permissive, NP: non-permissive. [a] MVA whose strain, variant or passage number was not stated. Data are summarized from Okeke *et al.* [133].

In non-permissive cells, the viral cycle of MVA follows the same first steps of the VACV life cycle. MVA enters to the cell, expresses the early genes, replicates the viral genome, expresses the intermediate and late genes, but the cycle is blocked in the viral assembly, leading to immature virus particles that stay inside the infected cells [119] or dense particles [287,289]. Thus, MVA cannot produce infectious progeny [124,284,286,287]. Recombinant MVA vectored influenza vaccine (MVA-HANP) has a similar cell permissiveness compared to MVA, except in A549 and NMULI that are non-permissive to MVA-HANP [287].

1.6 Evolution and phylogeny of orthopoxviruses

The orthopoxviruses, as dsDNA viruses with proofreading DNA polymerases, evolve slowly compared to RNA viruses [290]. However, OPXV are not static, they can suffer genomic and phenotypic changes. The evolution of OPXV is driven by several molecular mechanisms such as point mutations, gene duplication, gene loss, homologous and non-homologous recombination and gene gain by horizontal gene transfer [291]. These mechanisms play an important role in the evolution of OPXV [200,291].

The substitution rate of OPXV have been estimated as 1.7-6.5 x 10^{-6} substitutions per site per year (subs/site/year) [292–295]. It is thought that OPXV evolve slowly because of the high fidelity of DNA replication by DNA polymerase [256]. However, despite of their low mutation rate, OPXV can evolve rapidly as it has been observed in MPXV [291]. Since 2018, the MPXV genomes have accumulated 50 single nucleotide polymorphisms (SNP). These number of SNP is higher with respect of the estimated substitution rate of OPXV. The rapid evolution of the recent MPXV outbreak may be due to human adaptation [296]. In contrast, the VARV genome has been quite stable over the years as it was well adapted to its host (humans) [199]. However, point mutations have also been observed in the OPXV genomes during the course of passaging in the laboratory [297–299].

Another mechanism that plays a significant role in OPXV evolution is recombination [84,200]. Recombination has been observed *in vitro* and *in vivo* between strains of the same species (intraspecies) and between different species (interspecies) [7,71,72,77,300–304]. Additionally, recombination between OPXV species with non-OPXV has been described [305]. Among CPXV strains, there is evidence of recombination between different CPXV clusters [77]. Similarly, recombination has been observed between VACV strains [303,306]. Furthermore, interspecies recombination has been reported between AKPV and ECTV [7]. The study of Gigante *et al.* demonstrated that ECTV may contain AKPV genome sequence [7]. Another study also showed recombination between ECTV and other OPXV (i.e., CPXV) [71]. This work demonstrated evidence of recombination in a CPXV strain that contained an ECTV-like *atip* gene [71]. Another study described that AKMV may have undergone recombination with CPXV. Some AKMV isolates contained a sequence of 6 kbp similar to CPXV in the left terminal region [6,302].

The phylogenetic analyses of OPXV showed that its members were split into two groups: the New World OPXV (RCNV, SKPV and VPXV) and the Old World OPXV (MPXV, CPXV, VACV, TATV, CMLV, VARV, ECTV, Abatino and AKMV) [7,74,78,307]. AKPV branched separately between the two groups despite its place of isolation (the USA) [7,74,307]. Based on the AKPV gene content, AKPV was more similar to the Old World OPXV than the New World OPXV. However, AKPV contained seven genes (*AKPV009, 010, 024, 025, 203, 204* and *205*) that encoded proteins most similar to proteins of Murmansk and NY_014 poxviruses. The presence of these genes in the AKPV genome might be a result of more than one recombination event with Murmansk. Moreover, two putative recombinant regions between ECTV and AKPV were also found in the AKPV genome [7].

Within the Old World OPXV, AKMV formed the deepest branch [6,7,74,184,302,307]. The isolates from the same species formed monophyletic clades, except for CPXV that did not cluster as a monophyletic group [7,73–75,77,78,307]. CPXV isolates were closely related to the Old World OPXV, except for AKMV [7,74,78,302]. Despite the similar genomic region (recombinant region) between some AKMV isolates and CPXV, AKMV did not cluster with CPXV in the study of Jeske *et al*. that used the complete genomes [78].

The phylogenetic studies showed that CPXV isolates were separated into at least five clusters named CPXV-like 1, CPXV-like 2, CPXV-like 3, VACV-like CPXV and VARV-like CPXV [72–78,308]. [77,78,308]. The phylogenetic relationship between CPXV-like 1, 2 and 3 and the other OPXV varied in the phylogenetic studies [74,77,78,307,309]. VACV-like CPXV had a close phylogenetic relationship with VACV. VARV-like CPXV was closely related to VARV, TATV and CMLV [73,74,77,78,302,307].

Various phylogenetic studies showed that CPXV was the only polyphyletic member of OPXV and also demonstrated the genetic diversity in CPXV isolates [70,72–78]. Carrol *et al.* showed the diversity of CPXV isolates using the genetic and patristic distances between CPXV isolates using as threshold values the distances between TATV and VARV. Their study also revealed that CPXV comprised several (up to 5) species [75]. Another study also revealed that CPXV was

genetically heterogeneous and could be divided into six cluster species based on the phylogeny and the genetic and patristic distances (using the distances between TATV and CMLV as a threshold) [72]. Mauldin *et al*. suggested that there are five (up to 14) lineages in CPXV based on monophyly and genetic distance criteria [73].

Compared to the other OPXV, CPXV had the largest genome, containing an almost full repertoire of OPXV genes (including OPXV accesory genes) and had the widest host range [40,84,198,201]. Based on that, it has been proposed that the common ancestor of the Old world OPXV (except for AKMV) is a CPXV-like virus [40,84,198,201]. The molecular evolution of OPXV is still unclear. A study of the molecular evolution of OPXV revealed that the emergence of OPXV took place about 42,000 years ago [307]. An earlier study of Babkin *et al*. showed that OPXV emerged 51,000 years ago, although the new OPXV species (i.e. AKMV, AKPV and Abatino) were not part of the dataset [292]. The New World OPXV first separated from the other OPXV [307]. Then, AKPV diverged from the Old World OPXV approximately 19,000 years ago. The emergence of the Old World OPXV was about 11,000 years ago. Within the Old World OPXV, the first to diverge was AKMV and its emergence was at around 11,000 years ago. The remaining of the Old World OPXV emerged about 6,000 years ago. Then, ECTV, Abatino and CPXV-GerMKY2010 clade diverged from other OPXV, and their estimated time to the most recent common ancestor (tMRCA) was approximately 5,000 years ago. Later CPXV-like 2 segregated from other OPXV approximately 5,400 years ago. The tMRCA of MPXV, VACV and VACV-like CPXV was estimated as 3,500 years ago. MPXV originated approximately 600 years ago, ~1444 AD [307]. However, a more recent study suggested that MPXV emerged in 1970 AD [310], although this estimation is later than the date of the first MPXV isolation [159]. CPXV-like1 diverged from VARV, TATV, CMLV and VARV-like CPXV about 3,700 years ago. VARV originated approximately 1,746 years ago [307]. Although a recent study reported that VARV has emerged 4,000 years ago, which is consistent with the records of smallpox in Egyptian mummies [311].

1.7 Hazard characterization of Modified Vaccinia virus Ankara

Recombinant viral vector vaccines, such as recombinant MVA, are considered as genetically modified organisms (GMO). In the European Union (EU), the marketing authorization of recombinant vaccines are subject to additional requirements compared to non-recombinant vaccines, which are stipulated in Directive 2001/18/EC [312]. The directive seeks to protect human health and the environment when a GMO is placed on the market and released into the environment by requiring an Environmental risk assessment (ERA) for the approval of the recombinant vaccine. The purpose of the ERA is to assess potential risks to human health and the environment that may arise from the use and release of GMOs into environment. The ERA consists of six steps: hazard identification, hazard characterization, evaluation of the likelihood of the hazard, risk characterization, proposal of risk management strategies and determination of overall risk conclusion [312]. Step 2 (hazard characterization) consists of the evaluation of the

potential consequences of each possible adverse effect of a GMO on human health and the environment.

Despite the strong safety profile of MVA, there are still some knowledge gaps regarding MVA and MVA vectored vaccines such as recombination of MVA vectored vaccines with naturally circulating OPXV, nature and distribution of naturally occurring OPXV, the molecular basis of MVA host range restriction as well as the genetic stability of MVA and MVA vectored vaccines [133]. Hence, addressing these knowledge gaps through carefully planned experiments in cell cultures and animal models is essential for the hazard characterization of MVA and MVA vectored vaccines. Therefore, it would contribute to achieving a more robust ERA and further optimizations of MVA as a safe vaccine vector [133].

1.7.1 Host cell restriction of MVA

The host restriction range of MVA is one of the characteristics that make MVA a good candidate for the development of vaccines against infectious diseases. However, the genetic basis for MVA restriction is not completely elucidated. MVA has suffered six major deletions that may cause its restricted host range. However, the introduction of six major MVA deletions into CVA was not enough to recover the complete host range of MVA [285]. Similarly, the restoration of large deleted regions containing *K1L* and *C12L* did not restore wild type host range [313], but improved the ability of MVA to multiply in human cells [313]. However, the introduction of the *C12L* gene rescued MVA multiplication in only human MRC-15 cells [314]. Additionally, the insertion of *K1L* in MVA did not restore the capacity to productively grow in human cells [121,313,315], but restored the multiplication of MVA in rabbit RK13 cells [315].

Another host range gene that plays a role in multiplication of MVA in human cells is *C16L*. The repair of both the *C16L* and *C12L* genes rescued the ability of MVA to multiply in human cell lines (HeLa, 293T, A549 and MRC-5 cells) [316]. Although the insertion of both genes, unlike the introduction of only *C16,* did not enhance the multiplication of MVA in monkey BS-C-1 cells [316]. Nevertheless, the multiplication competent VACV-WR lacked the *C16L* gene, which suggested that it contained another gene with redundant function [316,317]. Yet, the role of the major deletions and small mutations in the host range defect of MVA it is still unclear.

A study by Erez *et al.* has shown that spontaneous single mutations altered the host range of MVA. These single mutations in the *D10L* gene arose during passaging of MVA in BS-C-1 cells and increased multiplication of MVA in monkey BS-C-1 cells and slightly in human cells [318]. Even though the *D10L* gene has never been associated with the host range. Another study demonstrated that it is possible to re-adapt MVA to human Caco2-cells by serial passages in Caco2-cells. MVA variants were able to undergo productive infection in human Caco2-cells [133]. These studies indicate that host defect of MVA could be reversible and the host range restriction of MVA might not be a stable feature [318]. Alternatively, most MVA strains may be polyclonal containing many variants and adaption in human and mammalian cells through serial

passages might have selected a variant with enhanced fitness and multiplication abilities in human cells.

1.7.2 Nature and distribution of naturally circulating orthopoxviruses

For the hazard characterization of the MVA and MVA vectored vaccines, it is necessary to have information about the nature and distribution of naturally occurring OPXV in the area where the recombinant vaccine is to be deployed due to potential recombination of MVA vectored vaccines with a multiplication competent OPXV, which may lead to restoration of MVA to wild type and transfer of the transgene into a competent OPXV [133].

Despite the relevance of OPXV, there is still lack of information regarding the natural reservoir, host range and geographic distribution of some OPXV [184,319]. The surveillance efforts and isolation of OPXV both in humans and animals are limited, except for a few countries [133]. In addition, many places where OPXV are endemic lack infrastructure and resources. Most information about OPXV has been collected after outbreaks, for instance, the current global Mpox outbreak. Thus, known OPXV are not a representation of what is in nature because most OPXV strains were isolated from humans and from a few places. The lack of information about the nature, distribution and evolution of OPXV hinders the prediction of emergence OPXV [319].

Moreover, there is also lack of information about the consequences of the possible adverse effects after releasing the OPXV vectored vaccines. There is no monitoring of the adverse effects associated with the interaction of the recombinant vaccine and naturally occurring OPXV. One example is the recombinant vaccinia-rabies vaccine (Raboral-VRG) used in foxes [320]. It has been monitored for efficacy of vaccination but not for the interaction of the vaccine with the wild OPXV in foxes as well as its possible adverse effects [321]. It is important to establish monitoring plans in place prior to releasing the recombinant vaccines as, for example, the spillover from vaccinated animals to the environment could cause changes in the diversity of the wild OPXVs.

It is difficult to make inference about adverse effects due to the interaction of OPXV vectored vaccines and the wild type OPXV when there is few or lack of information about the nature and distribution of naturally occurring OPXV before and after the release of OPXV vectored vaccines. Those are knowledge gaps in the hazard characterization of MVA vectored vaccines [133].

1.7.3 Recombination in co-infection and superinfection

The recombination between MVA vectored vaccines and naturally occurring OPXV could result in the restoration of MVA to wild type (due to the rescue of deleted and fragmented genes), the transfer of the transgene into a naturally occurring OPXV and the generation of progeny viruses with altered properties (such as virulence and host range) [133,322]. The information about the potential for recombination between OPXV vectored vaccines and naturally occurring OPXV are not mandatory in the ERA [133]. Even though the genetic transfer

could be a consequence of recombination and it is stipulated in the Directive 2001/18/EC as an indirect effect.

There is dearth of information about the potential for recombination between the poxvirus vectored vaccines and naturally occurring OPXV as well as its consequences. The recombination events between MVA vectored vaccines and naturally occurring OPXV are considered negligible because (1) the co-localization of the viruses in the same cell is unlikely, (2) MVA lost the ability to produce infectious virions in human and most mammalian cells, (3) OPXV are short-lived and (4) superinfection exclusion prevents the second infection of infected cells [323]. However, the likelihood of co-localization increases when there are OPXV circulating in the area of administration of MVA and when the vaccines are administrated to domesticated animals and wildlife since animals are the reservoirs and accidental hosts of natural OPXV [133,322]. Even the ongoing global Mpox outbreak would create scenarios for the interaction of MVA and zoonotic OPXV in humans due to the extensive use of MVA vaccines. Despite the short-lived of OPXV, DNAemia of CPXV can last until four weeks [324], which is a lapse of time for virus-virus interactions [133]. Even though MVA is unable to complete the viral cycle in non-permissive cells, the infection is blocked on the morphogenesis, thereby the viral DNA replication is unimpaired [119]. Hence, the recombination could take place in non-permissive cells because only 12 bp of overlapping homologous sequences in DNA sequences are sufficient for recombination [325]. In case of superinfections, the mechanisms of superinfection exclusion are not absolute as few viral cores of the superinfecting virions were observed in the cytoplasm of superinfected cells [218].

A study of *in vitro* co-infection with MVA vectored vaccines and naturally occurring OPXV showed that the viruses underwent recombination [326]. The co-infection was performed in permissive BHK-21 cells. The recombination resulted in hybrid viruses that displayed parental and non-parental characteristics [326,327]. The genomic characterization of these progeny viruses would give a better understanding of the recombination between these viruses.

Evidence for the natural recombination between a wild strain of capripoxvirus and a live attenuated vaccine in Russia has been reported [328]. The recombinant vaccine-like lumpy skin disease virus (LSDV) might be the result of the recombination between field LSDV strain and LSD vaccine. It was isolated after the introduction of the vaccine. The next outbreaks were caused by vaccine-like LSDV strains and not by wild LSDV strains that were observed in the previous years before the vaccination campaigns [329,330]. Although it has been suggested that the recombinant vaccine-like LSDV strains could be a spillover from vaccinated animals [331] .

Despite of the relevance of the recombination between OPXV vaccines or OPXV vectored vaccine and naturally circulating OPXV, the studies about this topic are scarce. Therefore, more studies examining recombination should be performed to obtain data about the potential hazard arising from recombination between MVA vectored vaccine and naturally occurring OPXV. Furthermore, the biological and genetic characterization of recombinant progeny viruses should

be performed to understand the recombination process, poxvirus host range, cytopathogenicity and transgene stability and integrity.

1.7.4 Homogeneity and genetic stability of MVA

The homogeneity and the genetic stability of OPXV vectored vaccines are the major concerns during the production of vaccines in large-scale. It is deemed that MVA was homogenous and stable after 570 passages in CEF and plaque purified [332]. Comparison of the genome sequence of five MVA strains showed that their genomes (excluding the ITR) were similar [333]. Another study showed that the genomes of three MVA strains were genetically identical, but the strains showed different phenotypic properties and safety profiles. The method employed in that study did not detect the variants in the MVA strains (which were polyclonal mixtures of viruses) because the method only evaluated the majority of viral genome in the sample [132]. In order to identify variants in the MVA strains and confirm the homogeneity, the strains should be subjected to deep sequencing [133].

The genetic instability could occur within and outside the transgene. One of the desirable characteristics for a virus to be used as recombinant vector vaccines is to be genetically stable. It has been observed that the MVA genome suffers spontaneous mutations during serial passages [318,334] and, hence, some variants could be raised during the production of the vaccine or recombinant vaccine stocks. The stability and integrity of the transgene is particular important in the development of recombinant viral vaccines to avoid losing or reducing expression of the transgene. Thus, understanding the viral and host determinants involved in the genetic instability will facility the development of MVA vectored vaccines.

Some studies have showed instability of the transgene in recombinant MVA vaccines [335–338]. A study by Wyatt *et al.* showed that the transgene expression changed during serial passages due to spontaneous mutations [338]. The mutations were found inside and outside the transgene [338]. The transgene stability of MVA-HANP has been examined in permissive IEC-6 cells. The expression of the transgene was unstable, after the third passage the expression was undetectable [327]. Similarly, it has been observed in the hybrid progeny viruses obtained from co-infection *in vitro* with MVA-HANP and a wild type CPXV. One hybrid virus completely lost the transgene expression after the third or fourth passage. Whereas the stability of transgene of other hybrid progeny viruses varied across different cell lines [326,327]. From a biosafety point of view the loss of the transgene is relevant because the transgene serves as a tool to monitor the spread of the recombinant vaccine to target and non-target organisms as well as its non-target effects.

In order to confirm the genome stability of recombinant MVA vaccine, it has been recommended to perform the genome sequencing of master seed virus for up to five passages [133]. In the ERA it is required to assess the adverse effects caused by the genetic stability but it is not mandatory to provide that information as well as whole genome sequences of the stocks to confirm homogeneity [133].

2. RATIONALE OF THIS STUDY

OPXV based vaccines, especially MVA, are being used as recombinant vector vaccine against infectious diseases and neoplasm in humans and animals. OPXV vectored vaccines are also being developed against well-known and emerging human diseases caused by viruses such as HIV, influenza virus, Ebola virus, Zika virus, respiratory syncytial virus and SARS-coranovirus-2. Moreover, oncolytic chimeric OPXV are in clinical trials for the treatment of cancer. It is worth considering some biosafety issues that may arise if OPXV vaccines or OPXV vectored vaccines are deployed extensively in the treatment of infectious diseases and cancers. MVA is considered an attractive vector for vaccination due to its host range restriction in human and mammalian cell lines. During the attenuation process MVA lost some virulence genes. However, various mammalian cells, even human cells, are still permissive and semi-permissive to MVA infection.

There are still knowledge gaps with respect to the hazard characterization of MVA. One of the biosafety concerns about the use of MVA vectored vaccine is the potential for recombination between MVA vectored vaccine and a naturally occurring OPXV in cells/hosts in which it multiplies poorly (semi-permissive/non-permissive cells). The recombination with multiplication competent OPXV during co-infection and superinfection may lead the rescue of deleted and/or truncated host range genes in MVA and, therefore, restore the ability to multiply efficiently in human and mammalian cells. The hybrid progenies could display higher virulence and non-parental characteristics, lose the transgene (which hinders the monitoring of OPXV vectored vaccine) and/or transfer the transgene to a multiplication competent OPXV.

In vitro studies on recombination between OPXV vectored vaccine and wild type OPXV are scarce because the risk of recombination has been considered negligible. This argument is based on MVA host restriction and superinfection exclusion. Nevertheless, viral DNA replication still occurs in non-permissive cells which is enough for recombination to take place. Therefore, studies of recombination *in vitro* between MVA vectored vaccine and natural circulating OPXV in semi-permissive cells during co-infection and superinfection should be performed. These studies are relevant to hazard characterization of MVA vectored vaccines.

There are putative scenarios where recombination between OPXV vectored vaccines and other OPXV such as post-exposure therapies of MVA to treat pre-existing OPXV infection in animals or humans can occur. A robust characterization of the potential for recombination between MVA vectored vaccines and naturally occurring OPXVs will require knowledge of the genetic diversity and evolution of naturally circulating OPXVs in regions in which the vaccine will be released since endemic OPXVs will serve as parental strains for recombination. Natural infection with an OPXV (for example MPXV) and vaccination with MVA vaccine (for example JYNEOUS) or prophylactic vaccination with MVA vaccine and natural infection with OPXV are plausible scenarios for co-infection and superinfection which may result in recombination. The surveillance and characterization of OPXV are limited, except for MPXV whose surveillance has increased recently due to the current global outbreak in several non-endemic

countries. OPXV circulated on every continent except Antarctica. For instance, CPXV is endemic to Eurasia. CPXV is a peculiar species among OPXV because it is genetically diverse and polyphyletic. It contains almost the full set of OPXV genes. Moreover, there is evidence of natural recombination in CPXV and between CPXV and other OPXV. The genomic characterization of CPXV isolates would provide insights into OPXV evolution, phylogeny and phylodynamic. Experimental *in vitro* co-infection and superinfection of cell cultures with naturally occurring CPXV and MVA vectored vaccine will serve as a model in which the potential for recombination and genome wide pattern of recombination will be explored. Taken together, the study of the diversity and evolution of OPXV circulating in the location of in which MVA vaccines may be released should be investigated because they are the baseline data to evaluate the potential for recombination and interrogate the genetic heterogeneity of CPXV.

3. GENERAL OBJECTIVE

The main objective of this thesis is to study the evolution and the genetic diversity of CPXV and examine recombination *in vitro* between a naturally occurring CPXV and MVA vectored vaccine in cells that MVA multiplies poorly. Thus, this study is aimed at improving OPXV vectored vaccine biosafety through genomic characterization of wild type CPXV and CPXV/MVA progeny viruses.

PAPER I

***Hypothesis*:** Recombinant CPXV viruses are circulating in nature.

***Specific objectives*:**

- To perform genomic characterization of a novel human CPXV.
- To detect potential recombination events in the genome of novel human CPXV.
- To determine the phylogenetic relationship of a novel human CPXV with other representative CPXV and OPXV strains.

PAPER II

Hypothesis: CPXV isolates have high genetic diversity and CPXV is not a single species.

Specific objectives:

- To determine the phylogenetic relationship of the Fennoscandian CPXV isolates with other representative CPXV and OPXV strains.
- To evaluate the genetic diversity in CPXV isolates
- To study the evolutionary history of CPXV.

PAPER III

Hypothesis: Recombination between MVA-HANP and a naturally occurring CPXV during co-infection and superinfection of cells (in which MVA multiplies poorly) leads the generation of progeny virus with novel genetic and biological characteristics.

Specific objectives:

- To examine the recombination *in vitro* MVA-HANP and naturally occurring Norwegian feline CPXV during co-infection and superinfection of semi-permissive Vero cells.
- To perform genome characterization of parental MVA-HANP and progeny viruses.

4. METHODOLOGY

4.1 Viruses, cells, co-infection and superinfection experiments

In **paper I**, we used the naturally occurring Norwegian human CPXV-No-H2 to examine the possibility of natural recombination in circulating Fennoscandian CPXV and map genome-wide recombination events. Evidence of natural recombination in CPXV-No-H2 based on limited genetic characterization was previously demonstrated [71]. CPXV was propagated in African green monkey kidney Vero cells because these cells are fully permissive to CPXV infection [121,124,284–287,327] (**paper I and II**).

In **paper II**, we characterized five naturally circulating CPXV strains (CPXV-No-H1, CPXV-No-F1, CPXV-No-F2, CPXV-Swe-H1 and CPXV-Swe-H2) that were isolated in the Fennoscandian region (Norway and Sweden) from human and felines [45,68–71]. Genome sequencing of these Fennoscandian CPXV, and phylogenomic analysis with other OPXV strains would contribute to the understanding of the diversity, phylogenetic relationship of CPXV and other OPXV and evolutionary history of CPXV.

In **paper III**, we evaluated the recombination between CPXV-No-F1 and MVA-HANP during *in vitro* co-infection and superinfection of semi-permissive cells to MVA-HANP. Vero cells were selected for these experiments because they are semi-permissive to MVA-HANP infection [287]. The feline isolate CPXV-No-F1 was selected instead of the human isolate CPXV-No-H1 because a possible scenario of human CPXV infection is by direct contact with infected domestic pets like cats. In addition, this is also a naturally occurring Fennoscandian CPXV.

MVA-HANP was previously chosen as a OPXV vectored vaccine since (1) MVA is used as smallpox vaccine and viral vector vaccine, (2) MVA is a multiplication incompetent poxvirus vector, and (3) MVA-HANP contains the influenza virus *hemagglutinin* (*HA;* A/PR/8/34) and *nucleoprotein* (*NP*) gene inserts, which makes it easier to monitor the transgenes by immunostaining. Overall, this is a safe model to test recombination *in vitro.*

The selection of the progeny viruses was in Vero cells. Unlike CPXV, MVA does not form plaques in Vero cells but expresses HA [326], which facilitates the identification (and selection) of the plaques from hybrid viruses and differentiate them from parental virus plaques by plaque phenotype and the HA expression. Two criteria used to select the progeny viruses were: plaque phenotype and the expression of the influenza virus HA protein.

The co-infection and superinfection experiments were done at a multiplicity of infection (moi) of 5.0 for each parental virus. Although the high moi of 5 might not be reflect the moi. under natural co-infection/superinfection, it assures the infection of all the cells in the primary infection and, therefore, guarantee the superinfection of Vero cells. Additionally, we performed different superinfection experiments: (1) primary infection with CPXV-No-F1 and superinfection with MVA-HANP after 4 hrs post primary infection (ppi), (2) primary infection with CPXV-No-F1 and superinfection with MVA-HANP after 6 hrs ppi, (3) primary infection

with MVA-HANP and superinfection with CPXV-No-F1 after 4 hrs ppi and (4) primary infection with MVA-HANP and superinfection with CPXV-No-F1 after 6 hrs ppi (Figure 4). These experiments would simulate different possible scenarios such as (1) the person/animal is infected with CPXV and receives the vaccine (MVA) and (2) when the person/animal received the vaccine (MVA) and then is infected with CPXV. The least possible scenario would be the co-infection when the person is infected by both viruses at the same time. But these experiments constitute cell culture-based models to examine recombination of MVA with other OPXV during co-infection of semi-permissive cells as well as evaluate the possibility of superinfection exclusion in preventing recombination.

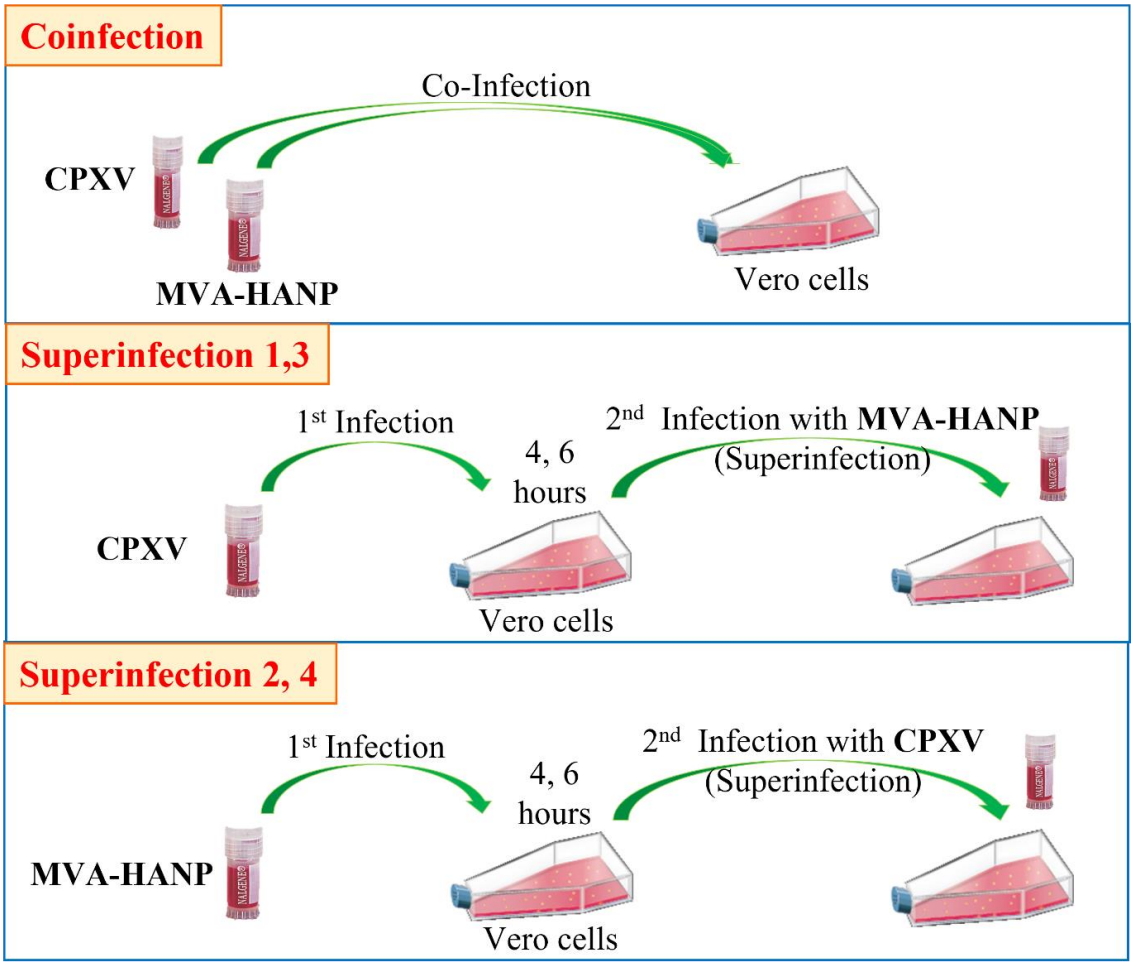

Figure 4. Co-infection and superinfection experiments in Vero cells. Co-infection, Vero cells were co-infected with CPXV-No-F1 and MVA-HANP. Superinfection 1, primary infection with CPXV-No-F1 and secondary infection with MVA-HANP at 4h post primary infection (ppi); Superinfection 2, primary infection with MVA-HANP and secondary infection with CPXV-No-F1 at 4h ppi; Superinfection 3, primary infection with CPXV-No-F1 and secondary infection with MVA-HANP at 6h ppi; Superinfection 4, primary infection with MVA-HANP and secondary infection with CPXV-No-F1 at 6h ppi.

4.2 Viral DNA extraction

The six CPXV isolates were semi-purified by sucrose gradient as previously described [209]. Viral DNA was extracted from Vero cells infected with the semi-purified virions (**paper I & II**). MVA-HANP was also semi-purified by sucrose gradient, but viral DNA was extracted from infected BKH-21 cells (**paper III**). The progeny viruses from co-infected and superinfected Vero cells were plaque purified and viral DNA was extracted from Vero cells infected with the plaque purified viruses (**paper III**).

The viral DNA extraction was performed following Dabrowski's protocol [76]. In order to release the viral particles, the infected cells were incubated on ice in cold hypertonic buffer (with Triton X-100 and β-mercaptoethanol) to solubilize the plasma membranes. The cell nuclei were removed from cytoplasmatic content by centrifugation. Then, the viral particles were isolated from the cytoplasmatic content by ultracentrifugation. The viral particles were incubated in cold hypotonic buffer to release viral core. For the following steps, we used a commercial kit for viral DNA extraction (and Qiagen Genomic DNA buffers). These kits have the advantages of extracting high-molecular weight DNA and yielding pure DNA of good quality. Moreover, reproducible DNA yield and quality is achieved.

4.3 Sequencing

Some sequencing technologies can be used for whole genome sequencing. These technologies are second generation sequencing (or next-generation sequencing, NGS) and third generation sequencing (TGS). NGS produces large amounts of short reads (up to a few hundred bp) with low error rate [339,340]. One disadvantage of NGS is that the short reads are not suitable for assembling genomes with long repeated regions and large structural variants [341]. In contrast to NGS, TGS yields much longer reads (>10 kbp), but with high error rate (~15%) [340–342]. The long reads are useful for *de novo* genome assembly. Both NGS and TGS have advantages and disadvantages; however, one technology overcomes the disadvantages of the other. The hybrid sequencing, that is combination of NGS (short-read sequencing) and TGS (long-read sequencing) platforms, resolves problems such as repetitive regions (e.g. ITR), deletions/insertions and produces genome assemblies with few or no gaps.

Whole genome sequencing of Fennoscandian CPXV isolates (**paper I and II**), MVA-HANP and the progeny viruses from co-infected and superinfected Vero cells (**paper III**) was performed using the hybrid sequencing approach. For this approach, we used Illumina Miseq platform for short-read sequencing (NGS) and Nanopore platform for long-read sequencing (TGS). Illumina MiSeq is suitable to sequence small genomes (like viral genomes) and generates up to 15 Gb of output and paired-end reads of 300 bp. Nanopore is more cost-effective for generating long reads [341,342].

4.4 Genome assembling and annotation

The raw Illumina reads were pre-processed before genome assembling (**paper I, II and III)**. The adapters, the low quality reads and short reads were trimmed using Trimmomatic [343]. It has been shown that read trimming increases the quality and reliability of downstream analysis and reduces computational requirements and execution time [344]. After trimming, the reads from contaminants (e.g. Vero cells) were removed using FastQ Screen v0.14.1 [345] with BWA aligner [346,347]. The reads were mapped to the possible contaminant genomes (Vero cells) and filtered. FastQ Screen v0.14.1 is a program that maps sequencing reads to one or more reference genomes (e.g. host cell, CPXV and MVA) using an aligner (e.g. BWA) and filters the reads mapping (or not mapping). [345]. Furthermore, the program allows you to create your own database with the genome of our interest and choose between three aligners. BWA was chosen because it is designed for aligning short and long reads [346,347].

The processed reads were used to assemble the viral genomes. The approach used in **paper I, II and III** was hybrid genome assembly (Nanopore and Illumina data) due to the structure of the OPXV genomes. These genomes contain repetitive regions and ITR that hinder the assembly with only Illumina data (short reads). The long reads from Nanopore sequencing overcome this problem. Different assemblers are available for hybrid genome assembly, such as SPAdes [348], PBcR [349], Unicycler [350] and MaSurCa [351]. The viral genomes were assembled using hybridSPAdes. The algorithm first assembles the short reads and then aligns the long reads to generate longer contigs, and generates accurate assemblies [348]. Unlike PBcR and MaSurCa, it has been designed to assemble small genomes (e.g. bacterial and viral genomes) [352].

The assembled genomes were annotated using Genome Annotation Transfer Utility (GATU) (**paper I, II and III**). GATU is a rapid annotation tool with a user-friendly graphical user interface. It transfers annotations from an annotated reference genome to the target genome, which makes the annotation process less time-consuming and less tedious. Additionally, it allows you to review the alignments of putative open reading frames (ORF) with the reference genes [353].

4.5 Gene content comparison

In **paper I**, we compared the gene content of CPXV-No-H2 with other poxvirus genomes. Previously evidence of recombination was detected in CPXV-No-H2 [71]. First, all predicted CPXV-NoH2 coding sequences (CDS) were translated and compared to the proteins of three OPXV reference genomes (ECTV-Moss, CPXV-BR and VACV-Cop) by BLASTP [354]. Some regions of the CPXV-No-H2 genome were more similar to either CPXV, ECTV or VACV, but others were less similar to the three OPXV. Hence, in order to detect CPXV-No-H2 genes more similar to other poxvirus genes, all predicted CPXV-NoH2 CDS were translated and compared to poxvirus proteins by BLASTp. The predicted CPXV-No-H2 genes that encode proteins with

the highest amino acid similarity to other OPXV proteins than CPXV proteins were compared to the OPXV genomes by BLASTn.

In **paper II,** we performed the gene content comparison of the five Fennoscandian CPXV with the reference genome CPXV-Br. Similar to procedure of **paper I**, the predicted CDS from five CPXV isolates were extracted, translated into amino acid sequences and compared to the CPXV-Br proteins using BLASTp [354].

4.6 Recombination analysis

Since it was suggested that CPXV-No-H2 might originate from a recombination between CPXV-like virus and ECTV-like virus [71], we performed the detection of the possible recombination events in the CPXV-No-H2 genome using RDP4 [355] and Simplot [356] (**paper I**). These programs have been widely used in other studies [6,71,357,358]. These programs required as input file the alignment of the recombinant sequence with the putative parental sequences. The CPXV-No-H2 genome with other genomes were aligned using Multiple Alignment Fast Fourier Transform (MAFFT). Compared to other aligners, MAFFT is a faster aligner and provides reliable and accurate multiple sequence alignments [359].

RDP4 is a recombination detection program that has implemented several methods (RDP [360], bootscan [361], maxchi [362], chimaera [363], 3seq [364], geneconv [365], lard [366], and siscan [367] to detect potential recombination events in the aligned sequences. It allows to analyse up to 2500 sequences of 10,000 kbp, which makes it suitable for our dataset (genome length < 225 kbp). Furthermore, RDP4 provides the recombination sequences, the sequences that are closely related to the minor and major parental and recombination breakpoints (the beginning and end breakpoints of the potential recombinant sequences) [355].

Simplot is another program to detect potential recombination. This software calculates the percent identity (similarity) of the query sequence compared to the other sequences and generates similarity plots (% similarity versus position). The potential recombination breakpoints are easily identified and visualized on the similarity plots. [356]. Compared to RDP4, Simplot provides fast results, but only allows to analyse up to 10 sequences. Besides the identification of the potential recombinant regions in CPXV-No-H2, we generated phylogenetic trees based on potential CPXV-No-H2 recombinant regions to corroborate the phylogenetic relationship between the putative parental virus (where the recombinant sequence was derived) and CPXV-No-H2. In **paper III**, we conducted recombination analysis of the progeny viruses from co-infected and superinfected Vero cells using the same methodology described above.

4.7 Phylogenetic analysis, patristic and genetic distances

The phylogenetic relationship of Fennoscandian CPXV strains with other CPXV and OPXV was investigated in **paper I and II**. The majority of the OPXV genomes used in this thesis were retrieved from the Viral Orthologous Clusters database (VOCs) [368] (**paper I and II**). VOCs is

a repository for large dsDNA viruses, including complete and fully annotated poxvirus genomes [369].

In **paper I and II,** three different alignments were used for the phylogenetic analysis: (1) OPXV core genome (the genomes without ITR), (2) OPXV whole genome (genomic region from the first gene until the last gene), and (3) OPXV orthologous genes. DNA sequences were aligned using MAFFT [370]. After aligning, the poorly aligned positions and gaps were removed from the whole and core genome alignments using Gblocks [371]. It is recommended to remove the problematic alignment regions in long alignments but not in short alignments (as orthologous gene alignment) to generate accurate phylogenetic trees [371]. The orthologous genes in OPXV genomes were identified using OrthoFinder [372]. OrthoFinder is fast, accurate and simple to use. It finds orthogroups, orthologs and gene duplication events and provides comparative genomics statistics [372]. The orthologs (present in ≥95% of the genomes) were aligned and concatenated.

Two methods of tree reconstruction were used for phylogenetic analysis: maximum likelihood (ML) and Bayesian inference (BI) method. These methods are more efficient than the neighbour joining method in obtaining accurate tree [373,374]. Although they are computationally expensive [375]. Before generating the phylogenetic trees, the best-fit models of DNA substitution for the datasets were selected because ML and BI methods use an explicit DNA substitution model. The models were selected by modelTest-NG [376]. ML analyses were performed using RAxML [377] and BI analyses were performed using MrBayes v.3.2.7 [378].

Recombination events within datasets may cause inconsistencies in the phylogenetic trees and, therefore, erroneous phylogenetic inferences [379,380]. In order to assess if recombination in three datasets affects the phylogenetic inferences between CPXV and OPXV in **paper II**, the three datasets were analyzed for recombination events using RDP4 and one additional dataset of 62 non-recombinant OPXV conserved genes was included. OPXV conserved genes were examined for recombination using RDP4 and only conserved genes that did not show recombination were selected. In addition, in **paper II** the phylogenetic signal of the four dataset was assessed by likelihood mapping analysis using IQ-TREE [381]. It is important to test the presence of phylogenetic signal because the lack of it can affect the reliability of the results [382].

The diversity of CPXV has been reported and it was proposed that CPXV might be more than one species [72,73,75,76,307]. Hence, in **paper II**, we used the genetic and patristic distances between and within CPXV clusters to demonstrate the genetic diversity among CPXV isolates. To separate CPXV isolates into sub-species, the genetic and patristic distances between the closest and distinct OPXV species (TATV and CMLV) were used as threshold values. The patristic and genetic distances were estimated using the program Patristic [383] and p-distances method, respectively.

4.8 Phylodynamic evolutionary analysis of CPXV

The molecular evolution of CPXV was reconstructed using 62 non-recombinant conserved genes of 55 CPXV (**paper II**). Different methods can be used to date the phylogeny: Bayesian [384], ML [385] or least-squares dating [386]. We used the Bayesian Markov chain Monte Carlo (MCMC) inference method implemented in *BEAST* [387]. Before carrying out the phylodynamic evolutionary analysis, we performed some preliminary analyses on the dataset. First, we checked the presence of phylogenetic signal in the dataset by IQtree [381]. Second, the conserved genes were examined for recombination by RPD4 [355]. Only conserved genes that did not show recombination were selected. Third, we assessed the temporal signal in the dataset using TempEst [388] because a dataset without temporal signal is not appropriate to calibrate a molecular clock and to infer evolutionary rate and time scale of the virus [382]. TempEst allows you to detect problematic sequences, for example sequences with assembly errors, annotation errors or incorrect sampling dates [388].

5. SUMMARY OF THE MAIN RESULTS

Paper I: "Genomic sequencing and analysis of a novel human *Cowpox virus* with mosaic sequences from North America and Old World orthopoxvirus"

- We presented the whole genome sequence of a human cowpox virus, CPXV-No-H2, from Norway. The length of the CPXV-No-H2 genome was 220,276 bp, containing 217 predicted genes.
- Among 217 predicted genes of CPXV-No-H2, seventeen encoded proteins were most similar to OPXV proteins from the Old World (ECTV and VACV), and North America (AKPV).
- Our analyses revealed that CPXV-No-H2 was a mosaic genome with genes most similar to other OPXV genes.
- The recombination analysis revealed that CPXV-No-H2 may have arisen out of several recombination events between OPXVs.
- One potential recombinant event with parental AKPV contained the *NoH2-210* gene that was most similar to *AKPV-203* and Murmansk gene.
- Within the seven putative recombinant regions in CPXV-No-H2, one was located in the conserved central genomic region.
- The phylogenetic analysis showed that CPXV-No-H2 with two German CPXV isolates (CPXV_GerMygEK938_17 and CPXV_Ger2010_MKY) formed a separate, new CPXV clade, which we named "ECTV-Abatino-like CPXV".
- CPXV_GerMygEK938_17 and CPXV_Ger2010_MKY shared 96.4% and 96.3% nucleotide identity with CPXV-No-H2, respectively.

Paper II: "Genomic Sequencing and Phylogenomics of *Cowpox Virus"*

- We reported the complete sequence of five Fennoscandian CPXV isolated from cats and humans.
- Their genome size ranged from 220-222 kbp, containing between 215 and 219 predicted CDS.
- The phylogenetic analysis based on the whole genomes, core genomes, orthologous genes and 62 non-recombinant conserved genes of 87 OPXV isolates (including the five Fennoscandian CPXV isolates) confirmed the separation of CPXV isolates into at least five distinct major clusters (CPXV-like 1, CPXV-like 2, VACV-like CPXV, VARV-like CPXV and ECTV-Abatino-like CPXV).
- CPXV strains were closely related to other the Old World OPXV, except for AKMV.
- Based on phylogenetic analysis and the genetic and patristic distances, CPXV isolates can be further divided into eighteen sub-species.
- We reconstructed the evolutionary history of CPXV using Bayesian time-scaled phylogeny of CPXV based on the concatenated 62 non-recombinant conserved genes of 55 CPXV. However, the emergence date of CPXV as well as CPXV clusters could not be accurately estimated.

- The mean evolution rate of CPXV was calculated to be 1.65×10^{-5} subs/site/year, with 95% high posterior density interval (HPD) of $4.36 \times 10^{-7} - 4.32 \times 10^{-5}$ subs/site/year.

Paper III: "Whole genome sequencing of recombinant viruses obtained from co-infection and superinfection of Vero cells with Modified Vaccinia virus Ankara vectored influenza vaccine and naturally occurring *Cowpox virus*"

- Recombination occurred between CPXV and MVA-HANP in co-infected and superinfected Vero cells.
- Some progeny viruses displayed plaque phenotype distinct of that of the parental viruses.
- The distribution of the recombinant events along the progeny virus genomes was random.
- The recombination events were located in both the conserved central region and the variable terminal regions.
- The transgene expression cassette was inserted (recombined) in the same position in the progeny virus genomes.
- The genomes of the recombinant progeny viruses have different lengths.
- Most recombinant progeny virus genomes were a mosaic of the two parental viruses (CPXV-No-F1 and MVA-HANP).
- The percentage of DNA derived from the parental viruses in the recombinant progeny viruses was variable.
- The recombinant viruses, more similar to MVA-HANP (>50%), rescued deleted and/or fragmented genes in MVA and gained new host ranges genes.
- Some recombinant progeny viruses carried the double expression cassette (harboring both influenza virus *HA* and *NP* transgenes) from MVA-HANP.
- The transgene of MVA-HANP was unstable, which led to the partially deletion of the double expression cassette.
- Resulting of the transgene instability of MVA-HANP one non-*HA*-transgene expressing progeny virus contained a fraction of the transgene expression cassette similar to the incomplete MVA-HANP.
- The progeny viruses suffered other genetic changes, such as the large deletion of 16,761 bp in two recombinant progeny viruses.

6. GENERAL DISCUSSION

MVA is a promising vector vaccine candidate. It is in pre-clinical and clinical trial studies for different diseases, including cancer [135,140,141,143,389]. However, despite the several studies about MVA and MVA vectored vaccine, there are still knowledge gaps about its potential for recombination with wild type OPXV as well as the distribution, genetic diversity and evolution of naturally circulating OPXV in regions in which MVA or MVA vectored vaccine will be administrated. The occurrence of natural recombination between MVA or MVA vectored vaccine and wild-type OPXV needs favourable scenarios where both viruses are present, that is, in environments where OPXV are circulating and MVA or MVA vectored vaccine is being administrated. Eurasia is a good scenario for recombination of MVA with CPXV since the latter is endemic in this region [31–37]. Several CPXV outbreaks and human CPXV infections have been reported [42,45,66,67,69,71,72]. Furthermore, MVA-BN has been approved as a smallpox and Mpox vaccine in Europe. Hence, the genomic characterization of CPXV strains isolated from different geographic locations is important to elucidate the genetic diversity and evolution of CPXV. This information is the baseline for evaluate the potential for recombination of MVA or MVA vectored vaccine with wild type OPXV.

In **paper I & II**, we reported the whole genome sequencing of six Fennoscandian CPXV isolates (CPXV-No-F1, CPXV-No-F2, CPXV-No-H1, CPXV-No-H2, CPXV-Swe-H1 and CPXV-Swe-H2). These isolates were from Norway and Sweden. Among them, there was one atypical CPXV isolate (CPXV-No-H2). It was classified as CPXV based on the presence of ATI, the sequence and phylogenetic analysis of *HA* gene, *cytokine response modifier B* (*crmB*) gene, and *Chinese hamster ovary host range* (*CHOhr*) genes [70,71]. However, it was an atypical CPXV because of its ATI phenotype ($V^{+/}$), presence of the ECTV *atip* gene and atypical CPXV *Hind III* restriction map [70,71].

In **paper I & II**, we studied the phylogenetic relationship of Fennoscandian CPXV with other OPXV. Our phylogenetic analyses revealed that CPXV did not form a monophyletic clade and their isolates were clustered into five major clusters: CPXV-like 1, CPXV-like 2, VARV-like CPXV, VACV-like CPXV and new CPXV clade. CPXV isolates were closely related to all Old World OPXV species, except for AKMV. These findings are in agreement with other phylogenetic studies [74,78,307]. The new CPXV clade was composed of CPXV-No-H2 and two German CPXV isolates, CPXV_GerMygEK938_17 and CPXV_Ger2010_MKY. CPXV-No-H2 shared most similarity to CPXV_GerMygEK_938_17. This new CPXV clade was closely related to ECTV and Abatino clade. Thus, we tentatively named this clade as "ECTV-Abatino-like CPXV". Previously it has been suggested that these two German CPXV isolates formed a new lineage (CPXV-like 3), but their phylogenetic relationship with ECTV and Abatino had a low bootstrap support [78]. A recently study showed that ECTV-Abatino-like CPXV did not cluster with ECTV and Abatino based on phylogenetic tree of conserved central region (*F11L - A23R*) [74]. In contrast, all our phylogenetic trees showed a closer phylogenetic relationship between ECTV-Abatino-like CPXV and ECTV/Abatino clade, regardless of the dataset used (OPXV whole- and core-genome, OPXV orthologous genes or 62 non-recombinant OPXV

conserved genes) (**paper I and II**). In addition, in our phylogenetic tree construction, we used both ML and BI methods which are more robust and accurate than the NJ method used by Bruneau *et al.* 2023 [74].

The Norwegian CPXV isolates grouped in separate CPXV clusters rather than clustering together (**paper I and II**). The Norwegian CPXV-No-H2 belonged to ECTV-Abatino-like CPXV, whereas the other Norwegian CPXV isolates clustered together in CPXV-like 2. Similarly, the Swedish CPXV isolates were grouped together in CPXV-like 2. These Norwegian and Sweden CPXV isolates were closely related to British and Danish isolates, respectively (**paper II**) The phylogenies generated in other studies also showed the close phylogenetic relationship of these Norwegian CPXV isolates with the British CPXV isolates [73,75,77].

Our findings in **paper I and II** revealed the genetic heterogeneity of CPXV isolates. Thus, in **paper II**, we examined the genetic diversity of CPXV using the genetic and patristic distances between and within CPXV clusters as previously reported [72,73]. Using the genetic and patristic distances between TATV and CMLV as a threshold value, the five CPXV clusters can be classified as five sub-species and even they can be further divided into 18 sub-species. This is in congruent with our phylogeny (**paper II).** The genetic diversity in CPXV could be attributed to recombination events in CPXV. It has been showed that some CPXV strains were mosaic genomes derived from different CPXV clades [77]. Even some studies suggested recombination between CPXV and other OPXV [6,84,302]. The reported genetic diversity of CPXV in **paper II** could not be a result of recombination events because we used a dataset of 62 non-recombinant OPXV conserved genes and despite the extensive recombination in the other three datasets, the phylogenies and genetic and patristic distances from the datasets with or without evidence of recombination were similar. This was surprisingly because recombination can lead to incongruences in the phylogeny and inaccurate phylogenetic inferences as has been observed in other studies [379,380]. Indeed, phylogenetic incongruency was observed when validating the recombinant regions singly in **paper I**. However, it appears that the phylogenetic signals of the recombinant regions were masked by signals from the larger, non-recombinant regions of the genome (**paper II**).

The definition of CPXV has been based on host specificity and two main criteria (ATI bodies and red hemorrhagic pocks on the CAM) [79], which allowed that several viruses were classified under the CPXV name. [80–83]. Mauldin *et al*. questioned the classification of CPXV as a single species because CPXV did not meet one of ICTV requirement (monophyly) to be classified as a species [73]. Our data presented herein substantiated the genetic diversity between and within CPXV clusters (**paper II**), which has also been noted by other researchers. [72,73,75–77,390]. Additionally, we demonstrated that CPXV was a polyphyletic assemblage, and it could be split into 18 sub-species (**paper II**). Earlier studies also suggested the division of CPXV [72,73,75]. Therefore, the reclassification of CPXV should be considered.

Within the OPXV, CPXV has the largest genome, broadest host range and contains almost the full set of OPXV genes [40,84,198,201]. These characteristics have led to the suggestion that a CPXV-like virus was the ancestor of all Old World OPXV (except for AKMV) [40,198,293,307]. However, the evolution of the CPXV as well as OPXV is not clear. In order to understand the evolution of CPXV, in **paper II** we studied the evolutionary history of CPXV based on the concatenated 62 non-recombinant conserved genes. We calculated CPXV substitution rate and the 95% HPD of our estimate overlapped the reported substitution rate of *Chordopoxvirinae* and OPXV [292–295]. The emergence and divergence dates of CPXV could not be accurately estimated; the 95% HPD intervals of the emergence dates were quite broad. We presumed that it could be because of (1) the high heterogeneity of CPXV isolates and (2) the low genetic information due to restricted number of isolates in term of location, age and host. However, these findings might support the proposed idea that lineages of CPXV are highly divergent and a reclassification of CPXV is warranted.

As mentioned above, CPXV-No-H2 is an atypical CPXV isolate that contains an ECTV *atip* gene [70,71]. A previous study of our research group suggested that CPXV-No-H2 could have acquired ECTV-*atip* gene by recombination with ECTV or and ECTV-like virus [71]. In order to characterize recombination in CPXV-No-H2, in **paper I** we sequenced the whole genome of CPXV-No-H2. Our analysis revealed that CPXV-No-H2 had a mosaic genome, containing genomic sequences more similar to North America OPXV (i.e., AKPV) and the Old World OPXV (i.e. ECTV and VACV). CPXV-No-H2 contained nine recombinant regions that may be a result of different recombination events between the parentals of AKPV and CPXV, ECTV and CPXV, and VACV and CPXV. Although two potential recombinant events with the parental AKPV overlapped with two potential recombination events with the parental ECTV. Curiously, AKPV may undergo recombination with ECTV in the same position of those overlapped recombinant regions and ECTV may contain AKPV-like sequences [7]. In addition, AKPV contained three genes (*AKPV-203*, *AKPV-204* and *AKPV-205*) that were most similar to Murmansk genes and they may be introduced from/to Murmansk by recombination [7]. One of the recombinant regions between AKPV and CPXV-No-H2 comprised a gene that was most similar to *AKPV-203* and Murmansk gene. Moreover, the phylogenetic analyses based on three recombinant regions between AKPV and CPXV suggested that AKPV-like sequences were introduced to CPXV-No-H2 rather than the other way (**paper I**).

Since CPXV-No-H2 produced atypical $V^{+/}$ ATI [71], we analysed the genes involved in the formation of ATI (**paper I**). Two of the three genes (*p4c and A27L)* were most similar to CPXV_GerMygEK_938_17 genes and the third gene (*atip*) was in the two overlapping recombinant regions between CPXV and AKPV, and CPXV and ECTV (**paper I**). Compared to CPXV-No-H2, AKMV and CPXV-Ger 2010 produced wild type V^{+} ATI [7,77,184]. On the other hand, ECTV_Hampstead displayed V^{+} and $V^{+/}$ ATI and other ECTV strains produced V^{-} ATI [174,183]. ECTV_Hampstead was the progenitor of the European ECTV outbreaks [391]. The ATI phenotype in CPXV_GerMygEK_938_17 was not reported but we presumed that CPXV_GerMygEK_938_17 produces the wild type V^{+} ATI because its *atip, p4c, and A27L* genes were similar to CPXV_Ger2010_MKY genes (**paper I**).

It is difficult to reconstruct the evolutionary history of CPXV-NoH2 due to the multiple recombination events. The mosaic genome of CPXV-No-H2 could be explained by symplesiomorphy since most recombinant regions were similar to more than one taxon. However, there was one AKPV-like sequence in CPXV-No-H2 that could not be explained by symplesiomorphy because it was only similar to AKPV. A plausible explanation about the origin of the recombinant regions in CPXV-No-H2 is that it was originated from the recombination of CPXV_GerMygEK_938_17-like virus and AKPV-like virus. Probably both viruses could have circulated in populations of rodents in Europe. Even though the isolation of AKPV was Alaska, its ancestor might circulate in Europe because AKPV contained genes similar to those of Russian *Murmansk virus* [7,305]. The recombinant progeny virus, CPXV-No-H2-like virus, could have suffered genomic changes linked to the adaptation to mice, resulting in ECTV-like virus. CPXV-like virus has been proposed as ancestor of ECTV [78]. Thus, these findings suggested that recombination between OPXV in nature is more common than we thought (**paper I**).

In **paper I and II,** we demonstrated that CPXV-No-H2 was a natural recombinant CPXV (**paper I**) and the extensive recombination in OPXV and CPXV (**paper II**). Recombination is not a foreign evolutionary mechanism in poxviruses. It has been demonstrated in different poxvirus species, both *in vivo* [6,7,71,77,302,392] and *in vitro* [326,393–396]. Hazard characterization of MVA vectored vaccines require the evaluation of potential recombination between the vector and naturally circulating OPXV. In our previous study, we performed co-infection and superinfection experiments of semi-permissive Vero cells with MVA-HANP and CPXV-No-F1 and showed that recombination occurred during *in vitro* co-infection and superinfection of Vero cells [133]. In **paper III**, we performed whole genome sequencing of these progeny viruses obtained from confection and superinfection of Vero cells. Our results confirmed the recombination with MVA-HANP and CPXV-No-F1 in cells where MVA poorly multiplies (Vero cells). It demonstrated that the recombination occurred in semi-permissive Vero cells, despite they did not form mature particles [287]. This is not surprising because viral DNA replication is unimpaired in non-permissive cells to MVA infection [119,286]. Therefore, MVA could undergo recombination in semi- and non-permissive cells because poxviral recombination only requires that the linear DNA molecules share 12 bp of homology [325]. On the other hand, the superinfection exclusion did not prevent the superinfection of Vero cells in spite of the superinfection time of 6 hours. It has been reported that 6 hours after primary infection with VACV produced 99% exclusion of superinfecting virus [397].

In **paper III,** the genomic characterization of progeny viruses derived from co-infected and superinfected Vero cells revealed that their genomes were a mosaic of the MVA-HANP and CPXV-No-F1 genomes, except for the progeny virus R9. The distribution of the recombination events in the progeny virus genomes was aleatory (**paper III**). Recombination events took place both in conserved central regions (*F4L - A24R*) and variable terminal regions (**paper III).** Similar observations were also made in the natural recombinant CPXV-No-H2 (**paper I**). However, it has been reported that the recombination events in OPXV are more common in the terminal genomic region than the central region [6,7,77,84,199,300]. Interestingly, there was a genomic

region (*CPXV-Br010* to *CPXV-Br043* gene) in the recombinant progeny viruses where recombination events did not occur (**paper III**). Although two recombinant viruses had suffered a large deletion in this region, from *CPXV-Br016* to *CPXV-Br029* gene (**paper III**).

The proportion of the parental genomes in the progeny virus genomes was not uniform. Most recombinant viruses comprised more CDS from CPXV-No-F1 (**paper III**). This could be because Vero cells were permissive to CPXV-No-F1 infection and the selection of progeny viruses based on visible plaques in Vero cells also biased selection in favor of viruses with more CPXV genomes since CPXV forms plaques in Vero while MVA/MVA-HANP does not. To gain a comprehensive understanding of recombination between MVA vector and naturally circulating CPXV, the limitations of culture-based selection can be overcome by metagenomic sequencing of co-infected and superinfected cells.

Various progeny viruses displayed plaque phenotypes distinct to that of parental viruses and some of them expressed the *HA* transgene (**paper III)**. Similar findings were observed in the progeny viruses from co-infected BHK-21 cells and superinfected Vero cells (using 2 hours) [133,326]. Our progeny viruses produced different plaques phenotypes, such as non-lytic plaques with comet formation (**paper III)**. The plaque morphology of the progeny viruses was affected by the presence or absence of genes involved in the syncytium and plaque formation (*F5L, F11L, F12L, F13L, A33R, A34R,* A36R, *A56R, B5R* and *K2L* genes) [250,252,253,259,262,263,398–401]. Some of these genes were fragmented (e.g. *F5L* and *F11L* gene) or have suffered small internal deletions (e.g. *A36R*) in MVA [120]. For instance, a recombinant progeny virus contained the *F5L, F11L, A36R, A33R, A34R* and *B5R* genes from MVA-HANP and formed small and non-lytic plaques with comet formation (**paper III)**.

Within the progeny viruses, there was a non-recombinant that formed plaques with syncytium formation. The genomic analysis revealed that its *K2L* gene had one non-synonymous single-nucleotide mutation (nsSNM) that caused the truncation of the gene (**paper III)**. It has been reported that the lack of the *K2L* gene caused the fusion of infected cells [251–253]. Besides nsSNMs, other genetic mutations such as deletion were detected in the progeny viruses. A large deletion (~16 kbp) was found in two recombinant viruses from superinfected Vero cells (**paper III)**.

A partial deletion of double expression cassette (harbouring both influenza virus *HA* and *NP* transgenes) was detected in the parental MVA-HANP as well as in one recombinant progeny virus (**paper III**). The instability of the *HA* transgene has been also observed in MVA-HANP and in recombinant progeny viruses from co-infected BHK-21 cells [327]. Other studies also showed the transgene instability in recombinant MVA vectors [335–338]. In MVA-HANP, the transgene was inserted in the hybrid genes A51/56, where MVA has suffered a deletion (deletion III) (**paper III**). One study compared the stability of the transgene inserted in different regions of the MVA genome (including deletion II, deletion III, the *CP77* gene locus and the *I8R-G1L* intergenic region) after 35 passages and showed that transgene was most stable in the intergenic region compared to the other regions (including deletion III) [402].

We observed that the recombinant progeny viruses, with more DNA derived from MVA (>50%), rescued some deleted and/or fragmented genes from CPXV, including host range genes (**paper III**). One of the main concerns about the recombination of MVA vectored vaccine with a multiplication competent OPXV is the rescue of missing or fragmented host range genes in MVA and, hence, restoring the wild-type phenotype [133,322]. Another concern is the transfer of the transgene from OPXV vectored vaccine into a multiplication competent OPXV [133,322]. Our data showed that the recombinant viruses with a genome more similar to CPXV-No-F1 contained the transgenic cassette from MVA-HANP (**paper III**).

The recombination of a wild type OPXV and a poxvirus vaccine has been reported [328]. A Russian recombinant virus showed evidence of 27 recombinant events. Their possible parentals were a field LSDV strain and an LSD vaccine [328]. In following LSDV outbreaks only vaccine-like LSDV strains have been detected instead of the wild type LSDV strains [329,330]. However, some researchers suggested the recombinant viruses could be a result of spillover from vaccinated animals [331] .

7. CONCLUSION AND FUTURE PERSPECTIVES

We have shown that recombination is a common evolutionary mechanism that occurred between OPXV in nature. CPXV-No-H2 was an example of a natural occurring CPXV that might have undergone several recombination events between different OPXV species isolated from different continents. Furthermore, CPXV, which is the potential candidate for recombination with MVA vectored vaccine, had a high genetic diversity and was an assemblage of several sub-species. Among CPXV strains, three CPXV strains (including CPXV-No-H2) were closely related to ECTV and Abatino and formed a new, distinct CPXV clade named "ECTV-Abatino-like CPXV". With the current genetic information of CPXV strains the evolutionary history of CPXV could not be elucidated. We demonstrated that progeny viruses obtained from co-infection and superinfection *in vitro* of semi-permissive Vero cells with MVA-HANP and CPXV-No-F1 displayed novel biological and genetic characteristics. Furthermore, the rescue of deleted or fragmented MVA genes in recombinant progeny viruses was possible as well the transfer of the transgene to CPXV. Overall, our findings provide relevant data for the hazard characterization of MVA vectored vaccines and, hence, improving the biosafety of MVA vectored vaccines.

The diversity and evolution of CPXV as well as the recombination between OPXV are still not completely elucidated. The diversity of CPXV has awoken debates about the reclassification of CPXV. However, for the re-classification of CPXV, the biological characterization of the CPXV strains is also required. Together, the genetic and biological characterization would provide a better understanding of diversity of CPXV as well as the evolution of CPXV and OPXV. In order to understand the evolution of CPXV, it is necessary to increase surveillance of OPXV (including CPXV) in different species and regions and acquire ancient CPXV strains. The recombination studies reported in this thesis were under *in vitro* conditions, which could differ from *in vivo* conditions. Thus, future studies should examine recombination *in vivo* particularly in immunocompetent and immunocompromised animal models.

8. REFERENCES

1. Moss, B. Poxviridae. in *Fields virology* (eds. Knipe, D. & Howley, P.) 2129–2159 (Lippincott Williams & Wilkins (LWW), 2013).

2. Diven, D. G. An overview of poxviruses. *Journal of the American Academy of Dermatology* **44**, (2001).

3. Silva, N. I. O., de Oliveira, J. S., Kroon, E. G., Trindade, G. de S. & Drumond, B. P. Here, There, and Everywhere: The Wide Host Range and Geographic Distribution of Zoonotic Orthopoxviruses. *Viruses* **13**, (2021).

4. Smithson, C. *et al.* The genomes of three North American orthopoxviruses. *Virus Genes* **53**, 21–34 (2017).

5. Cardeti, G. *et al.* Fatal Outbreak in Tonkean Macaques Caused by Possibly Novel Orthopoxvirus, Italy, January 2015 - Volume 23, Number 12—December 2017 - Emerging Infectious Diseases journal - CDC. *Emerg. Infect. Dis.* **23**, 1941–1949 (2017).

6. Gao, J. *et al.* Genome sequences of Akhmeta virus, an early divergent old world orthopoxvirus. *Viruses* **10**, (2018).

7. Gigante, C. M. *et al.* Genome of Alaskapox Virus, a Novel Orthopoxvirus Isolated from Alaska. *Viruses* **11**, (2019).

8. McFadden, G. Poxvirus tropism. *Nature Reviews Microbiology* **3**, (2005).

9. Behbehani, A. M. The smallpox story: Life and death of an old disease. *Microbiological Reviews* **47**, (1983).

10. Fenner, F., Henderson, D., Arita, I., Jezek, Z. & Ladnyi, D. *Smallpox and its eradication*. (WHO, 1988).

11. Berche, P. Life and death of smallpox. *Press. Medicale* **51**, 104117 (2022).

12. Moore, J. C. *The history of the small pox*. (1815).

13. Farhi, D. & Dupin, N. Origins of syphilis and management in the immunocompetent patient: Facts and controversies. *Clin. Dermatol.* **28**, (2010).

14. Hopkins, D. Ramses V: earliest know victim? 22–26 (1980).

15. Ellner, P. D. Smallpox: Gone but not forgotten. *Infection* **26**, (1998).

16. Deria, A., Jezek, Z., Markvart, K., Carrasco, P. & Weisfeld, J. The world's last endemic case of smallpox: surveillance and containment measures. *Bull. World Health Organ.* **58**, 279 (1980).

17. WHO. *The global eradication of smallpox : final report of the Global Commission for the Certification of Smallpox Eradication, Geneva, December 1979*. (1980).

18. Shchelkunova, G. A. & Shchelkunov, S. N. 40 Years without Smallpox. *Acta Naturae* **9**, (2017).

19. WHO. *A74/43 - Report by the Director-General - Smallpox eradication*. (2021).

20. Barquet, N. & Domingo, P. Smallpox: The triumph over the most terrible of the ministers of death. *Ann. Intern. Med.* **127**, (1997).

21. Jenner, E. The Three Original Publications On Vaccination Against Smallpox. in *The Harvard Classics, Vol. XXXVIII, Part 4* (1909).

22. Jenner, E. An inquiry into the causes and effects of the variolae vaccinae: a disease discovered in some of the western counties of England, particularly Gloucestershire, and known by the name of the cow pox. *Springf. [Mass.] Re-printed Dr. Samuel Cool. by Ashley Brew. 1802* 134 (1802).

23. Willis, N. J. Edward Jenner and the eradication of smallpox. *Scottish Medical Journal* **42**, (1997).

24. Tuells, J. Vaccinology: The name, the concept, the adjectives. *Vaccine* **30**, (2012).

25. Pearson, G. *An Examination of the Report of the Committee of the House of Commons on the Claims of Remuneration for the Vaccine Pock Inoculation*. (1802).

26. Esparza, J., Schrick, L., Damaso, C. R. & Nitsche, A. Equination (inoculation of horsepox): An early alternative to vaccination (inoculation of cowpox) and the potential role of horsepox virus in the origin of the smallpox vaccine. *Vaccine* **35**, 7222–7230 (2017).

27. Damaso, C. R. Revisiting Jenner's mysteries, the role of the Beaugency lymph in the evolutionary path of ancient smallpox vaccines. *The Lancet Infectious Diseases* **18**, (2018).

28. Brinkmann, A., Souza, A. R. V., Esparza, J., Nitsche, A. & Damaso, C. R. Re-assembly of nineteenth-century smallpox vaccine genomes reveals the contemporaneous use of horsepox and horsepox-related viruses in the USA. *Genome Biology* **21**, (2020).

29. Pead, P. J. Benjamin Jesty: New light in the dawn of vaccination. *Lancet* **362**, (2003).

30. Hammarsten, J. F., Tattersall, W. & Hammarsten, J. E. Who discovered smallpox vaccination? Edward Jenner or Benjamin Jesty? *Transactions of the American Clinical and Climatological Association* **Vol. 90**, (1978).

31. Chantrey, J. *et al.* Cowpox: reservoir hosts and geographic range. *Epidemiol. Infect.* **122**, 455 (1999).

32. Wolfs, T. F. W., Wagenaar, J. A., Niesters, H. G. M. & Osterhaus, A. D. M. E. Rat-to-Human Transmission of Cowpox Infection. *Emerg. Infect. Dis.* **8**, 1495 (2002).

33. Laakkonen, J. *et al.* Serological Survey for Viral Pathogens in Turkish Rodents. *J. Wildl. Dis.* **42**, 672–676 (2006).

34. Vorou, R. M., Papavassiliou, V. G. & Pierroutsakos, I. N. Cowpox virus infection: An emerging health threat. *Curr. Opin. Infect. Dis.* **21**, 153–156 (2008).

35. Popova, A. Y. *et al.* Cowpox in a human, Russia, 2015. *Epidemiol. Infect.* **145**, 755–759 (2017).

36. Diaz, J. H. The Disease Ecology, Epidemiology, Clinical Manifestations, Management, Prevention, and Control of Increasing Human Infections with Animal Orthopoxviruses. *Wilderness Environ. Med.* **32**, 528–536 (2021).

37. Ferrier, A. *et al.* Fatal cowpox virus infection in human fetus, france, 2017. *Emerg. Infect. Dis.*

27, 2570–2577 (2021).

38. Oliveira, G. P., Rodrigues, R. A. L., Lima, M. T., Drumond, B. P. & Abrahão, J. S. Poxvirus Host Range Genes and Virus–Host Spectrum: A Critical Review. *Viruses 2017, Vol. 9, Page 331* **9**, 331 (2017).

39. Bratke, K. A., McLysaght, A. & Rothenburg, S. A survey of host range genes in poxvirus genomes. *Infect. Genet. Evol.* **14**, 406–425 (2013).

40. Shchelkunov, S. N. *et al.* The genomic sequence analysis of the left and right species-specific terminal region of a cowpox virus strain reveals unique sequences and a cluster of intact ORFs for immunomodulatory and host range proteins. *Virology* **243**, 432–460 (1998).

41. Kinnunen, P. M. *et al.* Orthopox Virus Infections in Eurasian Wild Rodents. *https://home.liebertpub.com/vbz* **11**, 1133–1140 (2011).

42. Prkno, A. *et al.* Epidemiological investigations of four cowpox virus outbreaks in alpaca herds, Germany. *Viruses* **9**, 1–15 (2017).

43. Girling, S. J., Pizzi, R., Cox, A. & Beard, P. M. Fatal cowpox virus infection in two squirrel monkeys (Saimiri sciureus). *Vet. Rec.* **169**, 156–156 (2011).

44. Smith, K. C., Bennett, M. & Garrett, D. C. Skin lesions caused by orthopoxvirus infection in a dog. *J. Small Anim. Pract.* **40**, 495–497 (1999).

45. Tryland, M., Myrmel, H., Holtet, L., Haukenes, G. & Traavik, T. Clinical cowpox cases in Norway. *Scand. J. Infect. Dis.* **30**, 301–303 (1998).

46. Martina, B. E. E. *et al.* Cowpox Virus Transmission from Rats to Monkeys, the Netherlands. *Emerg. Infect. Dis.* **12**, 1005 (2006).

47. Essbauer, S., Pfeffer, M. & Meyer, H. Zoonotic poxviruses. *Vet. Microbiol.* **140**, 229–236 (2010).

48. Carletti, F. *et al.* Cat-to-human orthopoxvirus transmission, northeastern Italy. *Emerging Infectious Diseases* **15**, (2009).

49. Świtaj, K., Kajfasz, P., Kurth, A. & Nitsche, A. Cowpox after a cat scratch – case report from Poland. *Ann. Agric. Environ. Med.* **22**, (2015).

50. Hemmer, C. J. *et al.* Human cowpox virus infection acquired from a circus elephant in Germany. *Int. J. Infect. Dis.* **14**, (2010).

51. Kurth, A. *et al.* Cowpox virus outbreak in banded mongooses (mungos mungo) and jaguarundis (Herpailurus yagouaroundi) with a time-delayed infection to humans. *PLoS One* **4**, (2009).

52. Elsendoorn, A. *et al.* Severe ear chondritis due to cowpox virus transmitted by a pet rat. *J. Infect.* **63**, (2011).

53. Hobi, S. *et al.* Neurogenic inflammation and colliquative lymphadenitis with persistent orthopox virus DNA detection in a human case of cowpox virus infection transmitted by a domestic cat. *Br. J. Dermatol.* **173**, (2015).

54. Kurth, A. *et al.* Rat-to-Elephant-to-Human Transmission of Cowpox Virus. *Emerg. Infect. Dis.* **14**, 670 (2008).

55. Vogel, S. *et al.* The Munich outbreak of cutaneous cowpox infection: Transmission by infected pet rats. *Acta Derm. Venereol.* **92**, (2012).

56. Becker, C. *et al.* Cowpox Virus Infection in Pet Rat Owners: Not Always Immediately Recognized. *Dtsch. Arztebl. Int.* **106**, 329 (2009).

57. Ducournau, C. *et al.* Concomitant human infections with 2 cowpox virus strains in related cases, France, 2011. *Emerg. Infect. Dis.* **19**, (2013).

58. Favier, A. L. *et al.* Necrotic ulcerated lesion in a young boy caused by cowpox virus infection. *Case Rep. Dermatol.* **3**, (2011).

59. Bonnekoh, B. *et al.* Cowpox infection transmitted from a domestic cat. *JDDG* **6**, (2008).

60. Lawn, R. Risk of cowpox to small animal practitioners. *Veterinary Record* **166**, (2010).

61. Fassbender, P. *et al.* Generalized cowpox virus infection in a patient with HIV, Germany, 2012. *Emerging Infectious Diseases* **22**, (2016).

62. Gazzani, P. *et al.* Fatal disseminated cowpox virus infection in an adolescent renal transplant recipient. *Pediatr. Nephrol.* **32**, (2017).

63. Eis-Hubinger, A. M. *et al.* Fatal cowpox-like virus infection transmitted by cat. *The Lancet* **336**, (1990).

64. Willemse, A. & Egberink, H. F. Transmission of cowpox virus infection from domestic cat to man. *Lancet (London, England)* **1**, 1515 (1985).

65. Wendt, R. *et al.* Generalized cowpox virus infection in an immunosuppressed patient. *International Journal of Infectious Diseases* **106**, (2021).

66. Stagegaard, J. *et al.* Seasonal recurrence of cowpox virus outbreaks in captive cheetahs (Acinonyx jubatus). *PLoS One* **12**, (2017).

67. Antwerpen, M. H. *et al.* Use of next generation sequencing to study two cowpox virus outbreaks. *PeerJ* **2019**, 1–17 (2019).

68. Tryland, M. *et al.* Characteristics of four cowpox virus isolates from Norway and Sweden. *APMIS* **106**, 623–635 (1998).

69. Cronqvist, J., Ekdahl, K., Kjartansdottir, A., Bauer, B. & Klinker, M. [Cowpox--a cat disease in man] . *Lakartidningen* **88**, 2605–2606 (1991).

70. Hansen, H., Okeke, M. I., Nilssen, Ø. & Traavik, T. Comparison and phylogenetic analysis of cowpox viruses isolated from cats and humans in Fennoscandia. *Arch. Virol.* **154**, 1293–1302 (2009).

71. Okeke, M. I., Hansen, H. & Traavik, T. A naturally occurring cowpox virus with an ectromelia virus A-type inclusion protein gene displays atypical A-type inclusions. *Infect. Genet. Evol.* **12**, 160–168 (2012).

72. Okeke, M. I. *et al.* Molecular characterization and phylogenetics of Fennoscandian cowpox virus isolates based on the p4c and atip genes. *Virol. J.* **11**, 1–16 (2014).

73. Mauldin, M. R. *et al.* Cowpox virus: What's in a Name? *Viruses 2017, Vol. 9, Page 101* **9**, 101 (2017).

74. Bruneau, R. C., Tazi, L. & Rothenburg, S. Cowpox Viruses : A Zoo Full of Viral Diversity and Lurking Threats. (2023).

75. Carroll, D. S. *et al.* Chasing Jenner's vaccine: Revisiting Cowpox virus classification. *PLoS One* **6**, 4–9 (2011).

76. Dabrowski, P. W., Radonić, A., Kurth, A. & Nitsche, A. Genome-wide comparison of cowpox viruses reveals a new clade related to variola virus. *PLoS One* **8**, 1–9 (2013).

77. Franke, A. *et al.* Classification of cowpox viruses into several distinct clades and identification of a novel lineage. *Viruses* **9**, 1–14 (2017).

78. Jeske, K. *et al.* Molecular Detection and Characterization of the First Cowpox Virus Isolate Derived from a Bank Vole. *Viruses* **11**, (2019).

79. Downie, A. W. A study of the lesions produced experimentally by cowpox virus. *J. Pathol. Bacteriol.* **48**, (1939).

80. Pilaski, J. & Rösen-Wolff, A. Poxvirus Infection in Zoo-Kept Mammals. in (1988). doi:10.1007/978-1-4613-2091-3_5

81. Zwart, P., Gispen, R. & Peters, J. C. Cowpox in okapis Okapia johnstoni at Rotterdam zoo. *Br. Vet. J.* **127**, (1971).

82. Baxby, D. Laboratory Characteristics of British and Dutch Strains of Cowpox Virus. *Zentralblatt für Veterinärmedizin R. B* **22**, (1975).

83. Marennikova, S. S., Maltseva, N. N., Korneeva, V. I. & Garanina, N. M. Outbreak of pox disease among carnivora (Felidae) and edentata. *J. Infect. Dis.* **135**, (1977).

84. Gubser, C., Hué, S., Kellam, P. & Smith, G. L. Poxvirus genomes: A phylogenetic analysis. *J. Gen. Virol.* **85**, 105–117 (2004).

85. Molteni, C., Forni, D., Cagliani, R., Clerici, M. & Sironi, M. Genetic ancestry and population structure of vaccinia virus. *npj Vaccines* **7**, (2022).

86. Esparza, J. & Damaso, C. R. Searching for the origin of the smallpox vaccine: Edward Jenner and his little-known horsepox hypothesis. *Vaccine* **40**, (2022).

87. Singh, R. K., Balamurugan, V., Bhanuprakash, V., Venkatesan, G. & Hosamani, M. Emergence and reemergence of vaccinia-like viruses: Global scenario and perspectives. *Indian Journal of Virology* **23**, (2012).

88. de Oliveira, J. S. *et al.* Vaccinia virus natural infections in Brazil: The good, the bad, and the ugly. *Viruses* **9**, (2017).

89. Eltom, K. H., Samy, A. M., Wahed, A. A. El & Czerny, C. P. Buffalopox virus: An emerging virus in livestock and humans. *Pathogens* **9**, (2020).

90. Miranda, J. B. *et al.* Serologic and Molecular Evidence of Vaccinia Virus Circulation among Small Mammals from Different Biomes, Brazil. *Emerg. Infect. Dis.* **23**, 931 (2017).

91. Baxby, D. & Hill, B. J. Characteristics of a new poxvirus isolated from indian buffaloes. *Arch. Gesamte Virusforsch.* **35**, (1971).

92. Lima, M. T. *et al.* An update on the known host range of the brazilian vaccinia virus: An

outbreak in Buffalo Calves. *Front. Microbiol.* **10**, (2019).

93. Roy, P. & Chandramohan, A. Buffalopox Disease in Livestock and Milkers, India. *Emerg. Infect. Dis.* **27**, (2021).

94. MacNeill, A. L. Comparative Pathology of Zoonotic Orthopoxviruses. *Pathogens* **11**, 1–22 (2022).

95. Zafar, A. *et al.* Nosocomial Buffalopoxvirus Infection, Karachi, Pakistan. *Emerg. Infect. Dis.* **13**, 904 (2007).

96. Singh, R. K. *et al.* An outbreak of buffalopox in buffalo (Bubalus bubalis) dairy herds in Aurangabad, India. *OIE Rev. Sci. Tech.* **25**, (2006).

97. Franco-Luiz, A. P. M. *et al.* Spread of vaccinia virus to cattle herds, Argentina, 2011. *Emerging Infectious Diseases* **20**, (2014).

98. Usme-Ciro, J. A. *et al.* Detection and molecular characterization of zoonotic poxviruses circulating in the amazon region of Colombia, 2014. *Emerg. Infect. Dis.* **23**, (2017).

99. Medaglia, M. L. G., Pessoa, L. C. G. D., Sales, E. R. C., Freitas, T. R. P. & Damaso, C. R. Spread of Cantagalo virus to northern Brazil. *Emerging Infectious Diseases* **15**, (2009).

100. Trindade, G. S. *et al.* Belo Horizonte virus: A vaccinia-like virus lacking the A-type inclusion body gene isolated from infected mice. *J. Gen. Virol.* **85**, (2004).

101. Brum, M. C. S. *et al.* An outbreak of orthopoxvirus-associated disease in horses in southern Brazil. *J. Vet. Diagnostic Investig.* **22**, (2010).

102. Abrahão, J. S. *et al.* Vaccinia virus infection in monkeys, Brazilian Amazon. *Emerg. Infect. Dis.* **16**, (2010).

103. Damaso, C. R. A., Esposito, J. J., Condit, R. C. & Moussatché, N. An emergent poxvirus from humans and cattle in Rio de Janeiro state: Cantagalo virus may derive from brazilian smallpox vaccine. *Virology* **277**, (2000).

104. Bhanuprakash, V. *et al.* Zoonotic infections of buffalopox in India. *Zoonoses Public Health* **57**, (2010).

105. Laiton-Donato, K. *et al.* Progressive vaccinia acquired through zoonotic transmission in a patient with HIV/AIDS, Colombia. *Emerg. Infect. Dis.* **26**, (2020).

106. Oliveira, G. P. *et al.* Short report: Intrafamilial transmission of Vaccinia virus during a bovine vaccinia outbreak in Brazil: A new insight in viral transmission chain. *Am. J. Trop. Med. Hyg.* **90**, (2014).

107. Batista, V. H., Scremin, J., Aguiar, L. M. & Schatzmayr, H. G. VULVAR INFECTION AND POSSIBLE HUMAN-TO-HUMAN TRANSMISSION OF BOVINE POXVIRUS DISEASE. *VIRUS Rev. Res.* **14**, (2009).

108. Jacobs, B. L. *et al.* Vaccinia Virus Vaccines: Past, Present and Future. *Antiviral Res.* **84**, 1 (2009).

109. Sánchez-Sampedro, L. *et al.* The evolution of poxvirus vaccines. *Viruses* **7**, (2015).

110. Rosenthal, S. R., Merchlinsky, M., Kleppinger, C. & Goldenthal, K. L. Developing new

smallpox vaccines. *Emerg. Infect. Dis.* **7**, 920–926 (2001).

111. Qin, L., Liang, M. & Evans, D. H. Genomic analysis of vaccinia virus strain TianTan provides new insights into the evolution and evolutionary relationships between Orthopoxviruses. *Virology* **442**, (2013).

112. Belongia, E. A. & Naleway, A. L. Smallpox vaccine: the good, the bad, and the ugly. *Clinical medicine & research* **1**, (2003).

113. Kenner, J., Cameron, F., Empig, C., Jobes, D. V. & Gurwith, M. LC16m8: An attenuated smallpox vaccine. *Vaccine* **24**, 7009–7022 (2006).

114. Mayr, A., Stickl, H., Müller, H. K., Danner, K. & Singer, H. [The smallpox vaccination strain MVA: marker, genetic structure, experience gained with the parenteral vaccination and behavior in organisms with a debilitated defence mechanism (author's transl)]. *Zentralbl. Bakteriol. B.* **167**, (1978).

115. Tartaglia, J. *et al.* NYVAC: a highly attenuated strain of vaccinia virus. *Virology* **188**, 217–232 (1992).

116. Paran, N. & Sutter, G. Smallpox vaccines: New formulations and revised strategies for vaccination. *Human vaccines* **5**, (2009).

117. Kennedy, R. B., Ovsyannikova, I. & Poland, G. A. Smallpox vaccines for biodefense. *Vaccine* **27**, (2009).

118. Smith, G. L. & Moss, B. Infectious poxvirus vectors have capacity for at least 25 000 base pairs of foreign DNA. *Gene* **25**, (1983).

119. Volz, A. & Sutter, G. Modified Vaccinia Virus Ankara: History, Value in Basic Research, and Current Perspectives for Vaccine Development. in *Advances in Virus Research* **97**, (2017).

120. Antoine, G., Scheiflinger, F., Dorner, F. & Falkner, F. G. The complete genomic sequence of the modified vaccinia Ankara strain: Comparison with other orthopoxviruses. *Virology* **244**, (1998).

121. Meyer, H., Sutter, G. & Mayr, A. Mapping of deletions in the genome of the highly attenuated vaccinia virus MVA and their influence on virulence. *J. Gen. Virol.* **72**, (1991).

122. Meisinger-Henschel, C. *et al.* Genomic sequence of chorioallantois vaccinia virus Ankara, the ancestor of modified vaccinia virus Ankara. *J. Gen. Virol.* **88**, 3249–3259 (2007).

123. Blanchard, T. J., Alcamí, A., Andrea, P. & Smith, G. L. Modified vaccinia virus Ankara undergoes limited replication in human cells and lacks several immunomodulatory proteins: Implications for use as a human vaccine. *J. Gen. Virol.* **79**, (1998).

124. Carroll, M. W. & Moss, B. Host range and cytopathogenicity of the highly attenuated MVA strain of vaccinia virus: Propagation and generation of recombinant viruses in a nonhuman mammalian cell line. *Virology* **238**, (1997).

125. Hornemann, S. *et al.* Replication of Modified Vaccinia Virus Ankara in Primary Chicken Embryo Fibroblasts Requires Expression of the Interferon Resistance Gene E3L. *J. Virol.* **77**, (2003).

126. Pittman, P. R. *et al.* Phase 3 Efficacy Trial of Modified Vaccinia Ankara as a Vaccine against Smallpox. *N. Engl. J. Med.* **381**, (2019).

127. Mayr, A. Smallpox vaccination and bioterrorism with pox viruses. *Comp. Immunol. Microbiol. Infect. Dis.* **26**, (2003).

128. Mahnel, H. & Mayr, A. Experiences with immunization against orthopox viruses of humans and animals using vaccine strain MVA. *Berl. Munch. Tierarztl. Wochenschr.* **107**, (1994).

129. European Medicines Agency. EMA recommends approval of Imvanex for the prevention of monkeypox disease. (2022). Available at: https://www.ema.europa.eu/en/news/ema-recommends-approval-imvanex-prevention-monkeypox-disease. (Accessed: 1st January 2023)

130. U.S. Food and Drugs. Vaccines Licensed for Use in the United States. (2022). Available at: https://www.fda.gov/vaccines-blood-biologics/vaccines/vaccines-licensed-use-united-states.

131. Chopra, H. *et al.* FDA approved vaccines for monkeypox: Current eminence. *Int. J. Surg.* **105**, (2022).

132. Suter, M. *et al.* Modified vaccinia Ankara strains with identical coding sequences actually represent complex mixtures of viruses that determine the biological properties of each strain. *Vaccine* **27**, (2009).

133. Okeke, M. I. *et al.* Hazard characterization of modified vaccinia virus ankara vector: What are the knowledge gaps? *Viruses* **9**, (2017).

134. Orlova, O. V., Glazkova, D. V., Bogoslovskaya, E. V., Shipulin, G. A. & Yudin, S. M. Development of Modified Vaccinia Virus Ankara-Based Vaccines: Advantages and Applications. *Vaccines* **10**, (2022).

135. Joachim, A. *et al.* Potent functional antibody responses elicited by HIV-I DNA priming and boosting with heterologous HIV-1 recombinant MVA in healthy tanzanian adults. *PLoS One* **10**, (2015).

136. Nilsson, C. *et al.* Broad and potent cellular and humoral immune responses after a second late HIV-modified vaccinia virus ankara vaccination in HIV-DNA-primed and HIV-modified vaccinia virus ankara-boosted swedish vaccinees. *AIDS Res. Hum. Retroviruses* **30**, (2014).

137. Milligan, I. D. *et al.* Safety and immunogenicity of novel adenovirus type 26-and modified vaccinia Ankara-vectored Ebola vaccines: A randomized clinical trial. *JAMA - J. Am. Med. Assoc.* **315**, (2016).

138. Tapia, M. D. *et al.* Use of ChAd3-EBO-Z Ebola virus vaccine in Malian and US adults, and boosting of Malian adults with MVA-BN-Filo: a phase 1, single-blind, randomised trial, a phase 1b, open-label and double-blind, dose-escalation trial, and a nested, randomised, double-blind, placebo-controlled trial. *Lancet Infect. Dis.* **16**, (2016).

139. Callendret, B. *et al.* A prophylactic multivalent vaccine against different filovirus species is immunogenic and provides protection from lethal infections with Ebolavirus and Marburgvirus species in non-human primates. *PLoS One* **13**, (2018).

140. Fuentes, S., Ravichandran, S., Coyle, E. M., Klenow, L. & Khurana, S. Human Antibody Repertoire following Ebola Virus Infection and Vaccination. *iScience* **23**, (2020).

141. Jordan, E. *et al.* Broad Antibody and Cellular Immune Response from a Phase 2 Clinical Trial with a Novel Multivalent Poxvirus-Based Respiratory Syncytial Virus Vaccine. *J. Infect. Dis.* **223**, (2021).

142. Koch, T. *et al.* Safety and immunogenicity of a modified vaccinia virus Ankara vector vaccine

candidate for Middle East respiratory syndrome: an open-label, phase 1 trial. *Lancet Infect. Dis.* **20**, (2020).

143. Aldoss, I. *et al.* Poxvirus vectored cytomegalovirus vaccine to prevent cytomegalovirus viremia in transplant recipients: A phase 2, randomized clinical trial. *Ann. Intern. Med.* **172**, (2020).

144. Kreijtz, J. H. C. M. *et al.* Safety and immunogenicity of a modified-vaccinia-virus-Ankara-based influenza A H5N1 vaccine: A randomised, double-blind phase 1/2a clinical trial. *Lancet Infect. Dis.* **14**, (2014).

145. Puksuriwong, S. *et al.* Modified vaccinia Ankara-vectored vaccine expressing nucleoprotein and matrix protein 1 (M1) activates mucosal M1-specific T-Cell immunity and tissue-resident memory T Cells in human nasopharynx-associated lymphoid tissue. *J. Infect. Dis.* **222**, (2020).

146. Tameris, M. D. *et al.* Safety and efficacy of MVA85A, a new tuberculosis vaccine, in infants previously vaccinated with BCG: A randomised, placebo-controlled phase 2b trial. *Lancet* **381**, (2013).

147. Hodgson, S. H. *et al.* Evaluation of the efficacy of ChAd63-MVA vectored vaccines expressing circumsporozoite protein and ME-TRAP against controlled human malaria infection in malaria-naive individuals. in *Journal of Infectious Diseases* **211**, (2015).

148. Biswas, S. *et al.* Assessment of humoral immune responses to blood-stage malaria antigens following ChAd63-MVA immunization, controlled human malaria infection and natural exposure. *PLoS One* **9**, (2014).

149. Sebastian, S. & Gilbert, S. C. Recombinant modified vaccinia virus Ankara-based malaria vaccines. *Expert Review of Vaccines* **15**, (2016).

150. Sah, R. *et al.* Monkeypox deaths in 2022 outbreak across the globe : correspondence. *Ann. Med. Surg.* **85(1)**, 57–58 (2023).

151. Beer, E. M. & Bhargavi Rao, V. A systematic review of the epidemiology of human monkeypox outbreaks and implications for outbreak strategy. *PLoS Negl. Trop. Dis.* **13**, e0007791 (2019).

152. Mbala, P. K. *et al.* Maternal and Fetal Outcomes among Pregnant Women with Human Monkeypox Infection in the Democratic Republic of Congo. *J. Infect. Dis.* **216**, (2017).

153. Alakunle, E. & Okeke, M. Monkeypox virus: a neglected zoonotic pathogen spreads globally. *Nat. Rev. Microbiol.* **20**, 507–508 (2022).

154. Damon, I. K. Status of human monkeypox: Clinical disease, epidemiology and research. *Vaccine* **29**, (2011).

155. Kmiec, D. & Kirchhoff, F. Monkeypox: A New Threat? *Int. J. Mol. Sci.* **23**, (2022).

156. WHO. Disease Outbreak News; Multi-country monkeypox outbreak in non-endemic countries. (2022). Available at: https://www.who.int/emergencies/disease-outbreak-news/item/2022-DON385. (Accessed: 20th June 2022)

157. Happi, C. *et al.* Urgent need for a non-discriminatory and non-stigmatizing nomenclature for monkeypox virus. *PLoS Biol.* **20**, 1–6 (2022).

158. Bunge, E. M. *et al.* The changing epidemiology of human monkeypox—A potential threat? A

systematic review. *PLoS Negl. Trop. Dis.* **16**, (2022).

159. Magnus, P. von, Andersen, E. K., Petersen, K. B. & Birch-Andersen, A. A POX-LIKE DISEASE IN CYNOMOLGUS MONKEYS. *Acta Pathol. Microbiol. Scand.* **46**, (1959).

160. Alakunle, E., Moens, U., Nchinda, G. & Okeke, M. I. Monkeypox Virus in Nigeria: Infection Biology, Epidemiology, and Evolution. *Viruses* **12**, (2020).

161. Ladnyj, I. D., Ziegler, P. & Kima, E. A human infection caused by monkeypox virus in Basankusu Territory, Democratic Republic of the Congo. *Bull. World Health Organ.* **46**, (1972).

162. Lourie, B. *et al.* Human infection with monkeypox virus: laboratory investigation of six cases in West Africa. *Bull. World Health Organ.* **46**, (1972).

163. Yinka-Ogunleye, A. *et al.* Reemergence of human monkeypox in Nigeria, 2017. *Emerging Infectious Diseases* **24**, (2018).

164. Erez, N. *et al.* Diagnosis of Imported Monkeypox, Israel, 2018. *Emerg. Infect. Dis.* **25**, 980 (2019).

165. Ng, O. T. *et al.* A case of imported Monkeypox in Singapore. *Lancet. Infect. Dis.* **19**, 1166 (2019).

166. Rao, A. K. *et al.* Monkeypox in a Traveler Returning from Nigeria — Dallas, Texas, July 2021. *Morb. Mortal. Wkly. Rep.* **71**, 509 (2022).

167. Vaughan, A. *et al.* Two cases of monkeypox imported to the United Kingdom, September 2018. *Eurosurveillance* **23**, (2018).

168. CDC. Multistate Outbreak of Monkeypox— Illinois, Indiana, and Wisconsin, 2003. *JAMA* **290(1)**, 30–31 (2003).

169. Petersen, E. *et al.* Human Monkeypox: Epidemiologic and Clinical Characteristics, Diagnosis, and Prevention. *Infectious Disease Clinics of North America* **33**, (2019).

170. WHO. Disease Outbreak News; Monkeypox– United Kingdom of Great Britain and Northern Ireland. (2022).

171. WHO. 2022-23 Mpox Outbreak: Global Trends. (2023). Available at: https://worldhealthorg.shinyapps.io/mpx_global/.

172. Buller, R. M. Mousepox: A Small Animal Model for Biodefense Research. *Appl. Biosaf.* **9**, (2004).

173. Marchal, J. Infectious ectromelia. A hitherto undescribed virus disease of mice. *J. Pathol. Bacteriol.* **33**, (1930).

174. Mavian, C., López-Bueno, A., Martín, R., Nitsche, A. & Alcamí, A. Comparative pathogenesis, genomics and phylogeography of mousepox. *Viruses* **13**, 1146 (2021).

175. Mendez-Rios, J. D. *et al.* Genome sequence of erythromelalgia-related poxvirus identifies it as an ectromelia virus strain. *PLoS One* **7**, (2012).

176. Zheng, Z. M., Specter, S., Zhang, J. H., Friedman, H. & Zhu, W. P. Further characterization of the biological and pathogenic properties of erythromelalgia-related poxviruses. *J. Gen. Virol.*

73, (1992).

177. Neubauer, H., Pfeffer, M. & Meyer, H. Specific detection of mousepox virus by polymerase chain reaction. *Lab. Anim.* **31**, (1997).

178. Trentin, J. J. & Briody, B. A. *An outbreak of mouse-pox (infectious ectromelia) in the United States: II. Definitive diagnosis*. *Science* **117**, (1953).

179. Spohr de Faundez, I. *et al.* Electron microscopy, plaque assay and preliminary serological characterization of three ectromelia virus strains isolated in Poland in the period 1986-1988. *Arch. Virol.* **114**, (1990).

180. Lipman, N. S., Nguyen, H. & Perkins, S. Mousepox: A threat to U.S. mouse colonies. *Laboratory Animal Science* **49**, (1999).

181. Chapman, J. L., Nichols, D. K., Martinez, M. J. & Raymond, J. W. Animal models of orthopoxvirus infection. *Vet. Pathol.* **47**, (2010).

182. Esteban, D., Parker, S., Schriewer, J., Hartzler, H. & Buller, R. M. Mousepox, a small animal model of smallpox. *Methods Mol. Biol.* **890**, (2012).

183. Ichihashi, Y. & Matsumoto, S. Studies on the nature of marchal bodies (A-type inclusion) during ectromelia virus infection. *Virology* **29**, 264–275 (1966).

184. Springer, Y. P. *et al.* Novel Orthopoxvirus Infection in an Alaska Resident. *Clin. Infect. Dis. An Off. Publ. Infect. Dis. Soc. Am.* **64**, 1737 (2017).

185. Hyun, J. Poxvirus under the eyes of electron microscope. *Appl. Microsc.* **52**, (2022).

186. Peters, D. Morphology of resting vaccinia virus. *Nature* **178**, (1956).

187. Dales, S. The uptake and development of vaccinia virus in strain L cells followed with labeled viral deoxyribonucleic acid. *J. Cell Biol.* **18**, (1963).

188. Resch, W. & Moss, B. The Conserved Poxvirus L3 Virion Protein Is Required for Transcription of Vaccinia Virus Early Genes. *J. Virol.* **79**, (2005).

189. Peters, D. & Müller, G. The fine structure of the DNA-containing core of vaccinia virus. *Virology* **21**, (1963).

190. McFadden, B. D. H., Moussatche, N., Kelley, K., Kang, B. H. & Condit, R. C. Vaccinia virions deficient in transcription enzymes lack a nucleocapsid. *Virology* **434**, (2012).

191. Condit, R. C., Moussatche, N. & Traktman, P. In A Nutshell: Structure and Assembly of the Vaccinia Virion. *Advances in Virus Research* **65**, (2006).

192. Moussatche, N. & Condit, R. C. Fine structure of the vaccinia virion determined by controlled degradation and immunolocalization. *Virology* **475**, (2015).

193. Bidgood, S. R. *et al.* Poxviruses package viral redox proteins in lateral bodies and modulate the host oxidative response. *PLoS Pathog.* **18**, (2022).

194. Cyrklaff, M. *et al.* Cryo-electron tomography of vaccinia virus. *Proc. Natl. Acad. Sci. U. S. A.* **102**, (2005).

195. Rodrigues, T. C. S. *et al.* Genome characterization of cetaceanpox virus from a managed Indo-

Pacific bottlenose dolphin (Tursiops aduncus). *Virus Res.* **278**, (2020).

196. Tulman, E. R. *et al.* The Genome of Canarypox Virus. *J. Virol.* **78**, (2004).

197. Nakazawa, Y. *et al.* Phylogenetic and ecologic perspectives of a monkeypox outbreak, Southern Sudan, 2005. *Emerg. Infect. Dis.* **19**, (2013).

198. Hendrickson, R. C., Wang, C., Hatcher, E. L. & Lefkowitz, E. J. Orthopoxvirus Genome Evolution: The Role of Gene Loss. *Viruses* **2**, 1933–1967 (2010).

199. Esposito, J. J. *et al.* Genome sequence diversity and clues to the evolution of variola (smallpox) virus. *Science (80-.).* **313**, (2006).

200. Lefkowitz, E. J., Wang, C. & Upton, C. Poxviruses: Past, present and future. *Virus Res.* **117**, (2006).

201. Senkevich, T. G., Yutin, N., Wolf, Y. I., Koonin, E. V. & Moss, B. Ancient gene capture and recent gene loss shape the evolution of orthopoxvirus-host interaction genes. *MBio* **12**, (2021).

202. Upton, C., Slack, S., Hunter, A. L., Ehlers, A. & Roper, R. L. Poxvirus Orthologous Clusters: toward Defining the Minimum Essential Poxvirus Genome. *J. Virol.* **77**, (2003).

203. Seet, B. T. *et al.* Poxviruses and immune evasion. *Annual Review of Immunology* **21**, (2003).

204. Shchelkunov, S. N. Orthopoxvirus genes that mediate disease virulence and host tropism. *Advances in Virology* **2012**, (2012).

205. Moss, B. Membrane fusion during poxvirus entry. *Seminars in Cell and Developmental Biology* **60**, (2016).

206. Schmidt, F. I., Bleck, C. K. E., Helenius, A. & Mercer, J. Vaccinia extracellular virions enter cells by macropinocytosis and acid-activated membrane rupture. *EMBO J.* **30**, (2011).

207. Schmidt, F. I. *et al.* Vaccinia virus entry is followed by core activation and proteasome-mediated release of the immunomodulatory effector VH1 from lateral bodies. *Cell Rep.* **4**, (2013).

208. Mallardo, M. *et al.* Relationship between Vaccinia Virus Intracellular Cores, Early mRNAs, and DNA Replication Sites. *J. Virol.* **76**, (2002).

209. Pedersen, K. *et al.* Characterization of Vaccinia Virus Intracellular Cores: Implications for Viral Uncoating and Core Structure. *J. Virol.* **74**, (2000).

210. Carter, G. C. *et al.* Vaccinia virus cores are transported on microtubules. *Journal of General Virology* **84**, (2003).

211. Greseth, M. D. & Traktman, P. The Life Cycle of the Vaccinia Virus Genome. *Annu. Rev. Virol.* **9**, 239–259 (2022).

212. Ahn, B. Y. & Moss, B. RNA polymerase-associated transcription specificity factor encoded by vaccinia virus. *Proc. Natl. Acad. Sci. U. S. A.* **89**, (1992).

213. Yang, Z. *et al.* Expression Profiling of the Intermediate and Late Stages of Poxvirus Replication. *J. Virol.* **85**, (2011).

214. Yang, Z. *et al.* Deciphering Poxvirus Gene Expression by RNA Sequencing and Ribosome

Profiling. *J. Virol.* **89**, (2015).

215. Baldick, C. J. & Moss, B. Characterization and temporal regulation of mRNAs encoded by vaccinia virus intermediate-stage genes. *J. Virol.* **67**, (1993).

216. Turner, P. C. & Moyer, R. W. The vaccinia virus fusion inhibitor proteins SPI-3 (K2) and HA (A56) expressed by infected cells reduce the entry of superinfecting virus. *Virology* **380**, (2008).

217. Wagenaar, T. R. & Moss, B. Expression of the A56 and K2 Proteins Is Sufficient To Inhibit Vaccinia Virus Entry and Cell Fusion. *J. Virol.* **83**, (2009).

218. Laliberte, J. P. & Moss, B. A Novel Mode of Poxvirus Superinfection Exclusion That Prevents Fusion of the Lipid Bilayers of Viral and Cellular Membranes. *J. Virol.* **88**, (2014).

219. Tolonen, N., Doglio, L., Schleich, S. & Krijnse Locker, J. Vaccinia virus DNA replication occurs in endoplasmic reticulum-enclosed cytoplasmic mini-nuclei. *Mol. Biol. Cell* **12**, (2001).

220. Cairns, J. The initiation of vaccinia infection. *Virology* **11**, (1960).

221. Domi, A. & Beaud, G. The punctate sites of accumulation of vaccinia virus early proteins are precursors of sites of viral DNA synthesis. *J. Gen. Virol.* **81**, (2000).

222. Rochester, S. C. & Traktman, P. Characterization of the Single-Stranded DNA Binding Protein Encoded by the Vaccinia Virus I3 Gene. *J. Virol.* **72**, (1998).

223. Czarnecki, M. W. & Traktman, P. The vaccinia virus DNA polymerase and its processivity factor. *Virus Research* **234**, (2017).

224. Bersch, B., Tarbouriech, N., Burmeister, W. P. & Iseni, F. Solution Structure of the C-terminal Domain of A20, the Missing Brick for the Characterization of the Interface between Vaccinia Virus DNA Polymerase and its Processivity Factor. *J. Mol. Biol.* **433**, (2021).

225. Banham, A. H. & Smith, G. L. Vaccinia virus gene B1R encodes a 34-kDa serine/threonine protein kinase that localizes in cytoplasmic factories and is packaged into virions. *Virology* **191**, (1992).

226. Murcia-Nicolas, A., Bolbach, G., Blais, J. C. & Beaud, G. Identification by mass spectroscopy of three major early proteins associated with virosomes in vaccinia virus-infected cells. *Virus Res.* **59**, (1999).

227. Welsch, S., Doglio, L., Schleich, S. & Krijnse Locker, J. The Vaccinia Virus I3L Gene Product Is Localized to a Complex Endoplasmic Reticulum-Associated Structure That Contains the Viral Parental DNA. *J. Virol.* **77**, (2003).

228. McDonald, W. F., Crozel-Goudot, V. & Traktman, P. Transient expression of the vaccinia virus DNA polymerase is an intrinsic feature of the early phase of infection and is unlinked to DNA replication and late gene expression. *J. Virol.* **66**, (1992).

229. Boyle, K. A., Arps, L. & Traktman, P. Biochemical and Genetic Analysis of the Vaccinia Virus D5 Protein: Multimerization-Dependent ATPase Activity Is Required To Support Viral DNA Replication. *J. Virol.* **81**, (2007).

230. Evans, E., Klemperer, N., Ghosh, R. & Traktman, P. The vaccinia virus D5 protein, which is required for DNA replication, is a nucleic acid-independent nucleoside triphosphatase. *J. Virol.* **69**, (1995).

231. McDonald, W. F., Klemperer, N. & Traktman, P. Characterization of a processive form of the vaccinia virus DNA polymerase. *Virology* **234**, (1997).

232. Sèle, C. *et al.* Low-Resolution Structure of Vaccinia Virus DNA Replication Machinery. *J. Virol.* **87**, (2013).

233. Katsafanas, G. C. & Moss, B. Linkage of Transcription and Translation within Cytoplasmic Poxvirus DNA Factories Provides a Mechanism to Coordinate Viral and Usurp Host Functions. *Cell Host Microbe* **2**, (2007).

234. Vos, J. C. & Stunnenberg, H. G. Derepression of a novel class of vaccinia virus genes upon DNA replication. *EMBO J.* **7**, (1988).

235. Keck, J. G., Baldick, C. J. & Moss, B. Role of DNA replication in vaccinia virus gene expression: A naked template is required for transcription of three late trans-activator genes. *Cell* **61**, (1990).

236. Gershon, P. D. & Moss, B. Early transcription factor subunits are encoded by vaccinia virus late genes. *Proc. Natl. Acad. Sci. U. S. A.* **87**, (1990).

237. Yeh, W. W., Moss, B. & Wolffe, E. J. The Vaccinia Virus A9L Gene Encodes a Membrane Protein Required for an Early Step in Virion Morphogenesis. *J. Virol.* **74**, (2000).

238. Roberts, K. L. & Smith, G. L. Vaccinia virus morphogenesis and dissemination. *Trends in Microbiology* **16**, (2008).

239. Smith, G. L., Vanderplasschen, A. & Law, M. The formation and function of extracellular enveloped vaccinia virus. *Journal of General Virology* **83**, (2002).

240. Schmelz, M. *et al.* Assembly of vaccinia virus: the second wrapping cisterna is derived from the trans Golgi network. *J. Virol.* **68**, (1994).

241. Tooze, J., Hollinshead, M., Reis, B., Radsak, K. & Kern, H. Progeny vaccinia and human cytomegalovirus particles utilize early endosomal cisternae for their envelopes. *Eur. J. Cell Biol.* **60**, (1993).

242. Weisberg, A. S. *et al.* Enigmatic origin of the poxvirus membrane from the endoplasmic reticulum shown by 3D imaging of vaccinia virus assembly mutants. *Proc. Natl. Acad. Sci. U. S. A.* **114**, (2017).

243. Liu, L., Cooper, T., Howley, P. M. & Hayball, J. D. From crescent to mature virion: Vaccinia virus assembly and maturation. *Viruses* **6**, (2014).

244. Shida, H., Tanabe, K. & Matsumoto, S. Mechanism of virus occlusion into A-type inclusion during poxvirus infection. *Virology* **76**, (1977).

245. Okeke, M. I. *et al.* Comparative sequence analysis of A-type inclusion (ATI) and P4c proteins of orthopoxviruses that produce typical and atypical ATI phenotypes. *Virus Genes* **39**, (2009).

246. Patel, D. D. & Pickup, D. J. Messenger RNAs of a strongly-expressed late gene of cowpox virus contain 5'-terminal poly(A) sequences. *EMBO J.* **6**, 3787 (1987).

247. McKelvey, T. A., Andrews, S. C., Miller, S. E., Ray, C. A. & Pickup, D. J. Identification of the Orthopoxvirus p4c Gene, Which Encodes a Structural Protein That Directs Intracellular Mature Virus Particles into A-Type Inclusions. *J. Virol.* **76**, 11216 (2002).

248. Howard, A. R., Weisberg, A. S. & Moss, B. Congregation of Orthopoxvirus Virions in Cytoplasmic A-Type Inclusions Is Mediated by Interactions of a Bridging Protein (A26p) with a Matrix Protein (ATIp) and a Virion Membrane-Associated Protein (A27p). *J. Virol.* **84**, 7592 (2010).

249. Firth, C. *et al.* Using Time-Structured Data to Estimate Evolutionary Rates of Double-Stranded DNA Viruses. *Mol. Biol. Evol.* **27**, 2038–2051 (2010).

250. de Haven, B. C., Gupta, K. & Isaacs, S. N. The vaccinia virus A56 protein: A multifunctional transmembrane glycoprotein that anchors two secreted viral proteins. *Journal of General Virology* **92**, (2011).

251. Zhou, J., Sun, X. Y., Fernando, G. J. P. & Frazer, I. H. The vaccinia virus K2L gene encodes a serine protease inhibitor which inhibits cell-cell fusion. *Virology* **189**, (1992).

252. Law, K. M. & Smith, G. L. A vaccinia serine protease inhibitor which prevents virus-induced cell fusion. *J. Gen. Virol.* **73**, (1992).

253. Turner, P. C. & Moyer, R. W. An orthopoxvirus serpinlike gene controls the ability of infected cells to fuse. *J. Virol.* **66**, (1992).

254. Carpentier, D. C. J., Van Loggerenberg, A., Dieckmann, N. M. G. & Smith, G. L. Vaccinia virus egress mediated by virus protein A36 is reliant on the F12 protein. *J. Gen. Virol.* **98**, (2017).

255. Dodding, M. P., Newsome, T. P., Collinson, L. M., Edwards, C. & Way, M. An E2-F12 complex is required for intracellular enveloped virus morphogenesis during vaccinia infection. *Cell. Microbiol.* **11**, (2009).

256. Moss, B. Poxvirus DNA replication. *Cold Spring Harb. Perspect. Biol.* **5**, (2013).

257. Van Eijl, H., Hollinshead, M. & Smith, G. L. The vaccinia virus A36R protein is a type Ib membrane protein present on intracellular but not extracellular enveloped virus particles. *Virology* **271**, (2000).

258. Blasco, R. & Moss, B. Role of cell-associated enveloped vaccinia virus in cell-to-cell spread. *J. Virol.* **66**, (1992).

259. Roper, R. L., Wolffe, E. J., Weisberg, A. & Moss, B. The Envelope Protein Encoded by the A33R Gene Is Required for Formation of Actin-Containing Microvilli and Efficient Cell-to-Cell Spread of Vaccinia Virus. *J. Virol.* **72**, (1998).

260. Wolffe, E. J., Isaacs, S. N. & Moss, B. Deletion of the vaccinia virus B5R gene encoding a 42-kilodalton membrane glycoprotein inhibits extracellular virus envelope formation and dissemination. *J. Virol.* **67**, (1993).

261. Wolffe, E. J., Katz, E., Weisberg, A. & Moss, B. The A34R glycoprotein gene is required for induction of specialized actin-containing microvilli and efficient cell-to-cell transmission of vaccinia virus. *J. Virol.* **71**, (1997).

262. Katz, E., Wolffe, E. & Moss, B. Identification of Second-Site Mutations That Enhance Release and Spread of Vaccinia Virus. *J. Virol.* **76**, (2002).

263. Blasco, R., Sisler, J. R. & Moss, B. Dissociation of progeny vaccinia virus from the cell membrane is regulated by a viral envelope glycoprotein: effect of a point mutation in the lectin homology domain of the A34R gene. *J. Virol.* **67**, (1993).

264. Doceul, V., Hollinshead, M., Van Der Linden, L. & Smith, G. L. Repulsion of superinfecting virions: A mechanism for rapid virus spread. *Science (80-.).* **327**, (2010).

265. McFadden, G., Mohamed, M. R., Rahman, M. M. & Bartee, E. Cytokine determinants of viral tropism. *Nature Reviews Immunology* **9**, (2009).

266. McFadden, G., Pace, W. E., Purres, J. & Dales, S. Biogenesis of poxviruses: Transitory expression of Molluscum contagiosum early functions. *Virology* **94**, (1979).

267. Li, Y., Yuan, S. & Moyer, R. W. The non-permissive infection of insect (Gypsy Moth) LD-652 cells by vaccinia virus. *Virology* **248**, (1998).

268. Zhao, Y. *et al.* Non-replicating Vaccinia Virus TianTan Strain (NTV) Translation Arrest of Viral Late Protein Synthesis Associated With Anti-viral Host Factor SAMD9. *Front. Cell. Infect. Microbiol.* **10**, (2020).

269. Bengali, Z. *et al.* Drosophila S2 cells are non-permissive for vaccinia virus DNA replication following entry via low pH-dependent endocytosis and early transcription. *PLoS One* **6**, (2011).

270. Johnston, J. B. *et al.* Role of the Serine-Threonine Kinase PAK-1 in Myxoma Virus Replication. *J. Virol.* **77**, (2003).

271. Werden, S. J., Rahman, M. M. & McFadden, G. Chapter 3 Poxvirus Host Range Genes. *Advances in Virus Research* **71**, (2008).

272. Haller, S. L., Peng, C., McFadden, G. & Rothenburg, S. Poxviruses and the evolution of host range and virulence. *Infection, Genetics and Evolution* **21**, (2014).

273. Ramsey-Ewing, A. L. & Moss, B. Complementation of a vaccinia virus host-range K1L gene deletion by the nonhomologous CP77 gene. *Virology* **222**, (1996).

274. Spehner, D., Gillard, S., Drillien, R. & Kirn, A. A cowpox virus gene required for multiplication in Chinese hamster ovary cells. *J. Virol.* **62**, (1988).

275. Drillien, R., Koehren, F. & Kirn, A. Host range deletion mutant of vaccinia virus defective in human cells. *Virology* **111**, (1981).

276. Gillard, S., Spehner, D., Drillien, R. & Kirn, A. Localization and sequence of a vaccinia virus gene required for multiplication in human cells. *Proc. Natl. Acad. Sci. U. S. A.* **83**, (1986).

277. Perkus, M. E. *et al.* Vaccinia virus host range genes. *Virology* **179**, 276–286 (1990).

278. Meng, X., Chao, J. & Xiang, Y. Identification from diverse mammalian poxviruses of host-range regulatory genes functioning equivalently to vaccinia virus C7L. *Virology* **372**, (2008).

279. Beattie, E. *et al.* Host-range restriction of vaccinia virus E3L-specific deletion mutants. *Virus Genes* **12**, (1996).

280. Chang, H. W., Uribe, L. H. & Jacobs, B. L. Rescue of vaccinia virus lacking the E3L gene by mutants of E3L. *J. Virol.* **69**, (1995).

281. Langland, J. O. & Jacobs, B. L. The role of the PKR-inhibitory genes, E3L and K3L, in determining vaccinia virus host range. *Virology* **299**, (2002).

282. Shisler, J. L., Isaacs, S. N. & Moss, B. Vaccinia virus serpin-1 deletion mutant exhibits a host

range defect characterized by low levels of intermediate and late mRNAs. *Virology* **262**, (1999).

283. Ali, A. N., Brooks, M. A. & Moyer, R. W. The SPI-1 gene of rabbitpox virus determines host range and is required for hemorrhagic pock formation. *Virology* **202**, (1994).

284. Drexler, I., Heller, K., Wahren, B., Erfle, V. & Sutter, G. Highly attenuated modified vaccinia virus Ankara replicates in baby hamster kidney cells, a potential host for virus propagation, but not in various human transformed and primary cells. *J. Gen. Virol.* **79**, (1998).

285. Meisinger-Henschel, C. *et al.* Introduction of the Six Major Genomic Deletions of Modified Vaccinia Virus Ankara (MVA) into the Parental Vaccinia Virus Is Not Sufficient To Reproduce an MVA-Like Phenotype in Cell Culture and in Mice. *J. Virol.* **84**, (2010).

286. Sutter, G. & Moss, B. Nonreplicating vaccinia vector efficiently expresses recombinant genes. *Proc. Natl. Acad. Sci. U. S. A.* **89**, (1992).

287. Okeke, M. I., Nilssen, Ø. & Traavik, T. Modified vaccinia virus Ankara multiplies in the rat IEC-6 cells and limited production of mature virions occurs in other mammalian cell lines. *J. Gen. Virol.* **87**, (2006).

288. Jordan, I., Horn, D., Oehmke, S., Leendertz, F. H. & Sandig, V. Cell lines from the Egyptian fruit bat are permissive for modified vaccinia Ankara. *Virus Res.* **145**, (2009).

289. Meiser, A., Sancho, C. & Krijnse Locker, J. Plasma Membrane Budding as an Alternative Release Mechanism of the Extracellular Enveloped Form of Vaccinia Virus from HeLa Cells. *J. Virol.* **77**, (2003).

290. Hughes, A. L., Irausquin, S. & Friedman, R. The evolutionary biology of poxviruses. *Infect. Genet. Evol.* **10**, 50–59 (2010).

291. Brennan, G. *et al.* Molecular Mechanisms of Poxvirus Evolution. *MBio* **14**, (2023).

292. Babkin, I. V. & Babkina, I. N. A retrospective study of the orthopoxvirus molecular evolution. *Infect. Genet. Evol.* **12**, 1597–1604 (2012).

293. Zehender, G. *et al.* Bayesian reconstruction of the evolutionary history and cross-species transition of variola virus and orthopoxviruses. *J. Med. Virol.* **90**, 1134–1141 (2018).

294. Babkin, I. V. & Babkina, I. N. Molecular Dating in the Evolution of Vertebrate Poxviruses. *Intervirology* **54**, 253–260 (2011).

295. Babkin, I. V. & Shchelkunov, S. N. Molecular evolution of poxviruses. *Russ. J. Genet. 2008 448* **44**, 895–908 (2008).

296. Isidro, J. *et al.* Phylogenomic characterization and signs of microevolution in the 2022 multi-country outbreak of monkeypox virus. *Nat. Med.* **28**, 1569–1572 (2022).

297. Elde, N. C. *et al.* Poxviruses deploy genomic accordions to adapt rapidly against host antiviral defenses. *Cell* **150**, (2012).

298. Grossegesse, M., Doellinger, J., Tyshaieva, A., Schaade, L. & Nitsche, A. Combined proteomics/genomics approach reveals proteomic changes of mature virions as a novel poxvirus adaptation mechanism. *Viruses* **9**, (2017).

299. Brennan, G., Kitzman, J. O., Rothenburg, S., Shendure, J. & Geballe, A. P. Adaptive Gene

Amplification As an Intermediate Step in the Expansion of Virus Host Range. *PLoS Pathog.* **10**, (2014).

300. Coulson, D. & Upton, C. Characterization of indels in poxvirus genomes. *Virus Genes* **42**, 171–177 (2011).

301. Smithson, C., Purdy, A., Verster, A. J. & Upton, C. Prediction of Steps in the Evolution of Variola Virus Host Range. *PLoS One* **9**, e91520 (2014).

302. Doty, J. B. *et al.* Isolation and Characterization of Akhmeta Virus from Wild-Caught Rodents (Apodemus spp.) in Georgia . *J. Virol.* **93**, (2019).

303. Qin, L., Favis, N., Famulski, J. & Evans, D. H. Evolution of and Evolutionary Relationships between Extant Vaccinia Virus Strains. *J. Virol.* **89**, 1809 (2015).

304. Qin, L., Upton, C., Hazes, B. & Evans, D. H. Genomic Analysis of the Vaccinia Virus Strain Variants Found in Dryvax Vaccine. *J. Virol.* **85**, 13049 (2011).

305. Smithson, C. *et al.* Two novel poxviruses with unusual genome rearrangements: NY_014 and Murmansk. *Virus Genes* **53**, 883–897 (2017).

306. Qin, L. & Evans, D. H. Genome Scale Patterns of Recombination between Coinfecting Vaccinia Viruses. *J. Virol.* **88**, 5277–5286 (2014).

307. Babkin, I. V., Babkina, I. N. & Tikunova, N. V. An Update of Orthopoxvirus Molecular Evolution. *Viruses 2022, Vol. 14, Page 388* **14**, 388 (2022).

308. Hoffmann, D. *et al.* Out of the Reservoir: Phenotypic and Genotypic Characterization of a Novel Cowpox Virus Isolated from a Common Vole. *J. Virol.* **89**, (2015).

309. Gruber, C. E. M. *et al.* Whole genome characterization of orthopoxvirus (Opv) abatino, a zoonotic virus representing a putative novel clade of old world orthopoxviruses. *Viruses* **10**, 1. – 12 of 12 (2018).

310. Guan, H. *et al.* Emergence, phylogeography, and adaptive evolution of mpox virus. *New Microbes New Infect.* **52**, 101102 (2023).

311. Forni, D., Molteni, C., Cagliani, R., Clerici, M. & Sironi, M. Analysis of variola virus molecular evolution suggests an old origin of the virus consistent with historical records. *Microb. Genomics* **9**, 1–7 (2023).

312. European Parliament and Council. Directive 2001/18/EC of the European Parliament and of the Council of 12 March on the deliberate release into the environment of genetically modified organisms and repealing Council Directive 90/220/EEC. 1–39 (2001).

313. Wyatt, L. S. *et al.* Marker rescue of the host range restriction defects of modified vaccinia virus Ankara. *Virology* **251**, (1998).

314. Liu, R. *et al.* SPI-1 is a missing host-range factor required for replication of the attenuated modified vaccinia ankara (MVA) vaccine vector in human cells. *PLoS Pathog.* **15**, (2019).

315. Zwilling, J., Sliva, K., Schwantes, A., Schnierle, B. & Sutter, G. Functional F11L and K1L genes in modified vaccinia virus Ankara restore virus-induced cell motility but not growth in human and murine cells. *Virology* **404**, (2010).

316. Peng, C. & Moss, B. Repair of a previously uncharacterized second host-range gene

contributes to full replication of modified vaccinia virus Ankara (MVA) in human cells. *Proc. Natl. Acad. Sci. U. S. A.* **117**, (2020).

317. Sutter, G. A vital gene for modified vaccinia virus Ankara replication in human cells. *Proceedings of the National Academy of Sciences of the United States of America* **117**, (2020).

318. Erez, N., Wyatt, L. S., Americo, J. L., Xiao, W. & Moss, B. Spontaneous and Targeted Mutations in the Decapping Enzyme Enhance Replication of Modified Vaccinia Virus Ankara (MVA) in Monkey Cells. *J. Virol.* **95**, (2021).

319. Reynolds, M. G., Guagliardo, S. A. J., Nakazawa, Y. J., Doty, J. B. & Mauldin, M. R. Understanding orthopoxvirus host range and evolution: from the enigmatic to the usual suspects. *Curr. Opin. Virol.* **28**, 108–115 (2018).

320. Brochier, B. M. *et al.* Use of recombinant vaccinia-rabies virus for oral vaccination of fox cubs (Vulpes vulpes, L) against rabies. *Vet. Microbiol.* **18**, (1988).

321. Freuling, C. M. *et al.* The elimination of fox rabies from Europe: Determinants of success and lessons for the future. *Philos. Trans. R. Soc. B Biol. Sci.* **368**, (2013).

322. Verheust, C., Goossens, M., Pauwels, K. & Breyer, D. Biosafety aspects of modified vaccinia virus Ankara (MVA)-based vectors used for gene therapy or vaccination. *Vaccine* **30**, (2012).

323. Goossens, M., Pauwels, K., Willemarck, N. & Breyer, D. Environmental Risk Assessment of Clinical Trials Involving Modified Vaccinia Virus Ankara (MVA)-Based Vectors. *Curr. Gene Ther.* **13**, (2014).

324. Nitsche, A., Kurth, A. & Pauli, G. Viremia in human Cowpox virus infection. *J. Clin. Virol.* **40**, (2007).

325. Willer, D. O., Yao, X. D., Mann, M. J. & Evans, D. H. In vitro concatemer formation catalyzed by vaccinia virus DNA polymerase. *Virology* **278**, (2000).

326. Hansen, H., Okeke, M. I., Nilssen, Ø. & Traavik, T. Recombinant viruses obtained from co-infection in vitro with a live vaccinia-vectored influenza vaccine and a naturally occurring cowpox virus display different plaque phenotypes and loss of the transgene. *Vaccine* **23**, 499–506 (2004).

327. Okeke, M. I., Nilssen, I., Moens, U., Tryland, M. & Traavik, T. In vitro host range, multiplication and virion forms of recombinant viruses obtained from co-infection in vitro with a vaccinia-vectored influenza vaccine and a naturally occurring cowpox virus isolate. *Virol. J.* **6**, (2009).

328. Sprygin, A. *et al.* Analysis and insights into recombination signals in lumpy skin disease virus recovered in the field. *PLoS One* **13**, (2018).

329. Sprygin, A. *et al.* Evidence of recombination of vaccine strains of lumpy skin disease virus with field strains, causing disease. *PLoS One* **15**, (2020).

330. Shumilova, I. *et al.* Overwintering of recombinant lumpy skin disease virus in northern latitudes, Russia. *Transbound. Emerg. Dis.* **69**, (2022).

331. Vandenbussche, F. *et al.* Recombinant LSDV Strains in Asia: Vaccine Spillover or Natural Emergence? *Viruses* **14**, (2022).

332. Mayr, A., Hochstein-Mintzel, V. & Stickl, H. Abstammung, Eigenschaften und Verwendung

des attenuierten Vaccinia-Stammes MVA. *Infection* **3**, (1975).

333. Cottingham, M. G. & Carroll, M. W. Recombinant MVA vaccines: Dispelling the myths. *Vaccine* **31**, (2013).

334. Jordan, I., Horn, D., John, K. & Sandig, V. A genotype of modified vaccinia Ankara (MVA) that facilitates replication in suspension cultures in chemically defined medium. *Viruses* **5**, (2013).

335. Burgers, W. A. *et al.* Construction, characterization, and immunogenicity of a multigene modified vaccinia Ankara (MVA) vaccine based on HIV Type 1 subtype C. *AIDS Res. Hum. Retroviruses* **24**, (2008).

336. Wyatt, L. S., Belyakov, I. M., Earl, P. L., Berzofsky, J. A. & Moss, B. Enhanced cell surface expression, immunogenicity and genetic stability resulting from a spontaneous truncation of HIV Env expressed by a recombinant MVA. *Virology* **372**, (2008).

337. Wang, Z. *et al.* Modified H5 promoter improves stability of insert genes while maintaining immunogenicity during extended passage of genetically engineered MVA vaccines. *Vaccine* **28**, (2010).

338. Wyatt, L. S. *et al.* Elucidating and Minimizing the Loss by Recombinant Vaccinia Virus of Human Immunodeficiency Virus Gene Expression Resulting from Spontaneous Mutations and Positive Selection. *J. Virol.* **83**, (2009).

339. Stoler, N. & Nekrutenko, A. Sequencing error profiles of Illumina sequencing instruments. *NAR Genomics Bioinforma.* **3**, (2021).

340. Heather, J. M. & Chain, B. The sequence of sequencers: The history of sequencing DNA. *Genomics* **107**, (2016).

341. Van Dijk, E. L., Jaszczyszyn, Y., Naquin, D. & Thermes, C. The Third Revolution in Sequencing Technology. *Trends Genet.* **34**, (2018).

342. Cui, J. *et al.* Analysis and comprehensive comparison of PacBio and nanopore-based RNA sequencing of the Arabidopsis transcriptome. *Plant Methods* **16**, (2020).

343. Bolger, A. M., Lohse, M. & Usadel, B. Trimmomatic: a flexible trimmer for Illumina sequence data. *Bioinformatics* **30**, 2114–2020 (2014).

344. Del Fabbro, C., Scalabrin, S., Morgante, M. & Giorgi, F. M. An extensive evaluation of read trimming effects on illumina NGS data analysis. *PLoS One* **8**, (2013).

345. Wingett, S. W. & Andrews, S. FastQ Screen: A tool for multi-genome mapping and quality control. *F1000Research* **7**, 1338 (2018).

346. Li, H. & Durbin, R. Fast and accurate short read alignment with Burrows–Wheeler transform. *Bioinformatics* **25**, 1754–1760 (2009).

347. Li, H. & Durbin, R. Fast and accurate long-read alignment with Burrows-Wheeler transform. *Bioinformatics* **26**, (2010).

348. Antipov, D., Korobeynikov, A., McLean, J. S. & Pevzner, P. A. HybridSPAdes: An algorithm for hybrid assembly of short and long reads. *Bioinformatics* **32**, (2016).

349. Koren, S. *et al.* Hybrid error correction and de novo assembly of single-molecule sequencing

reads. *Nat. Biotechnol.* **30**, (2012).

350. Wick, R. R., Judd, L. M., Gorrie, C. L. & Holt, K. E. Unicycler: Resolving bacterial genome assemblies from short and long sequencing reads. *PLoS Comput. Biol.* **13**, (2017).

351. Zimin, A. V. *et al.* The MaSuRCA genome assembler. *Bioinformatics* **29**, (2013).

352. Haghshenas, E., Asghari, H., Stoye, J., Chauve, C. & Hach, F. HASLR: Fast Hybrid Assembly of Long Reads. *iScience* **23**, (2020).

353. Tcherepanov, V., Ehlers, A. & Upton, C. Genome Annotation Transfer Utility (GATU): rapid annotation of viral genomes using a closely related reference genome. *BMC Genomics* **7**, 150 (2006).

354. Camacho, C. *et al.* BLAST+: architecture and applications. *BMC Bioinformatics* **10**, 421 (2009).

355. Martin, D. P., Murrell, B., Golden, M., Khoosal, A. & Muhire, B. RDP4: Detection and analysis of recombination patterns in virus genomes. *Virus Evolution* **1**, (2015).

356. Lole, K. S. *et al.* Full-Length Human Immunodeficiency Virus Type 1 Genomes from Subtype C-Infected Seroconverters in India, with Evidence of Intersubtype Recombination. *Journal of Virology* **73**, 160 (1999).

357. Mühlemann, B. *et al.* Diverse variola virus (smallpox) strains were widespread in northern Europe in the Viking Age. *Science (80-.).* **369**, (2020).

358. Gyuranecz, M. *et al.* Worldwide Phylogenetic Relationship of Avian Poxviruses. *J. Virol.* **87**, (2013).

359. Pais, F. S. M., Ruy, P. de C., Oliveira, G. & Coimbra, R. S. Assessing the efficiency of multiple sequence alignment programs. *Algorithms Mol. Biol.* **9**, (2014).

360. Martin, D. & Rybicki, E. RDP: detection of recombination amongst aligned sequences. *Bioinformatics* **16**, 562–563 (2000).

361. Salminen, M. O., Carr, J. K., Burke, D. S. & Mccutchan, F. E. Identification of Breakpoints in Intergenotypic Recombinants of HIV Type 1 by Bootscanning. *AIDS Res. Hum. Retroviruses* **11**, (1995).

362. Smith, J. M. Analyzing the mosaic structure of genes. *Journal of Molecular Evolution 1992 34:2* **34**, 126–129 (1992).

363. Posada, D. & Crandall, K. A. Evaluation of methods for detecting recombination from DNA sequences: Computer simulations. *Proceedings of the National Academy of Sciences* **98**, 13757–13762 (2001).

364. Boni, M. F., Posada, D. & Feldman, M. W. An Exact Nonparametric Method for Inferring Mosaic Structure in Sequence Triplets. *Genetics* **176**, 1035–1047 (2007).

365. Padidam, M., Sawyer, S. & Fauquet, C. M. Possible Emergence of New Geminiviruses by Frequent Recombination. *Virology* **265**, 218–225 (1999).

366. Holmes, E. C., Worobey, M. & Rambaut, A. Phylogenetic evidence for recombination in dengue virus. *Mol. Biol. Evol.* **16**, (1999).

367. Gibbs, M. J., Armstrong, J. S. & Gibbs, A. J. Sister-Scanning: a Monte Carlo procedure for assessing signals in recombinant sequences. *Bioinformatics* **16**, 573–582 (2000).

368. Ehlers, A., Osborne, J., Slack, S., Roper, R. L. & Upton, C. Poxvirus Orthologous Clusters (POCs). *Bioinformatics* **18**, 1544–1545 (2002).

369. McLeod, K. & Upton, C. Virus Databases. in *Reference Module in Biomedical Sciences* (2017). doi:10.1016/b978-0-12-801238-3.95728-3

370. Katoh, K. & Standley, D. M. MAFFT Multiple Sequence Alignment Software Version 7: Improvements in Performance and Usability. *Molecular Biology and Evolution* **30**, 772–780 (2013).

371. Talavera, G. & Castresana, J. Improvement of Phylogenies after Removing Divergent and Ambiguously Aligned Blocks from Protein Sequence Alignments. *Systematic Biology* **56**, 564–577 (2007).

372. Emms, D. M. & Kelly, S. OrthoFinder: solving fundamental biases in whole genome comparisons dramatically improves orthogroup inference accuracy. *Genome Biology* **16**, (2015).

373. Ogden, T. H. & Rosenberg, M. S. Multiple sequence alignment accuracy and phylogenetic inference. *Syst. Biol.* **55**, (2006).

374. Hall, B. G. Comparison of the accuracies of several phylogenetic methods using protein and DNA sequences. *Mol. Biol. Evol.* **22**, (2005).

375. Holder, M. & Lewis, P. O. Phylogeny estimation: Traditional and Bayesian approaches. *Nature Reviews Genetics* **4**, (2003).

376. Darriba, Di. *et al.* ModelTest-NG: A New and Scalable Tool for the Selection of DNA and Protein Evolutionary Models. *Molecular Biology and Evolution* **37**, 294 (2020).

377. Stamatakis, A., Hoover, P. & Rougemont, J. A Rapid Bootstrap Algorithm for the RAxML Web Servers. *Syst. Biol.* **57**, 758–771 (2008).

378. Ronquist, F. *et al.* MrBayes 3.2: Efficient Bayesian Phylogenetic Inference and Model Choice Across a Large Model Space. *Systematic Biology* **61**, 539–542 (2012).

379. Smithson, C., Kampman, S., Hetman, B. M. & Upton, C. Incongruencies in vaccinia virus phylogenetic trees. *Computation* **2**, (2014).

380. Rousseau, C. M. *et al.* Extensive Intrasubtype Recombination in South African Human Immunodeficiency Virus Type 1 Subtype C Infections. *J. Virol.* **81**, (2007).

381. Minh, B. Q. *et al.* IQ-TREE 2: New Models and Efficient Methods for Phylogenetic Inference in the Genomic Era. *Mol. Biol. Evol.* **37**, 1530–1534 (2020).

382. Mavian, C., Marini, S., Prosperi, M. & Salemi, M. A snapshot of SARS-CoV-2 genome availability up to April 2020 and its implications: Data analysis. *JMIR Public Heal. Surveill.* **6**, (2020).

383. Fourment, M. & Gibbs, M. J. PATRISTIC: a program for calculating patristic distances and graphically comparing the components of genetic change. *BMC Evolutionary Biology* **6**, 1 (2006).

384. Drummond, A. J. & Rambaut, A. BEAST: Bayesian evolutionary analysis by sampling trees. *BMC Evol. Biol.* **7**, (2007).

385. Sagulenko, P., Puller, V. & Neher, R. A. TreeTime: Maximum-likelihood phylodynamic analysis. *Virus Evol.* **4**, (2018).

386. To, T. H., Jung, M., Lycett, S. & Gascuel, O. Fast Dating Using Least-Squares Criteria and Algorithms. *Syst. Biol.* **65**, (2016).

387. Suchard, M. A. *et al.* Bayesian phylogenetic and phylodynamic data integration using BEAST 1.10. *Virus Evol.* **4**, (2018).

388. Rambaut, A., Lam, T. T., Carvalho, L. M. & Pybus, O. G. Exploring the temporal structure of heterochronous sequences using TempEst (formerly Path-O-Gen). *Virus Evol.* **2**, (2016).

389. Demaria, P. J. *et al.* Phase 1 open-label trial of intravenous administration of MVA-BN-brachyury-TRICOM vaccine in patients with advanced cancer. *J. Immunother. Cancer* **9**, (2021).

390. Kaysser, P., von Bomhard, W., Dobrzykowski, L. & Meyer, H. Genetic diversity of feline cowpox virus, Germany 2000-2008. *Vet. Microbiol.* **141**, (2010).

391. Mavian, C. *et al.* The genome sequence of ectromelia virus Naval and Cornell isolates from outbreaks in North America. *Virology* **462**–**463**, 218–226 (2014).

392. Gershon, P. D., Kitching, R. P., Hammond, J. M. & Black, D. N. Poxvirus genetic recombination during natural virus transmission. *J. Gen. Virol.* **70**, (1989).

393. Lin, Y.-C. J. & Evans, D. H. Vaccinia Virus Particles Mix Inefficiently, and in a Way That Would Restrict Viral Recombination, in Coinfected Cells. *J. Virol.* **84**, 2432–2443 (2010).

394. Chernos, V. I., Antonova, T. P. & Senkevich, T. G. Recombinants between vaccinia and ectromelia viruses bearing the specific pathogenicity markers on both parents. *J. Gen. Virol.* **66**, (1985).

395. Ball, L. A. High-frequency homologous recombination in vaccinia virus DNA. *J. Virol.* **61**, (1987).

396. Fathi, Z., Dyster, L. M., Seto, J., Condit, R. C. & Niles, E. G. Intragenic and intergenic recombination between temperature-sensitive mutants of vaccinia virus. *J. Gen. Virol.* **72**, (1991).

397. Christen, L., Seto, J. & Niles, E. G. Superinfection exclusion of vaccinia virus in virus-infected cell cultures. *Virology* **174**, (1990).

398. Dobson, B. M. *et al.* Vaccinia virus F5 is required for normal plaque morphology in multiple cell lines but not replication in culture or virulence in mice. *Virology* **456**–**457**, (2014).

399. Dobson, B. M. & Tscharke, D. C. Truncation of gene F5L partially masks rescue of vaccinia virus strain MVA growth on mammalian cells by restricting plaque size. *J. Gen. Virol.* **95**, (2014).

400. Morales, I. *et al.* The vaccinia virus F11L gene product facilitates cell detachment and promotes migration. *Traffic* **9**, (2008).

401. Zhang, W.-H., Wilcock, D. & Smith, G. L. Vaccinia Virus F12L Protein Is Required for Actin

Tail Formation, Normal Plaque Size, and Virulence. *J. Virol.* **74**, (2000).

402. Atukorale, V. N., Weir, J. P. & Meseda, C. A. Stability of the hsv-2 us-6 gene in the del ii, del iii, cp77, and i8r-g1l sites in modified vaccinia virus ankara after serial passage of recombinant vectors in cells. *Vaccines* **8**, (2020).

Paper I

frontiers | Frontiers in Microbiology

ORIGINAL RESEARCH
published: 03 May 2022
doi: 10.3389/fmicb.2022.868887

Genomic Sequencing and Analysis of a Novel Human Cowpox Virus With Mosaic Sequences From North America and Old World Orthopoxvirus

Diana Diaz-Cánova[1], Ugo L. Moens[1], Annika Brinkmann[2], Andreas Nitsche[2] and Malachy Ifeanyi Okeke[3]**

[1] Molecular Inflammation Research Group, Department of Medical Biology, UiT - The Arctic University of Norway, Tromsø, Norway, [2] Highly Pathogenic Viruses, Centre for Biological Threats and Special Pathogens, WHO Reference Laboratory for SARS-CoV-2 and WHO Collaborating Centre for Emerging Infections and Biological Threats, Robert Koch Institute, Berlin, Germany, [3] Section of Biomedical Sciences, Department of Natural and Environmental Sciences, School of Arts and Sciences, American University of Nigeria, Yola, Nigeria

OPEN ACCESS

Edited by:
Vladimir N. Uversky, University of South Florida, United States

Reviewed by:
David Hugh Evans, University of Alberta, Canada
Sergei Shchelkunov, State Research Center of Virology and Biotechnology VECTOR (ISTC), Russia

***Correspondence:**
Ugo L. Moens
ugo.moens@uit.no
Malachy Ifeanyi Okeke
malachy.okeke@aun.edu.ng

Specialty section:
This article was submitted to Virology, a section of the journal Frontiers in Microbiology

Received: *03 February 2022*
Accepted: *24 February 2022*
Published: *03 May 2022*

Citation:
Diaz-Cánova D, Moens UL, Brinkmann A, Nitsche A and Okeke MI (2022) Genomic Sequencing and Analysis of a Novel Human Cowpox Virus With Mosaic Sequences From North America and Old World Orthopoxvirus. Front. Microbiol. 13:868887. doi: 10.3389/fmicb.2022.868887

Orthopoxviruses (OPXVs) not only infect their natural hosts, but some OPXVs can also cause disease in humans. Previously, we partially characterized an OPXV isolated from an 18-year-old male living in Northern Norway. Restriction enzyme analysis and partial genome sequencing characterized this virus as an atypical cowpox virus (CPXV), which we named CPXV-No-H2. In this study, we determined the complete genome sequence of CPXV-No-H2 using Illumina and Nanopore sequencing. Our results showed that the whole CPXV-No-H2 genome is 220,276 base pairs (bp) in length, with inverted terminal repeat regions of approximately 7 kbp, containing 217 predicted genes. Seventeen predicted CPXV-No-H2 proteins were most similar to OPXV proteins from the Old World, including *Ectromelia virus* (ECTV) and *Vaccinia virus*, and North America, *Alaskapox virus* (AKPV). CPXV-No-H2 has a mosaic genome with genes most similar to other OPXV genes, and seven potential recombination events were identified. The phylogenetic analysis showed that CPXV-No-H2 formed a separate clade with the German CPXV isolates CPXV_GerMygEK938_17 and CPXV_Ger2010_MKY, sharing 96.4 and 96.3% nucleotide identity, respectively, and this clade clustered closely with the ECTV-OPXV Abatino clade. CPXV-No-H2 is a mosaic virus that may have arisen out of several recombination events between OPXVs, and its phylogenetic clustering suggests that ECTV-Abatino-like cowpox viruses form a distinct, new clade of cowpox viruses.

Keywords: poxvirus, phylogenetics, Fennoscandian, Norway, recombination

INTRODUCTION

Poxvirus is a family of double-stranded DNA viruses that can infect a broad range of hosts, including mammals, birds, reptiles, and insects (International Committee on Taxonomy of Viruses, ICTV[1]). Based on the host, *Poxviridae* is divided into two subfamilies: *Chordopoxvirinae* (poxviruses that infect vertebrates) and *Entomopoxvirinae* (poxviruses that infect insects)

[1]https://talk.ictvonline.org/taxonomy/

(MacLachlan and Dubovi, 2017). Within the subfamily *Chordopoxvirinae*, there is the genus *Orthopoxvirus* (OPXV). They are viruses with large, linear, double-stranded DNA genomes ranging in size from 170 to 250 kbp (Hendrickson et al., 2010).

One of the best-known species among OPXV is *Variola virus* (VARV), the causative agent of smallpox. It was one of the deadliest viruses in human history and was declared to be successfully eradicated in 1980 after a worldwide smallpox vaccination campaign (Strassburg, 1982). Other members of the OPXV genus also cause human diseases, such as *Cowpox virus* (CPXV), *Monkeypox virus* (MPXV), and vaccinia-like virus (Vora et al., 2015; Reynolds et al., 2018; Diaz, 2021; Silva et al., 2021), but those are zoonotic OPXVs. *Variola virus* is the only OPXV that exclusively infected humans in nature. Among the most studied members of OPXVs, *Vaccinia virus* (VACV) is the prototype species. Several VACV strains were used as smallpox vaccines during the world vaccination campaign (Jacobs et al., 2009).

OPXVs can be further divided into New World and Old World OPXVs according to their endemism. The Old World or African-Eurasian OPXV group contains seven species: *VARV*, *VACV*, *MPXV*, *CPXV*, *Camelpox virus* (CMLV), *Ectromelia virus* (ECTV), and *Taterapox virus* (TATV). The New World OPXV group comprises three species that are endemic to North America: *Raccoonpox virus* (RCNV), *Volepox virus* (VPXV), and *Skunkpox virus* (SKPV) (Smithson et al., 2017b).

In recent times, the increased number of reported OPXV infections as well as the emergence of new OPXVs or re-emergence of existing OPXVs has been reported in several countries across the world (Abrahão et al., 2015; Kalthan et al., 2018). Three novel OPXV species have recently been discovered: *Abatino macacapox virus* (OPXV Abatino) in Italy (Cardeti et al., 2017), *Ahkmeta virus* (AKMV) in Georgia (Gao et al., 2018), and *Alaskapox virus* (AKPV) in the United States (Gigante et al., 2019).

The increasing number of OPXV infections in humans could be due to low population immunity against smallpox after the cessation of smallpox vaccination. The vaccinia-like virus infections were reported in different places and host species (Dumbell and Richardson, 1993; Abrahão et al., 2015; Miranda et al., 2017), including humans (Damaso et al., 2007; Megid et al., 2012). In different countries in Africa, human cases of MPXV infections have been reported (Nakoune et al., 2017; Durski et al., 2018; Yinka-Ogunleye et al., 2019; Alakunle et al., 2020); imported MPXV cases were as well reported in Israel, the United Kingdom and Singapore (Vaughan et al., 2018; Erez et al., 2019; Ng et al., 2019). In Europe, cases of cowpox were reported (Tryland et al., 1998; Kalthoff et al., 2014; Ferrier et al., 2021). The distribution of CPXV is in Eurasia (Chantrey et al., 1999; Wolfs et al., 2002; Laakkonen et al., 2006; Vorou et al., 2008; Popova et al., 2017; Diaz, 2021; Ferrier et al., 2021). The natural reservoirs of CPXV are wild rodents (Chantrey et al., 1999; Kinnunen et al., 2011). CPXV has a wide host spectrum, including humans, monkeys, cats, dogs, horses, and farmed llamas (Tryland et al., 1998; Smith et al., 1999; Girling et al., 2011; Prkno et al., 2017; Diaz, 2021). CPXV's broad range is associated with its large genome, which is the largest genome among OPXVs (Gubser et al., 2004; Carroll et al., 2011). CPXV is polyphyletic (Carroll et al., 2011; Okeke et al., 2014; Franke et al., 2017; Mauldin et al., 2017), and their strains cluster in at least five clades (Mauldin et al., 2017; Jeske et al., 2019). Among them, some clades are more genetically similar to VACV (VACV-like virus) and VARV (VARV-like virus), whereas other CPXV strains appear as single branches and have a mosaic genome that contains genomic parts from different clades (Franke et al., 2017). The genetic heterogeneity inside CPXV could partially be due to recombination processes with other OPXV species or between CPXV clades (Okeke et al., 2012, 2014; Franke et al., 2017).

A poxvirus was isolated from an 18-year-old man living in the county Nordland, Norway (Hansen et al., 2009). Based on the detection of A-type inclusion (ATI) bodies, the sequence and phylogenetic analysis of hemagglutinin (*HA*) gene, cytokine response modifier B (*crmB*) gene, and Chinese hamster ovary host range (*CHOhr*) genes as well as *Hind III* restriction map, this virus was classified as a CPXV and was tentatively named CPXV-No-H2 (Hansen et al., 2009; Okeke et al., 2012). This isolate produces an atypical ATI phenotype, $V^{+/}$, in which the virions are encrusted only in the periphery of ATI (Okeke et al., 2012). The sequencing of two of the three genes (*atip*, *p4c*, and *A27L*) involved in the production of ATI with virions embedded into ATI (V^{+}) (Patel and Pickup, 1987; McKelvey et al., 2002; Howard et al., 2010) showed that it has intact *atip* and *p4c* genes. Furthermore, interestingly, the *atip* gene of CPXV-No-H2 closely related to that of ECTV with a bootstrap support of 100%, whereas the *p4c* gene was more diverse compared to the orthologs in other OPXVs (Okeke et al., 2012, 2014).

In this study, we report the whole sequence and genomic characterization of a Norwegian human CPXV isolate, CPXV-No-H2. We annotated the open reading frames, performed recombination analysis, and determined phylogenetic relationships with other OPXV genomes.

MATERIALS AND METHODS

Cell, Virus Culture, and DNA Isolation

The Fennoscandian CPXV No-H2 strain was isolated in 2001 from a human patient from Northern Norway (Hansen et al., 2009; Okeke et al., 2012). CPXV-No-H2 was cultured on a monolayer of Vero cells (ATCC No. CCL-81) in 175-cm^2 flasks (NUNC Sweden) as previously described (Okeke et al., 2012). Viral DNA was extracted from semi-purified virions using QIAGEN Genomic-tip 100/G and QIAGEN Genomic DNA Buffer Set, following the manufacturer's instructions (Qiagen, Hilden, Germany). DNA concentration was measured using NanoDrop 2000 spectrophotometer (Thermo Fischer Scientific^{TM}, Waltham, MA, United States).

Whole-Genome Sequencing

The genome of CPXV-No-H2 was sequenced using Illumina and Oxford Nanopore Technologies (ONT; Oxford, United Kingdom), respectively. The preparation of sequencing libraries and next-generation sequencing with Illumina was

performed at the Norwegian Sequencing Centre, Oslo. ThruPLEX DNA-Seq kit with an input DNA of 50 ng was used for the library preparation. Whole-genome sequencing was performed on an Illumina MiSeq instrument (Illumina Inc., San Diego, CA, United States) using MiSeq Reagent v3 (600 cycles), producing 2×300-bp paired-end reads. For nanopore sequencing, sequencing libraries were prepared using the Ligation Sequencing Kit SQK-LSK109 (ONT, Oxford, United Kingdom) and native barcoding expansion kit EXP-NBD104 and EXP-NBD114 (ONT). Up to 14 samples were multiplexed on R9.4 flow cells (FLO-MIN106). The run was performed on GridION X5 (Oxford, United Kingdom) using MinKNOW v20.10.6. Library preparation and nanopore sequencing were performed at the Genomics Support Centre Tromsø at UiT-The Arctic University of Norway.

Genome Assembly

Raw sequencing data from Illumina MiSeq were evaluated for their quality using FastQC software v0.11.8 (Andrews, 2010). Adapter removal and quality filtering were conducted using Trimmomatic v0.39 (Parameters: ILLUMINACLIP:TruSeq3-PE-2.fa:2:30:10 LEADING:3 TRAILING:3 SLIDINGWINDOW:4:20 MINLEN:36) (Bolger et al., 2014). In order to remove reads corresponding to host cells, filtered reads were mapped against *Chlorocebus sabaeus* (GCF_000409795.2) using FastQ Screen v0.14.1 (Wingett and Andrews, 2018) with BWA v.0.7.17 (Li and Durbin, 2009). The remaining reads were used in the genome assembly. Raw nanopore data (fast5 files) were base called using Guppy 4.2.3 in MinKNOW 20.10.6, with a qscore of 7 as filter, to produce Fastq formatted sequence files. Fastq sequences were demultiplexed using Guppy 4.2.3—likewise with barcode removal. Host sequences were filtered out using FastQ Screen v0.14.1 (Wingett and Andrews, 2018) with BWA v.0.7.17 (Li and Durbin, 2009) as described above. SPAdes v3.15.3 (Bankevich et al., 2012) was used to combine the ONT long reads and the Illumina reads to produce a hybrid assembly (with nanopore option and default parameters). Contigs were screened using BLAST[2] to remove host contamination. In order to assemble the complete genome, the Illumina reads were mapped to the contigs using Geneious mapper implemented in Geneious Prime 2020.2.4 (Biomatters, Inc., Newark, NJ, United States). Then, the extended contigs were merged into one by Geneious assembler in Geneious Prime 2020.2.4.

Genome Annotation

The assembled genome was annotated using Genome Annotation Transfer Utility (GATU) software from the Viral Bioinformatics Resource Centre (Tcherepanov et al., 2006). ECTV Moscow strain (ECTV_Mos), CPXV Brighton Red strain (CPXV_Br), and VACV Copenhagen strain (VACV_Cop) were used as reference genomes. These reference sequences were retrieved from the Viral Orthologous Clusters (VOCs) database (Ehlers et al., 2002). The GATU parameters included open reading frames (ORFs) longer than 30 amino acids, with a maximum overlap of 25%. Gene annotations from the reference genomes were transferred to the CPXV-No-H2 genome when the level of similarity was ≥80%. The putative coding sequences (CDS) with low similarity to the reference genes were subjected to a BLASTp analysis against the proteins belonging to the *Poxviridae* family from the NCBI database. Putative CDS with high similarity to other poxviruses were annotated. Similarly, the unassigned ORFs were investigated using BLASTp searches to find orthologous genes. In cases where more than one CDS were found in the same genomic region, the CDS with the highest similarity was selected. Geneious Prime 2020.2.4 was used to visualize, edit, and correct the annotations, if needed.

[2]https://blast.ncbi.nlm.nih.gov/Blast.cgi

Phylogenetic Analysis

For phylogenetic analysis, 75 OPXV genomes were retrieved from the VOCs database (Ehlers et al., 2002), except for CPXV_GerMygEK938_17, which was retrieved from GenBank. The OPXV genomes used in this study are listed in **Supplementary Table 1**. The alignments of (1) the genomes, excluding the inverted terminal repeats (ITRs; called core genome), (2) the genomic region from the first gene until the last gene (referred to as the whole genome), and (3) the orthologous genes of the 76 OPXVs (including CPXV-No-H2) were performed using MAFFT v1.4.0 (with default parameters; Katoh and Standley, 2013) implemented in Geneious Prime 2020.2.4. The poorly aligned positions were removed from the alignments (1 and 2) with Gblocks 0.91b using default parameters (Talavera and Castresana, 2007). The orthologous genes were identified using OrthoFinder v2.5.2 (Emms and Kelly, 2015). The orthologs (present in ≥95% of the genomes) were aligned as described above and concatenated in Geneious Prime 2020.2.4.

The phylogenetic relationship among these OPXVs was inferred by the maximum likelihood (ML) and Bayesian inference (BI) methods. ML trees were constructed in RAxML v.8.2.12 (Stamatakis, 2014) using the best-fitting nucleotide substitution model and 1,000 bootstrap replicates. The best-fit nucleotide substitution model for the alignment data was selected using the modelTest-NG v.0.1.6 (Darriba et al., 2020). BI analyses were performed using MrBayes v.3.2.7 (Ronquist et al., 2012) under the best-fitting substitution model with the following parameters: 2 million generations, nchains = 4, samplefreq = 500, and burninfrac = 0.25. The phylogenetic trees were visualized using FigTree v1.4.4 (Rambaut, 2018).

Gene Content Comparison

Predicted CDS from isolate CPXV-No-H2 were extracted, translated into amino acid sequences, and compared to the CPXV_Br, ECTV_Mos, or VACV_Cop proteins using BLASTp (ncbi-blast+ v2.11.0) (Camacho et al., 2009). To find the closest annotated proteins for all predicted CPXV-No-H2 CDS, every translated CPXV-No-H2 CDS was analyzed by BLASTp search against proteins of the *Poxviridae* family. A BLASTn identity analysis was performed on predicted CPXV-No-H2 CDS that encode proteins with a higher identity to other OPXV proteins than CPXV proteins. When the first hit in BLASTp or BLAStn was CPXV-No-H2 protein or genome, the second hit was used.

Investigation of Potential Recombination Events

The genome sequence of CPXV-No-H2 was examined for potential recombination events using recombination detection program 4 (RPD4) (Martin et al., 2015) and SimPlot v3.5.1 (Lole et al., 1999). A putative recombinant event was taken into account if it was identified by RDP4 and/or Simplot analysis and the sequence was most similar to the possible minor parental. The whole genome of CPXV-No-H2 was aligned to other OPXV genomes used as putative parentals (AKPV, CPXV_Gri, CPXV_GerMygEK938_17, ECTV_Mos, MPXV_Zaire, and VACV_LC16m8), with MAFFT v1.4.0 (Katoh and Standley, 2013) implemented in Geneious Prime 2020.2.4. Gaps were not removed from the multiple alignments. Similarity plots were performed on the multiple alignments using the SimPlot program (Lole et al., 1999) with default settings. Putative recombination breakpoints were determined by maximization of χ^2 analysis (Lole et al., 1999; Lim et al., 2011). For recombination analysis with RPD4, seven methods [RDP (Martin and Rybicki, 2000), GENECONV (Padidam et al., 1999), Bootscan (Martin et al., 2005), MaxChi (Smith, 1992), Chimaera (Posada and Crandall, 2001), SiScan (Gibbs et al., 2000), and 3Seq (Boni et al., 2007)] were used to detect potential recombination events. RDP4 was used with the default parameters, except for the option "require topological evidence." The recombination events that were identified by 6 of 7 methods with significant *p*-values ($p \leq 0.01$) were considered potential recombinant events. The beginning and end of the breakpoints of these events suggested by RPD4 were used to identify the potential recombinant sequence. When the breakpoints were not identified by RDP4, the range of positions of the breakpoints obtained by Simplot analysis was used. Those potential recombinant sequences were utilized to build an ML tree using RAxML v.8.2.12 (Stamatakis, 2014). Phylogenetic tree incongruence was further used to map potential recombination sequences. Furthermore, a BLASTn identity analysis was performed on those potential recombinant sequences.

RESULTS

Genome Assembly and Genome Annotation

Two large contigs (>1000 bp) were obtained with the hybrid assembly and after removing the host contamination. The average coverage of the major and minor contig was 1502X and 735X, respectively. The mean genomic coverage of CPXV-No-H2 was 1370X. The assembled whole-genome length of CPXV-No-H2 was 220,276 bp. The ITR regions were approximately 7 kbp, and the central region was 206,204 bp. The A+T content of the CPXV-No-H2 genome was 66.6%. Genome annotation predicted 217 potential genes in the CPXV-No-H2 genome (**Figure 1** and **Supplementary Table 2**). The overlapping genes were excluded from the annotation process. However, there were 20 predicted overlapping genes (**Supplementary Table 3**). Some of them were homologs of CPXV_Br genes (*CPXV004*, *CXPV47*, *CPXV51A*, *CPXV058*, *CPXV078A*, *CPXV096*, *CPXV116*, *CPXV119A*, *CPXV130*, *CPXV152A*, *CPXV160*, *CPXV170*, and *CPXV214*). The whole genome sequence is deposited in GenBank with accession number OM460002.

Phylogenetic Analysis

The phylogenetic analysis showed that the ML tree topologies were similar to the phylogenetic trees generated by the BI method, regardless of the alignments used. The BI phylogenetic trees had strong posterior probabilities in most nodes (≥0.95) (**Figures 2–4**). Unlike the BI trees, the ML trees had low clade support (<70%) in some of the nodes (**Supplementary Figures 2–4**). The BI phylogenetic trees of 76 OPXV whole genomes, 76 OPXV core genomes, and 134 OPXV orthologous genes are shown in **Figures 2–4**, respectively. The Old World and New World OPXV were separated into two groups in the phylogenetic trees generated from 76 OPXV whole genomes (**Figure 2**), 76 OPXV core genomes (**Figure 3**), and 134 OPXV orthologous genes (**Figure 4**). Within the Old World OPXV, the strains from the same OPXV species were grouped into clusters, except for CPXV strains that formed more than one cluster. CPXV was divided into clusters: CPXV-like 1, CPXV-like 2, VARV-like, VACV-like, and new clade (Franke et al., 2017). Although the strains of VACV-like did not form a proper cluster, they were closely related VACV (**Figures 2–4**).

The new clade comprised CPXV-No-H2 and two German CPXV isolates: CPXV_GerMygEK938_17 and CPXV_Ger2010_MKY (posterior probabilities of 1.0 and bootstrap values of 100%) (**Figures 2–4** and **Supplementary Figures 2–4**). The CPXV-No-H2 genome was most similar to the CPXV_GerMygEK_938_17 genome (96.38% identical), and the second most similar virus was CPXV_Ger2010_MKY (96.26% identical), based on the alignment of 76 OPXV whole genomes. The new clade was closely related to the ECTV/Abatino clade. Both clades formed a major clade together (posterior probabilities of 1.0 and bootstrap values > 89%) (**Figures 2–4** and **Supplementary Figures 2–4**). In this study, the new clade (CPXV-No-H2/CPXV_GerMygEK938_17/ CPXV_Ger2010_MKY) was tentatively named "ECTV-Abatino-like."

In phylogenetic trees derived from the 134 OPXV orthologous genes, the ECTV-Abatino-like/ECTV/OPXV Abatino clade clustered with CPXV_Ger1998/CPXV-like 2 clade with a strong posterior probability (1.0), but with a low bootstrap support value (46%) (**Figure 4** and **Supplementary Figure 4**), whereas the phylogeny of the 76 OPXV whole and core genomes showed that the ECTV-Abatino-like/ECTV/OPXV Abatino clade was separated from the other Old World OPXV, which formed a major polyphyletic clade (posterior probability of 1.0 and bootstrap values > 81%) (**Figures 2**, **3** and **Supplementary Figures 2, 3**). This major polyphyletic clade was further resolved in two groups: the CPXV_Ger1998/CPXV-like 2 clade (posterior probability of 1.0 and bootstrap values of 100%) and a larger group containing CPXV-like 1, VARV-like, VARV-TATV-CMLV, CPXV_HumLit08, VACV-like, MPXV, RPXV, and VACV clades (posterior probabilities of 1.0 and bootstrap values of 100%) (**Figures 2**, **3** and **Supplementary Figures 2, 3**). The clustering

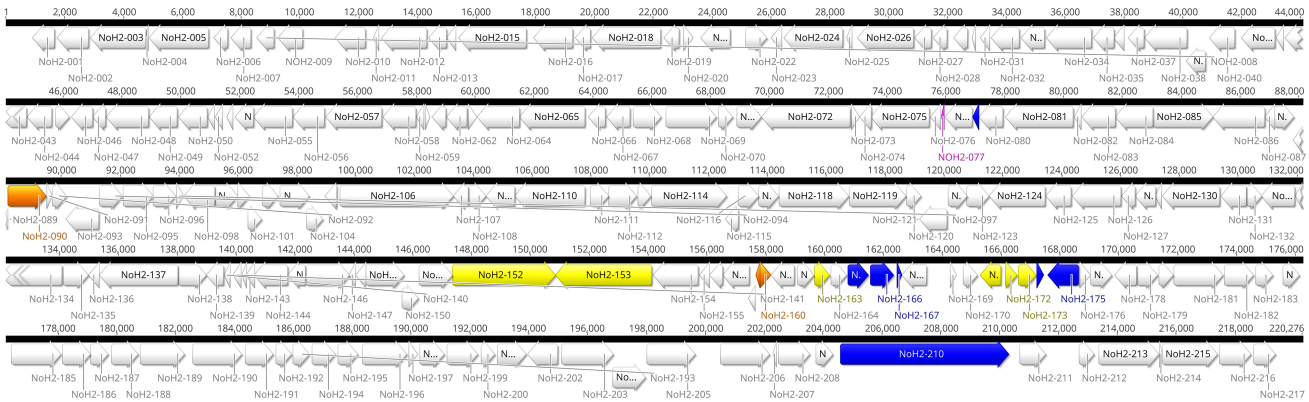

FIGURE 1 | Genome map of CPXV-No-H2. Localization of 217 predicted coding sequences (CDS) and nine putative recombination events in the CPXV-No-H2 genome. Green blocks represent the putative recombination events. Other colors were used to visualize the amino acid sequence similarity between translated CDS to other OPXV proteins: blue blocks represent CDS with a higher similarity to *Alaskapox virus* proteins, yellow blocks represent CDS with a higher similarity to *Ectromelia virus* (ECTV) proteins, orange blocks represent CDS with a higher similarity to *Vaccinia virus* (VACV) proteins, and fuchsia block represents the CDS with a higher similarity to ECTV, VACV, and *Horsepox virus* proteins.

within this monophyletic group apparently differs between the tree based on 76 OPXV whole genomes and the trees built from 76 OPXV core genomes and 134 OPXV orthologous genes (**Figures 2–4** and **Supplementary Figures 2–4**). In the former, CPXV-like 1 branches separated from other members of the large polyphyletic group (**Figure 2** and **Supplementary Figure 2**). These members formed a cluster and were further split into two clusters: the VARV-like/TATV/CMLV/VARV cluster and the CPXV_HumLit08/VACV-like/MPXV/RPXV/VACV cluster. Both clusters were supported by strong posterior probabilities (1.0) and bootstrap values (100%) (**Figure 2** and **Supplementary Figure 2**), while 76 OPXV core genomes and 134 OPXV orthologous gene phylogenies grouped CPXV-like 1 into the same cluster with VARV-like/TATV/CMLV/VARV, with posterior probabilities of 0.99 and 1.0 and bootstrap values of 51 and 99%, respectively (**Figures 3**, **4** and **Supplementary Figures 3, 4**). Additionally, CPXV_HumLit08, VACV-like, MPXV, RPXV, and VACV were grouped into the same cluster, with posterior probabilities of 1.0 and bootstrap values of 100%.

However irrespective of the aforementioned differences between the whole genome tree on one hand and the core genome and the concatenated 134 orthologous genes on the other, the following topologies were consistent in all the trees generated from the three distinct datasets: (i) ECTV-Abatino-like CPXV clustered closely with ECTV-OPXV Abatino clade, (ii) VACV-like CPXV grouped together with VACV, (iii) VARV-like CPXV clustered closely with VARV-TATV-CMLV clade, (iv) CPXV-like 1 clade is sister to VACV-like clade, and (vi) AKPV/AKMV are intermediate between Old World and New World OPXV.

Gene Content Comparison

The gene content and organization of the CPXV-No-H2 genome were similar to that of the CPXV_Br and ECTV_Mos genomes. All CPXV_Br genes (excluding ITR genes) were found in the CPXV-No-H2 genome, except for *CPXV221* (encodes CrmD protein) and *CPXV192* (encodes CPXV192 protein). The last gene is truncated in CPXV-No-H2 and overlapped to a major predicted gene. Similarly, comparing CPXV-No-H2 and ECTV_Mos, it was shown that *EVM003/170* (homolog to *CPXV221*) was missing in the CPXV-No-H2 genome. Additionally, the *EVM006* gene (encodes C-type lectin) was absent in the CPXV-No-H2 genome.

The predicted gene *NoH2-154* encodes an intact p4c protein compared to CPXV_Br, whose *p4c* gene is disrupted in two fragments (*CPXV159* and *CPXV161*). Similarly, this gene is fragmented in ECTV_Mos (Chen et al., 2003). The BLASTp analysis for NoH2-154 revealed that the best hit was an inclusion protein III from *Buffalopox virus*, with 87.7% identity. This protein (501 aa) was smaller than the p4c protein from CPXV-No-H2 (512 aa). The next best BLASTp hits were longer proteins of 527 aa from CPXV_Ger2010_MKY and 523 aa from CPXV_GerMygEK938_17, which shared 88.6 and 89.12% identity with p4c protein from CPXV-No-H2, respectively. BLASTn showed that the CPXV-No-H2 *p4c* gene was most similar to the *p4c* gene from CPXV_GerMygEK938_17.

Within ITRs of CPXV-No-H2, five of eight duplicate CPXV_Br genes were found (*CPXV003/227*, *CPXV005/226*, *CPXV006/225*, *CPXV007/224*, and *CPXV008/223*). The terminal *CPXV004* gene was also found in both ITRs of CPXV-No-H2 (*NoH2-A* and *NoH2-T*) (**Supplementary Table 3**), but they overlapped two major predicted genes (*NoH2-002* and *NoH2-216*). Interestingly, *NoH2-006*, the ortholog of *CPXV009/222*, was found as a single copy downstream of the left ITR of the CPXV-No-H2 genome (**Figure 1**).

All predicted genes in CPXV-No-H2 were found to have homologs in either CPXV_Br, ECTV_Mos, or VACV_Cop, except for *NoH2*-008 and *NoH2-212*. The translated *NoH2-008* CDS shared 100% amino acid identity with the hypothetical protein CPXV0285 of CPXV_FM2292 (CRL86746.1) and CPXV_Ger2007_Vole (SBN49117.1). The predicted gene *NoH2-212* was a homolog of *CPXV-GRI-K3R* (encodes CrmE protein). The BLASTp analysis of this translated CDS showed

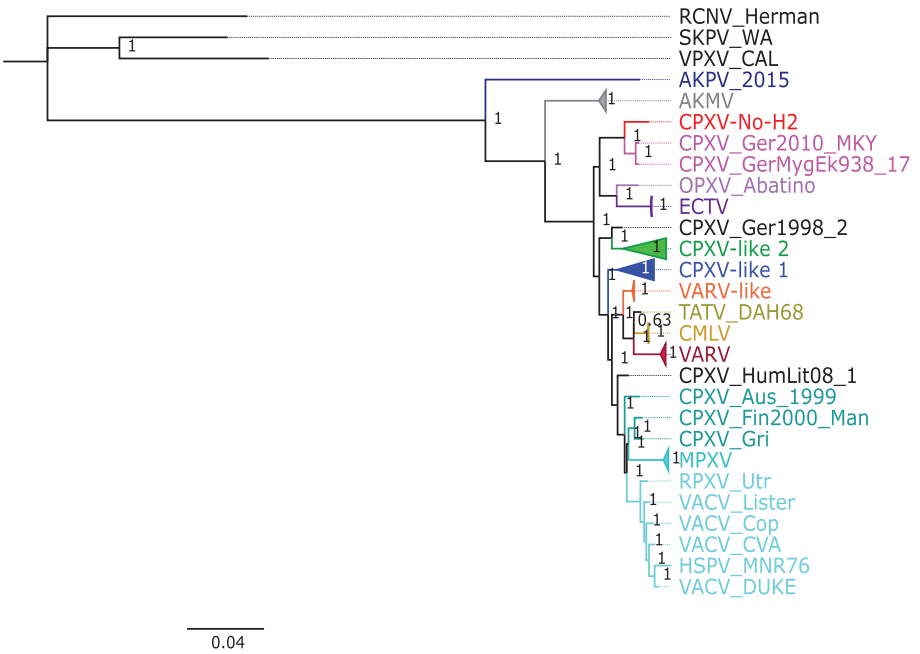

FIGURE 2 | Bayesian inference phylogenetic tree based on 76 orthopoxvirus whole genomes. Posterior probabilities are shown on the right side of each node, and only posterior probabilities above 0.6 are shown. The cowpox virus strains were grouped into different clades: CPXV-like 1, CPXV-like 2, and VARV-like (Franke et al., 2017). The scale bar represents the expected substitutions per site.

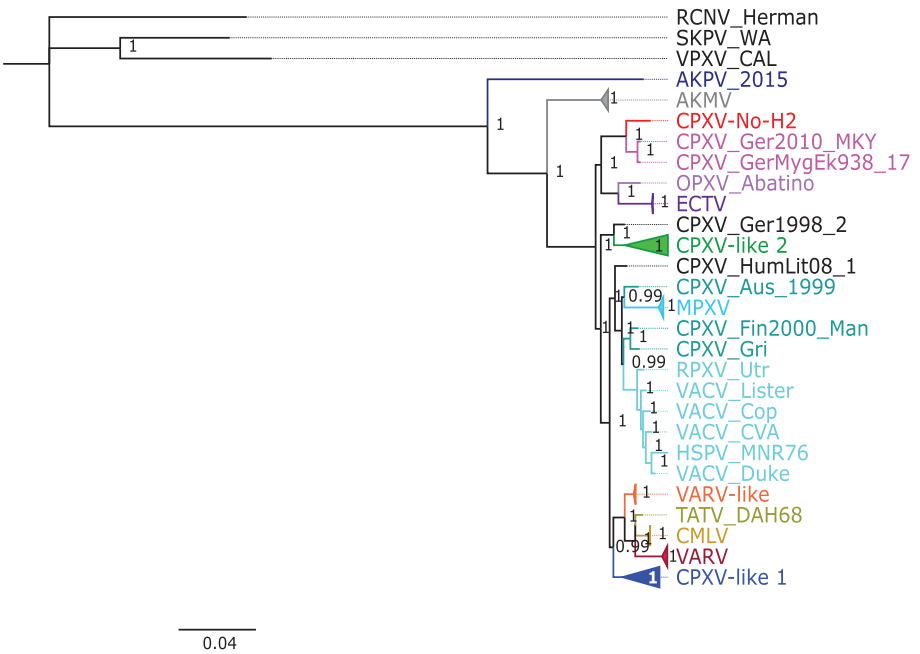

FIGURE 3 | Bayesian inference phylogenetic tree based on 76 orthopoxvirus core genomes. Posterior probabilities are shown on the right side of each node, and only posterior probabilities above 0.6 are shown. The cowpox virus (CPXV) strains were grouped into different clades: CPXV-like 1, CPXV-like 2, and VARV-like (Franke et al., 2017). The scale bar represents the expected substitutions per site.

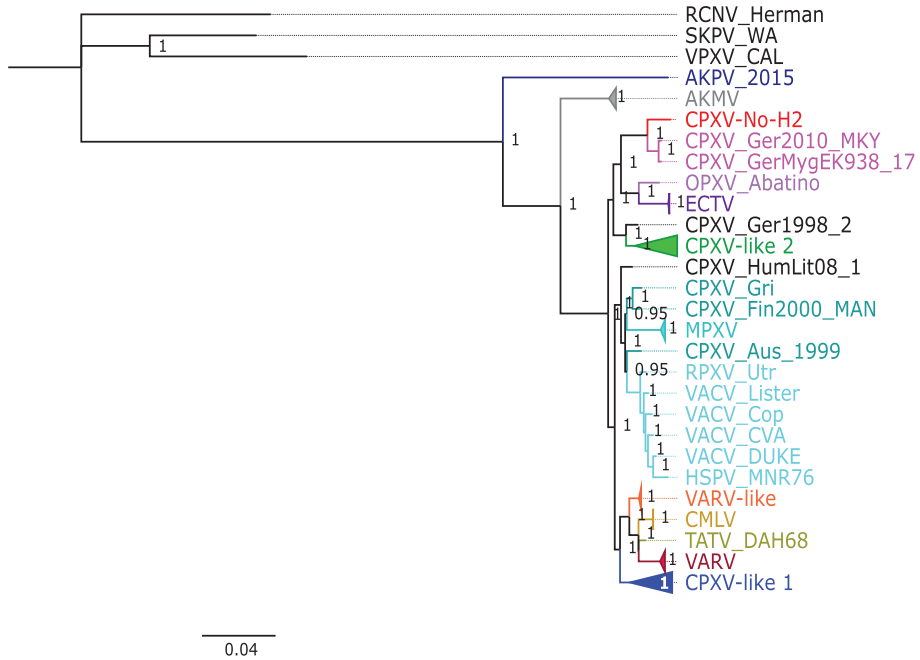

FIGURE 4 | Bayesian inference phylogenetic tree based on 134 orthopoxvirus orthologous genes. Posterior probabilities are shown on the right side of each node, and only posterior probabilities above 0.6 are shown. The cowpox virus (CPXV) strains were grouped into different clades: CPXV-like 1, CPXV-like 2, and VARV-like (Franke et al., 2017). The scale bar represents the expected substitutions per site.

that it shared the highest amino acid identity (95.2%) with a CPXV_GerMygEK938_17 protein (hypothetical protein pCPXV003 CAB5514210.1). The *NoH2-212* gene was located upstream of the right ITR of CPXV-No-H2 (**Figure 1**).

Of the 217 predicted genes of CPXV-No-H2, 17 coded for proteins that were most similar to other OPXV proteins than CPXV proteins. Seven of them shared high similarity to North American OPXV proteins, AKPV, and 10 genes were most similar to Old World OPXV proteins, including ECTV and VACV (**Supplementary Table 4**). The seven predicted CPXV-No-H2 proteins were most similar (i.e., >92% amino acid identity) to AKPV proteins, including NoH2-079, NoH2-165, NoH2-166, NoH2-167, NoH2-174, NoH2-175, and NoH2-210. The BLASTn analysis of their seven predicted CPXV-No-H2 genes revealed that *NoH2-079*, *NoH2-165*, *NoH2-166*, *NoH2-167*, *NoH2-174*, and *NoH2-210* shared the highest similarity (i.e., > 97% nucleotide identity) with *AKPV-076*, *AKPV-162*, *AKPV-163*, *AKPV-164*, *AKPV-171*, and *AKPV-203*, respectively, whereas *NoH2-175* shared the highest nucleotide similarity with CPXV_GerMygEK938_17/CPXV_Ger2010_MKY. However, the BLASTn analysis of *NoH2-175* with the intergenic region between *NoH2-174* and *NoH2-175* revealed the highest similarity with AKPV (93.98% nucleotide identity).

The six predicted proteins most identical (i.e., > 94% amino acid identity) to ECTV proteins were NoH2-152, NoH2-153, NoH2-163, NoH2-171, NoH2-172, and NoH2-173. At the nucleotide level, *NoH2-152*, *NoH2-153*, *NoH2-171*, *NoH2-172*, and *NoH2-173* had > 95% identity with the corresponding ECTV *EVM127*, *EVM128*, *EVM140*, *EVM141*, and *EVM142* genes. The *NoH2-163* gene, however, was most similar to *CPXV169* from CPXV_GerMygEK938_17 and CPXV_Ger2010_MKY (98.6% identity), whereas the next best BLASTn hit was an ECTV gene with 98.4% identity. The difference between their percent identities was due to one identical nucleotide (**Supplementary Figure 1**).

The three CPXV-No-H2 predicted proteins most similar to VACV proteins included NoH2-090, NoH2-159, and NoH2-160. The BLASTn search of these predicted genes revealed that *NoH2-159* shared 100% nucleotide identity with VACV, BPXV, and CPXV genomes, and *NoH2-160* was 98.4% identical to VACV LC16m8 (*m8197R*) and VACV LC16mO genes (*mO197R*). The predicted protein of the gene *NoH2-077* was 100% identical to ECTV, HSPV, and VACV proteins. However, the BLASTn of this predicted gene showed that it was 100% identical to CPXV_GerMygEK938_17 genome, but this region was not annotated.

Overlapping genes were excluded from the annotation process. There were 20 overlapping predicted genes (**Supplementary Table 3**). Fourteen of them were homologs of CPXV_Br (*CPXV004*, *CXPV47*, *CPXV51A*, *CPXV058, CPXV078A*, *CPXV096*, *CPXV116*, *CPXV119A*, *CPXV130*, *CPXV152A*, *CPXV160*, *CPXV170*, and *CPXV214*). Another six overlapping genes did not correspond to any annotated CPXV gene. The BLASTp analysis of the protein encoded by the six overlapping genes revealed that five shared the highest similarity (> 83% amino acid identity) to CMLV_0408151v (NoH2-B), OPXV Abatino (NoH2-H), VACV_CEyV1

(NoH2-G and NoH2-N), or VACV_Lister (NoH2-R) proteins (**Supplementary Table 3**).

Recombination Analysis

Previous studies by our group had identified a putative crossover event downstream of the *atip* gene (Okeke et al., 2012). Consequently, the complete CPXV-No-H2 genome was examined for recombination because it contained genomic regions with predicted genes similar to AKPV, ECTV, or VACV genomes. Nine putative recombination events were predicted by RDP4 and Simplot analysis for the CPXV-No-H2 genome (**Table 1** and **Figure 1**). Six potential recombination regions were a result of recombination events between the parentals of AKPV and CPXV (putative recombination events 1–6), two originated from recombination events between the parental ECTV and CPXV (putative recombination events 7 and 8), and one was a product of a recombination event between the parental VACV and CPXV (putative recombination event 9) (**Table 1**). Within the nine putative recombinant regions in CPXV-No-H2, only one recombinant region (putative recombination event 6) was close to terminal regions, whereas the other eight recombinant regions were located in the central region of the genome.

The first potential recombinant region in the CPXV-No-H2 genome (putative recombination event 1) comprised the *NoH2-079* gene and started from position 76,946 bp in the CPXV-No-H2. The ending breaking could be between positions 77,201 and 77,208 bp in the CPXV-No-H2 genome based on Simplot analysis. The next potential recombinant region (putative recombination event 2) was almost 500 bp downstream of the first one. It was located between 77,741 and 78,243 bp in the CPXV-No-H2 genome and contained parts of *NoH2-080* and *NoH2-081*. These two putative recombinant regions shared the highest similarity to the AKPV genome (>98% identical) (**Supplementary Table 5**).

The third potential recombinant region (putative recombination event 3) spanned approximately 4,500 bp, from position 150,156 to 154,530 bp in the CPXV-No-H2 genome. However, it overlapped with the predicted recombinant region between the parental ECTV and CPXV (putative recombination event 7), located between 150,119 and 153,968 bp in the CPXV-No-H2 genome. The latter encompassed only two genes, *NoH2-152* and *No-153*, compared to the former that also contained part of the *NoH2-154* gene. The BLASTn analysis of the third potential recombinant region revealed the highest similarity with the AKPV genome (96.89% identical), whereas the putative recombinant region between the parental ECTV and CPXV was most similar to the ECTV genomes, with 97.93% nucleotide identity (**Supplementary Table 5**).

The fourth potential recombinant region in the CPXV-No-H2 genome (putative recombination event 4) included the genes *NoH2-165*, *NoH2-166*, and *NoH2-167* and part of *NoH2-168*. The Simplot analysis revealed that the beginning and ending breakpoints were located between 160,774 and 160,878 bp and between 162,909 and 162,948 bp in the CPXV-No-H2 genome, respectively. This genomic region was most similar to the AKPV genome, sharing 97.66% nucleotide identity (**Supplementary Table 5**). The fifth potential recombinant region (putative recombination event 5) started from 165,874 to 168,063 bp in the CPXV-No-H2 genome. It overlapped with another putative recombinant region between the parental ECTV and CPXV (putative recombination event 8), which was located between 165,847 and 167,892 bp in the CPXV-No-H2 genome. Both regions contained part of *NoH2-171*, *NoH2-172*, *NoH2-173*, and *NoH2-174* and part of *NoH2-175*. The BLASTn analysis of these two putative recombination regions revealed that the first hit was the AKPV genome, with > 97% nucleotide identity (**Supplementary Table 5**).

A sixth potential recombinant event between the parental AKPV and CPXV (putative recombination event 6) was detected only by Simplot analysis. The cross-over points lay between 204,960 and 204,977 bp and between 209,488 and 209,901 bp in the CPXV-No-H2 genome. It contained a major part of the *NoH2-210* gene, which was most similar to AKPV-203 (97.15% identical) and also shared similarity with the Murmansk-007 gene (91.44% identical). Furthermore, this putative recombinant sequence showed its highest identity with the AKPV genome (98.4% identical), followed by the *Murmansk microtuspox virus* genome (91.44% identical).

One putative recombination event between the parental VACV and CPXV (putative recombination event 9) was detected. The breakpoints were undetermined by RDP4, but the Simplot analysis revealed that the putative recombinant sequence started from position 164,400–164,525 bp and ended at position 164,756–164,768 bp in the CPXV-No-H2 genome. This region contained a small part of *NoH2-169* and a major part of *NoH2-170*. The latter gene shared 94.44% identity with the genes of CPXV and RPXV and the VACV strains, such as Lister, Cantagalo, CVA, and NYCBH.

The phylogenetic analysis of the six putative recombinant regions between the parental AKPV and CPXV showed that CPXV-No-H2 clustered with AKPV with a bootstrap support of > 91%, except for the phylogenetic tree based on the fifth putative recombinant region (165,874–168,063 bp in the CPXV-No-H2 genome), where CPXV-No-H2 clustered with ECTV with a low bootstrap support (55%), and they were grouped with AKPV (bootstrap value of 100%) (**Supplementary Figures 5–10**). CPXV-No-H2 likewise clustered with ECTV in the phylogenetic tree generated from the potential recombinant region between the parental ECTV and CPXV (165,847–167,892 bp in the CPXV-No-H2 genome) that overlapped the fifth putative recombinant region (**Supplementary Figure 12**). Unlike the previous phylogenetic tree, the bootstrap support for this clade was higher (93%) though.

Based on the phylogenetic analysis of the putative recombinant sequence between the parental ECTV and CPXV (150,119–153,968 bp in the CPXV-No-H2 genome), CPXV-No-H2 formed a cluster with ECTV (**Supplementary Figure 11**). This cluster was most closely related to AKPV and formed a major clade, with AKPV and AKMV, separating them from other Old World OPXV. However, the phylogenetic tree of the recombinant region between the parental AKPV and CPXV (150,156–154,530 bp in the CPXV-No-H2 genome), which overlapped that recombinant region, clustered CPXV-No-H2 with AKPV, and both isolates were closely related to ECTV

TABLE 1 | Predicted recombination events in the CPXV-No-H2 genome using recombination detection program 4 (RPD4) and Simplot analysis.

Putative parental strains	Major parental	Minor parental	Recombinant virus	Recombination event	RDP4			Simplot	
					Breakpoint in CPXV-No-H2		Recombination detection programs	Breakpoint interval in CPXV-No-H2	
					Begin (bp)	End (bp)		Begin (bp)	End (bp)
AKPV, CPXV_GerMygEK938_17, CPXV_Gri, CPXV-No-H2	CPXV_GerMygEK938_17	AKPV	CPXV-No-H2	1	76,946	77,244*	RDP, GENECONV, Bootscan, MaxChi, Chimaera, 3Seq	76,679–76,957	77,201–77,208
	CPXV_GerMygEK938_17	AKPV	CPXV-No-H2	2	77,741	78,243	RDP, GENECONV, Bootscan, MaxChi, Chimaera, 3Seq	77,717–77,765	78,237–78,399
	CPXV_GerMygEK938_17	AKPV	CPXV-No-H2	3	150,156	154,530	GENECONV, Bootscan, MaxChi, Chimaera, SiScan, 3Seq	150041–150158	154,524–154,570
	CPXV_GerMygEK938_17	AKPV	CPXV-No-H2	4	160,988*	162,917*	RDP, GENECONV, Bootscan, MaxChi, Chimaera, SiScan, 3Seq	160,774–160,878	162,909–162,948
	CPXV_GerMygEK938_17	AKPV	CPXV-No-H2	5	165,874	168,063	RDP, GENECONV, Bootscan, MaxChi, Chimaera, SiScan, 3Seq	165,828–165,878	168,042–168,066
	CPXV_GerMygEK938_17	AKPV	CPXV-No-H2	6	-	-	-	204,960–204,977	209,498–209,901
ECTV_Mos, CPXV_GerMygEK938_17, CPXV_Gri, CPXV-No-H2	CPXV_GerMygEK938_17	ECTV_Mos	CPXV-No-H2	7	150,119	153,968	GENECONV, Bootscan, MaxChi, Chimaera, SiScan, 3Seq	149,993–150,158	153,952–154,180
	CPXV_GerMygEK938_17	ECTV_Mos	CPXV-No-H2	8	165,847	167,892	RDP, GENECONV, Bootscan, MaxChi, Chimaera, SiScan, 3Seq	165,678–165,855	167,879–167,943
VACV_LC16m8, CPXV_GerMygEK938_17, CPXV_Gri, CPXV-No-H2	CPXV_GerMygEK938_17	VACV_LC16m8	CPXV-No-H2	9	164,419*	165,036*	RDP, Bootscan, MaxChi, Chimaera, SiScan, 3Seq	164,399–164,525	164,756–164,768

The breakpoint that was undetermined is marked with an asterisk. AKPV, Alaskapox virus; CPXV, Cowpox virus; ECTV, Ectromelia virus; VACV, Vaccinia virus. The breakpoint that was undetermined is marked with an asterisk.

(**Supplementary Figure 7**). The phylogenetic tree based on the putative recombinant sequence between the parental VACV and CPXV placed CPXV-No-H2 inside the VACV cluster (**Supplementary Figure 13**).

DISCUSSION

CPXV-No-H2 is an isolate from a human in Northern Norway that was classified as an atypical CPXV based on ATI phenotype, sequence of the *atip* and *p4c* genes, and Hind III restriction map (Hansen et al., 2009; Okeke et al., 2012). Our phylogeny analysis indicated that CPXV-No-H2 is most closely related to the German CPXV isolates CPXV_GerMygEK938_17 and CPXV_Ger2010_MKY (**Figures 2–4**). Similarly, phylogenetic analysis based on the *HA* gene also resolved CPXV_Ger2010_MKY and CPXV-No-H2 in the same cluster (Kalthoff et al., 2014). The three CPXV isolates (CPXV_GerMygEK938_17, CPXV_Ger2010_MKY, and CPXV-No-H2) may be part of a novel CPXV lineage separated from the other CPXV strains. It was previously suggested that CPXV_Ger2010_MKY and CPXV_GerMygEK938_17 were part of a new cluster provisionally called CPXV-like 3 (Franke et al., 2017; Jeske et al., 2019). However, this cluster was supported by a low bootstrap value (Jeske et al., 2019). The phylogenetic analysis reported in our study indicated that the new clade (CPXV-No-H2/CPXV_GerMygEK938_17/CPXV_Ger2010_MKY) was more closely related to ECTV and OPXV Abatino than other OPXVs, with strong posterior probabilities and bootstrap values (**Figures 2–4** and **Supplementary Figures 2–4**). Thus, we tentatively named this clade as "ECTV-Abatino-like."

The ECTV-Abatino-like/ECTV/OPXV Abatino clade was separated from the Old World OPXV in 76 OPXV whole- and core-genome phylogenetic trees, while a phylogenetic tree based on 134 OPXV orthologous genes showed that this clade clustered closely with CPXV_Ger1998/CPXV-like 2 but with poor bootstrap support (46%). We suggest that the separation of ECTV-Abatino-like/ECTV/OPXV Abatino from the other Old World OPXV may be due to the presence of some genes (or genomic regions) located in the core genome, which are not included within the 134 OPXV orthologous genes. A previous study showed that CPXV_GerMygEK938_17/CPXV_Ger2010_MKY/ECTV/OPXV Abatino clustered with CPXV-like 2 but with low bootstrap support (< 70%) (Jeske et al., 2019), although AKPV was not included in their phylogenetic analysis compared to our study that included AKPV and more OPXV strains. When AKPV was excluded from the construction of our phylogenetic trees, the ECTV-Abatino-like/ECTV/OPXV Abatino clade clustered with CPXV_Ger1998/CPXV-like 2 in 75 OPXV whole- and core-genome phylogenetic trees but with low bootstrap support (**Supplementary Figures 14–17**). In contrast, the bootstrap value in the node that clustered these clades increased from 46 to 82% in the phylogenetic tree based on 134 OPXV orthologous genes (**Supplementary Figures 18, 19**). We suspect that the genes or genomic regions that separated those clades have homologs in AKPV—for instance, homologs of *NoH2-166*, *NoH2-167*, *NoH2-174*, and *NoH2-210* genes, which were most similar to the AKPV genes, were not included in the construction of the phylogenetic tree based on 134 OPXV orthologous genes.

In fact, CPXV-No-H2 has a mosaic genome with genes most similar to the OPXV genes from the Old World, including ECTV and VACV, and the North America, AKPV. Previously, we have shown that the *atip* gene from CPXV-No-H2 displayed the highest similarity to the corresponding ECTV gene, and the insertion of the ECTV *atip* gene may be a result of the recombination between CPXV and ECTV or an ECTV-like virus (Okeke et al., 2012). Our present study suggested similar findings and indicated that CPXV-No-H2 has also undergone recombination events between AKPV and VACV. A recombination between OPXVs has been reported by others (Gubser et al., 2004; Coulson and Upton, 2011; Qin et al., 2011, 2015; Okeke et al., 2012; Smithson et al., 2014, 2017a; Franke et al., 2017; Gao et al., 2018; Gigante et al., 2019).

CPXV-No-H2 displays recombination events with OPXVs that were isolated from different places and species. CPXV-No-H2 is a strain from Northern Norway (Okeke et al., 2012). Its closest relatives CPXV_GerMygEK938_17 and CPXV_Ger2010_MKY were isolated in Germany, but they were isolated from different species: bank vole and cotton-top tamarin, respectively (Kalthoff et al., 2014; Jeske et al., 2019). It was suggested that the infection of cotton-top tamarin was mediated by bank vole infected with CPXV (Jeske et al., 2019; Weber et al., 2020). In contrast, AKPV was isolated from a human patient in North America (Alaska, the United States). The patient's infection source is unknown, but it is presumable that she was infected by a small mammal (Springer et al., 2017; Gigante et al., 2019). VACV and ECTV have been reported around the world (Dumbell and Richardson, 1993; Miranda et al., 2017; Mavian et al., 2021). ECTV infects laboratory mice worldwide (Trentin and Briody, 1953; Mavian et al., 2021; Wang et al., 2021). The first discovered ECTV strain, ECTV_Hampstead, was isolated in the United Kingdom and was the progenitor of the European outbreaks. Only one ECTV strain (ECTV_MouKre) was isolated from a wild mouse in Germany (Mavian et al., 2021). The worldwide presence of ECTV in animals suggests their presence also in Norwegian fauna and hence the possibility to recombine with CPXV.

Among the nine potential recombination events in the CPXV-No-H2 genome, two potential recombination events with the parental AKPV (putative recombination events 3 and 5) overlap with two potential recombination events with the parental ECTV (putative recombination events 6 and 7). Interestingly, in the same position of these recombinant regions, AKPV has undergone a potential recombination with ECTV, and it was suggested that ECTV contains an AKPV-like sequence (Gigante et al., 2019).

These recombinant regions (putative recombination events 5 and 8) contain the *atip* gene, which is one of the three genes (*atip*, *p4c*, and *A27L*) required for the formation of the V^+ ATI phenotype (Patel and Pickup, 1987; McKelvey et al., 2002; Howard et al., 2010). CPXV-No-H2 contains an intact ECTV-like *atip*, *p4c*, and *A27L* genes. Those latter genes

were most similar to CPXV_GerMygEK938_17 genes. CPXV-No-H2 produces mainly virions encrusted on the surface of ATI ($V^{+/}$) similar to ECTV_Hampstead, which produces both V^+ and $V^{+/}$ ATI phenotype (Ichihashi and Matsumoto, 1966; Okeke et al., 2012; Mavian et al., 2021). ECTV_Hampstead encodes a full-length p4c protein compared to other ECTV isolates with V^- ATI phenotype. Besides this, it contains the *atip* and *A27L* genes (Mavian et al., 2021). AKPV and CPXV_Ger2010_MKY also comprise these three genes and produce the V^+ ATI phenotype (Franke et al., 2017; Springer et al., 2017; Gigante et al., 2019). There is no report of the production of ATI bodies in CPXV_GerMygEK938_17; however, its *atip*, *p4c*, and *A27L* genes are most similar to those of CPXV_Ger2010_MKY.

The potential recombination event between the parental AKPV and CPXV (putative recombinant event 6) located close to the terminal region contains part of the *NoH2-210* gene that shared similarity with *AKPV-203* and the Murmansk gene. *AKPV-203* is one of the three AKPV genes that may be introduced from/to Murmansk poxvirus by recombination (Gigante et al., 2019). Murmansk is a non-OPXV that belongs to the genus *Centapoxvirus* that was isolated in Murmansk, Russia (Smithson et al., 2017a). In three of the six recombination events with the parental AKPV (putative recombination events 1, 4, and 6), it seems that CPXV-No-H2 contains AKPV-like sequences rather than AKPV containing CPXV-No-H2-like sequences because the phylogenetic trees showed that CPXV-No-H2 is not part of the ECTV-Abatino-like clade and was placed next to AKPV (**Supplementary Figures 5, 8, 10**). In contrast, the overlapping recombinant regions seem to be CPXV-No-H2-like sequences that were introduced to AKPV based on the phylogenetic tree and the sequence similarity (**Supplementary Figures 7, 9, 11, 12**).

Reconstructing the evolutionary history of CPXV-No-H2 is difficult since it displays several potential recombination events with different OPXVs, especially when it is suspected that recombination events occurred between these OPXVs (such as AKPV and ECTV) (Gigante et al., 2019). Additionally, these OPXVs were isolated from different continents (Springer et al., 2017; Mavian et al., 2021). One plausible hypothesis about the mosaic genome of CPXV-No-H2 is that the CPXV_GerMygEK938_17-like virus was probably circulating in a population of rodents in Europe, and it underwent recombination with the AKPV-like virus. The resultant virus, CPXV-No-H2-like virus, could have suffered genomic changes and adapted to mice, which could be the possible ancestor of ECTV. The origin of ECTV from the CPXV-like ancestor was previously proposed (Jeske et al., 2019) since ECTV has a shorter genome (ranging from 204 to 208 kbp) and reduced number of genes compared to CPXV that has the largest genome among OPXVs, about 220 kbp (Chen et al., 2003; Hendrickson et al., 2010; Carroll et al., 2011; Dabrowski et al., 2013; Mavian et al., 2014, 2021). Our results suggest that CPXV-No-H2 could be derived from a CPXV_GerMygEK938_17-like virus because (1) CPXV_GerMygEK938_17 shares the highest similarity with CPXV-No-H2, (2) it did not show any significant recombination event (Kalthoff et al., 2014; Jeske et al., 2019), (3) none of the seven recombination regions in CPXV-No-H2 was highly similar to either CPXV_GerMygEK938_17 or CPXV_Ger2010_MKY, (4) there is high similarity between their *p4c* and *A27L* genes, (5) its place of isolation was also in Europe, and (6) we speculated that it has V^+ ATI phenotype similar to CPXV_Ger2010_MKY due to the similarity between their *atip*, *p4c*, and *A27L* genes.

The recombination may have occurred between CPXV_GerMygEK938_17-like virus and AKPV-like virus rather than ECTV-like virus because, aside from two recombination events with the parental AKPV that overlapped a recombination event with the parental ECTV, there are other four recombinant events with the parental AKPV which cannot be viewed as a simple coincidence. In addition, the two suspected recombination regions in the ECTV genome (Gigante et al., 2019) were more similar to CPXV-No-H2 than AKPV (data not shown). Furthermore, hypothetically, CPXV_GerMygEK938_17 may produce V^+ ATI similar to AKPV, while CPXV-No-H2 and ECTV_Hampstead produce both V^+ and $V^{+/}$ ATI phenotypes (Ichihashi and Matsumoto, 1966; Okeke et al., 2012; Mavian et al., 2021). It seems that the putative progeny virus, CPXV-No-H2-like virus, may have reduced its ability to embed virions into ATI bodies. This was also observed in the derivates of ECTV_Hampstead that produces the V^- ATI phenotype (Mavian et al., 2021). We speculated that the recombination between CPXV_GerMygEK938_17-like virus and AKPV-like virus could take place in a rodent in Europe because AKPV contains genes from a Russian poxvirus, Murmansk, which was isolated from a root vole (Smithson et al., 2017a; Gigante et al., 2019), and CPXV_GerMygEK938_17 was isolated from bank vole in Europe (Jeske et al., 2019). Furthermore, CPXV-No-H2 was isolated in Europe, likewise with CPXV_Ger2010_MKY and ECTV_Hampstead (the source of the European outbreaks) (Hansen et al., 2009; Okeke et al., 2012; Kalthoff et al., 2014; Mavian et al., 2021).

However, it is pertinent to note that recombination detection programs predict hypothetical recombination events across genomes, and the outputs are sensitive to input parameter settings, particularly the sliding window size. To increase the likelihood of putative recombination events being real, we recommend the following: (i) use of these programs at default settings, (ii) identification of the exact recombination event by at least two different programs and algorithms, (iii) discountenance of recombination events without very high statistical support, (iv) confirmation of recombination breakpoints by manual inspection of similarity plots, and (v) incongruence of phylogenetic trees.

Another explanation for the presence of the OPXV-like genomic regions in CPXV-No-H2 could be symplesiomorphy because most genomic regions were similar to more than one taxon—for instance, the two CPXV-No-H2 genomic regions that were similar to ECTV and AKPV may be inherited from a common ancestral virus, likewise with the AKPV-like genomic region that contains part of the *NoH2-210* similar to AKPV and Murmansk. However, symplesiomorphy does not explain the presence of the AKPV-like genomic region of 2,150 bp in CPXV-No-H2, which did not share high similarity with

other taxa. The only plausible explanation is that CPXV-No-H2 may have obtained this sequence from an AKPV-like virus by recombination.

Overall, the genetic analysis of the atypical CPXV-No-H2 suggested that it contains sequences similar to other OPXVs, and one of the plausible explanations for their presence was recombination events with other OPXVs. In addition, CPXV-No-H2 is part of a new CPXV clade that was more phylogenetically related to ECTV and OPXV Abatino than other CPXV strains. Our findings provide some insight into the evolutionary history of CPXV and strongly support the genetic heterogeneity of the species CPXV. The discovery of new CPXV isolates and their phylogenetic relationship with OPXVs as well their genomic characterization will contribute to the further elucidation of the complex evolutionary history of CPXV.

DATA AVAILABILITY STATEMENT

The original contributions presented in the study are publicly available. This data can be found here: https://www.ncbi.nlm.nih.gov/genbank/, OM460002.

AUTHOR CONTRIBUTIONS

DD-C conducted the experiments, analyzed the data, and wrote the manuscript. MO and UM conceptualized the study, supervised the design and execution of the project, and wrote the manuscript. AB and AN contributed to data interpretation and revision of the manuscript for improved intellectual content. All authors contributed to the article and approved the submitted version.

FUNDING

This study was supported by the University of Tromsø, the Arctic University of Norway (project A212100108) and the National Graduate School in Infection Biology and Antimicrobials (grant no. 249062). Article processing charge was paid UiT - The Arctic University of Norway.

ACKNOWLEDGMENTS

We thank Jessin Janice and Juan Daniel Montenegro Cabrera for their assistance during the bioinformatics analysis.

SUPPLEMENTARY MATERIAL

The Supplementary Material for this article can be found online at: https://www.frontiersin.org/articles/10.3389/fmicb.2022.868887/full#supplementary-material

REFERENCES

Abrahão, J. S., Campos, R. K., De Souza Trindade, G., Da Fonseca, F. G., Ferreira, P. C. P., and Kroon, E. G. (2015). Outbreak of Severe Zoonotic Vaccinia Virus Infection, Southeastern Brazil. *Emerg. Infect. Dis.* 21:695. doi: 10.3201/EID2104.140351

Alakunle, E., Moens, U., Nchinda, G., and Okeke, M. I. (2020). Monkeypox Virus in Nigeria: infection Biology, Epidemiology, and Evolution. *Viruses* 12:1211157. doi: 10.3390/V12111257

Andrews, S. (2010). *A Quality Control tool for High Throughput Sequence Data*. Available online at: https://www.bioinformatics.babraham.ac.uk/projects/fastqc/ (accessed October 16, 2020).

Bankevich, A., Nurk, S., Antipov, D., Gurevich, A. A., Dvorkin, M., Kulikov, A. S., et al. (2012). SPAdes: a New Genome Assembly Algorithm and Its Applications to Single-Cell Sequencing. *J. Comput. Biol.* 19:477. doi: 10.1089/CMB.2012.0021

Bolger, A. M., Lohse, M., and Usadel, B. (2014). Trimmomatic: a flexible trimmer for Illumina sequence data. *Bioinformatics* 30, 2114–2020. doi: 10.1093/BIOINFORMATICS/BTU170

Boni, M. F., Posada, D., and Feldman, M. W. (2007). An Exact Nonparametric Method for Inferring Mosaic Structure in Sequence Triplets. *Genetics* 176, 1035–1047. doi: 10.1534/GENETICS.106.068874

Camacho, C., Coulouris, G., Avagyan, V., Ma, N., Papadopoulos, J., Bealer, K., et al. (2009). BLAST+: architecture and applications. *BMC Bioinform.* 10:421. doi: 10.1186/1471-2105-10-421

Cardeti, G., Gruber, C. E. M., Eleni, C., Carletti, F., Castilletti, C., Manna, G., et al. (2017). Fatal Outbreak in Tonkean Macaques Caused by Possibly Novel Orthopoxvirus, Italy, January 2015 - Volume 23, Number 12—December 2017 - Emerging Infectious Diseases journal - CDC. *Emerg. Infect. Dis.* 23, 1941–1949. doi: 10.3201/EID2312.162098

Carroll, D. S., Emerson, G. L., Li, Y., Sammons, S., Olson, V., Frace, M., et al. (2011). Chasing Jenner's vaccine: Revisiting Cowpox virus classification. *PLoS One* 6, 4–9. doi: 10.1371/journal.pone.0023086

Chantrey, J., Meyer, H., Baxby, D., Begon, M., Bown, K. J., Hazel, S. M., et al. (1999). Cowpox: reservoir hosts and geographic range. *Epidemiol. Infect.* 122:455. doi: 10.1017/S0950268899002423

Chen, N., Danila, M. I., Feng, Z., Buller, R. M. L., Wang, C., Han, X., et al. (2003). The genomic sequence of ectromelia virus, the causative agent of mousepox. *Virology* 317, 165–186. doi: 10.1016/S0042-6822(03)00520-8

Coulson, D., and Upton, C. (2011). Characterization of indels in poxvirus genomes. *Virus Genes* 42, 171–177. doi: 10.1007/S11262-010-0560-X/FIGURES/4

Dabrowski, P. W., Radoniæ, A., Kurth, A., and Nitsche, A. (2013). Genome-wide comparison of cowpox viruses reveals a new clade related to variola virus. *PLoS One* 8, 1–9. doi: 10.1371/journal.pone.0079953

Damaso, C. R. A., Reis, S. A., Jesus, D. M., Lima, P. S. F., and Moussatché, N. (2007). A PCR-based assay for detection of emerging vaccinia-like viruses isolated in Brazil. *Diagn. Microbiol. Infect. Dis.* 57, 39–46. doi: 10.1016/J.DIAGMICROBIO.2006.07.012

Darriba, D., Posada, D., Kozlov, A. M., Stamatakis, A., Morel, B., and Flouri, T. (2020). ModelTest-NG: A New and Scalable Tool for the Selection of DNA and Protein Evolutionary Models. *Mol. Biol. Evol.* 37:294. doi: 10.1093/MOLBEV/MSZ189

Diaz, J. H. (2021). The Disease Ecology, Epidemiology, Clinical Manifestations, Management, Prevention, and Control of Increasing Human Infections with Animal Orthopoxviruses. *Wilderness Environ. Med.* 32, 528–536. doi: 10.1016/J.WEM.2021.08.003

Dumbell, K., and Richardson, M. (1993). Virological investigations of specimens from buffaloes affected by buffalopox in Maharashtra State, India between 1985 and 1987. *Arch. Virol.* 128, 257–267. doi: 10.1007/BF01309438

Durski, K. N., McCollum, A. M., Nakazawa, Y., Petersen, B. W., Reynolds, M. G., Briand, S., et al. (2018). Emergence of Monkeypox — West and Central

Africa, 1970–2017. *Morb. Mortal. Wkly. Rep.* 67:310. doi: 10.15585/MMWR.MM6710A5

Ehlers, A., Osborne, J., Slack, S., Roper, R. L., and Upton, C. (2002). Poxvirus Orthologous Clusters (POCs). *Bioinformatics* 18, 1544–1545. doi: 10.1093/BIOINFORMATICS/18.11.1544

Emms, D. M., and Kelly, S. (2015). OrthoFinder: solving fundamental biases in whole genome comparisons dramatically improves orthogroup inference accuracy. *Genome Biol.* 16:2. doi: 10.1186/S13059-015-0721-2

Erez, N., Achdout, H., Milrot, E., Schwartz, Y., Wiener-Well, Y., Paran, N., et al. (2019). Diagnosis of Imported Monkeypox, Israel, 2018. *Emerg. Infect. Dis.* 25:980. doi: 10.3201/EID2505.190076

Ferrier, A., Frenois-Veyrat, G., Schvoerer, E., Henard, S., Jarjaval, F., Drouet, I., et al. (2021). Fatal cowpox virus infection in human fetus, france, 2017. *Emerg. Infect. Dis.* 27, 2570–2577. doi: 10.3201/eid2710.204818

Franke, A., Pfaff, F., Jenckel, M., Hoffmann, B., Höper, D., Antwerpen, M., et al. (2017). Classification of cowpox viruses into several distinct clades and identification of a novel lineage. *Viruses* 9, 1–14. doi: 10.3390/v9060142

Gao, J., Gigante, C., Khmaladze, E., Liu, P., Tang, S., Wilkins, K., et al. (2018). Genome sequences of Akhmeta virus, an early divergent old world orthopoxvirus. *Viruses* 10:50252. doi: 10.3390/v10050252

Gibbs, M. J., Armstrong, J. S., and Gibbs, A. J. (2000). Sister-Scanning: a Monte Carlo procedure for assessing signals in recombinant sequences. *Bioinformatics* 16, 573–582. doi: 10.1093/BIOINFORMATICS/16.7.573

Gigante, C. M., Gao, J., Tang, S., McCollum, A. M., Wilkins, K., Reynolds, M. G., et al. (2019). Genome of Alaskapox Virus, a Novel Orthopoxvirus Isolated from Alaska. *Viruses* 11:1080708. doi: 10.3390/V11080708

Girling, S. J., Pizzi, R., Cox, A., and Beard, P. M. (2011). Fatal cowpox virus infection in two squirrel monkeys (Saimiri sciureus). *Vet. Rec.* 169, 156–156. doi: 10.1136/VR.D4005

Gubser, C., Hué, S., Kellam, P., and Smith, G. L. (2004). Poxvirus genomes: A phylogenetic analysis. *J. Gen. Virol.* 85, 105–117. doi: 10.1099/VIR.0.19565-0/CITE/REFWORKS

Hansen, H., Okeke, M. I., Nilssen, O., and Traavik, T. (2009). Comparison and phylogenetic analysis of cowpox viruses isolated from cats and humans in Fennoscandia. *Arch. Virol.* 154, 1293–1302. doi: 10.1007/S00705-009-0442-5/FIGURES/3

Hendrickson, R. C., Wang, C., Hatcher, E. L., and Lefkowitz, E. J. (2010). Orthopoxvirus Genome Evolution: the Role of Gene Loss. *Viruses* 2, 1933–1967. doi: 10.3390/V2091933

Howard, A. R., Weisberg, A. S., and Moss, B. (2010). Congregation of Orthopoxvirus Virions in Cytoplasmic A-Type Inclusions Is Mediated by Interactions of a Bridging Protein (A26p) with a Matrix Protein (ATIp) and a Virion Membrane-Associated Protein (A27p). *J. Virol.* 84:7592. doi: 10.1128/JVI.00704-10

Ichihashi, Y., and Matsumoto, S. (1966). Studies on the nature of marchal bodies (A-type inclusion) during ectromelia virus infection. *Virology* 29, 264–275. doi: 10.1016/0042-6822(66)90033-X

Jacobs, B. L., Langland, J. O., Kibler, K. V., Denzler, K. L., White, S. D., Holechek, S. A., et al. (2009). Vaccinia virus vaccines: past, present and future. *Antiviral Res.* 84, 1–13. doi: 10.1016/J.ANTIVIRAL.2009.06.006

Jeske, K., Weber, S., Pfaff, F., Imholt, C., Jacob, J., Beer, M., et al. (2019). Molecular Detection and Characterization of the First Cowpox Virus Isolate Derived from a Bank Vole. *Viruses* 11:1111075. doi: 10.3390/V11111075

Kalthan, E., Tenguere, J., Ndjapou, S. G., Koyazengbe, T. A., Mbomba, J., Marada, R. M., et al. (2018). Investigation of an outbreak of monkeypox in an area occupied by armed groups, Central African Republic. *Méd. Mal. Infect.* 48, 263–268. doi: 10.1016/J.MEDMAL.2018.02.010

Kalthoff, D., Bock, W. I., Hühn, F., Beer, M., and Hoffmann, B. (2014). Fatal cowpox virus infection in cotton-top tamarins (Saguinus oedipus) in Germany. *Vector-Borne Zoonotic Dis.* 14, 303–305. doi: 10.1089/VBZ.2013.1442

Katoh, K., and Standley, D. M. (2013). MAFFT Multiple Sequence Alignment Software Version 7: improvements in Performance and Usability. *Mol. Biol. Evol.* 30, 772–780. doi: 10.1093/MOLBEV/MST010

Kinnunen, P. M., Henttonen, H., Hoffmann, B., Kallio, E. R., Korthase, C., Laakkonen, J., et al. (2011). Orthopox Virus Infections in Eurasian Wild Rodents. *Vector Borne Zoonotic Dis.* 11, 1133–1140. doi: 10.1089/VBZ.2010.0170

Laakkonen, J., Kallio-Kokko, H., Öktem, M. A., Blasdell, K., Plyusnina, A., Niemimaa, J., et al. (2006). Serological Survey for Viral Pathogens in Turkish Rodents. *J. Wildl. Dis.* 42, 672–676. doi: 10.7589/0090-3558-42.3.672

Li, H., and Durbin, R. (2009). Fast and accurate short read alignment with Burrows–Wheeler transform. *Bioinformatics* 25, 1754–1760. doi: 10.1093/BIOINFORMATICS/BTP324

Lim, T. H., Lee, H. J., Lee, D. H., Lee, Y. N., Park, J. K., Youn, H. N., et al. (2011). An emerging recombinant cluster of nephropathogenic strains of avian infectious bronchitis virus in Korea. *Infect. Genet. Evol.* 11, 678–685. doi: 10.1016/J.MEEGID.2011.01.007

Lole, K. S., Bollinger, R. C., Paranjape, R. S., Gadkari, D., Kulkarni, S. S., Novak, N. G., et al. (1999). Full-Length Human Immunodeficiency Virus Type 1 Genomes from Subtype C-Infected Seroconverters in India, with Evidence of Intersubtype Recombination. *J. Virol.* 73:160. doi: 10.1128/jvi.73.1.152-160.1999

MacLachlan, N. J., and Dubovi, E. J. (eds) (2017). "Poxviridae," in *Fenner's Veterinary Virology*, (Boston: Academic Press), 157–174. doi: 10.1016/B978-0-12-800946-8.00007-6

Martin, D. P., Murrell, B., Golden, M., Khoosal, A., and Muhire, B. (2015). RDP4: Detection and analysis of recombination patterns in virus genomes. *Virus Evol.* 1:3. doi: 10.1093/VE/VEV003

Martin, D. P., Posada, D., Crandall, K. A., and Williamson, C. (2005). A Modified Bootscan Algorithm for Automated Identification of Recombinant Sequences and Recombination Breakpoints. *AIDS Res. Hum. Retrovir.* 21, 98–102. doi: 10.1089/AID.2005.21.98

Martin, D., and Rybicki, E. (2000). RDP: detection of recombination amongst aligned sequences. *Bioinformatics* 16, 562–563. doi: 10.1093/BIOINFORMATICS/16.6.562

Mauldin, M. R., Antwerpen, M., Emerson, G. L., Li, Y., Zoeller, G., Carroll, D. S., et al. (2017). Cowpox virus: What's in a Name? *Viruses* 2017:101. doi: 10.3390/V9050101

Mavian, C., López-Bueno, A., Bryant, N. A., Seeger, K., Quail, M. A., Harris, D., et al. (2014). The genome sequence of ectromelia virus Naval and Cornell isolates from outbreaks in North America. *Virology* 462–463, 218–226. doi: 10.1016/j.virol.2014.06.010

Mavian, C., López-Bueno, A., Martín, R., Nitsche, A., and Alcamí, A. (2021). Comparative pathogenesis, genomics and phylogeography of mousepox. *Viruses* 13:13061146. doi: 10.3390/v13061146

McKelvey, T. A., Andrews, S. C., Miller, S. E., Ray, C. A., and Pickup, D. J. (2002). Identification of the Orthopoxvirus p4c Gene, Which Encodes a Structural Protein That Directs Intracellular Mature Virus Particles into A-Type Inclusions. *J. Virol.* 76:11216. doi: 10.1128/JVI.76.22.11216-11225.2002

Megid, J., Borges, I. A., Abrahão, J. S., Trindade, G. S., Appolinário, C. M., Ribeiro, M. G., et al. (2012). Vaccinia Virus Zoonotic Infection, São Paulo State, Brazil. *Emerg. Infect. Dis.* 18:189. doi: 10.3201/EID1801.110692

Miranda, J. B., Borges, I. A., Campos, S. P. S., Vieira, F. N., De Ázara, T. M. F., Marques, F. A., et al. (2017). Serologic and Molecular Evidence of Vaccinia Virus Circulation among Small Mammals from Different Biomes, Brazil. *Emerg. Infect. Dis.* 23:931. doi: 10.3201/EID2306.161643

Nakoune, E., Lampaert, E., Ndjapou, S. G., Janssens, C., Zuniga, I., Van Herp, M., et al. (2017). A Nosocomial Outbreak of Human Monkeypox in the Central African Republic. *Open Forum Infect. Dis.* 4:168. doi: 10.1093/OFID/OFX168

Ng, O. T., Lee, V., Marimuthu, K., Vasoo, S., Chan, G., Lin, R. T. P., et al. (2019). A case of imported Monkeypox in Singapore. *Lancet. Infect. Dis.* 19:1166. doi: 10.1016/S1473-3099(19)30537-7

Okeke, M. I., Hansen, H., and Traavik, T. (2012). A naturally occurring cowpox virus with an ectromelia virus A-type inclusion protein gene displays atypical A-type inclusions. *Infect. Genet. Evol.* 12, 160–168. doi: 10.1016/J.MEEGID.2011.09.017

Okeke, M. I, Okoli, A. S., Nilssen, O., Moens, U., Tryland, M., Bøhn, T., et al. (2014). Molecular characterization and phylogenetics of Fennoscandian cowpox virus isolates based on the p4c and atip genes. *Virol. J.* 11, 1–16. doi: 10.1186/1743-422X-11-119/TABLES/5

Padidam, M., Sawyer, S., and Fauquet, C. M. (1999). Possible Emergence of New Geminiviruses by Frequent Recombination. *Virology* 265, 218–225. doi: 10.1006/VIRO.1999.0056

Patel, D. D., and Pickup, D. J. (1987). Messenger RNAs of a strongly-expressed late gene of cowpox virus contain 5'-terminal poly(A) sequences. *EMBO J.* 6:3787. doi: 10.1002/J.1460-2075.1987.TB02714.X

Popova, A. Y., Maksyutov, R. A., Taranov, O. S., Tregubchak, T. V., Zaikovskaya, A. V., Sergeev, A. A., et al. (2017). Cowpox in a human, Russia, 2015. *Epidemiol. Infect.* 145, 755–759. doi: 10.1017/S0950268816002922

Posada, D., and Crandall, K. A. (2001). Evaluation of methods for detecting recombination from DNA sequences: Computer simulations. *Proc. Natl. Acad. Sci.* 98, 13757–13762. doi: 10.1073/PNAS.241370698

Prkno, A., Hoffmann, D., Goerigk, D., Kaiser, M., van Maanen, A. C. F., Jeske, K., et al. (2017). Epidemiological investigations of four cowpox virus outbreaks in alpaca herds, Germany. *Viruses* 9, 1–15. doi: 10.3390/v9110344

Qin, L., Favis, N., Famulski, J., and Evans, D. H. (2015). Evolution of and Evolutionary Relationships between Extant Vaccinia Virus Strains. *J. Virol.* 89:1809. doi: 10.1128/JVI.02797-14

Qin, L., Upton, C., Hazes, B., and Evans, D. H. (2011). Genomic Analysis of the Vaccinia Virus Strain Variants Found in Dryvax Vaccine. *J. Virol.* 85:13049. doi: 10.1128/JVI.05779-11

Rambaut, A. (2018). *FigTree*. Available online at: http://tree.bio.ed.ac.uk/software/figtree/ [accessed February 19, 2021]

Reynolds, M. G., Guagliardo, S. A. J., Nakazawa, Y. J., Doty, J. B., and Mauldin, M. R. (2018). Understanding orthopoxvirus host range and evolution: from the enigmatic to the usual suspects. *Curr. Opin. Virol.* 28, 108–115. doi: 10.1016/J.COVIRO.2017.11.012

Ronquist, F., Teslenko, M., Van Der Mark, P., Ayres, D. L., Darling, A., Höhna, S., et al. (2012). MrBayes 3.2: Efficient Bayesian Phylogenetic Inference and Model Choice Across a Large Model Space. *Syst. Biol.* 61, 539–542. doi: 10.1093/SYSBIO/SYS029

Silva, N. I. O., de Oliveira, J. S., Kroon, E. G., Trindade, G., de, S., and Drumond, B. P. (2021). Here, There, and Everywhere: The Wide Host Range and Geographic Distribution of Zoonotic Orthopoxviruses. *Viruses* 2021:13. doi: 10.3390/V13010043

Smith, J. M. (1992). Analyzing the mosaic structure of genes. *J. Mol. Evol.* 342, 126–129. doi: 10.1007/BF00182389

Smith, K. C., Bennett, M., and Garrett, D. C. (1999). Skin lesions caused by orthopoxvirus infection in a dog. *J. Small Anim. Pract.* 40, 495–497. doi: 10.1111/J.1748-5827.1999.TB03003.X

Smithson, C., Tang, N., Sammons, S., Frace, M., Batra, D., Li, Y., et al. (2017b). The genomes of three North American orthopoxviruses. *Virus Genes* 53, 21–34. doi: 10.1007/S11262-016-1388-9/TABLES/2

Smithson, C., Meyer, H., Gigante, C. M., Gao, J., Zhao, H., Batra, D., et al. (2017a). Two novel poxviruses with unusual genome rearrangements: NY_014 and Murmansk. *Virus Genes* 53, 883–897. doi: 10.1007/S11262-017-1501-8/FIGURES/5

Smithson, C., Purdy, A., Verster, A. J., and Upton, C. (2014). Prediction of Steps in the Evolution of Variola Virus Host Range. *PLoS One* 9:e91520. doi: 10.1371/JOURNAL.PONE.0091520

Springer, Y. P., Hsu, C. H., Werle, Z. R., Olson, L. E., Cooper, M. P., Castrodale, L. J., et al. (2017). Novel Orthopoxvirus Infection in an Alaska Resident. *Clin. Infect. Dis. An Off. Publ. Infect. Dis. Soc. Am.* 64:1737. doi: 10.1093/CID/CIX219

Stamatakis, A. (2014). RAxML version 8: a tool for phylogenetic analysis and post-analysis of large phylogenies. *Bioinformatics* 30:1313. doi: 10.1093/BIOINFORMATICS/BTU033

Strassburg, M. A. (1982). The global eradication of smallpox. *Am. J. Infect. Control* 10, 53–59. doi: 10.1016/0196-6553(82)90003-7

Talavera, G., and Castresana, J. (2007). Improvement of Phylogenies after Removing Divergent and Ambiguously Aligned Blocks from Protein Sequence Alignments. *Syst. Biol.* 56, 564–577. doi: 10.1080/10635150701472164

Tcherepanov, V., Ehlers, A., and Upton, C. (2006). Genome Annotation Transfer Utility (GATU): rapid annotation of viral genomes using a closely related reference genome. *BMC Gen.* 7:150. doi: 10.1186/1471-2164-7-150

Trentin, J. J., and Briody, B. A. (1953). An outbreak of mouse-pox (infectious ectromelia) in the United States: II. *Definit. Diag.* 1953, 227. doi: 10.1126/science.117.3035.227

Tryland, M., Myrmel, H., Holtet, L., Haukenes, G., and Traavik, T. (1998). Clinical cowpox cases in Norway. *Scand. J. Infect. Dis.* 30, 301–303. doi: 10.1080/00365549850160972

Vaughan, A., Aarons, E., Astbury, J., Balasegaram, S., Beadsworth, M., Beck, C. R., et al. (2018). Two cases of monkeypox imported to the United Kingdom, September 2018. *Eurosurveillance* 23:1800509. doi: 10.2807/1560-7917.ES.2018.23.38.1800509

Vora, N. M., Li, Y., Geleishvili, M., Emerson, G. L., Khmaladze, E., Maghlakelidze, G., et al. (2015). Human Infection with a Zoonotic Orthopoxvirus in the Country of Georgia. *N. Engl. J. Med.* 372:1223. doi: 10.1056/NEJMOA1407647

Vorou, R. M., Papavassiliou, V. G., and Pierroutsakos, I. N. (2008). Cowpox virus infection: An emerging health threat. *Curr. Opin. Infect. Dis.* 21, 153–156. doi: 10.1097/QCO.0B013E3282F44C74

Wang, J., Liu, X., Zhu, Q., Wu, Q., Tang, S., Zhang, L., et al. (2021). Identification, Isolation, and Characterization of an Ectromelia Virus New Strain from an Experimental Mouse. *Virol. Sin.* 36, 155–158. doi: 10.1007/s12250-020-00263-w

Weber, S., Jeske, K., Ulrich, R. G., Imholt, C., Jacob, J., Beer, M., et al. (2020). In vivo characterization of a bank vole-derived cowpox virus isolate in natural hosts and the rat model. *Viruses* 12:12020237. doi: 10.3390/v12020237

Wingett, S. W., and Andrews, S. (2018). FastQ Screen: a tool for multi-genome mapping and quality control. *F1000Research* 7:1338. doi: 10.12688/F1000RESEARCH.15931.2

Wolfs, T. F. W., Wagenaar, J. A., Niesters, H. G. M., and Osterhaus, A. D. M. E. (2002). Rat-to-Human Transmission of Cowpox Infection. *Emerg. Infect. Dis.* 8:1495. doi: 10.3201/EID0812.020089

Yinka-Ogunleye, A., Aruna, O., Dalhat, M., Ogoina, D., McCollum, A., Disu, Y., et al. (2019). Outbreak of human monkeypox in Nigeria in 2017–18: a clinical and epidemiological report. *Lancet Infect. Dis.* 19, 872–879. doi: 10.1016/S1473-3099(19)30294-4

Conflict of Interest: The authors declare that the research was conducted in the absence of any commercial or financial relationships that could be construed as a potential conflict of interest.

Publisher's Note: All claims expressed in this article are solely those of the authors and do not necessarily represent those of their affiliated organizations, or those of the publisher, the editors and the reviewers. Any product that may be evaluated in this article, or claim that may be made by its manufacturer, is not guaranteed or endorsed by the publisher.

Supplementary Material

1 Supplementary Figures

Supplementary Figure S1. Schematic diagram of alignment of CPXV-No-H2, CPXV_GerMygEK938_17, CPXV_Ger2010_MKY and ECTV_Mos showing the *NoH2-163* gene and their homologs, using Geneious software 2021.2.2. Grey regions indicate conserved bases while colors (red, blue, yellow, green) indicate differences (A, C, G, T, respectively) from CPXV-No-H2.

Supplementary Figure S2. Maximum-Likelihood phylogenetic tree based on 76 orthopoxvirus whole genomes. Bootstrap values were determined from 1000 replica sampling. *Cowpox virus* (CPXV) strains were grouped into different clades: CPXV-like 1, CPXV-like 2, and VARV-like (Franke et al., 2017). The scale bar represents expected substitutions per site.

Supplementary Figure S3. Maximum-Likelihood phylogenetic tree on 76 orthopoxvirus core genomes. Bootstrap values were determined from 1000 replica sampling. *Cowpox virus* (CPXV) strains were grouped into different clades: CPXV-like 1, CPXV-like 2, and VARV-like (Franke et al., 2017). The scale bar represents expected substitutions per site.

Supplementary Figure S4. Maximum-Likelihood phylogenetic tree of 134 orthopoxvirus orthologous genes. Bootstrap values were determined from 1000 replica sampling. *Cowpox virus* (CPXV) strains were grouped into different clades: CPXV-like 1, CPXV-like 2, and VARV-like (Franke et al., 2017). The scale bar represents expected substitutions per site.

Supplementary Figure S5. Maximum-Likelihood phylogenetic tree based on the putative recombinant region 1 between the parental AKPV and CPXV (potential recombinant event 1). Bootstrap values were determined from 1000 replica sampling. Clades are identified with colors.

Supplementary Figure S6. Maximum-Likelihood phylogenetic tree based on the putative recombinant region 2 between the parental AKPV and CPXV (potential recombinant event 2). Bootstrap values were determined from 1000 replica sampling. Clades are identified with colors.

Supplementary Figure S7. Maximum-Likelihood phylogenetic tree based on the putative recombinant region 3 between the parental AKPV and CPXV (potential recombinant event 3). Bootstrap values were determined from 1000 replica sampling. Clades are identified with colors.

Supplementary Figure S8. Maximum-Likelihood phylogenetic tree based on the putative recombinant region 4 between the parental AKPV and CPXV (potential recombinant event 4). Bootstrap values were determined from 1000 replica sampling. Clades are identified with colors.

Supplementary Figure S9. Maximum-Likelihood phylogenetic tree based on the putative recombinant region 5 between the parental AKPV and CPXV (potential recombinant event 5). Bootstrap values were determined from 1000 replica sampling. Clades are identified with colors.

Supplementary Figure S10. Maximum-Likelihood phylogenetic tree based on the putative recombinant region 6 between the parental AKPV and CPXV (potential recombinant event 6). Bootstrap values were determined from 1000 replica sampling. Clades are identified with colors.

Supplementary Figure S11. Maximum-Likelihood phylogenetic tree based on the putative recombinant region 1 between the parental ECTV and CPXV (potential recombinant event 7). Bootstrap values were determined from 1000 replica sampling. Clades are identified with colors.

Supplementary Figure S12. Maximum-Likelihood phylogenetic tree based on the putative recombinant region 2 between the parental ECTV and CPXV (potential recombinant event 8). Bootstrap values were determined from 1000 replica sampling. Clades are identified with colors.

Supplementary Figure S13. Maximum-Likelihood phylogenetic tree based on the putative recombinant region between the parental VACV and CPXV (potential recombinant event 9). Bootstrap values were determined from 1000 replica sampling. Clades are identified with colors.

Supplementary Figure S14. Maximum-Likelihood phylogenetic tree based on 75 OPXV whole genomes. Bootstrap values were determined from 1000 replica sampling. Clades are identified with colors.

Supplementary Figure S15. Bayesian Inference phylogenetic tree based on 75 OPXV whole genomes. Clades are identified with colors.

Supplementary Figure S16. Maximum-Likelihood phylogenetic tree based on 75 OPXV core genomes. Bootstrap values were determined from 1000 replica sampling. Clades are identified with colors.

Supplementary Figure S17. Bayesian Inference phylogenetic tree based on 75 OPXV core genomes. Clades are identified with colors.

Supplementary Figure S18. Maximum-Likelihood phylogenetic tree based on 134 orthologous genes from 75 OPXV genomes. Bootstrap values were determined from 1000 replica sampling. Clades are identified with colors.

Supplementary Figure S19. Bayesian Inference phylogenetic tree based on 134 orthologous genes from 75 OPXV genomes. Clades are identified with colors.

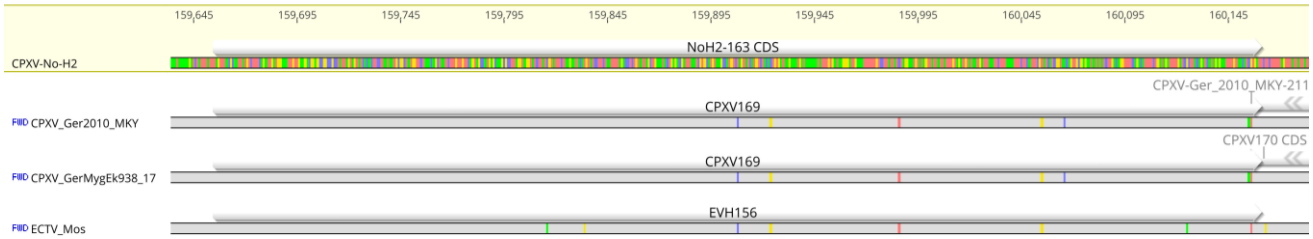

Supplementary Figure S1. Schematic diagram of alignment of CPXV-No-H2, CPXV_GerMygEK938_17, CPXV_Ger2010_MKY and ECTV_Mos showing the *NoH2-163* gene and their homologs, using Geneious software 2021.2.2. Grey regions indicate conserved bases while colors (red, blue, yellow, green) indicate differences (A, C, G, T, respectively) from CPXV-No-H2.

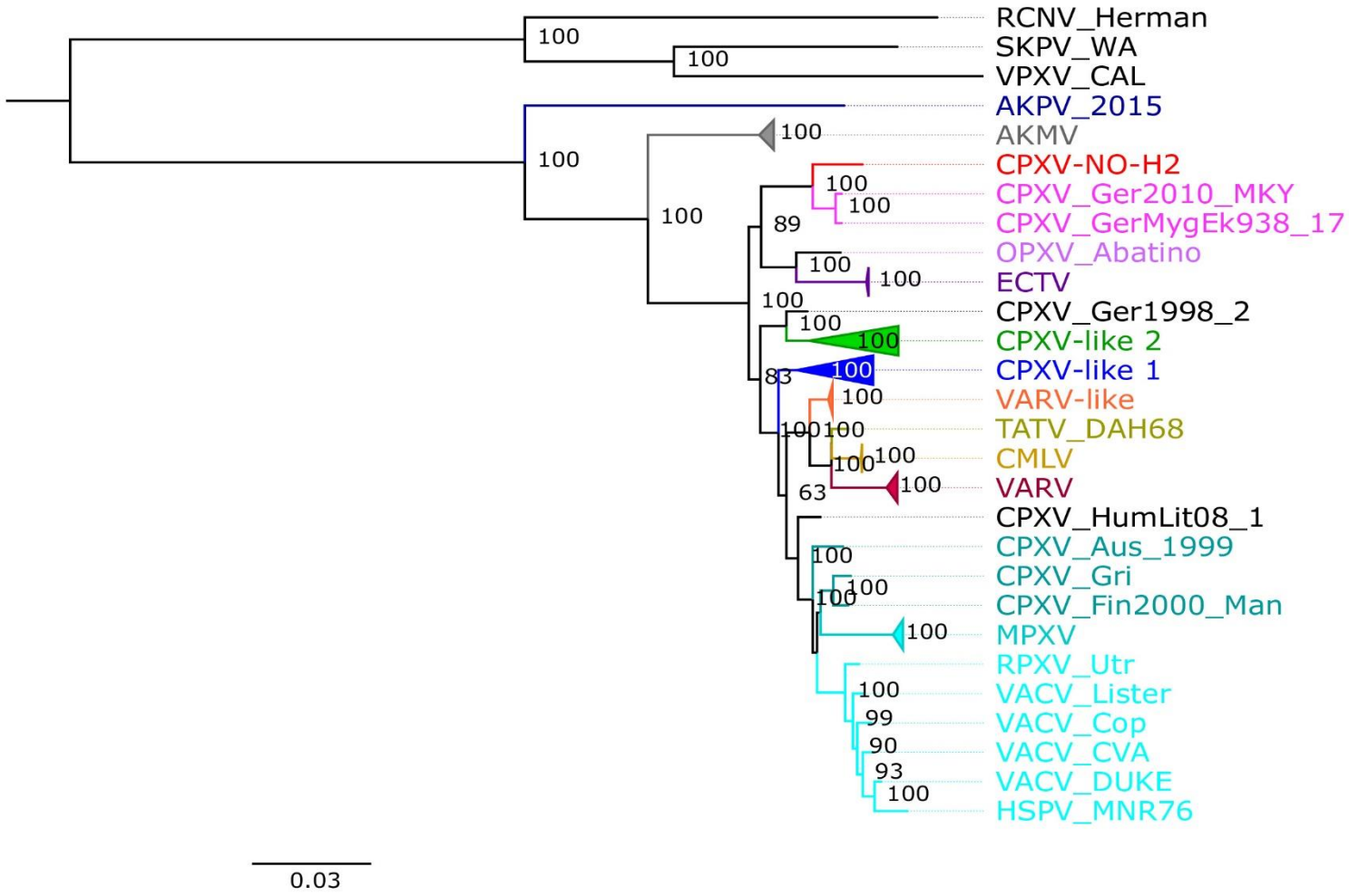

Supplementary Figure S2. Maximum-Likelihood phylogenetic tree based on 76 orthopoxvirus whole genomes. Bootstrap values were determined from 1000 replica sampling. *Cowpox virus* (CPXV) strains were grouped into different clades: CPXV-like 1, CPXV-like 2, and VARV-like (Franke et al., 2017). The scale bar represents expected substitutions per site.

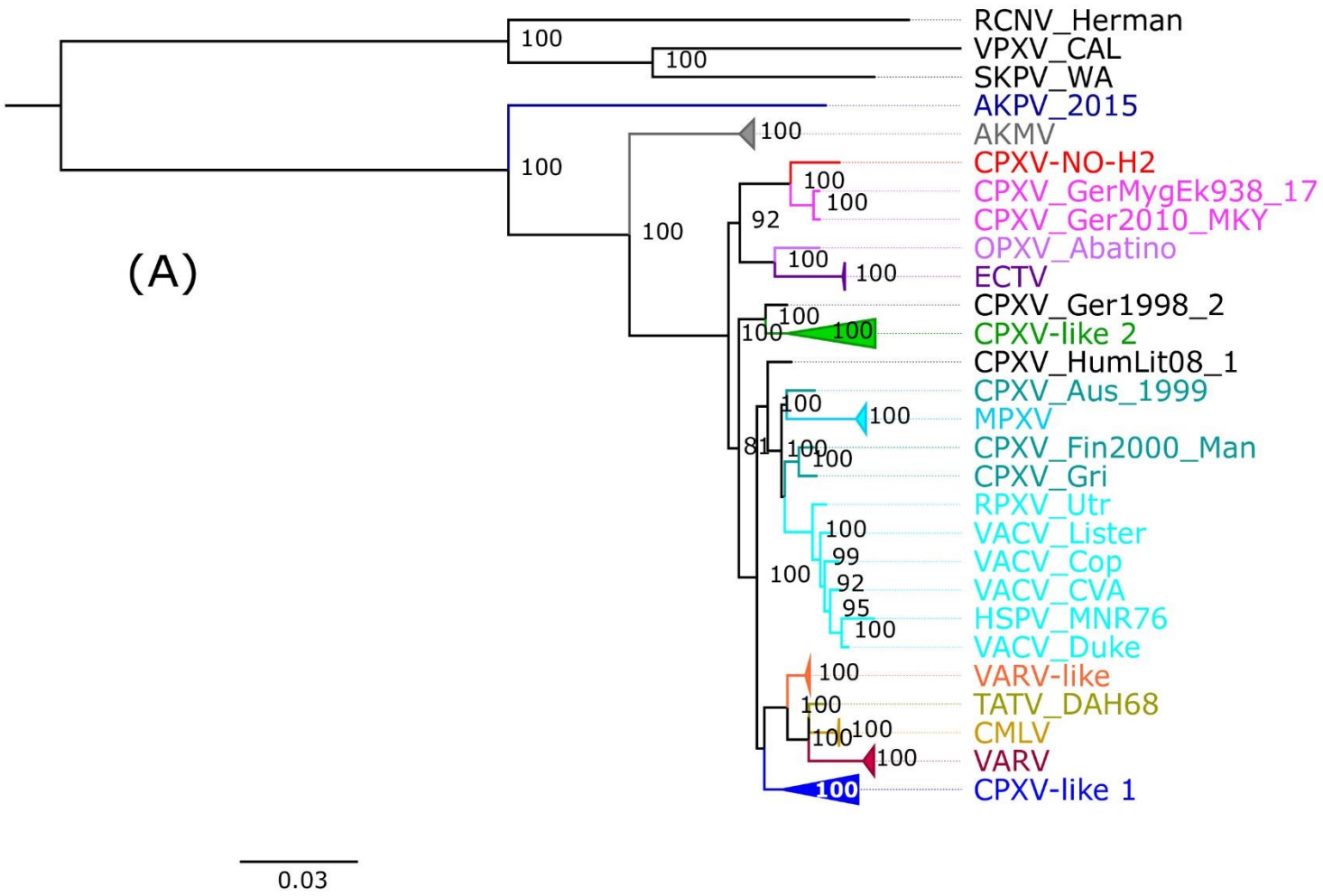

Supplementary Figure S3. Maximum-Likelihood phylogenetic tree on 76 orthopoxvirus core genomes. Bootstrap values were determined from 1000 replica sampling. *Cowpox virus* (CPXV) strains were grouped into different clades: CPXV-like 1, CPXV-like 2, and VARV-like (Franke et al., 2017). The scale bar represents expected substitutions per site.

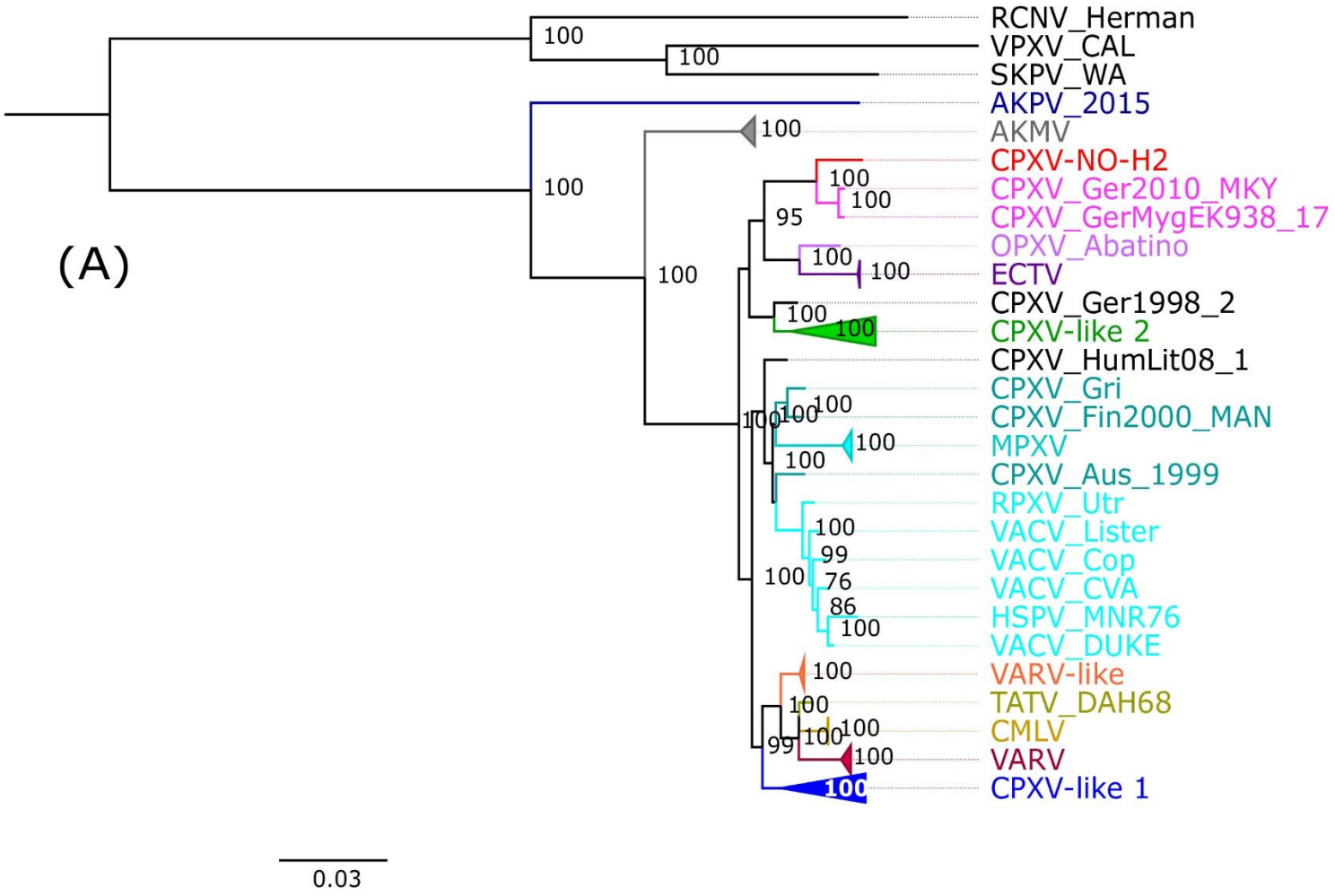

Supplementary Figure S4. Maximum-Likelihood phylogenetic tree of 134 orthopoxvirus orthologous genes. Bootstrap values were determined from 1000 replica sampling. *Cowpox virus* (CPXV) strains were grouped into different clades: CPXV-like 1, CPXV-like 2, and VARV-like (Franke et al., 2017). The scale bar represents expected substitutions per site.

Supplementary Figure S5. Maximum-Likelihood phylogenetic tree based on the putative recombinant region 1 between the parental AKPV and CPXV (potential recombinant event 1). Bootstrap values were determined from 1000 replica sampling. Clades are identified with colors.

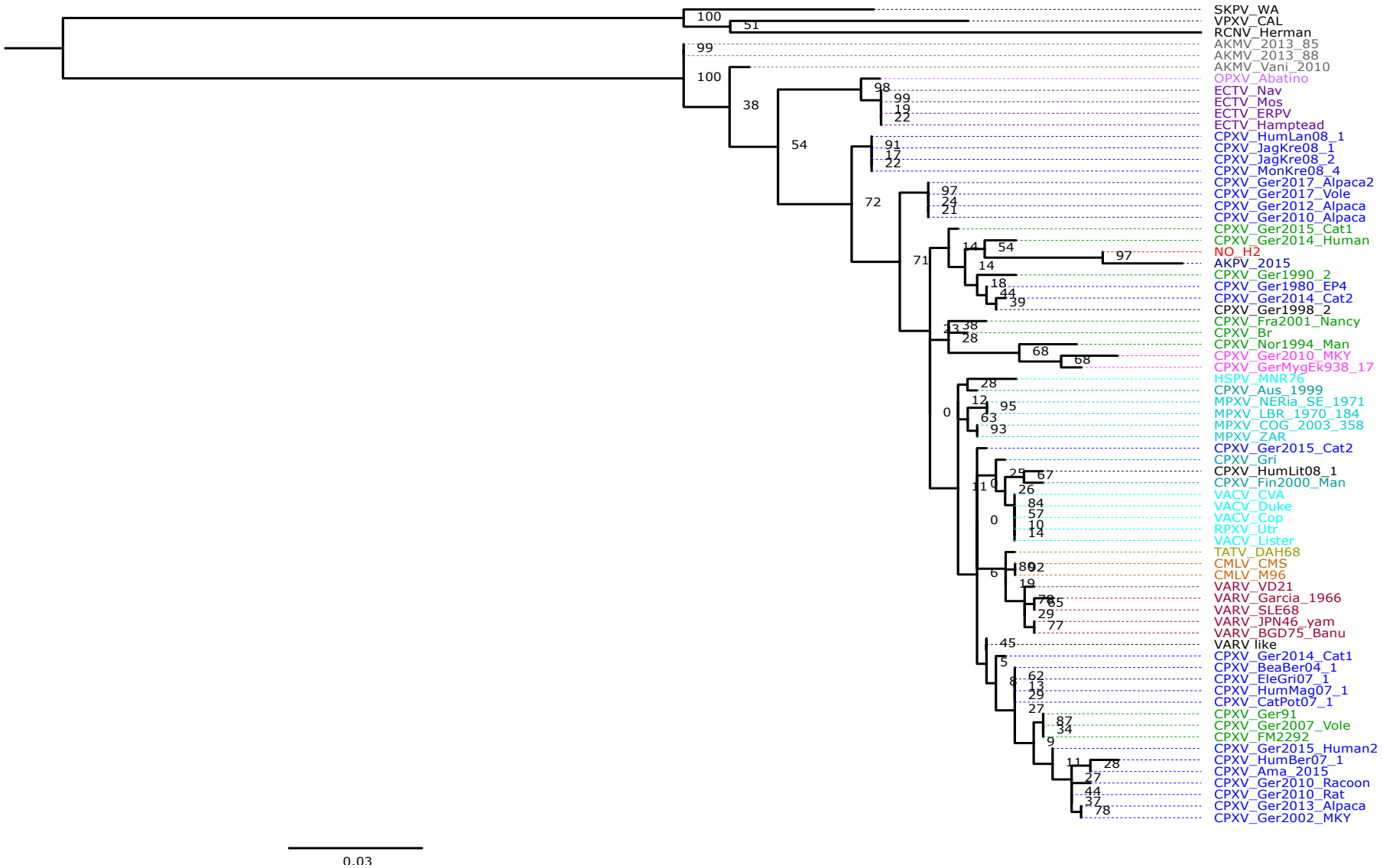

Supplementary Figure S6. Maximum-Likelihood phylogenetic tree based on the putative recombinant region 2 between the parental AKPV and CPXV (potential recombinant event 2). Bootstrap values were determined from 1000 replica sampling. Clades are identified with colors.

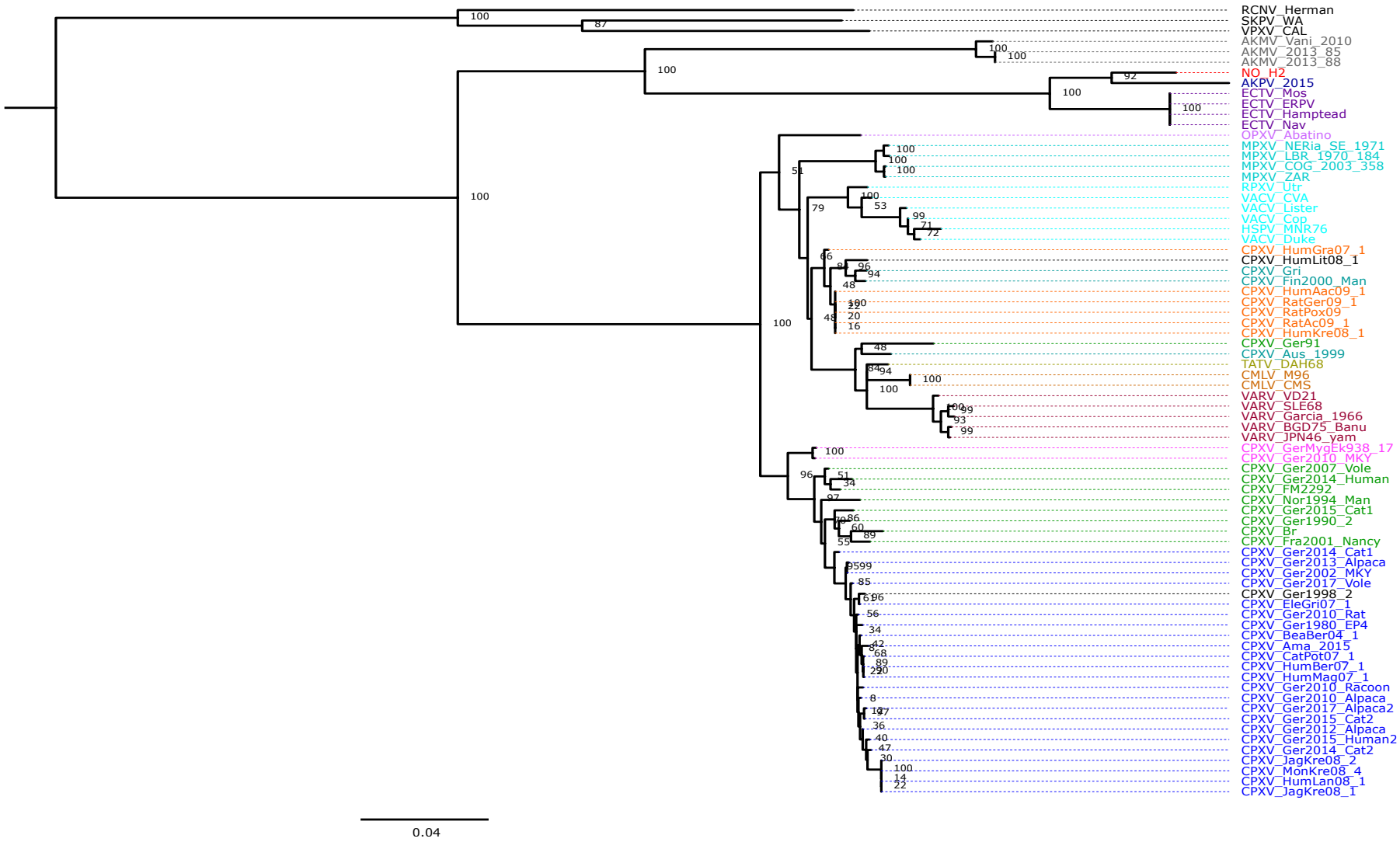

Supplementary Figure S7. Maximum-Likelihood phylogenetic tree based on the putative recombinant region 3 between the parental AKPV and CPXV (potential recombinant event 3). Bootstrap values were determined from 1000 replica sampling. Clades are identified with colors.

Supplementary Figure S8. Maximum-Likelihood phylogenetic tree based on the putative recombinant region 4 between the parental AKPV and CPXV (potential recombinant event 4). Bootstrap values were determined from 1000 replica sampling. Clades are identified with colors.

Supplementary Figure S9. Maximum-Likelihood phylogenetic tree based on the putative recombinant region 5 between the parental AKPV and CPXV (potential recombinant event 5). Bootstrap values were determined from 1000 replica sampling. Clades are identified with colors.

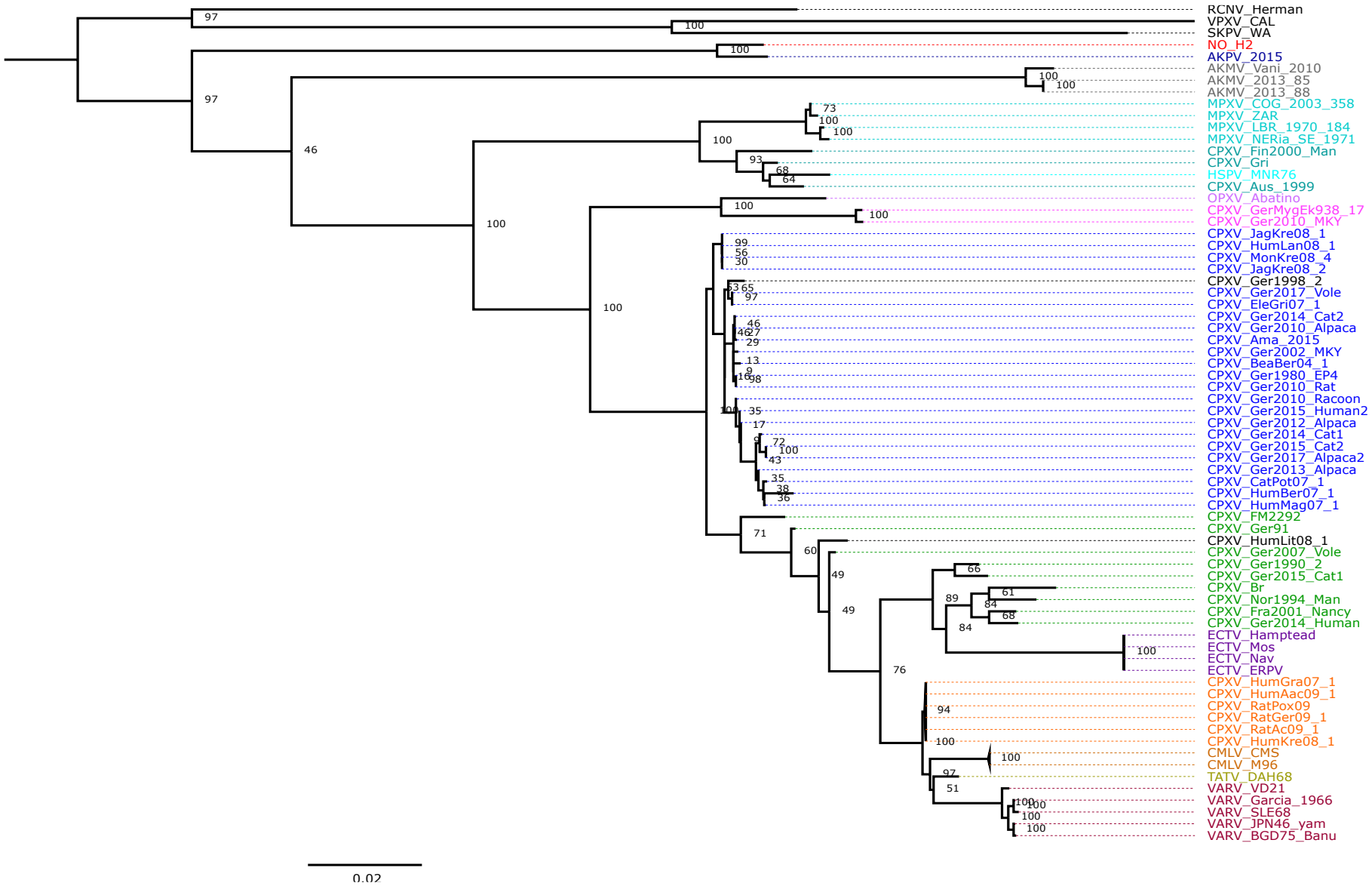

Supplementary Figure S10. Maximum-Likelihood phylogenetic tree based on the putative recombinant region 6 between the parental AKPV and CPXV (potential recombinant event 6). Bootstrap values were determined from 1000 replica sampling. Clades are identified with colors.

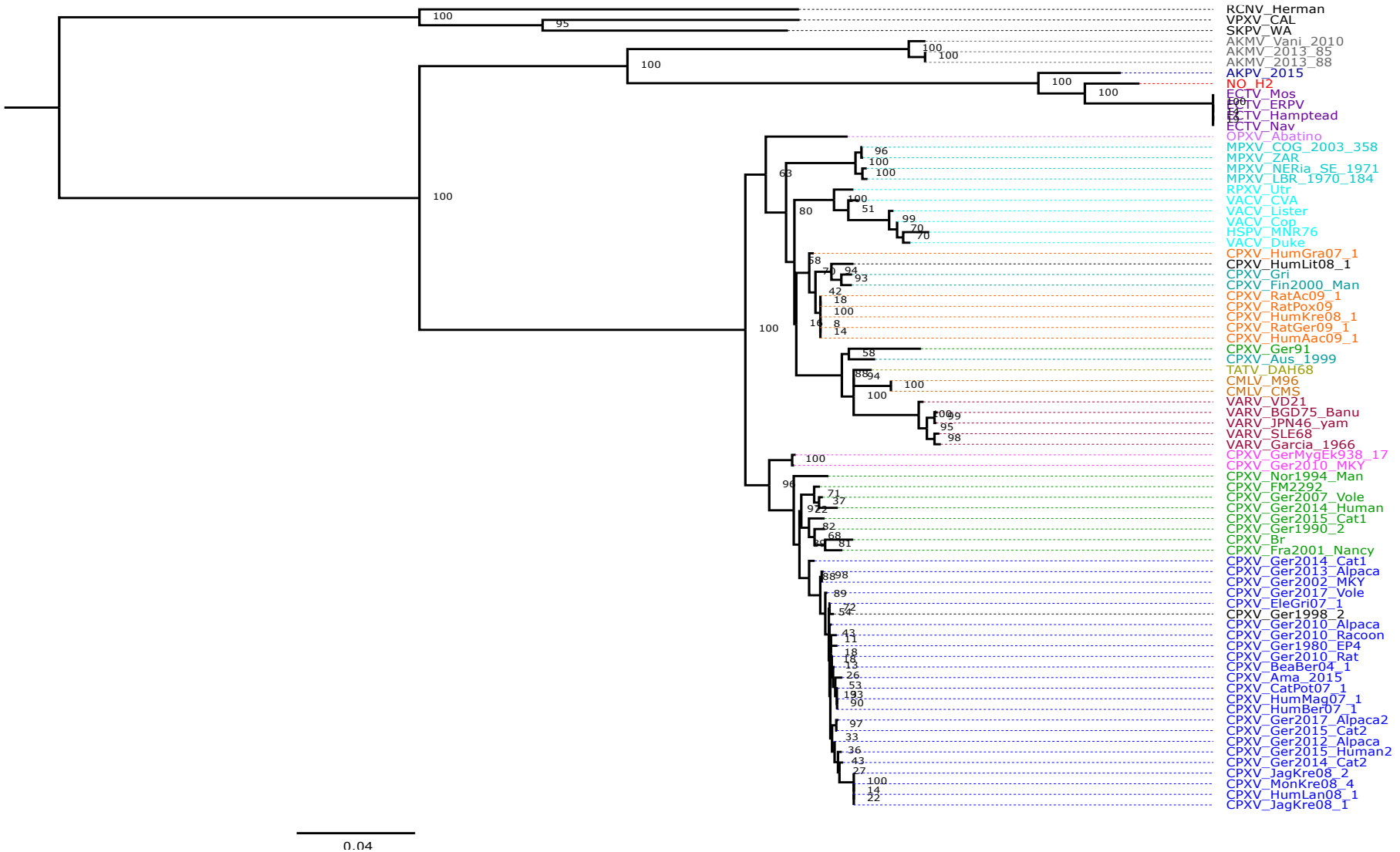

Supplementary Figure S11. Maximum-Likelihood phylogenetic tree based on the putative recombinant region 1 between the parental ECTV and CPXV (potential recombinant event 7). Bootstrap values were determined from 1000 replica sampling. Clades are identified with colors.

Supplementary Figure S12. Maximum-Likelihood phylogenetic tree based on the putative recombinant region 2 between the parental ECTV and CPXV (potential recombinant event 8). Bootstrap values were determined from 1000 replica sampling. Clades are identified with colors.

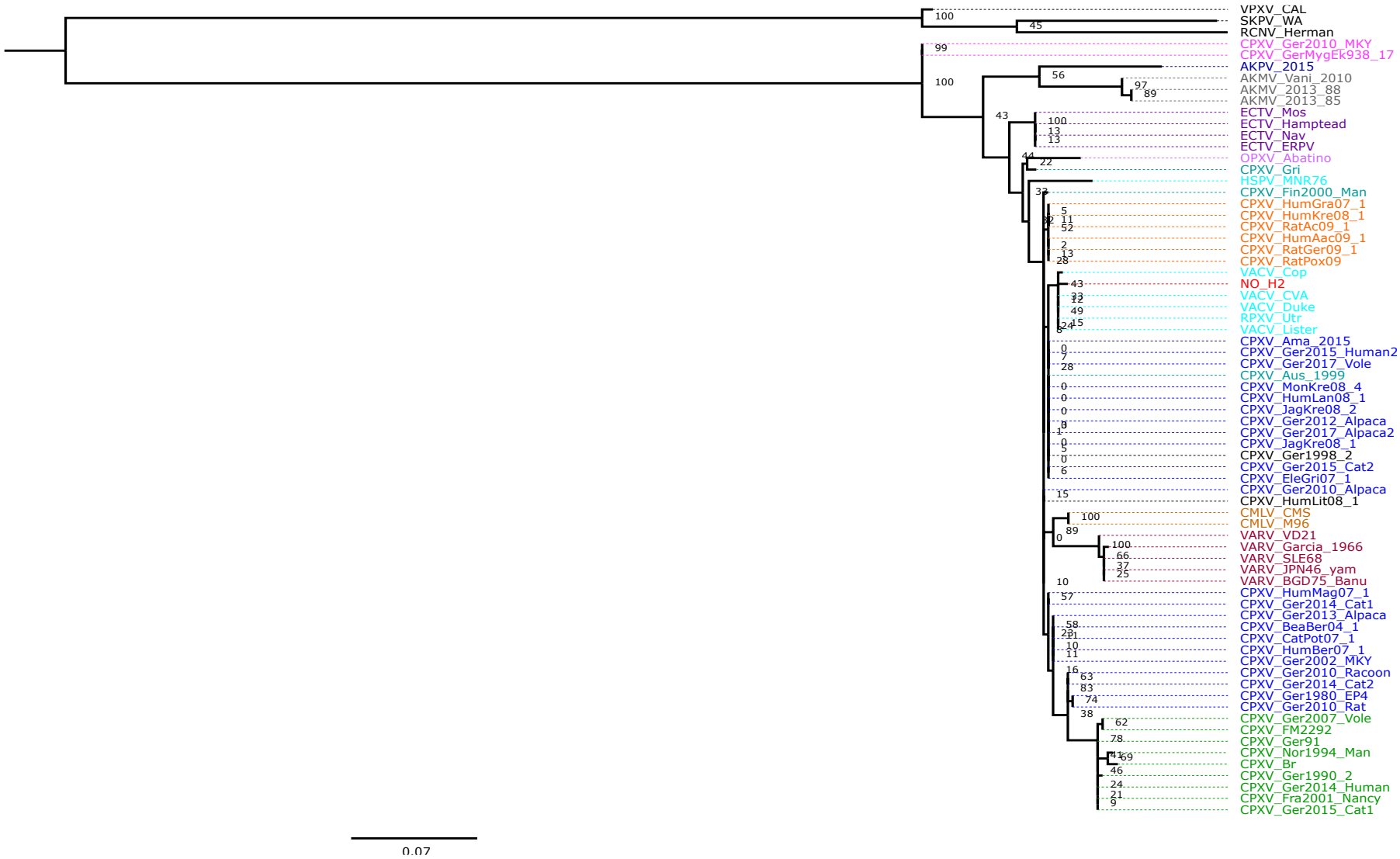

Supplementary Figure S13. Maximum-Likelihood phylogenetic tree based on the putative recombinant region between the parental VACV and CPXV (potential recombinant event 9). Bootstrap values were determined from 1000 replica sampling. Clades are identified with colors.

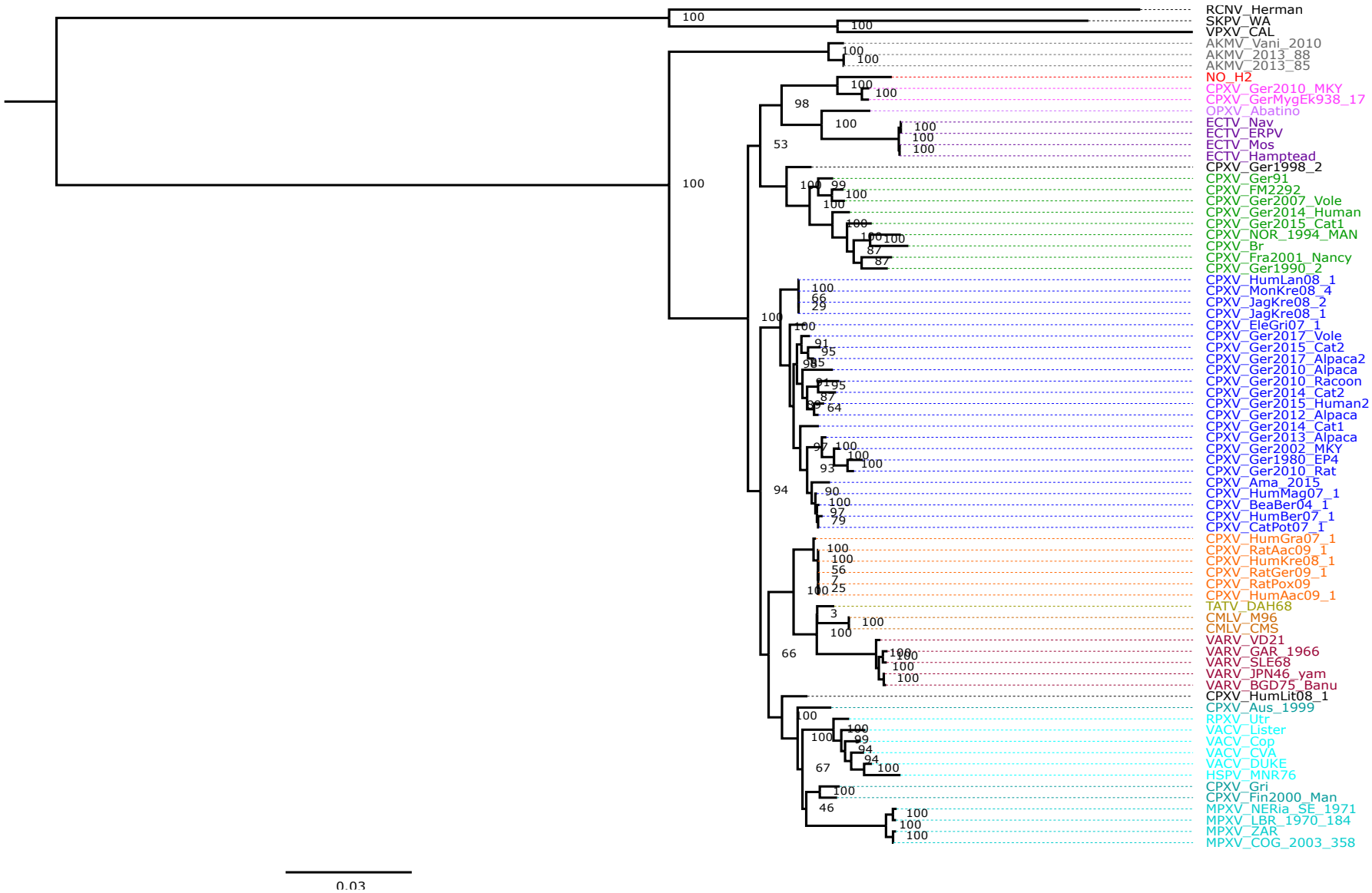

Supplementary Figure S14. Maximum-Likelihood phylogenetic tree based on 75 OPXV whole genomes. Bootstrap values were determined from 1000 replica sampling. Clades are identified with colors.

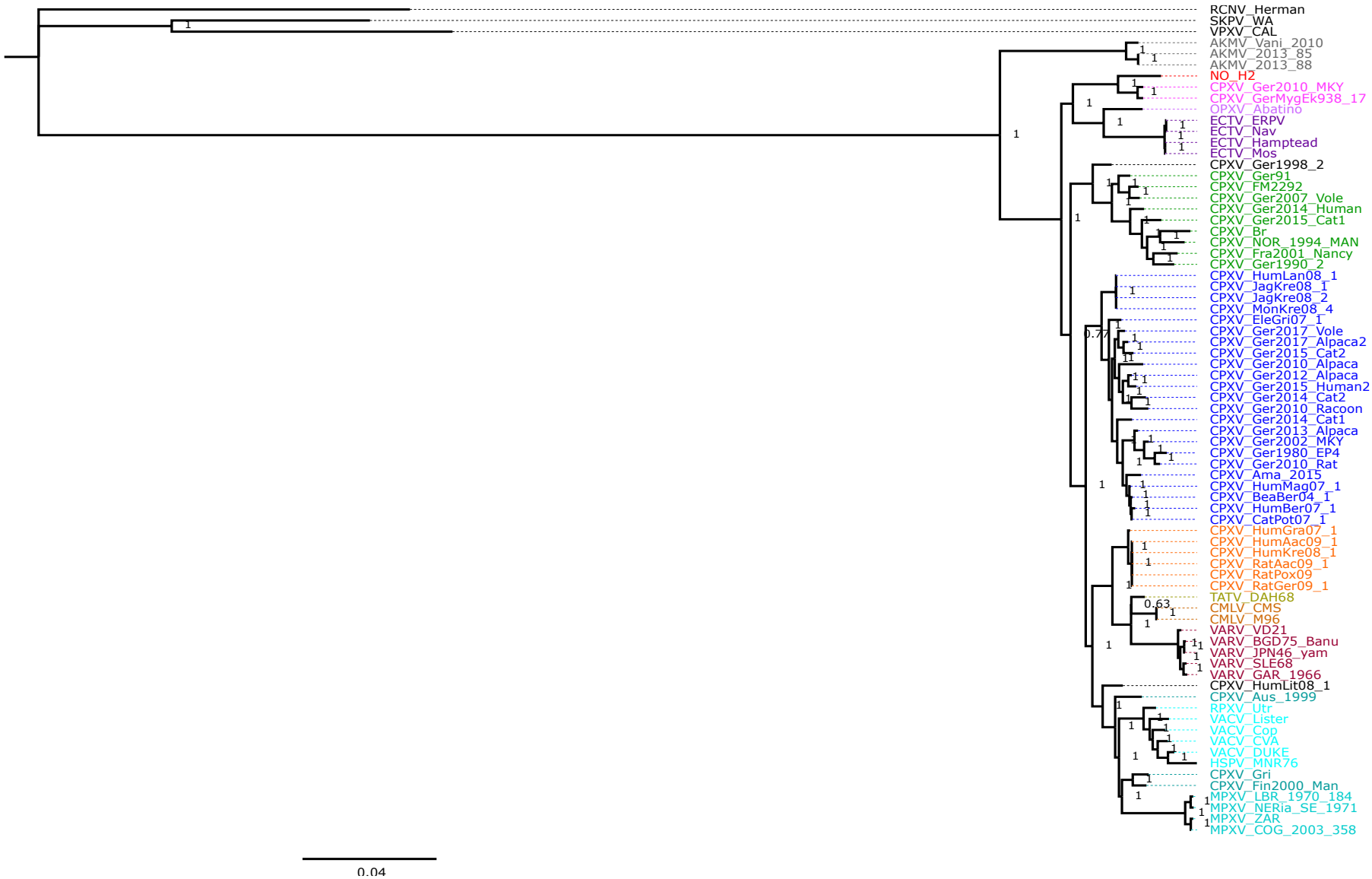

Supplementary Figure S15. Bayesian Inference phylogenetic tree based on 75 OPXV whole genomes. Clades are identified with colors.

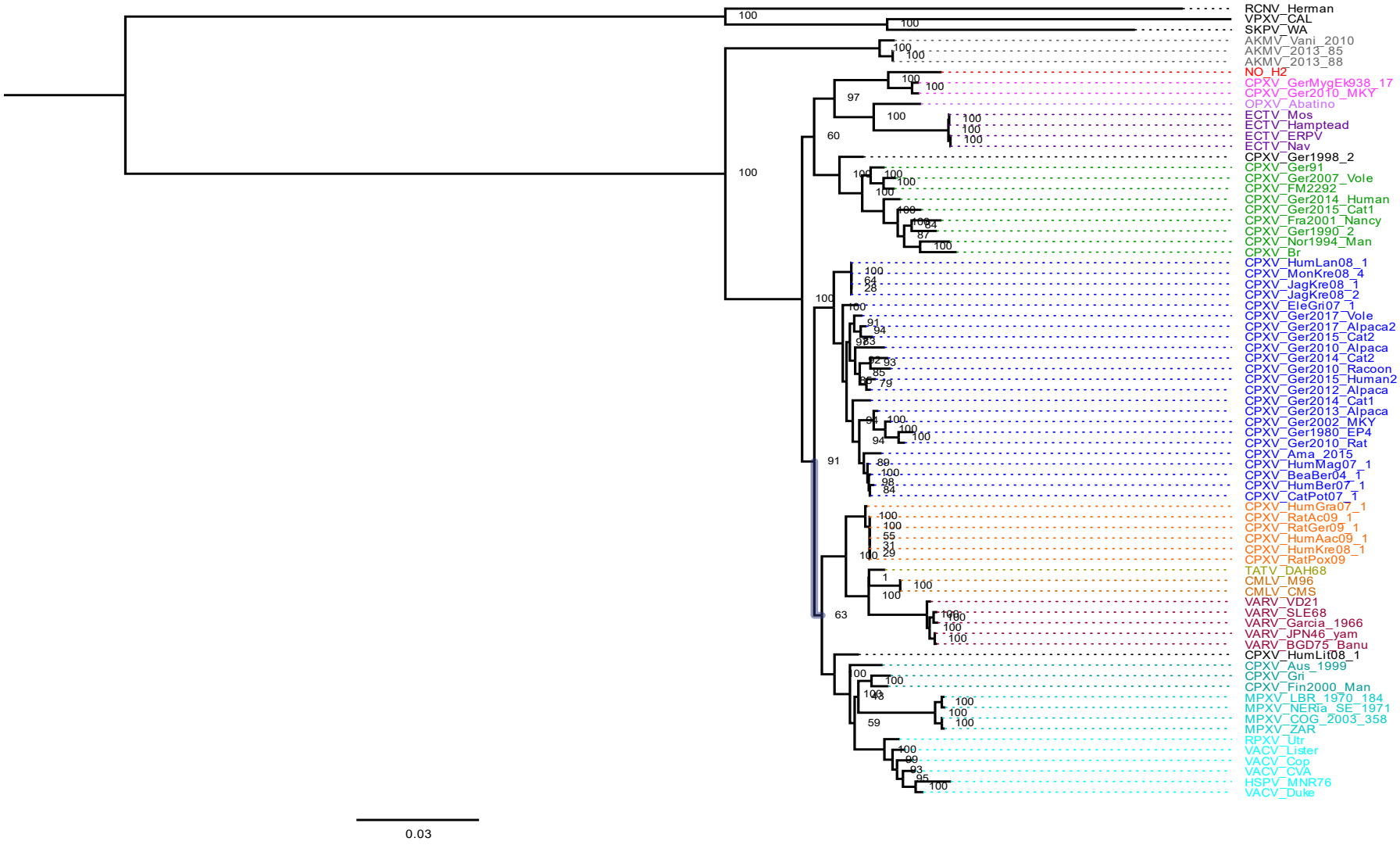

Supplementary Figure S16. Maximum-Likelihood phylogenetic tree based on 75 OPXV core genomes. Bootstrap values were determined from 1000 replica sampling. Clades are identified with colors.

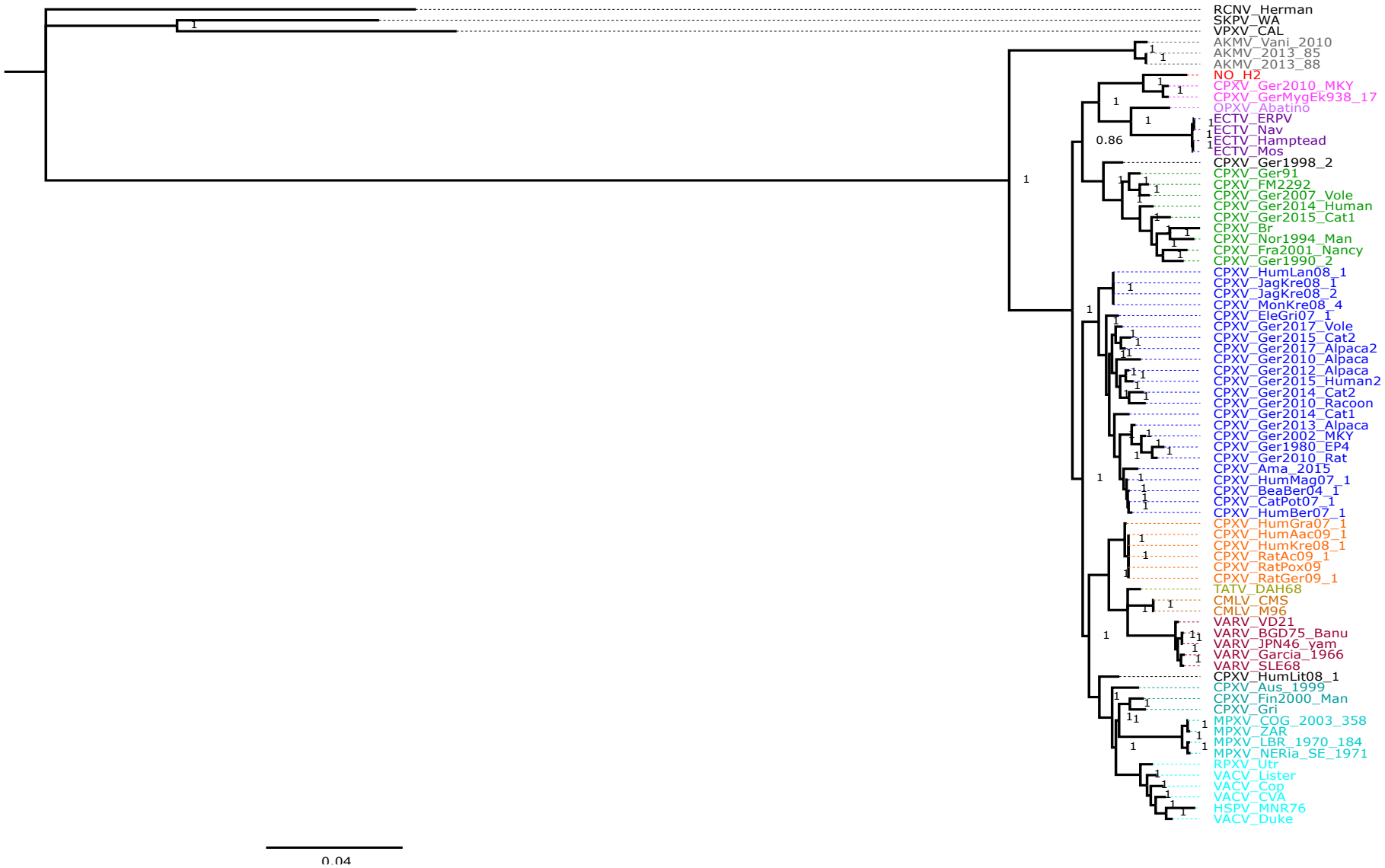

Supplementary Figure S17. Bayesian Inference phylogenetic tree based on 75 OPXV core genomes. Clades are identified with colors.

Supplementary Figure S18. Maximum-Likelihood phylogenetic tree based on 134 orthologous genes from 75 OPXV genomes. Bootstrap values were determined from 1000 replica sampling. Clades are identified with colors.

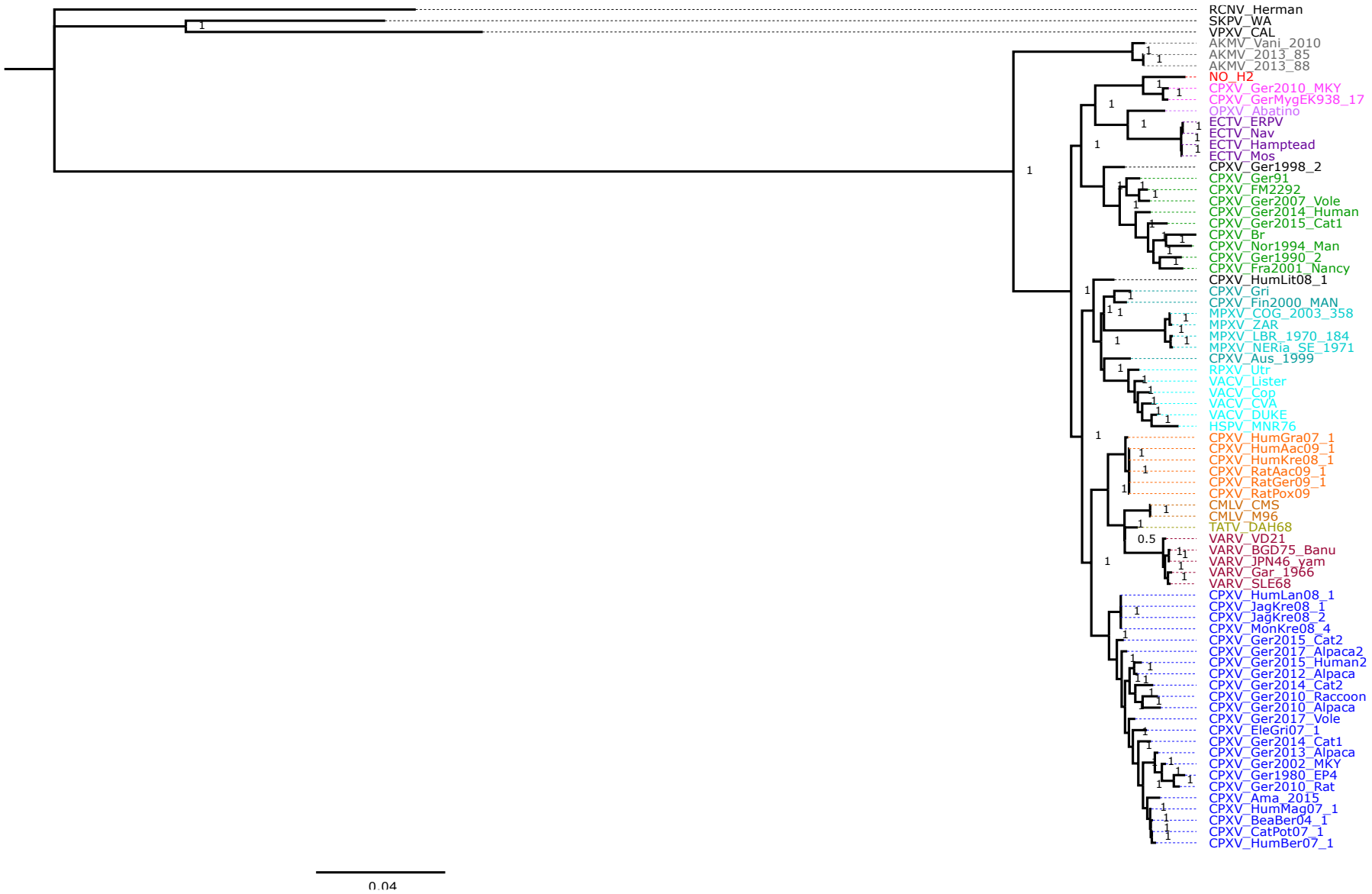

Supplementary Figure S19. Bayesian Inference phylogenetic tree based on 134 orthologous genes from 75 OPXV genomes. Clades are identified with colors.

Supplementary Table S1. List of strains used in this study.

Virus species	Strain	GenBank number accession	Abbreviation
Akhmeta virus	2013-85	MH607142	AKMV_2013_85
	2013-88	MH607141	AKMV_2013_88
	Vani_2010	MH607143	AKMV_Vani_2010
Alaskapox virus	2015	MN240300	AKPV_2015
Camelpox virus	CMS	AY009089	CMLV_CMS
	M96	NC_003391	CMLV_M96
Cowpox virus	Amadeus 2015	LN879483	CPXV_AMA_2015
	Austria 1999	HQ407377	CPXV_AUS_1999
	BeaBer04/1	KC813491.1	CPXV_BeaBer04_1
	Brighton Red	NC_003663	CPXV_BR
	CatPot07/1	KC813506.1	CPXV_CatPot07/1
	EleGri07/1	KC813507	CPXV_EleGRi07/1
	Finland 2000 MAN	HQ420893	CPXV_FIN_2000_MAN
	FM2292	LN864566	CPXV_FM2292
	France 2001 Nancy	HQ420894	CPXV_FRA_2001_Nancy
	Germany 91-3	DQ437593	CPXV_Ger91
	Germany 1980 EP4	HQ420895	CPXV_Ger1980_EP4
	Germany 1990 2	HQ420896	CPXV_Ger1990_2
	Germany 1998 2	HQ420897	CPXV_Ger1998_2
	Germany 2002 MKY	HQ420898	CPXV_Ger2002_MKY
	Ger/2007/Vole	LT896722	CPXV_Ger2007_Vole
	Ger/2010/Alpaca	LT896718	CPXV_Ger2010_Alpaca
	Ger/2010/MKY	LT896721	CPXV_Ger2010_MKY
	Ger/2010/Raccoon	LT896730	CPXV_Ger2010_Racoon
	Ger/2010/Rat	LT896728	CPXV_Ger2010_Rat
	Ger/2012/Alpaca	LT896726	CPXV_Ger2012_Alpaca
	Ger/2013/Alpaca	LT896719	CPXV_Ger2013_Alpaca
	Ger/2014/Cat1	LT896723	CPXV_Ger2014_Cat1
	Ger/2014/Cat2	LT896725	CPXV_Ger2014_Cat2
	Ger/2014/Human	LT993226	CPXV_Ger2014_Human
	Ger/2015/Cat1	LT896724	CPXV_Ger2015_Cat1
	Ger/2015/Cat2	LT896727	CPXV_Ger2015_Cat2
	Ger/2015/Human2	LT993232	CPXV_Ger2015_Human2
	Ger/2017/Alpaca2	LT896732	CPXV_Ger2017_Alpaca2
	Ger/2017/CommonvoleFMEimka	LT993228	CPXV_Ger2017_Vole
	GerMygEK938/17	LR812035	CPXV_GerMygEk93_17
	GRI-90	X94355	CPXV_GRI
	HumAac09/1	KC813508.1	CPXV_HumAac09_1
	HumBer07/1	KC813509.1	CPXV_HumBer07_1
	HumGra07/1	KC813510.1	CPXV_HumGra07_1
	HumKre08/1	KC813512.1	CPXV_HumKre08_1
	HumLan08/1	KC813492.1	CPXV_HumLan08_1
	HumLit08/1	KC813493.1	CPXV_HumLit08_1
	HumMag07/1	KC813495.1	CPXV_HumMag07_1
	JagKre08/1	KC813497.1	CPXV_JagKre08_1
	JagKre08/2	KC813498.1	CPXV_JagKre08_2
	MonKre08/4	KC813500.1	CPXV_MonKre08_4
	Norway1994MAN	HQ420899	CPXV_NOR_1994_MAN
	RatAac09/1	KC813501.1	CPXV_RatAac09_1
	RatGer09/1	KC813503.1	CPXV_RatGer09_1
	Ratpox09	LN864565	CPXV_RatPox09
Ectromelia virus	ERPV culture-collection ATCC:VR-1431	JQ410350	ECTV_ERPV
	Hampstead	KY554976	ECTV_Hampstead
	Moscow	NC_004105	ECTV_Mos
	Naval	KJ563295	ECTV_Nav
Horsepox virus	MNR-76	DQ792504	HSPV_MNR76
Monkeypox virus	Congo_2003_358	DQ011154	MPXV_COG_2003_358
	Liberia_1970_184	DQ011156	MPXV_LBR_1970_184
	Nigeria-SE-1971	KJ642617	MPXV_NERia_SE_1971
	Zaire	NC_003310	MPXV_ZAR
Abatino macacapox virus	-	MH816996	OPXV_Abatino
Raccoonpox virus	Herman	KP143769	RCNV_Herman
Rabbitpox virus	Utrecht	AY484669	RPXV_Utr
Skunkpox virus	WA	NC_031038.1	SKPV_WA
Taterapox virus	Dahomey 1968	NC_008291	TATV_DAH68
Vaccinia virus	Copenhagen	M35027	VACV_Cop
	Chorioallantois Ankara (CVA)	AM501482	VACV_CVA
	DUKE	DQ439815	VACV_DUKE
	Lister	AY678276	VACV_Lister
Variola virus	Bangladesh 1975 v75-550 Banu	DQ437581	VARV_BGD75_Banu
	Garcia 1966	Y16780	VARV_GARV_1966
	Japan 1946 (Yamada MS-2(A) Tokyo)	DQ441429	VARV_JPN46_yam
	Sierra Leone 1969 (V68-258)	DQ441437	VARV_SLE68
	VD21	KY358055	VARV_VD21
Volepox virus	CA	NC_031033.1	VPXV_CAL

Supplementary Table S2. Predicted genes in CPXV-No-H2 compared to reference genomes CPXV-Brighton (CPXV_BR), ECTV-Moscow (ECTV_Mos) and VACV-Copenhagen (VACV_Cop).

CDS	Start	Stop	Length (bp)	Direction	Function	CPXV_BR	Similarity (%)	ECTV_Mos	Similarity (%)	VACV_Cop	Similarity (%)
NoH2-001	897	1637	741	reverse	Chemokine binding protein (Cop-C23L)	vCCI/CPXV003	91.94	EVM001	83.00	B29R/C23L	79.01
NoH2-002	1746	2795	1050	reverse	TNF receptor (CrmB) (Cop-C22L)	crmB/CPXV005	92.96	-	-	B28R/C22L	75.00
NoH2-003	2873	4756	1884	reverse	Ankyrin (Cop-C19L)	CPXV006	87.30	EVM002	84.33	B25R/C19L	79.12
NoH2-004	4744	4833	90	reverse	Ankyrin-like repeat containing protein	CPXV007	100.00	-	-	-	-
NoH2-005	4871	6892	2022	reverse	Ankyrin (Cop-C17L)	CPXV008	95.38	-	-	B23R/C17L	87.57
NoH2-006	7064	7525	462	reverse	Hypothetical protein (Cop-C16L)	PXV009/CPXV22	55.56	-	-	B22R/C16L	55.92
NoH2-007	7643	8311	669	reverse	Alpha amanatin target protein (Cop-N2L)	CPXV010	89.59	-	-	-	-
NoH2-008	8529	9101	573	reverse	Hypothetical protein (Cop-C14L)	-	-	-	-	-	-
NoH2-009	9249	10070	822	reverse	BTB Kelch-domain containing protein; CRL comple x (Cop-A55R)	-	-	EVM004	82.05	-	-
NoH2-010	11192	12205	1014	reverse	Ankyrin (Cop-B20R)	CPXV011	92.88	EVM005	88.72	-	-
NoH2-011	12481	12681	201	reverse	C-type lectin domain containing protein	CPXV012	100.00	EVM007	67.44	-	-
NoH2-012	12765	14300	1536	reverse	BTB Kelch-domain containing protein; CRL comple x (Cop-A55R)	CPXV013	91.85	-	-	-	-
NoH2-013	14370	14966	597	reverse	TNF receptor (CrmB) (Cop-C22L)	CPXV014	83.85	EVM008	79.69	-	-
NoH2-014	14963	15289	327	reverse	TNF-alpha receptor like protein	vCD30/CPXV015	97.22	EVM009	90.83	-	-
NoH2-015	15389	17683	2295	reverse	Ankyrin (Cop-B18R)	CPXV016	91.89	EVM010	93.19	-	-
NoH2-016	17946	19250	1305	reverse	Ankyrin (CPXV-017)	CPXV017	92.87	-	-	-	-
NoH2-017	19346	19867	522	reverse	MPV-Z-N3R	CPXV018	86.71	-	-	-	-
NoH2-018	19927	22242	2316	reverse	Ankyrin (Cop-B18R)	CPXV019	86.43	-	-	-	-
NoH2-019	22358	22876	519	reverse	Host range protein	CPXV020	91.28	-	-	-	-
NoH2-020	23038	23364	327	forward	Secreted EGF-like protein (Cop-C11R)	VGF/CPXV021	82.57	-	96.39	C11R	79.82
NoH2-021	23610	24611	1002	reverse	IL-1 receptor antagonist (Cop-C10L)	CPXV022	93.39	EVM011	93.09	C10L	91.89
NoH2-022	25143	25871	729	forward	Zinc finger-like protein	CPXV023	94.22	EVM012	92.15	-	-
NoH2-023	26001	26381	381	reverse	Soluble IL-18 binding protein (Bsh-D7L)	CPXV024	92.06	EVM013	90.08	-	-
NoH2-024	26439	28445	2007	reverse	Ankyrin|Host Range (Bang-D8L)	VHR1/CPXV025	94.01	-	-	-	-
NoH2-025	28582	28770	189	reverse	ANK-containing protein	CPXV026	90.00	EVM014	75.47	-	-
NoH2-026	28947	30857	1911	reverse	Ankyrin; Type I IFN resistance (Cop-C9L)	CPXV027	89.21	-	-	C9L	82.91
NoH2-027	30898	31455	558	reverse	Unknown (Cop-C8L)	CPXV028	89.19	-	-	C8L	87.57
NoH2-028	31525	31977	453	reverse	Type 1 IFN inhibitor (Cop-C7L)	CPXV029	96.67	EVM015	93.33	C7L	96.67
NoH2-029	32209	32679	471	reverse	Bcl-2-like protein, IFN-beta inhibitor (Cop-C6L)	CPXV030	92.11	EVM016	92.76	C6L	92.67
NoH2-030	32834	32956	123	reverse	Kelch-like protein (Cop-C5L)	CPXV031	66.67	-	-	-	-
NoH2-031	33111	33431	321	reverse	Kelch-like protein (Cop-C5L)	CPXV032	92.45	-	-	C5L	91.35
NoH2-032	33492	34442	951	reverse	IL-1 receptor antagonist (Cop-C10L)	CPXV033	95.57	-	-	C4L	95.89
NoH2-033	34519	35304	786	reverse	Complement binding (secreted) (Cop-C3L)	CPXV034	89.35	EVM017	91.57	C3L	89.35
NoH2-034	35361	36899	1539	reverse	POZ|BTB Kelch domain protein (Cop-C2L)	CPXV035	97.07	EVM018	95.90	C2L	98.05
NoH2-035	36966	37655	690	reverse	Putative TLR signalling inhibitor (Cop-C1L)	CPXV036	92.21	-	-	C1L	91.93
NoH2-036	37642	37998	357	reverse	Anti-apoptotic Bcl-2-like protein (Cop-N1L)	CPXV037	91.53	EVM019	93.22	N1L	90.68
NoH2-037	38136	38672	537	reverse	Alpha amanatin target protein (Cop-N2L)	CPXV038	87.08	EVM020	84.36	N2L	83.62
NoH2-038	38714	40129	1416	reverse	ANK-containing protein; apoptosis inhibitor (C op-M1L)	CPXV039	95.35	EVM021	96.82	M1L	96.82
NoH2-039	40107	40769	663	reverse	NFkB inhibitor (Cop-M2L)	CPXV040	92.27	-	-	M2L	92.27
NoH2-040	40903	41760	858	reverse	Ankyrin|NFkB inhibitor (Cop-K1L)	CPXV041	96.47	EVM022	95.44	K1L	95.05
NoH2-041	41992	43119	1128	reverse	Serpin 1,2,3 (Cop-K2L)	SPI3/CPXV042	95.73	H14-B/EVM023	93.60	K2L	92.27
NoH2-042	43169	43435	267	reverse	IFN resistance, PKR|eIF-alpha inhibitor (Cop-K3 L)	CPXV043	92.05	-	-	K3L	87.50
NoH2-043	43485	44759	1275	reverse	Phospholipase-D-like protein (Cop-K4L)	CPXV044	98.11	-	-	K4L	96.93
NoH2-044	44781	45614	834	reverse	Monoglyceride lipase (Cop-K5L)	CPXV045	98.18	H14-E/EVM024	96.73	K5L	88.89
NoH2-045	45752	46201	450	forward	Host immune response repressor (Cop-K7R)	CPXV046	97.32	-	-	K7R	95.97
NoH2-046	46275	46997	723	reverse	Caspase-9 (apoptosis) inhibitor (mitochondrial- associated) (Cop-F1L)	CPXV048	83.20	EVM025	86.98	F1L	88.56
NoH2-047	46997	47440	444	reverse	dUTPase (Cop-F2L)	CPXV049	98.64	EVM026	98.64	F2L	97.96
NoH2-048	47464	48906	1443	reverse	Kelch-like protein (Cop-F3L)	CPXV050	94.38	EVM027	94.57	F3L	93.33
NoH2-049	48917	49876	960	reverse	Ribonucleotide reductase small subunit (Cop-F4L)	CPXV051	97.49	EVM028	98.12	F4L	97.49
NoH2-050	49912	50898	987	reverse	36kDa major membrane protein (Cop-F5L)	CPXV052	86.28	-	-	F5L	82.32
NoH2-051	50928	51152	225	reverse	Hypothetical protein (Cop-F6L)	CPXV053	85.14	EVM029	90.54	F6L	91.89
NoH2-052	51166	51426	261	reverse	Hypothetical protein (Cop-F7L)	CPXV054	81.40	EVM030	87.21	F7L	82.61
NoH2-053	51574	51777	204	reverse	Cytoplasmic protein (Cop-F8L)	CPXV055	96.88	EVM031	95.31	F8L	98.44
NoH2-054	51837	52475	639	reverse	S-S bond formation pathway protein substrate (Cop-F9L)	CPXV056	98.59	EVM032	97.17	F9L	98.11
NoH2-055	52462	53781	1320	reverse	Essential Ser|Thr kinase morph (Cop-F10L)	CPXV057	99.32	EVM033	99.09	F10L	99.54
NoH2-056	53804	54868	1065	reverse	RhoA signalling inhibitor, virus release protei n (Cop-F11L)	CPXV059	98.31	EVM034	97.74	F11L	99.15
NoH2-057	54926	56830	1905	reverse	EEV maturation protein (Cop-F12L)	CPXV060	98.11	EVM035	97.63	F12L	96.85
NoH2-058	56876	57994	1119	reverse	Palmitylated EEV membrane glycoprotein (Cop-F13 L)	CPXV061	99.19	EVM036	100.00	F13L	99.46
NoH2-059	58012	58263	252	reverse	Unknown (Cop-F14L)	CPXV062	77.11	EVM037	71.08	F14L	75.90
NoH2-060	58308	58466	159	forward	CPV-B-063	CPXV063	90.39	-	-	-	-
NoH2-061	58536	59012	477	reverse	Unknown conserved protein (Cop-F15L)	CPXV064	96.20	EVM038	98.73	F15L	98.10
NoH2-062	59030	59713	684	reverse	Non-functional Serine Recombinase (Cop-F16L)	CPXV065	94.71	EVM039	95.60	F16L	96.92
NoH2-063	59776	60081	306	forward	DNA-binding phosphoprotein (VP11); mTOR antagon ist (Cop-F17R)	CPXV066	98.02	EVM040	97.03	F17R	99.01
NoH2-064	60078	61517	1440	reverse	Poly (A) polymerase catalytic subunit (VP55) (C op-E1L)	CPXV067	99.58	EVM041	98.96	E1L	99.17
NoH2-065	61514	63727	2214	reverse	IEV morphogenesis (Cop-E2L)	CPXV068	99.05	EVM042	97.97	E2L	98.24
NoH2-066	63851	64423	573	reverse	dsRNA-binding protein, IFN resistance|PKR inhib itor (Z-DNA binding) (Cop-E3L)	CPXV069	92.11	EVM043	90.00	E3L	90.53
NoH2-067	64479	65258	780	reverse	RNA polymerase subunit (RPO30) (Cop-E4L)	CPXV070	98.08	EVM044	99.61	E4L	99.61
NoH2-068	65378	66337	960	forward	Virosome component (Cop-E5R)	CPXV071	95.93	EVM045	87.77	E5R	90.91
NoH2-069	66498	68201	1704	forward	Virion protein (Cop-E6R)	CPXV072	99.30	EVM046	98.41	E6R	99.12
NoH2-070	68282	68767	486	forward	Myristylated protein (Cop-E7R)	CPXV073	93.17	EVM047	90.68	E7R	93.17
NoH2-071	68907	69728	822	forward	ER-localized membrane protein, virion core prot ein (Cop-E8R)	CPXV074	98.17	EVM048	97.80	E8R	99.27
NoH2-072	69735	72755	3021	reverse	DNA polymerase (Cop-E9L)	CPXV075	99.40	EVM049	97.82	E9L	98.51
NoH2-073	72787	73074	288	forward	Sulfhydryl oxidase (FAD-linked) (Cop-E10R)	CPXV076	98.95	EVM050	97.90	E10R	100.00
NoH2-074	73069	73458	390	reverse	Virion core protein (Cop-E11L)	CPXV077	97.67	EVM051	94.57	E11L	96.12
NoH2-075	73445	75445	2001	reverse	Membrane protein (Cop-O1L)	CPXV078	97.90	EVM052	96.40	O1L	97.45
NoH2-076	75493	75819	327	reverse	Glutaredoxin 1 (Cop-O2L)	CPXV079	98.15	EVM053	99.07	O2L	100.00
NoH2-077	75843	75950	108	reverse	Virus entry|fusion complex component (Cop-O3L)	-	-	-	-	O3L	100.00
NoH2-078	75965	76903	939	reverse	DNA-binding core protein (Cop-I1L)	CPXV080	99.68	EVM054	98.72	I1L	99.68
NoH2-079	76910	77128	219	reverse	IMV membrane protein (Cop-I2L)	CPXV081	84.93	EVM055	86.30	I2L	86.30
NoH2-080	77129	77938	810	reverse	ssDNA-binding phosphoprotein (Cop-I3L)	CPXV082	99.63	EVM056	98.51	I3L	98.14
NoH2-081	78021	80336	2316	reverse	Ribonucleotide reductase large subunit (Cop-I4L)	CPXV083	98.83	EVM057	96.50	I4L	98.70
NoH2-082	80363	80602	240	reverse	IMV protein VP13 (Cop-I5L)	CPXV084	98.73	EVM058	97.47	I5L	100.00
NoH2-083	80621	81769	1149	reverse	Telomere-binding protein (Cop-I6L)	CPXV085	99.22	EVM059	99.22	I6L	99.74
NoH2-084	81762	83033	1272	reverse	Virion core cysteine protease (Cop-I7L)	CPXV086	98.82	EVM060	98.11	I7L	98.11
NoH2-085	83039	85069	2031	forward	RNA helicase, DExH-NPH-II domain (Cop-I8R)	CPXV087	96.01	EVM061	96.60	I8R	95.56
NoH2-086	85073	86848	1776	reverse	Metalloprotease (Cop-G1L)	CPXV088	98.48	EVM062	98.48	G1L	98.65
NoH2-087	86845	87180	336	reverse	Entry|fusion complex component (Cop-G3L)	CPXV089	98.20	EVM063	96.40	G3L	97.30
NoH2-088	87174	87836	663	forward	VLTF (late transcription elongation factor) (Co p-G2R)	CPXV090	98.64	EVM064	98.18	G2R	100.00
NoH2-089	87806	88180	375	reverse	Glutaredoxin-like protein (Cop-G4L)	CPXV091	99.19	EVM065	100.00	G4L	99.19
NoH2-090	88183	89487	1305	forward	FEN1-like nuclease (Cop-G5R)	CPXV092	98.16	EVM066	97.93	G5R	98.62
NoH2-091	89495	89686	192	forward	RNA polymerase subunit (RPO7) (Cop-G5.5R)	CPXV093	100.00	EVM067	100.00	G5.5R	100.00
NoH2-092	89688	90185	498	forward	NLPc|P60 superfamily protein (Cop-G6R)	CPXV094	96.36	EVM068	97.58	G6R	96.36
NoH2-093	90150	91265	1116	reverse	Virion phosphoprotein, early morphogenesis (Cop -G7L)	CPXV095	99.73	EVM069	99.19	G7L	99.19
NoH2-094	91296	92078	783	forward	VLTF-1 (late transcription factor 1) (Cop-G8R)	CPXV097	99.62	EVM070	100.00	G8R	100.00
NoH2-095	92098	93120	1023	forward	Entry|fusion complex component, myristyl|protein (Cop-G9R)	CPXV098	97.94	EVM071	96.47	G9R	98.53
NoH2-096	93121	93873	753	forward	IMV membrane protein (Cop-L1R)	CPXV099	98.40	EVM072	98.40	L1R	98.80
NoH2-097	93905	94171	267	forward	Viral membrane assembly proteins (VMAP) (Cop-L2 R)	CPXV100	98.86	EVM073	90.91	L2R	92.05
NoH2-098	94161	95213	1053	reverse	Internal virion protein (Cop-L3L)	CPXV101	98.00	EVM074	92.66	L3L	97.43
NoH2-099	95238	95993	756	forward	ss|dsDNA binding protein (VP8) (Cop-L4R)	CPXV102	98.81	EVM075	98.81	L4R	98.41
NoH2-100	96003	96389	387	forward	Entry and Fusion IMV protein (Cop-L5R)	CPXV103	99.22	EVM076	100.00	L5R	100.00
NoH2-101	96346	96807	462	forward	Virion morph (Cop-J1R)	CPXV104	100.00	EVM077	100.00	J1R	98.69
NoH2-102	96823	97356	534	forward	Thymidine kinase (Cop-J2R)	CPXV105	97.18	EVM078	96.61	J2R	99.44
NoH2-103	97422	98423	1002	forward	Poly (A) polymerase small subunit (VP39) (Cop-J 3R)	CPXV106	99.40	EVM079	99.40	J3R	98.50
NoH2-104	98338	98895	558	forward	RNA polymerase subunit (RPO22) (Cop-J4R)	CPXV107	99.46	EVM080	98.92	J4R	99.46
NoH2-105	98956	99357	402	reverse	IMV membrane protein (Cop-J5L)	CPXV108	99.25	EVM081	99.25	J5L	98.50
NoH2-106	99464	103324	3861	forward	RNA polymerase subunit (RPO147) (Cop-J6R)	CPXV109	99.15	EVM082	99.07	J6R	99.22
NoH2-107	103321	103836	516	reverse	Tyr|Ser phosphatase, IFN-gamma inhibitor (Cop-H 1L)	CPXV110	99.42	EVM083	99.42	H1L	99.42
NoH2-108	103850	104419	570	forward	IMV membrane protein (Cop-H2R)	CPXV111	99.47	EVM084	98.94	H2R	98.41
NoH2-109	104422	105399	978	reverse	IMV heparin binding surface protein (Cop-H3L)	CPXV112	97.22	EVM085	96.00	H3L	96.92
NoH2-110	105400	107787	2388	reverse	RAP94 (RNA pol assoc protein) (Cop-H4L)	CPXV113	99.37	EVM086	98.62	H4L	99.12

NoH2-111	107973	108602	630	forward	VLTF-4 (late transcription factor 4) (Cop-H5R)	CPXV114	95.22	EVM087	88.38	H5R	88.24
NoH2-112	108603	109547	945	forward	DNA topoisomerase type I (Cop-H6R)	CPXV115	99.05	EVM088	99.05	H6R	99.68
NoH2-113	109585	110025	441	forward	Viral membrane assembly proteins (VMAP) (Cop-H7 R)	CPXV117	95.89	EVM089	95.21	H7R	96.58
NoH2-114	110069	112600	2532	forward	mRNA capping enzyme large subunit (Cop-D1R)	CPXV118	99.29	EVM090	99.05	D1R	98.70
NoH2-115	112559	112999	441	reverse	Virion core (Cop-D2L)	CPXV119	99.32	EVM091	97.95	D2L	98.63
NoH2-116	112992	113705	714	forward	Virion core (Cop-D3R)	CPXV120	98.73	EVM092	98.73	D3R	97.47
NoH2-117	113705	114361	657	forward	Uracil-DNA glycosylase, DNA polymerase processi vity factor (Cop-D4R)	CPXV121	97.25	EVM093	97.71	D4R	98.62
NoH2-118	114393	116750	2358	forward	NTPase, DNA primase (Cop-D5R)	CPXV122	97.83	EVM094	97.83	D5R	98.47
NoH2-119	116791	118704	1914	forward	Morphogenesis, VETF-s (early transcription fact or small) (Cop-D6R)	CPXV123	99.53	EVM095	98.74	D6R	99.06
NoH2-120	118731	119216	486	forward	RNA polymerase subunit (RPO18) (Cop-D7R)	CPXV124	98.76	EVM096	98.76	D7R	98.76
NoH2-121	119179	120096	918	reverse	Carbonic anhydrase, GAG-binding IMV membrane pr otein (Cop-D8L)	CPXV125	97.38	EVM097	95.41	D8L	93.12
NoH2-122	120138	120779	642	forward	mRNA decapping enzyme (Cop-D9R)	CPXV126	100.00	EVM098	99.53	D9R	99.53
NoH2-123	120776	121528	753	forward	mRNA decapping enzyme (Cop-D10R)	CPXV127	98.78	EVM099	97.60	D10R	98.37
NoH2-124	121525	123420	1896	reverse	ATPase, NPH1 (Cop-D11L)	CPXV128	99.68	EVM100	98.73	D11L	99.53
NoH2-125	123455	124318	864	reverse	mRNA capping enzyme small subunit (Cop-D12L)	CPXV129	99.65	EVM101	99.30	D12L	99.65
NoH2-126	124349	126004	1656	reverse	Trimeric virion coat protein (rifampicin res) (Cop-D13L)	CPXV131	99.09	EVM102	99.09	D13L	99.09
NoH2-127	126028	126480	453	reverse	VLTF-2 (late transcription factor 2) (Cop-A1L)	CPXV132	98.67	EVM103	98.67	A1L	99.33
NoH2-128	126501	127175	675	reverse	VLTF-3 (late transcription factor 3) (Cop-A2L)	CPXV133	99.11	EVM104	98.21	A2L	99.55
NoH2-129	127172	127402	231	reverse	S-S bond formation pathway protein (Cop-A2.5L)	CPXV134	96.05	EVM105	96.05	A2.5L	93.42
NoH2-130	127417	129354	1938	reverse	P4b precursor (Cop-A3L)	CPXV135	97.67	EVM106	97.36	A3L	97.52
NoH2-131	129407	130258	852	reverse	39kDa virion core protein (Cop-A4L)	CPXV136	88.14	EVM107	91.52	A4L	92.23
NoH2-132	130296	130790	495	forward	RNA polymerase subunit (RPO19) (Cop-A5R)	CPXV137	98.17	EVM108	96.95	A5R	98.17
NoH2-133	130787	131905	1119	reverse	Viral membrane assembly proteins (VMAP), core p rotein (Cop-A6L)	CPXV138	98.12	EVM109	98.12	A6L	99.19
NoH2-134	131929	134061	2133	reverse	VETF-L (early transcription factor large) (Cop- A7L)	CPXV139	98.45	EVM110	98.87	A7L	99.72
NoH2-135	134115	134981	867	forward	VITF-3 34kda subunit (Cop-A8R)	CPXV140	98.96	EVM111	98.26	A8R	98.61
NoH2-136	134974	135336	363	reverse	Viral membrane associated, early morphogenesis protein (Cop-A9L)	CPXV141	96.00	EVM112	79.49	A9L	84.04
NoH2-137	135337	138012	2676	reverse	P4a precursor (Cop-A10L)	CPXV142	94.74	EVM113	95.96	A10L	95.85
NoH2-138	138027	138983	957	forward	Viral membrane assembly proteins (VMAP) (Cop-A1 1R)	CPXV143	100.00	EVM114	99.37	A11R	99.69
NoH2-139	138980	139558	579	reverse	Virion core and cleavage processing protein (Co p-A12L)	CPXV144	92.19	EVM115	95.31	A12L	98.44
NoH2-140	139582	139788	207	reverse	IMV membrane protein, virion maturation (Cop-A1 3L)	CPXV145	87.14	EVM116	86.77	A13L	87.14
NoH2-141	139896	140168	273	reverse	Essential IMV membrane protein (Cop-A14L)	CPXV146	98.89	EVM117	100.00	A14L	98.89
NoH2-142	140185	140346	162	reverse	Non-essential IMV membrane protein (Cop-A14.5L)	CPXV147	100.00	EVM117.5	100.00	A14.5L	100.00
NoH2-143	140336	140620	285	reverse	Core protein (Cop-A15L)	CPXV148	100.00	EVM118	97.87	A15L	100.00
NoH2-144	140604	141737	1134	reverse	Myristylated protein, essential for entry|fusio n (Cop-A16L)	CPXV149	97.88	EVM119	96.82	A16L	98.68
NoH2-145	141740	142351	612	reverse	IMV membrane protein (Cop-A17L)	CPXV150	96.06	EVM120	96.06	A17L	98.03
NoH2-146	142366	143847	1482	forward	DNA helicase, transcript release factor (Cop-A1 8R)	CPXV151	96.76	EVM121	97.77	A18R	98.38
NoH2-147	143828	144061	234	reverse	Zinc finger-like protein (Cop-A19L)	CPXV152	100.00	EVM122	97.40	A19L	100.00
NoH2-148	144062	144415	354	reverse	IMV membrane protein, entry|fusion complex component (Cop-A21L)	CPXV153	98.29	EVM123	97.46	A21L	100.00
NoH2-149	144414	145694	1281	forward	DNA polymerase processivity factor (Cop-A20R)	CPXV154	97.89	EVM124	97.42	A20R	97.89
NoH2-150	145624	146187	564	forward	Holliday junction resolvase (Cop-A22R)	CPXV155	99.47	EVM125	98.40	A22R	98.86
NoH2-151	146206	147354	1149	forward	VITF-3 45kda subunit (Cop-A23R)	CPXV156	99.22	EVM126	98.17	A23R	99.22
NoH2-152	147351	150845	3495	forward	RNA polymerase subunit (RPO132) (Cop-A24R)	rpo132/CPXV157	99.23	EVM127	99.83	A24R	99.14
NoH2-153	150838	154107	3270	reverse	A-type inclusion protein (Cop-A25L)	CPXV158	51.73	EVM128	94.82	-	-
NoH2-154	154153	155691	1539	reverse	P4c precursor (Cop-A26L)	CPXV161	87.06	-	-	A26L	92.39
NoH2-155	155743	156075	333	reverse	IMV surface protein, fusion protein (Cop-A27L)	CPXV162	98.18	EVM129	96.36	A27L	97.27
NoH2-156	156076	156516	441	reverse	IMV MP|Virus entry (Cop-A28L)	CPXV163	97.95	EVM130	97.26	A28L	97.26
NoH2-157	156517	157434	918	reverse	RNA polymerase subunit (RPO35) (Cop-A29L)	CPXV164	98.36	EVM131	98.03	A29L	99.02
NoH2-158	157397	157630	234	reverse	IMV protein (Cop-A30L)	CPXV165	96.10	EVM132	97.40	A30L	98.70
NoH2-159	157663	157791	129	reverse	Viral membrane assembly proteins (VMAP) (Cop-A 30.5L)	165.5	95.24	-	-	A30.5L	100.00
NoH2-160	157790	158170	381	forward	Hypothetical protein (Cop-A31R)	CPXV166	89.29	EVM133	93.65	A31R	96.03
NoH2-161	158174	158950	777	reverse	ATPase|DNA packaging protein (Cop-A32L)	CPXV167	98.44	EVM134	98.44	A32L	97.66
NoH2-162	159068	159631	564	forward	EEV membrane phosphoglycoprotein, C-type lectin -like domain (Cop-A33R)	CPXV168	91.98	EVM135	88.24	A33R	88.24
NoH2-163	159655	160161	507	forward	C-type lectin-like IEV|EEV glycoprotein (Cop-A34R)	CPXV169	94.05	EVM136	97.62	A34R	92.86
NoH2-164	160204	160734	531	forward	MHC class II antigen presentation inhibitor (Co p-A35R)	CPXV171	97.73	EVM137	94.89	A35R	97.73
NoH2-165	160801	161481	681	forward	IEV transmembrane phosphoprotein (Cop-A36R)	CPXV172	74.14	137.5f	67.88	A36R	74.56
NoH2-166	161546	162340	795	forward	Hypothetical protein (Cop-A37R)	CPXV173	84.03	-	-	A37R	84.73
NoH2-167	162451	162630	180	forward	Unknown (Gar-A43R)	CPXV174	70.18	-	-	-	-
NoH2-168	162627	163460	834	reverse	CD47-like, integral membrane protein (Cop-A38L)	CPXV175	95.67	EVM138	94.95	A38L	94.95
NoH2-169	164256	164471	216	forward	Semaphorin (Cop-A39R)	CPXV176	82.76	EVM139	90.39	A39R	82.76
NoH2-170	164706	165185	480	forward	Lectin homolog (Cop-A40R)	CPXV177	91.25	-	-	A40R	97.08
NoH2-171	165294	165971	678	reverse	Chemokine binding protein (Cop-A41L)	CPXV178	90.05	EVM140	95.11	A41L	90.67
NoH2-172	166133	166537	405	forward	Profilin-like protein, ATI-localized (Cop-A42R)	CPXV179	90.91	EVM141	100.00	A42R	90.91
NoH2-173	166577	167188	612	forward	Type I membrane glycoprotein (Cop-A43R)	CPXV180	65.03	EVM142	99.51	A43R	66.01
NoH2-174	167207	167431	225	forward	Hypothetical protein (Cop-A43.5R)	CPXV181	73.61	-	-	A43.5R	91.43
NoH2-175	167586	168626	1041	reverse	3 beta-hydroxysteroid dehydrogenase|delta 5->4 isomerase (Cop-A44L)	CPXV182	92.44	EVM143	95.09	A44L	92.78
NoH2-176	168673	169050	378	forward	Inactive Cu-Zn superoxide dismutase-like virion protein (Cop-A45R)	CPXV183	95.20	EVM144	94.40	A45R	93.60
NoH2-177	169040	169762	723	forward	IL-1|TLR signaling inhibitor (Cop-A46R)	CPXV184	98.75	EVM145	97.50	A46R	97.30
NoH2-178	169850	170584	735	reverse	Immunoprevalent protein (Cop-A47L)	CPXV185	98.77	EVM146	95.90	A47L	95.90
NoH2-179	170617	171300	684	forward	Thymidylate kinase (Cop-A48R)	CPXV186	99.12	EVM147	98.68	A48R	99.02
NoH2-180	171350	171838	489	forward	Putative phosphotransferase|anion transport pro tein (Cop-A49R)	CPXV187	95.06	-	-	A49R	97.53
NoH2-181	171870	173528	1659	forward	ATP-dependent DNA ligase (Cop-A50R)	CPXV188	96.39	EVM148	95.31	A50R	96.56
NoH2-182	173579	174583	1005	forward	Hypothetical protein (Cop-A51R)	CPXV189	94.31	EVM149	93.11	A51R	94.91
NoH2-183	174656	175231	576	forward	Toll|IL-1 receptor-like protein, IL-1, NFkB sig nalling inhibitor (Cop-A52R)	CPXV190	96.34	-	-	A52R	95.29
NoH2-184	175568	176125	558	forward	TNF receptor (CrmC) (Cop-A53R)	CrmC/CPXV191	85.56	-	-	A53R	78.18
NoH2-185	176400	178094	1695	forward	BTB Kelch-domain containing protein; CRL comple x (Cop-A55R)	CPXV193	95.57	EVM150	95.04	A55R	95.39
NoH2-186	178143	179087	945	forward	Hemagglutinin (Cop-A56R)	CPXV194	84.18	EVM151	77.29	A56R	85.76
NoH2-187	179105	179698	594	forward	Guanylate kinase (Cop-A56.5R)	CPXV195	98.48	-	-	A57R	96.69
NoH2-188	179818	180717	900	forward	Ser|Thr Kinase (Cop-B1R)	CPXV196	97.99	EVM152	96.32	B1R	94.63
NoH2-189	180787	182304	1518	forward	Schlafen (Cop-B2R)	CPXV197	94.65	EVM153	90.68	B2R	89.35
NoH2-190	182565	184253	1689	forward	Ankyrin (Cop-B4R)	CPXV198	96.09	EVM154	92.53	B4R	93.24
NoH2-191	184357	185313	957	forward	EEV type-1 membrane glycoprotein, protective an tigen (Cop-B5R)	CPXV199	89.62	C1R/EVM155	91.20	B5R	91.82
NoH2-192	185401	185946	546	forward	Ankyrin-like protein (Cop-B6R)	CPXV200	90.61	C2R/EVM156	89.50	B6R	88.40
NoH2-193	185985	186539	555	forward	Virulence, ER resident (Cop-B7R)	CPXV201	90.76	C3R/EVM157	90.76	B7R	90.22
NoH2-194	186626	187426	801	forward	Soluble IFN-g receptor-like protein (Cop-B8R)	CPXV202	89.10	C4R/EVM158	85.71	B8R	88.21
NoH2-195	187506	188183	678	forward	ER-localized apoptosis regulator (Cop-B9R)	CPXV203	93.33	-	-	B9R	81.16
NoH2-196	188342	189850	1509	forward	Kelch-like protein (Cop-B10R)	CPXV204	92.03	-	-	B10R	89.51
NoH2-197	189924	190220	297	forward	Hypothetical protein (Cop-B11R)	CPXV205	97.02	C5R/EVM159	93.94	B11R	89.39
NoH2-198	190288	191136	849	forward	Ser|Thr Kinase (Cop-B12R)	CPXV206	97.87	C6R/EVM160	92.23	B12R	96.79
NoH2-199	191229	192260	1032	forward	Serpin 1,2,3 (Cop-K2L)	CrmA/CPXV207	95.03	C7R/EVM161	92.11	B14R	94.44
NoH2-200	192386	192835	450	forward	Hypothetical protein (Cop-C16L)	CPXV208	95.30	C8R/EVM162	93.29	B15R	93.29
NoH2-201	192926	193903	978	forward	IL-1 beta receptor (Cop-B16R)	CPXV209	95.09	C9R/EVM163	81.10	B16R	90.35
NoH2-202	193951	194973	1023	reverse	IL-1 beta inhibitor (Cop-B17L)	CPXV210	96.77	C10L/EVM164	92.04	B17L	96.77
NoH2-203	195115	196881	1767	forward	Ankyrin (Cop-B18R)	CPXV211	95.24	C11R/EVM165	92.77	B18R	92.77
NoH2-204	196856	197953	1098	forward	IFN-alpha|beta receptor glycoprotein (Cop-B19R)	CPXV212	92.08	C12R/EVM166	81.43	B19R	85.51
NoH2-205	198015	199643	1629	forward	Ankyrin (Cop-B20R)	CPXV213	95.60	-	-	B20R	82.26
NoH2-206	200512	202185	1674	forward	kelch-like protein (EV-M-167)	CPXV215	96.59	C13R/EVM167	78.04	-	-
NoH2-207	202304	202405	102	reverse	Hypothetical protein (Cop-C11.5R)	CPXV216	92.00	-	-	C11.5R	84.00
NoH2-208	202477	203556	1080	forward	Serpin 1,2,3 (Cop-K2L)	CPXV217	94.99	C14R/EVM168	94.43	C12L	92.48
NoH2-209	203746	204333	588	forward	Hypothetical protein (Cop-C14L)	CPXV218	95.39	-	-	C14L	89.86
NoH2-210	204592	210315	5724	forward	Surface glycoprotein	CPXV219	82.22	C15R/EVM169	83.35	B20.5R	80.77
NoH2-211	210688	211563	876	forward	Ankyrin (Cop-C19L)	CPXV220	86.01	-	-	-	-
NoH2-212	212705	213208	504	forward	TNF-alpha receptor (CPXV-GRI-K3R)	-	-	-	-	-	-
NoH2-213	213385	215406	2022	forward	Ankyrin (Cop-C17L)	CPXV223	95.38	-	-	B23R/C17L	87.57
NoH2-214	215444	215533	90	forward	Ankyrin-like repeat containing protein	CPXV224	100.00	-	-	-	-
NoH2-215	215521	217404	1884	forward	Ankyrin (Cop-C19L)	CPXV225	87.30	K1R/EVM171	84.33	B25R/C19L	79.12
NoH2-216	217482	218531	1050	forward	TNF receptor (CrmB) (Cop-C22L)	crmB/CPXV226	92.96	-	-	B28R/C22L	75.00
NoH2-217	218640	219380	741	forward	Chemokine binding protein (Cop-C23L)	vCCI/CPXV227	91.94	K2R/EVM172	83.00	B29R/C23L	79.01

Supplementary Table S3. Predicted overlapping genes in CPXV-No-H2 and BLAST analysis.

CDS	Start	Stop	CPXV_Br	Identity (%)	BLASTp		BLASTn	
					OPXV Genome with Highest Identity	Aminoacid identity (%)	OPXV Genome with Highest Identity	Nucleotide identity (%)
NoH2-A	1636	1845	CPXV004	74.65	CPXV	76.1	CPXV GerMygEK938/17	98.1
NoH2-B	38093	38188	-	-	CMLV 0408151v	83.3	CPXV GerMygEK938/17	99.0
NoH2-C	45836	46030	-	-	CPXV GerMygEK938/17, CPXVGer2010MKY	100.0	CPXV GerMygEK938/17, CPXVGer2010MKY	100.0
NoH2-D	46234	46413	CPXV047	83.05	CPXV Ger 2010 MKY	94.9	CPXV Ger 2010 MKY	98.3
NoH2-E	49188	49424	CPXV051A	97.44	CPXV GerMygEK938/17, CPXVGer2010MKY	100.0	CPXV GerMygEK938/17, CPXVGer2010MKY	99.2
NoH2-F	53895	54017	CPXV058	97.5	CPXV, VACV	97.5	ECTV	100.0
NoH2-G	54768	54890	-	-	VACV CEyV1	87.5	CPXV	99.2
NoH2-H	58313	58462	-	-	OPXV Abatino	98.0	CPXV GerMygEK938/17, CPXVGer2010MKY	100.0
NoH2-I	75455	75643	CPXV078A	96.77	CPXV GerMygEK938/17, CPXVGer2010MKY	98.4	CPXV GerMygEK938/17, CPXVGer2010MKY	99.5
NoH2-J	91226	91435	CPXV096	100	AKMV, CMLV, CPXV, VACV	100.0	CPXV,VACV	100.0
NoH2-K	109530	109703	CPXV116	94.12	CPXV, VACV	96.1	CPXV	98.3
NoH2-L	112614	112856	CPXV119A	100	CPXV	100.0	CPXV,OPXVA	99.2
NoH2-M	124280	124498	CPXV130	100	CPXV	100.0	CPXV	99.5
NoH2-N	139869	139985	-	-	VACV CEyV1	94.7	CPXV, VACV	100.0
NoH2-O	144031	144159	CPXV152A	95.24	CPXV	97.6	CPXV,TATV, VARV	100.0
NoH2-P	154705	154911	CPXV160	88.24	CPXV Ger2010MKY	97.1	CPXV Ger2010MKY	98.6
NoH2-Q	160152	160364	CPXV170	94.34	CPXV	100.0	CPXV	99.4
NoH2-R	179029	179130	-	-	VACV Lister	97.0	VACV_VK01	99.0
NoH2-S	200439	200600	CPXV214	84	CPXV Ger2010MKY	94.0	CPXV Ger2010MKY	97.5
NoH2-T	218432	218641	CPXV004	74.65	CPXV	76.1	CPXV GerMygEK938/17	98.1

Supplementary Table S4. BLASTn analysis of predicted genes in CPXV-No-H2 that encode proteins with highest aminoacid similarity to other OPXV proteins than CPXV proteins.

CDS	Start	Stop	Length (bp)	BLASTp		BLASTn	
				OPV Genome with Highest Identity	Aminoacid identity (%)	OPV Genome with Highest Identity	Nucleotide identity (%)
NoH2-077	75843	75950	108	ECTV, HSPV, VACV	100.0	CPXV GerMygEK938/17	100.0
NoH2-079	76910	77128	219	AKPV	98.592	AKPV	98.2
NoH2-090	88183	89487	1305	VACV WAU86/88-1	99.5	CPXV GerMygEK938/17	99.2
NoH2-152	147351	150845	3495	ECTV	99.828	ECTV	98.9
NoH2-153	150838	154107	3270	ECTV*	94.82	ECTV	98.3
NoH2-159	157663	157791	129	VACV	100	BPXV, CPXV , VACV	100
NoH2-160	157790	158170	381	VACV	98.425	VACV LC16m8, VACV LC16mO	98.4
NoH2-163	159655	160161	507	ECTV	97.6	CPXV Ger2010MKY, CPXV GerMygEK938/17	98.6
NoH2-165	160801	161481	681	AKPV	92.92	AKPV	95.2
NoH2-166	161546	162340	795	AKPV	98.485	AKPV	99.1
NoH2-167	162451	162630	180	AKPV	98.305	AKPV	99.4
NoH2-171	165294	165971	678	ECTV	95.556	ECTV_Mill-Hill, ECTV_Hampstead-Egg	95.9
NoH2-172	166133	166537	405	ECTV	100	ECTV	99.8
NoH2-173	166577	167188	612	ECTV	99.507	ECTV	99.7
NoH2-174	167207	167431	225	AKPV	97.297	AKPV	98.7
NoH2-175	167586	168626	1041	AKPV	95.1	CPXV GerMygEK938/17, CPXV Ger2010MKY	94.4
NoH2-210	204592	210315	5724	AKPV	94.905	AKPV	97.2

Supplementary Table S5. Position of the putative recombinant regions in the CPXV-No-H2 genome and BLASTn analysis

Putative recombination event	CPXV-No-H2 genome		BLASTn	
	Start	End	OPXV Genome with Highest Identity	Identity (%)
1	76946	77205	AKPV	98.33
2	77741	78243	AKPV	98.21
3	150156	154530	AKPV	96.89
4	160786	162936	AKPV	97.66
5	165874	168063	AKPV	97.37
6	204966	209636	AKPV	98.42
7	150119	153968	ECTV	97.93
8	165847	167892	AKPV	97.29
9	164405	164766	VACV	99.44

Paper II

viruses

MDPI

Article

Genomic Sequencing and Phylogenomics of Cowpox Virus

Diana Diaz-Cánova [1], Carla Mavian [2], Annika Brinkmann [3], Andreas Nitsche [3], Ugo Moens [1,*] and Malachy Ifeanyi Okeke [4,*]

1 Molecular Inflammation Research Group, Department of Medical Biology, UiT—The Arctic University of Norway, N-9037 Tromsø, Norway
2 Emerging Pathogens Institute, Department of Pathology, College of Medicine, University of Florida, Gainesville, FL 32610, USA
3 Highly Pathogenic Viruses, Centre for Biological Threats and Special Pathogens, WHO Reference Laboratory for SARS-CoV-2 and WHO Collaborating Centre for Emerging Infections and Biological Threats, Robert Koch Institute, 1335 Berlin, Germany
4 Section of Biomedical Sciences, Department of Natural and Environmental Sciences, School of Arts and Sciences, American University of Nigeria, Yola PMB 2250, Nigeria
* Correspondence: ugo.moens@uit.no (U.M.); malachy.okeke@aun.edu.ng (M.I.O.)

Abstract: *Cowpox virus* (CPXV; genus *Orthopoxvirus*; family *Poxviridae*) is the causative agent of cowpox, a self-limiting zoonotic infection. CPXV is endemic in Eurasia, and human CPXV infections are associated with exposure to infected animals. In the Fennoscandian region, five CPXVs isolated from cats and humans were collected and used in this study. We report the complete sequence of their genomes, which ranged in size from 220–222 kbp, containing between 215 and 219 open reading frames. The phylogenetic analysis of 87 orthopoxvirus strains, including the Fennoscandian CPXV isolates, confirmed the division of CPXV strains into at least five distinct major clusters (CPXV-like 1, CPXV-like 2, VACV-like, VARV-like and ECTV-Abatino-like) and can be further divided into eighteen sub-species based on the genetic and patristic distances. Bayesian time-scaled evolutionary history of CPXV was reconstructed employing concatenated 62 non-recombinant conserved genes of 55 CPXV. The CPXV evolution rate was calculated to be 1.65×10^{-5} substitution/site/year. Our findings confirmed that CPXV is not a single species but a polyphyletic assemblage of several species and thus, a reclassification is warranted.

Keywords: phylogenetic; orthopoxvirus; poxviridae; molecular clock; Fennoscandian; phylodynamics; cowpox virus

Citation: Diaz-Cánova, D.; Mavian, C.; Brinkmann, A.; Nitsche, A.; Moens, U.; Okeke, M.I. Genomic Sequencing and Phylogenomics of Cowpox Virus. *Viruses* **2022**, *14*, 2134. https://doi.org/10.3390/v14102134

Academic Editor: Stefan Rothenburg

Received: 17 August 2022
Accepted: 24 September 2022
Published: 28 September 2022

1. Introduction

Cowpox virus (CPXV) is an orthopoxvirus species, belonging to the subfamily *Chordopoxvirinae* of the family *Poxviridae* [1]. Orthopoxvirus (OPXV) comprises several species from the New World and Old World. The most representative species from the New World are raccoonpox virus (RCNV), volepox virus (VPXV) and skunkpox virus (SKPV) [2]. Within Old World OPXV, there are several species: ectromelia virus (ECTV), vaccinia virus (VACV), monkeypox virus (MPXV), variola virus (VARV), taterapox virus (TATV), camelpox virus (CMLV) and CPXV [3–5]. In the last decade, new OPXV species were discovered in the United States (alaskapox virus, AKPV), Italy (abatino macacapox virus, Abatino) and Georgia (akhmeta virus, AKMV) [6–8].

The most notable member of OPXV genus is VARV, the etiologic agent of smallpox. However, after a large, massive vaccination campaign, smallpox was eradicated in 1980 [9]. The last natural cases of smallpox in humans were in Somalia in 1977 [10]. OPXV species, such as CPXV and MPXV, can cause zoonotic diseases [11–14]. MPXV and CPXV are the causative agents of monkeypox and cowpox, respectively, and have a wide host range [13,15]. Recently, a multi-country human monkeypox outbreak in 50 countries has been reported [16]. Compared to MPXV that occurs in Central and Western Africa [17],

CPXV is endemic of Eurasia, mainly present in Europe [12,18–23]. The natural reservoirs of CPXV are wild rodents [18,24]. Nevertheless, CPXV is also able to infect felines, monkeys, dogs, alpacas, rats, horses and humans [12,25–29]. The first zoonotic case was reported in the Netherlands in 1985, where CPXV was transmitted from a domestic cat to a woman [30]. In Fennoscandian, human cases of CPXV infections have been reported (CPXV-No-H1, CPXV-No-H2, CPXV-Swe-H1 and CPXV-Swe-H2) as well as feline cases (CPXV-No-F1 and CPXV-No-F2) [27,31–35]. CPXV has been classified as a single species; however, it has been proposed that CPXV should be considered as a polyphyletic species [33,35–40]. Based on phylogenetic studies, CPXV was divided into at least five clades: CPXV-like 1, CPXV-like 2, ECTV-Abatino-like, VACV-like and VARV-like [38,40–42]. Among OPXV, CPXV has the largest genome [43] and contains the highest number of orthopoxviral genes [42,44]. It was suggested that CPXV-like virus was the ancestor of Old World OPXV, except for AKPV and AKMV [39,44,45]. Until now, the evolutionary history of CPXV is still unclear. Most studies have focused on the molecular evolution of VARV, but few studies were focused on OPXV and, specially, on CPXV [39,45–49].

In this study, we present the whole genome sequence of five Fennoscandian CPXV isolates. We determined the phylogenetic relationship of CPXV, including the Fennoscandian isolates, with other OPXV and studied the evolutionary history of CPXV based on the concatenated 62 non-recombinant conserved genes of several representatives CPXV isolates from the different CPXV clades. Furthermore, we propose a new classification of CPXV.

2. Materials and Methods

2.1. Cell, Virus Culture and DNA Isolation

Five Fennoscandian isolates were used in this study: CPXV-No-H1, CPXV-No-F1, CPXV-No-F2, CPXV-Swe-H1 and CPXV-Swe-H2. The isolates were cultured on a monolayer of Vero cells (ATCC No. CCL-81), and the viral DNA was extracted from semi-purified virions, as previously described [34,40]. The origin of the five CPXV isolates has been described elsewhere [27,31–34].

2.2. Whole Genome Sequencing, Genome Assembly and Genome Annotation

The genomes of the five Fennoscandian isolates (CPXV-No-H1, CPXV-No-F1, CPXV-No-F2, CPXV-Swe-H1 and CPXV-Swe-H2) were sequenced using Oxford Nanopore Technology GridION (ONT; Oxford, UK) and Illumina MiSeq using reagent kit v3 with 2 × 300 bp paired-end reads, as previously described [40]. Illumina sequencing was performed at the Norwegian Sequencing Centre, Oslo, and Nanopore sequencing was performed at the Genomics Support Centre Tromsø at UiT—The Arctic University of Norway. The genomes were assembled using SPAdes v3.15.3 [50] and annotated with Genome Annotation Transfer Utility (GATU) [51], as previously reported [40].

2.3. Gene Content Comparison

The five Fennoscandian CPXV genomes were compared to CPXV-Br genome. Predicted CDS from five CPXV isolates were extracted, translated into amino acid sequences and compared to the CPXV-Br proteins using BLASTp (ncbi-blast+ v2.11.0) [52].

2.4. Phylogenetic Analysis, Patristic and Genetic Distances

A total of 87 OPXV genomes, including the five Fennoscandian genomes, were used in this study (Table S1). Eighty-two OPXV genomes were retrieved from the Viral Orthologous Clusters (VOCs) database [53], with the exception of CPXV_GerMygEK938_17 (retrieved from GenBank). The genes and genomes were aligned using MAFFT v7.450 (with default parameters) [54], as implemented in Geneious Prime 2022.0.2. Four different alignments were used to build the phylogenetic trees: (1) 87 OPXV whole genome alignment, (2) 87 OPXV core genome alignment, (3) OPXV orthologous gene alignment (Table S2) and (4) 62 conserved genes alignment (Table S3), as previously described [40].

Recombination detection program 4 (RDP4) [55] was used to detect genome-wide recombination in the datasets. Recombination events identified by 5 of 7 methods (RDP [56], GENECONV [57], Bootscan [58], MaxChi [59], Chimaera [60], SiScan [61] and 3Seq [62]) with significant *p*-values ($p \leq 0.01$) were considered credible evidences of recombination. Whole genome, core genome and orthologous gene alignments were generated without removing the putative recombinant regions.

The conserved gene alignment was generated by examining the 90 Chordopoxvirus (ChPV) conserved genes for recombination using RDP4 [55], as described above. The 62 conserved genes identified as non-recombinant were aligned singly and the 62 single gene alignments were concatenated to generate the conserved gene dataset.

Gblocks 0.91b was used to remove poorly aligned positions from 87 OPXV whole and core genome alignments [63]. The presence of phylogenetic signal of the datasets was assessed by likelihood mapping analysis with the evaluation of 2000 random quartets using IQ-TREE v.2.0.3. [64] (Figure S1). The best-fit nucleotide substitution model for the alignment data was selected using the modelTest-NG v.0.1.6 [65]. Two inference methods, maximum likelihood (ML) and Bayesian inference (BI), were conducted with RAxML v8.2.12 [66] using a rapid bootstrap algorithm [67] and MrBayes v3.2.7 [68], respectively, as previously described [40]. The Markov Chain Monte Carlo (MCMC) analysis was run until reaching convergence. The phylogenetic trees were visualized applying FigTree v1.4.4 (http://tree.bio.ed.ac.uk/software/figtree/, accessed on 19 February 2021). The BI phylogenetic tree based on the OPXV orthologous genes was not built because MCMC analysis did not reach convergence after 50,000,000 generations.

Patristic distances between different groups were calculated from the ML/BI trees of concatenated 62 conserved non-recombinant genes using the program Patristic version 1.0 [69]. The genetic distances between the different groups were estimated by p-distances, as implemented in MEGA version 11 [70]. For patristic and genetic distances, the distances were averaged across taxa to produce a single value. The genetic and patristic distances between TATV and CMLV were used as threshold values since they are closest and distinct OPXV species. These threshold values were used to compare the distance between CPXV clusters and OPXV species and separate them in different sub-species if they were equal or greater than TATV-CMLV threshold values.

2.5. Phylodynamic Evolutionary Analysis of CPXV

A Bayesian MCMC inference method implemented in BEAST 1.10.4 [71] was used to estimate evolutionary rates and the divergence times. Evolutionary analysis was carried out on alignment of concatenated 62 conserved non-recombinant genes of 55 CPXV strains (listed in Table S4). The temporal signal was assessed from the ML tree of 62 conserved genes of 55 CPXV by regression of genetic divergence (root-to-tip genetic distance) and the sampling date using TempEst v.1.5.3 [72] (Figure S2). In the analysis, we did not include other OPXV species because the dataset did not contain temporal signal (correlation coefficient = −0.15, value of R2 = 0.02). The presence of phylogenetic signal of the dataset was evaluated using IQ-TREE v.2.0.3. [64], as described above (Figure S2).

The Bayesian phylodynamic analysis was calibrated using the following parameters: log-normal relaxed clock, coalescent Bayesian skyline population, HKY substitution model and four gamma categories. MCMC chain was run for 1 billion generations. The effective sampling size (ESS) values were checked in Tracer v1.7.2 [73]. Only the Effective Sampling Size (ESS) values > 200 (after burn-in) were accepted. The maximum clade credibility (MCC) tree was generated using TreeAnnotator v1.10.4, visualized using FigTree v1.4.4 and edited graphically using the ggtree package available in R [74].

3. Results

3.1. Genome Assembly, Genome Annotation and Gene Content

The whole genomes of five Fennoscandian CPXV isolates (CPXV-No-H1, CPXV-No-F1, CPXV-No-F2, CPXV-Swe-H1 and CPXV-Swe-H2) were assembled, and the coverage of the

assembled genomes varied from 300X to 2400X, as shown in Table 1. The genome size of the Fennoscandian CPXV isolates ranges from 220,808 to 222,178 bp and the length of inverted terminal repeats (ITRs) were approximately 8 kbp (Table 1). The whole genome sequences of these isolates are available in GenBank, with Accession Number: OP125537, OP125538, OP125539, OP125540, OP125541.

Table 1. Genome size, number of predicted coding sequences (CDS) and genome coverage of the Fennoscandian CPXV isolates sequenced in this study.

Name	Genome Size (bp)	CDS	Genome Coverage	
			Illumina	Nanopore
CPXV-No-H1	221,926	215	300X	600X
CPXV-No-F1	221,334	217	820X	1519X
CPXV-No-F2	222,178	217	940X	1480X
CPXV-Swe-H1	220,981	217	700X	2500X
CPXV-Swe-H2	220,808	217	990X	2400X

Gene annotation of the five Fennoscandian CPXV genomes (CPXV-No-H1, CPXV-No-F1, CPXV-No-F2, CPXV-Swe-H1 and CPXV-Swe-H2) revealed 212, 219, 217, 217 and 217 predicted coding sequences (CDS), respectively. A comparison of the predicted CDS of the five Fennoscandian CPXV isolates with the CPXV-Br genome is shown in Table S5. The genome content of the five Fennoscandian CXPV isolates was similar to CXPV-Br genome. The majority of predicted CDS of the five CXPV strains were found to have homologs in CPXV-Br, except for few predicted CDS. *NoF1-009, NoF2-009* and *NoH1-008*, present in the Norwegian isolates, were homologs of *EVM004* that encodes a BTB Kelch-domain containing protein. The Swedish isolates contain a CDS (*SweH1-210* and *SweH2-210*) that was homolog of *CPXV-GRI-K3R* (codes for CrmE protein). The five Fennoscandian isolates contain a homolog of *VACV-Cop O3L*, encoding a virus entry/fusion complex component.

The five Fennoscandian CPXV strains lacked homologs of *CPXV001* and *CPXV216*. Furthermore, *CPXV002* and *CPXV191* (*CrmC*) were absent in CPXV-No-H1 and CPXV-No-F1 genomes, respectively.

3.2. Phylogenetic Analysis

The recombination analysis evidenced the extensive recombination in OPXV core genomes (Figure S3) as well as in the datasets of OPXV whole genomes and orthologous genes (data not shown). Recombination regions were not removed from the alignments used to generate the phylogenetic trees for the whole genome, core genome and orthologous genes. To examine if the recombinant regions in the three datasets biased the phylogenetic signal, we generated some fourth data, in which 62 OPXV conserved genes without any evidence of recombination were used in phylogenetic reconstruction, as described in methods. The ML and BI phylogenetic trees built from concatenated 62 conserved genes without recombination is shown in Figure 1 and Figure S4, respectively.

The topology of the phylogenetic trees based on 87 OPXV core genomes (Figure 2 and Figure S5) was identical to that of trees generated from 87 OPXV whole genomes (Figures S6 and S7) and similar to that of the phylogenetic tree built based on OPXV orthologous genes (Figure S8). Whereas the topology of phylogenetic trees based on 62 conserved genes (Figure 1 and Figure S4) slightly differed from that of the phylogenetic trees generated from 87 OPXV core genomes (Figure 2 and Figure S5).

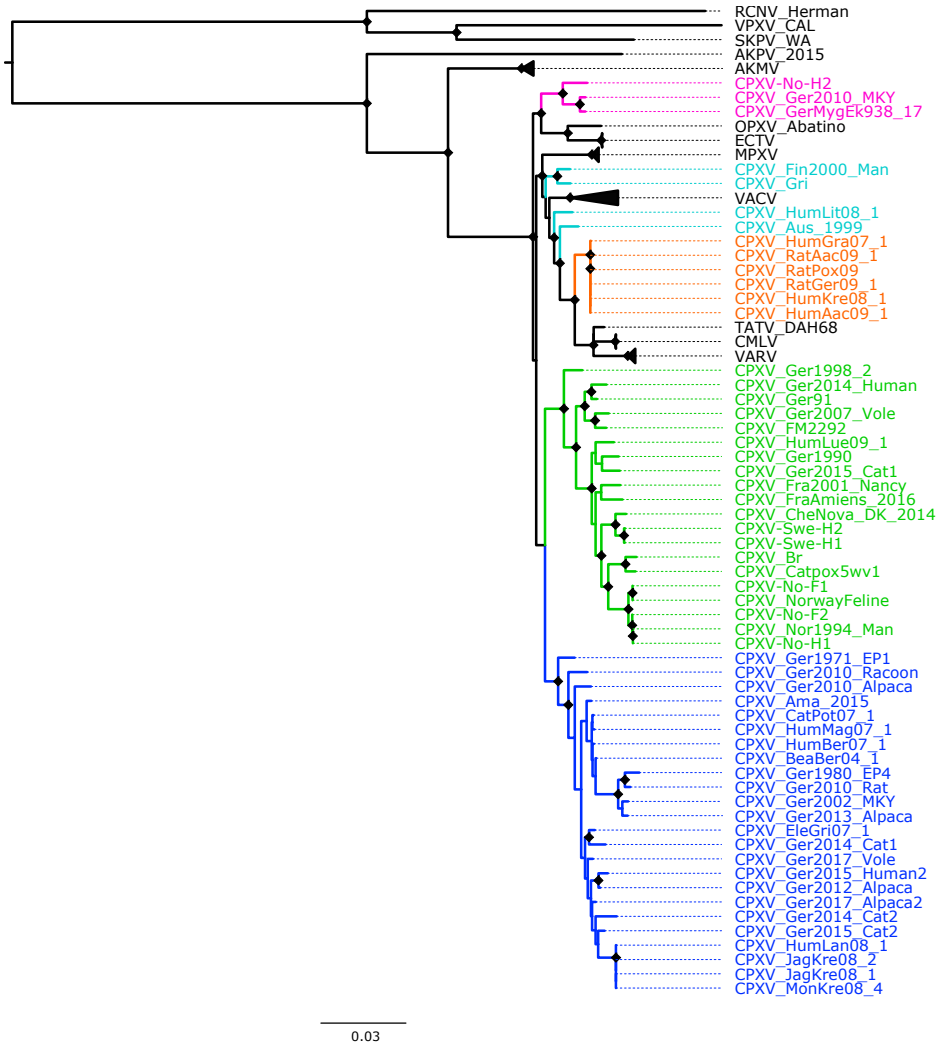

Figure 1. Maximum likelihood phylogenetic tree of 62 conserved genes from 87 orthopoxviruses. Bootstrap values were inferred from 1000 rapid bootstrap replicates. Diamonds at the nodes indicate bootstrap values > 80%. The scale indicates substitution per site. The main five cowpox virus (CPXV) clusters were highlighted in different colors: pink (Ectromelia-Abatino-like CPXV), blue (CPXV-like 1), green (CPXV-like 2), turquoise blue (Vaccinia-like CPXV) and orange (Variola-like CPXV).

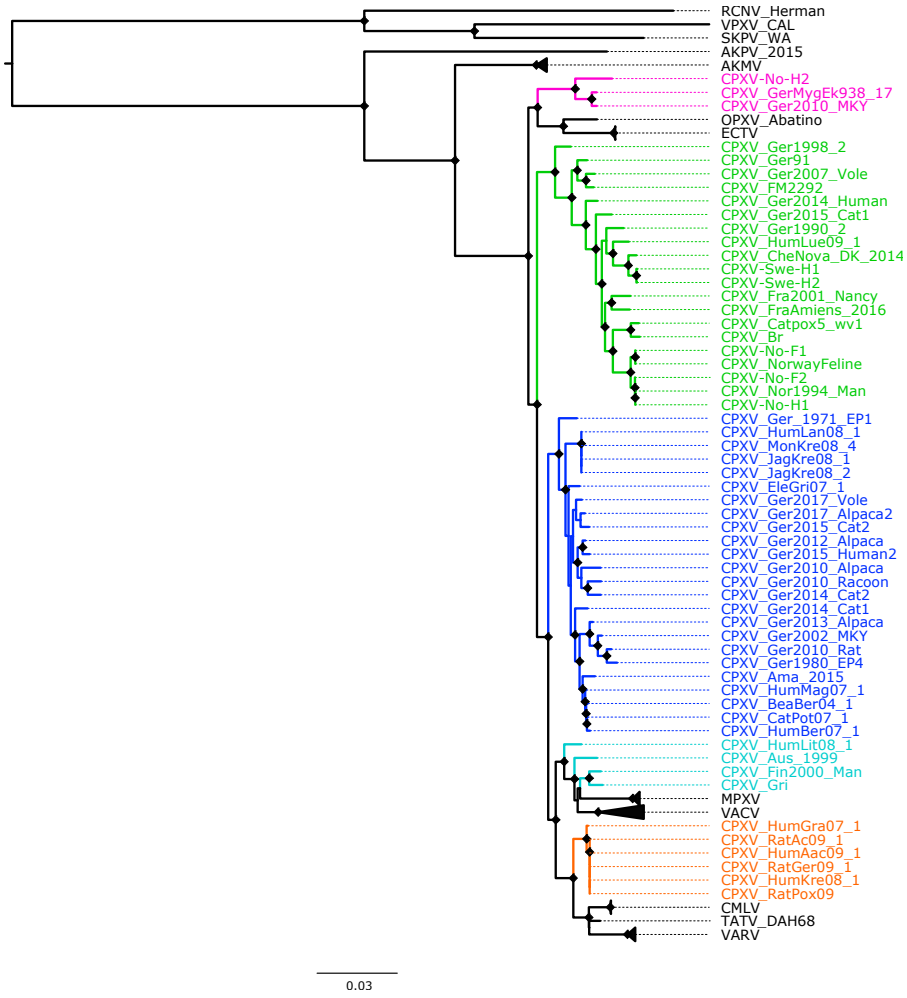

Figure 2. Maximum likelihood phylogenetic tree of 87 orthopoxvirus core genome. Bootstrap values were inferred from 1000 rapid bootstrap replicates. Diamonds at the nodes indicate bootstrap values > 80%. The scale indicates substitution per site. The main five cowpox virus (CPXV) clusters were highlighted in different colors: pink (Ectromelia-Abatino-like CPXV), blue (CPXV-like 1), green (CPXV-like 2), turquoise blue (Vaccinia-like CPXV) and orange (Variola-like CPXV).

As expected, in all phylogenetic trees, the New World and Old World OPXV were separated and AKPV and AKMV clades were placed between them (Figure 1, Figure 2 and Figures S4–S8). Within the Old OPXV, the strains from the same species formed distinct clades, except for CPXV strains. They formed separated clusters with different OPXV species such as VACV, VARV, ECTV and Abatino. CPXV isolates were separated in five clusters: ECTV-Abatino-like CPXV, CPXV-like 1, CPXV-like 2, VACV-like CPXV and VARV-like CPXV. Even though CPXV strains from VACV-like did not form a cluster, they were closely related to VACV clade. ECTV/Abatino group was clustered with ECTV-Abatino-like clade, which includes one Fennoscandian isolate (CXPV-No-H2) and two German isolates. ECTV/Abatino/ECTV-Abatino-like CPXV clade clustered with a major clade that contains: CPXV-like 2, CPXV-like 1, VACV-like, VACV, MPXV, VARV-like, VARV, TATV and CMLV clusters (PP = 1.0 and bootstrap values = 100%). In the phylogenetic trees based on 87 OPXV core genomes (Figure 2 and Figure S5), CPXV-like 2 was separated from the other CPXV clusters and OPXV. Furthermore, CPXV-like 1 clade was sister to a major clade that comprised VACV-like, VACV, MPXV, VARV-like, TATV, CMLV and VARV (PP = 1.0 and bootstrap values = 100%). Within this major clade VACV-like/VACV/MPXV cluster was separated from VARV-like, TATV, CMLV and VARV. Whereas the phylogenetic trees generated from 62 conserved genes (Figure 2 and Figure S6) showed that CPXV-like 1 and

CPXV-like 2 were sister clades (PP = 1 and bootstrap values = 70%) and these clustered together with a clade that contains VACV-like, VACV, MPXV, VARV-like, VARV, TATV and CMLV, but with low bootstrap support (48%) and PP of 0.93. In comparison to a phylogenetic tree built from 87 OPXV core genomes, VACV-like/VACV/MPXV did not form separate from VARV-like.

All Fennoscandian CPXV isolates except CPXV-No-H2 were grouped into CPXV-like 2 clade (Figure 1, Figure 2 and Figures S4–S8). This clade also contains CPXV strains from Germany, Denmark, Russia, The United Kingdom (UK) and France. Within CPXV-like 2, CPXV-Ger1998_2 formed a deeper single branch and the remaining CPXV isolates were divided in two main sub-clusters. In the phylogenetic trees built from 87 OPXV core genomes (Figure 2 and Figure S5), the sub-cluster one contained three German isolates (CPXV_Ger91, CPXV_Ger2007_Vole and CPXV_FM2292) and sub-cluster two comprised 16 CPXV isolates, including the five Fennoscandian CPXV isolates reported in this study (CPXV_Ger2014_Human, CPXV_Ger2015_cat1, CPXV_Ger1990_2, CPXV_HumLue09_1, CPXV_CheNova_DK_2014, CPXV-Swe-H1, CPXV-Swe-H2, CPXV-Fra2001-Nancy, CPXV-FraAmiens_2016, CPXV-Catpox5-wv1, CPXV-Br, CPXV-No-F1, CPXV-Norwayfeline, CPXV-No-F2, CPXV-No-H1 and CPXV-Nor1994_Man). Whereas sub-cluster one of the phylogenetic tree based on 62 conserved genes contained an additional CPXV strain, CPXV_Ger0214 _Human (Figure 1 and Figure S4). In all phylogenetic trees, the Norwegian isolates were closely related to the UK isolates (CPXV-Br and CPXV- Catpox5_wv1), while Swedish isolates were closer to the Danish isolate. CPXV-like 1 clade was the largest CPXV clade and comprises only German CPXV isolates as well as VARV-like clade. This clade was sister group of VARV/CMLV/TATV. VACV-like contains CPXV strains from Austria, Russia, Finland and Lithuania. These strains were closely related to VACV and MPXV. Compared to VACV-like, VARV-like and ECTV-Abatino-like, CPXV-like 1 and CPXV-like 2 did not cluster together with other OPXV species (Figure 1, Figure 2 and Figures S4–S8). Overall, all phylogenetic trees (based on 87 OPXV whole genomes, core genomes, orthologous genes and conserved genes) showed the five major CPXV clusters and the clustering of the CPXV-like 2 strains were similar. Thus, although recombination among CPXV is extensive, tree topology from datasets with recombinant regions and datasets without evidence of recombination were very similar.

3.3. Patristic and Genetic Distances

Based on the genetic and patristic distances, CPXV strains can be classified into 18 sub-species (Figure 3). The genetic and patristic distances between CPXV clusters and OPXV species were higher than the TATV-CMLV genetic and patristic distance threshold (Tables S6 and S7). Furthermore, the genetic and patristic distances within some CPXV clusters, such as CPXV-like 2, were higher than the threshold values (Table S8). According to the genetic and patristic distances between CPXV-like 2 strains, CPXV-like 2 was further divided into ten sub-species: group one (CPXV-Ger1998_2), group two (CPXV_Ger2014_Human, CPXV_Ger91, CPXV_Ger2007_Vole and CPXV_FM2292), group three (CPXV_HumLue09_1), group four (CPXV_Ger1990_2), group five (CPXV_Ger2015_cat1), group six (CPXV-Fra2001-Nancy), group seven (CPXV-FraAmiens_2016), group eight (CPXV_CheNova_DK_2014, CPXV-Swe-H1 and CPXV-Swe-H2), group nine (CPXV-Catpox5-wv1 and CPXV-Br) and group ten (CPXV-No-F1, CPXV-Norwayfeline, CPXV-No-F2, CPXV-No-H1 and CPXV-Nor1994_Man) (Tables S9 and S10). The isolates were grouped together according to their origin, except for the German and French isolates that were separated into five and two distinct sub-species, respectively.

Figure 3. New classification of cowpox virus (CPXV) based on phylogenetic tree inference from 62 conserved genes without evidence of recombination, patristic and genetic distances. Diamonds at the nodes indicate bootstrap values > 80%. The main five CPXV clusters were highlighted in different colors: pink (Ectromelia-Abatino-like CPXV), blue (CPXV-like 1), green (CPXV-like 2), turquoise blue (Vaccinia-like CPXV) and orange (Variola-like CPXV).

Similarly, in the ECTV-Abatino-like clade, the genetic and patristic distances between the Norwegian human isolate, CPXV-No-H2, and the German isolates (CPXV_GerMygEk938_17 and CPXV_Ger201_MKY) exceeded the distances between TATV and CMLV (Table S11). Within VACV-like, the distances between the CPXV strains were higher than the threshold values, except for the distances between CXPV-Gri and CPXV-Fin2000-Man (Tables S12 and S13). VACV-like strains were divided into three different sub-species: sub-species one, CPXV_HumLit08_1;

sub-species two, CPXV_Aus_1999; sub-species three, CPXV_Gri and CPXV_Fin2000_Man (Figure 3). In CPXV-like 1, CPXV_Ger_1971_EP1 was classified as one sub-species and the remaining CPXV-like 1 strains as another sub-species, according to the genetic and patristic distances (Table S14). However, the patristic distances between CPXV_Ger2010_Alpaca and other CPXV-like 1 strains were higher than the threshold value, but some genetic distances were lower than the threshold values (Tables S15 and S16). VARV-like strains remained together as one sub-species based on the genetic and patristic distances and phylogeny. Curiously, these strains contain a genomic region of approximately 5860 bp that was also identified in some CPXV-like 2 strains (CPXV_Ger91, CPXV_2007_vole, CPXV_FM2291 and CPXV_Fra2001_Nancy), VARV and CMLV.

3.4. Evolutionary Analysis of CPXV

The phylodynamic analysis was performed based on the 62 conserved genes of CPXV genomes. The dataset exhibited a positive correlation between the genetic divergence and the sampling time, which indicates the presence of temporal signal in the sequence dataset (correlation efficient = 0.48; R2 = 0.23). The mean evolution rate of CPXV was estimated to be 1.65×10^{-5} substitutions per site per year (subs/site/year), with 95% high posterior density interval (HPD) of $4.36 \times 10^{-7} - 4.32 \times 10^{-5}$ subs/site/year.

The MCC tree showed that CPXV strains were divided into two main clusters (Figure S9). The minor cluster contained CPXV-like 2 clade (PP = 0.88) and the major cluster comprised ECTV-Abatino-like, VACV-like, VARV-like and CXPV-like 1 clades (PP = 0.89) (Figure S9). However, the emergence date of CPXV as well as major CPXV clusters could not be accurately estimated since the 95% HPD intervals were wide, especially in the deepest nodes. As compared to the 95% HPD intervals tMRCA for recent nodes, tMRCA for deeper internal nodes were quite broad and showed some degree of overlap.

4. Discussion

CPXV strains examined in this study were isolated from different countries in Eurasia, with most of CPXV isolates from Germany. We included five CPXV isolates collected from Fennoscandian as well as our previously published CPXV isolate, CPXV-No-H2 [40]. These five Fennoscandian isolates were previously classified as CPXV based on Hind III restriction map of virus DNA, phylogenetic analysis of multiple conserved genes and the possession of two copies of the intact *cytokine response modifier B (CrmB)* gene [33–35].

CPXV is classified as one species, but this has been debated in many studies due to its genetic heterogeneity and polyphyletic character [33,35–40]. The genetic heterogeneity among CPXV strains could be due to recombination processes [34,35,41] since it is part of the evolution of OPXV [8,34,40,41,43,75–79]. It has been suggested that recombination can affect the accuracy of the phylogenetic inferences [80]. Since the extensive recombination in OPXV genomes has been reported by others [41], we included in our study a dataset of 62 non-recombinant conserved genes to avoid inaccuracy of phylogenetic estimation due the presence of recombination in 87 OPXV whole genomes, core genomes and orthologous genes.

Our phylogenetic analysis using different datasets always showed that CPXV isolates were divided into at least five clusters: CPXV-like 1, CPXV-like 2, VACV-like CPXV, VARV-like CPXV and ECTV-Abatino-like CPXV (Figure 1, Figure 2 and Figures S3–S7). Similar phylogenetic clustering of CPXV has been reported in other studies [40,81]. Three of the five CPXV clusters were closely related to other OPXV species, such as ECTV, Abatino, VARV and VACV. Previous studies have also showed this phylogenetic relationship of CPXV with other OPXV [35,37,38,40,41,43,81].

The German isolates were present in all CPXV clusters, except for VACV-like, while the Fennoscandian CPXV isolates clustered into CPXV-like 2 and grouped into separate clusters according to their country of origin (Norway, Sweden and Denmark), except for CPXV-No-H2. These results are in agreement with the phylogenetic analysis based on single genes (*atip*, *p4c*, *CrmB*, *HA*, complete *CHOhr* or partial *CHOhr*) reported in our previous studies [33,35]. However, not all Fennoscandian isolates were closely related. The

Norwegian isolates were closely related to the UK strains, whereas the Swedish CPXV isolates were closer to the Danish CPXV isolate. The phylogenetic relationship of the Norwegian and UK isolates has been previously reported [38,41]. In our previous studies the relationship of the Fennoscandian isolates with other CPXV isolates varied depending on the single gene used in the phylogenetic analysis [33,35]. However, in the present study, the phylogenetic relationship between the Norwegian and UK isolates as well as the Swedish and Danish isolates were consistent, regardless of the alignment used (87 OPXV whole genomes, core genomes, orthologous genes or 62 conserved genes).

Genetic and patristic distances have been previously used to examine the diversity of CPXV [35,36,38]. We used the genetic and patristic distances between TATV and CMLV to classify OPXV into the same or different species because they are the closest and recognized OPXV species. Our examination of the genetic and patristic distances between and within CPXV clusters revealed that the five CPXV clusters can be considered distinct CPXV sub-species and that even the CPXV strains can be separated into 18 sub-species (Figure 3). The heterogeneity of CPXV was not only demonstrated between CPXV clusters, but it was also present within some clusters. Among them, CPXV-like 2 was the most heterogeneous. Their isolates were classified into ten sub-species based on the genetic and patristic distances. This clade comprised isolates of diverse geographic origins (Norway, Sweden, Denmark, UK, Germany and France) and its classification followed their geographical origin. Only German and French isolates were separated into more than one sub-species.

Large genetic variation was also found within VACV-like strains, which were closely related to VACV and MPXV, as previously described [38,40,41]. These strains split into three different sub-species based on the genetic and patristic distances. This division is in agreement with phylogenetic work reported in other previous studies [38,40,41]. Among VACV-like strains, it has been reported that CPXV-HumLit08/1 is a recombinant virus that contains genomic regions related to VACV, VACV-like and VARV-like [41]. However, our findings based on 62 non-recombinant conserved genes evidenced that CPXV-HumLit08/1 can be considered as one sub-species. Similarly, within ECTV-Abatino-like clade, CPXV-No-H2 has undergone recombination with other OPXV [40] and our data supported the separation of CPXV-No-H2 and the other ECTV-Abatino-like strains into different sub-species.

The most genetically homogeneous CPXV cluster was the VARV-like group. The origin of these strains was associated with infected pet rats, probably imported from the Czech Republic [37,82]. Overall, our findings are in concordance with the results of Mauldin et al. [38]. They reported that CPXV-like 1 strains were split into more than one cluster (referred in the study as E1, E2, E3, E4 and E5), VACV-like strains were divided into three groups (referred in the study as A, B and C) and VARV-like strains were clustered into a single group.

Despite the evidence of recombination in the datasets of 87 OPXV whole genomes, core genomes and orthologous genes, their phylogeny, genetic and patristic distances agreed with and are very similar to the phylogeny, patristic and genetic distances reconstructed from the dataset of 62 conserved genes without evidence of recombination. All four datasets suggested that CPXV strains can be divided into at least 18 sub-species (Figure 3, Figure S10 and Tables S6–S16). However, biological characterization of CPXV is required to accurately infer the taxonomic level to which these 18 sub-species of CPXV belong. Furthermore, our phylogenetic analysis evidenced that recombination did not change the phylogenetic relationship between CPXV strains and OPXV despite the extensive recombination between OPXV genomes. Taking into cognizance the extensive recombination present in CPXV genomes, it is rather surprising that recombination appears not to alter the clustering pattern in OPXV phylogeny. Plausible reasons may be that recombination among CPXVs occurred very early in CPXV/OPXV evolution, recombination regions occurred in small batch sizes compared to the whole genomes and the phylogenetic signals from recombinant regions were small and was diluted out by larger phylogenetic signals from other parts of the genome.

We estimated the evolution rate of CPXV based on 62 conserved genes of 55 CPXV to be 1.65×10^{-5} substitution/site/year (95% HPD, 4.36×10^{-7}–4.32×10^{-5} subs/site/year). The 95% HPD of our estimate overlapped the reported substitution rates of *Chordopoxvirinae*, 0.5–8.8 $\times 10^{-6}$ substitutions/site/year, and OPXV, 1.7–6.5 $\times 10^{-6}$ substitutions/site/year [45–47,49]. The divergence times of CPXV could not be accurately estimated using 62 conserved genes of 55 CPXV genomes (Figure S9), even using conserved central region (F4L-A24L) of CPXV genomes (data not shown), since the broad 95% HPD intervals of the divergence time were quite broad. It could be due to the high heterogeneity of CXPV strains and the limited number of samples in terms of location, host and sample age. The majority of CPXV strains were isolated in Germany and from infections in humans. Furthermore, most CPXV strains were isolated in the last decades, there were no ancient CPXV isolates. Therefore, the low genetic information and the high genetic distances between the current CPXV strains increase the uncertainty of the node ages. In our opinion, our result strengthens the proposed idea that lineages of CPXV are highly divergent and a reclassification is needed, rather than showing a lack of a good calibration (tempest indicated presence of temporal signal). It has been proposed that the CXPV-like virus was the ancestor of Old World OPXV, excluding AKPV and AKMV, [39,44,45,83] due to its large genome, broadest host range and the presence of the most orthopoxviral genes [42,43,83,84]. Thus, despite the exclusion of other OPXV in our analysis due to the lack of temporal signal in the dataset, the evolutionary analysis of only CPXV may reflect the genomic history of all OPXV taking into account the high genetic heterogeneity among CPXV, the suggestion that CPXV or cowpox-like virus may be the ancestor to Old World OPXV species and the phylogenetic evidence of CPXV being the only OPXV that clusters with all Old World OPXV. However, the phylodynamic analysis of only CPXV has limitations because of oversampling of CPXV strains from Germany, from human zoonotic events and lack of ancient isolates. To improve the reconstruction of the evolutionary history of CPXV, increased genomic surveillance of CPXV across different regions of Eurasia and in multiple species or by the acquisition of ancient CPXV strains are required. These will result in a more accurate estimation of the time-scale of CPXV evolution.

5. Conclusions

In conclusion, the present study demonstrated the high genetic heterogeneity among CPXV isolates and the polyphyletic character of CPXV. Furthermore, our findings confirmed that CPXV was not a single species but a polyphyletic assemblage of several (up to 18) sub-species. Therefore, the current classification of CPXV as one single species should be re-evaluated. We also provided the first reconstruction of the evolutionary history of only CPXV. Overall, this study has shed significant insight on the evolution, phylogeny and classification of CPXV.

Supplementary Materials: The following supporting information can be downloaded at: https://www.mdpi.com/article/10.3390/v14102134/s1, Figure S1. Presence of phylogenetic signal was evaluated by likelihood mapping checking for alternative topologies (tips), unresolved quartets (center) and partly resolved quartets (edges) for 87 OPXV whole genomes (a), core genomes (b), OPXV orthologous genes (c) and 62 conserved genes. Figure S2. Phylogenetic and temporal signal analyses. (a) Presence of phylogenetic signal was evaluated by likelihood mapping checking for alternative topologies (tips), unresolved quartets (center) and partly resolved quartets (edges) for 62 conserved genes of 55 CPXV strains. (b) Linear regression of root-to-tip genetic distance in a maximum likelihood phylogeny against sampling time for 62 conserved genes of 55 CPXV strains. Figure S3. Recombination analysis of 87 orthopoxvirus (OPXV) core genomes with RPD4. Schematic sequence display depicting color-coded representations of the analyzed sequences and the locations of detected recombination events in the 87 OPXV core genomes. The detected recombination events were detected for at least 5 of 7 methods (RDP, GENECONV, Bootscan, MaxChi, Chimaera, SiScan and 3Seq) with significant p-values ($p \leq 0.01$). Figure S4. Bayesian inference phylogenetic tree of 62 conserved genes from 87 orthopoxviruses. Diamonds at the nodes indicate posterior probabilities > 0.9. The scale bar represents expected substitutions per site. The main five cowpox virus (CPXV) clus-

ters were highlighted in different colors: pink (Ectromelia-Abatino-like CPXV), blue (CPXV-like 1), green (CPXV-like 2), turquoise blue (Vaccinia-like CPXV) and orange (Variola-like CPXV). Figure S5. Bayesian inference phylogenetic tree of 87 OPXV core genomes. Posterior probabilities are shown on the right side of each node and only posterior probabilities above 0.9 are shown. The scale bar represents expected substitutions per site. The main five cowpox virus (CPXV) clusters were highlighted in different colors: pink (Ectromelia-Abatino-like CPXV), blue (CPXV-like 1), green (CPXV-like 2), turquoise blue (Vaccinia-like CPXV) and orange (Variola-like CPXV). Figure S6. Maximum likelihood phylogenetic tree of 87 orthopoxvirus whole genome. Bootstrap values were inferred from 1000 rapid bootstrap replicates. Diamonds at the nodes indicate bootstrap values > 80%. The scale bar indicates substitution per site. The main five cowpox virus (CPXV) clusters were highlighted in different colors: pink (Ectromelia-Abatino-like CPXV), blue (CPXV-like 1), green (CPXV-like 2), turquoise blue (Vaccinia-like CPXV) and orange (Variola-like CPXV). Figure S7. Bayesian inference phylogenetic tree of 87 OPXV whole genomes. Diamonds at the nodes indicate posterior probabilities > 0.9. The scale bar represents expected substitutions per site. The main five cowpox virus (CPXV) clusters were highlighted in different colors: pink (Ectromelia-Abatino-like CPXV), blue (CPXV-like 1), green (CPXV-like 2), turquoise blue (Vaccinia-like CPXV) and orange (Variola-like CPXV). Figure S8. Maximum likelihood phylogenetic tree based on orthopoxvirus orthologous genes. Bootstrap values were inferred from 1000 rapid bootstrap replicates. Diamonds at the nodes indicate bootstrap values > 80%. The scale indicates substitution per site. The main five cowpox virus (CPXV) clusters were highlighted in different colors: pink (Ectromelia-Abatino-like CPXV), blue (CPXV-like 1), green (CPXV-like 2), turquoise blue (Vaccinia-like CPXV) and orange (Variola-like CPXV). Figure S9. Bayesian maximum clade credibility (MCC) tree of 62 non-recombinant conserved genes of 55 CPXV genomes. The MCC tree was generated using BEAST 1, using a log-normal relaxed clock, coalescent Bayesian skyline population, HKY substitution model and four gamma categories. The numbers on the nodes indicate the time of the most recent common ancestor of the clades. Diamonds at the nodes indicate posterior probability values > 0.9. The main five CPXV clusters were highlighted in different colors: pink (Ectromelia-Abatino-like CPXV), blue (CPXV-like 1), green (CPXV-like 2), turquoise blue (Vaccinia-like CPXV) and orange (Variola-like CPXV). Figure S10. New classification of Cowpox virus (CPXV) based on phylogenetic inference (from 87 OPXV whole genomes, core genomes and orthologous genes), patristic and genetic distances. Diamonds at the nodes indicate bootstrap values > 80%. The main five CPXV clusters were highlighted in different colors: pink (Ectromelia-Abatino-like CPXV), blue (CPXV-like 1), green (CPXV-like 2), turquoise blue (Vaccinia-like CPXV) and orange (Variola-like CPXV). Table S1: List of strains used in the phylogenetic analysis. Table S2: List of orthologous genes from 87 orthopoxviruses used in this study. Table S3: List of 62 conserved genes from 87 orthopoxviruses used in this study. Table S4: List of strains used in the evolution molecular analysis. Table S5. Predicted genes in CPXV-No-F1, CPXV-No-F2, CPXV-No-H1, CPXV-Swe-H1 and CPXV-Swe-H2 compared to reference genomes CPXV-Brighton (CPXV_BR). Table S6. Patristic distances between CPXV clusters and OPXV species calculated from the Maximum likelihood (ML) and Bayesian inference (BI) trees of 62 conserved genes, 87 OPXV whole genomes, core genomes and orthologous genes. Table S7. Genetic distances between CPXV clusters and OPXV species estimated by p-distances from the alignment of 62 conserved genes (A), 87 OPXV whole genomes (B), core genomes (C) and orthologous genes (D). Table S8. Patristic and genetic distances within CPXV clusters calculated from the Maximum likelihood (ML) and Bayesian inference (BI) trees of 62 conserved genes, 87 OPXV core genomes, whole genomes and orthologous genes and their alignments, respectively. Table S9. Patristic distances within CPXV-like 2 calculated from the Maximum likelihood (ML) and Bayesian inference (BI) trees of 62 conserved genes, 87 OPXV whole genomes, core genomes and orthologous genes. Table S10. Genetic distances within CPXV-like 2 estimated by p-distances from the alignment of 62 conserved genes (A), 87 OPXV whole genomes (B), core genomes (C) and orthologous genes (D). Table S11. Patristic and genetic distances within ECTV-Abatino-like calculated from the Maximum likelihood (ML) and Bayesian inference (BI) trees of 62 conserved genes, 87 OPXV whole genomes, core genomes and orthologous genes and their alignments, respectively. Table S12. Patristic distances within VACV-like calculated from the Maximum likelihood (ML) and Bayesian inference (BI) trees of 62 conserved genes, 87 OPXV whole genomes, core genomes and orthologous genes. Table S13. Genetic distances within VACV-like clade estimated by p-distances from the alignment of 62 conserved genes (A), 87 OPXV whole genomes (B), core genomes (C) and orthologous genes (D). Table S14. Patristic and genetic distances within CPXV-like 1 calculated from the Maximum likelihood (ML) and Bayesian inference (BI) trees of 87 OPXV whole genomes, core

genomes and orthologous genes and their alignments, respectively. Table S15. Patristic distances within CPXV-like 1 calculated from the Maximum likelihood (ML) and Bayesian inference (BI) trees of 62 conserved genes, 87 OPXV whole genomes, core genomes and orthologous genes. Table S16. Genetic distances within CPXV-like 1 estimated by p-distances from the alignment of 62 conserved genes (A), 87 OPXV whole genomes (B), core genomes (C) and orthologous genes (D).

Author Contributions: Conceptualization, D.D.-C., U.M. and M.I.O.; Methodology, D.D.-C., C.M., U.M. and M.I.O.; Supervision, U.M. and M.I.O.; Writing—original draft, D.D.-C., C.M., U.M. and M.I.O.; Writing—review and editing, D.D.-C., C.M., A.N., A.B., U.M. and M.I.O. All authors have read and agreed to the published version of the manuscript.

Funding: This research was funded by UiT—The Arctic University of Norway, grant number A212100108 and the National Graduate School in Infection Biology and Antimicrobials, grant number 249062. The APC was funded by UiT—The Arctic University of Norway.

Institutional Review Board Statement: Not applicable.

Informed Consent Statement: Not applicable.

Data Availability Statement: The original contributions presented in the study are publicly available. These data can be found here: https://www.ncbi.nlm.nih.gov/genbank/ (accessed on 2 August 2022), OP125537, OP125538, OP125539, OP125540, OP125541.

Conflicts of Interest: The authors declare no conflict of interest.

References

1. MacLachlan, N.J.; Dubovi, E.J. (Eds.) Poxviridae. In *Fenner's Veterinary Virology*; Academic Press: Boston, MA, USA, 2017; pp. 157–174. ISBN 9780128009468.
2. Smithson, C.; Tang, N.; Sammons, S.; Frace, M.; Batra, D.; Li, Y.; Emerson, G.L.; Carroll, D.S.; Upton, C. The Genomes of Three North American Orthopoxviruses. *Virus Genes* **2017**, *53*, 21–34. [CrossRef]
3. International Committee on Taxonomy of Viruses (ICTV). Available online: https://talk.ictvonline.org/taxonomy/ (accessed on 16 July 2022).
4. Gubser, C.; Smith, G.L. The Sequence of Camelpox Virus Shows It Is Most Closely Related to Variola Virus, the Cause of Smallpox. *J. Gen. Virol.* **2002**, *83*, 855–872. [CrossRef] [PubMed]
5. Mavian, C.; López-Bueno, A.; Martín, R.; Nitsche, A.; Alcamí, A. Comparative Pathogenesis, Genomics and Phylogeography of Mousepox. *Viruses* **2021**, *13*, 1146. [CrossRef] [PubMed]
6. Cardeti, G.; Gruber, C.E.M.; Eleni, C.; Carletti, F.; Castilletti, C.; Manna, G.; Rosone, F.; Giombini, E.; Selleri, M.; Lapa, D.; et al. Fatal Outbreak in Tonkean Macaques Caused by Possibly Novel Orthopoxvirus, Italy, January 2015. *Emerg. Infect. Dis. J.* **2017**, *23*, 1941–1949. [CrossRef] [PubMed]
7. Springer, Y.P.; Hsu, C.H.; Werle, Z.R.; Olson, L.E.; Cooper, M.P.; Castrodale, L.J.; Fowler, N.; Mccollum, A.M.; Goldsmith, C.S.; Emerson, G.L.; et al. Novel Orthopoxvirus Infection in an Alaska Resident. *Clin. Infect. Dis.* **2017**, *64*, 1737. [CrossRef] [PubMed]
8. Gao, J.; Gigante, C.; Khmaladze, E.; Liu, P.; Tang, S.; Wilkins, K.; Zhao, K.; Davidson, W.; Nakazawa, Y.; Maghlakelidze, G.; et al. Genome Sequences of Akhmeta Virus, an Early Divergent Old World Orthopoxvirus. *Viruses* **2018**, *10*, 252. [CrossRef] [PubMed]
9. Strassburg, M.A. The Global Eradication of Smallpox. *Am. J. Infect. Control* **1982**, *10*, 53–59. [CrossRef]
10. Deria, A.; Jezek, Z.; Markvart, K.; Carrasco, P.; Weisfeld, J. The World's Last Endemic Case of Smallpox: Surveillance and Containment Measures. *Bull. World Health Organ.* **1980**, *58*, 279.
11. Vora, N.M.; Li, Y.; Geleishvili, M.; Emerson, G.L.; Khmaladze, E.; Maghlakelidze, G.; Navdarashvili, A.; Zakhashvili, K.; Kokhreidze, M.; Endeladze, M.; et al. Human Infection with a Zoonotic Orthopoxvirus in the Country of Georgia. *N. Engl. J. Med.* **2015**, *372*, 1223. [CrossRef] [PubMed]
12. Diaz, J.H. The Disease Ecology, Epidemiology, Clinical Manifestations, Management, Prevention, and Control of Increasing Human Infections with Animal Orthopoxviruses. *Wilderness Environ. Med.* **2021**, *32*, 528–536. [CrossRef]
13. Silva, N.I.O.; de Oliveira, J.S.; Kroon, E.G.; de Souza Trindade, G.; Drumond, B.P. Here, There, and Everywhere: The Wide Host Range and Geographic Distribution of Zoonotic Orthopoxviruses. *Viruses* **2021**, *13*, 43. [CrossRef] [PubMed]
14. Alakunle, E.; Moens, U.; Nchinda, G.; Okeke, M.I. Monkeypox Virus in Nigeria: Infection Biology, Epidemiology, and Evolution. *Viruses* **2020**, *12*, 1257. [CrossRef] [PubMed]
15. Reynolds, M.G.; Guagliardo, S.A.J.; Nakazawa, Y.J.; Doty, J.B.; Mauldin, M.R. Understanding Orthopoxvirus Host Range and Evolution: From the Enigmatic to the Usual Suspects. *Curr. Opin. Virol.* **2018**, *28*, 108–115. [CrossRef] [PubMed]
16. WHO. Disease Outbreak News; Multi-Country Monkeypox Outbreak: Situation Update. Available online: https://www.who.int/emergencies/disease-outbreak-news/item/2022-DON396 (accessed on 9 July 2022).
17. WHO. Disease Outbreak News; Multi-Country Monkeypox Outbreak in Non-Endemic Countries. Available online: https://www.who.int/emergencies/disease-outbreak-news/item/2022-DON385 (accessed on 20 June 2022).

18. Chantrey, J.; Meyer, H.; Baxby, D.; Begon, M.; Bown, K.J.; Hazel, S.M.; Jones, T.; Montgomery, W.I.; Bennett, M. Cowpox: Reservoir Hosts and Geographic Range. *Epidemiol. Infect.* **1999**, *122*, 455. [CrossRef] [PubMed]
19. Wolfs, T.F.W.; Wagenaar, J.A.; Niesters, H.G.M.; Osterhaus, A.D.M.E. Rat-to-Human Transmission of Cowpox Infection. *Emerg. Infect. Dis.* **2002**, *8*, 1495. [CrossRef]
20. Laakkonen, J.; Kallio-Kokko, H.; Öktem, M.A.; Blasdell, K.; Plyusnina, A.; Niemimaa, J.; Karataş, A.; Plyusnin, A.; Vaheri, A.; Henttonen, H. Serological Survey for Viral Pathogens in Turkish Rodents. *J. Wildl. Dis.* **2006**, *42*, 672–676. [CrossRef]
21. Vorou, R.M.; Papavassiliou, V.G.; Pierroutsakos, I.N. Cowpox Virus Infection: An Emerging Health Threat. *Curr. Opin. Infect. Dis.* **2008**, *21*, 153–156. [CrossRef]
22. Popova, A.Y.; Maksyutov, R.A.; Taranov, O.S.; Tregubchak, T.V.; Zaikovskaya, A.V.; Sergeev, A.A.; Vlashchenko, I.V.; Bodnev, S.A.; Ternovoi, V.A.; Alexandrova, N.S. Cowpox in a Human, Russia, 2015. *Epidemiol. Infect.* **2017**, *145*, 755–759. [CrossRef]
23. Ferrier, A.; Frenois-Veyrat, G.; Schvoerer, E.; Henard, S.; Jarjaval, F.; Drouet, I.; Timera, H.; Boutin, L.; Mosca, E.; Peyrefitte, C.; et al. Fatal Cowpox Virus Infection in Human Fetus, France, 2017. *Emerg. Infect. Dis.* **2021**, *27*, 2570–2577. [CrossRef]
24. Kinnunen, P.M.; Henttonen, H.; Hoffmann, B.; Kallio, E.R.; Korthase, C.; Laakkonen, J.; Niemimaa, J.; Palva, A.; Schlegel, M.; Ali, H.S.; et al. Orthopox Virus Infections in Eurasian Wild Rodents. *Vector-Borne Zoonotic Dis.* **2011**, *11*, 1133–1140. [CrossRef]
25. Girling, S.J.; Pizzi, R.; Cox, A.; Beard, P.M. Fatal Cowpox Virus Infection in Two Squirrel Monkeys (*Saimiri sciureus*). *Vet. Rec.* **2011**, *169*, 156. [CrossRef] [PubMed]
26. Smith, K.C.; Bennett, M.; Garrett, D.C. Skin Lesions Caused by Orthopoxvirus Infection in a Dog. *J. Small Anim. Pract.* **1999**, *40*, 495–497. [CrossRef] [PubMed]
27. Tryland, M.; Myrmel, H.; Holtet, L.; Haukenes, G.; Traavik, T. Clinical Cowpox Cases in Norway. *Scand. J. Infect. Dis.* **1998**, *30*, 301–303. [CrossRef] [PubMed]
28. Martina, B.E.E.; Van Doornum, G.; Dorrestein, G.M.; Niesters, H.G.M.; Stittelaar, K.J.; Wolters, M.A.B.I.; Van Bolhuis, H.G.H.; Osterhaus, A.D.M.E. Cowpox Virus Transmission from Rats to Monkeys, the Netherlands. *Emerg. Infect. Dis.* **2006**, *12*, 1005. [CrossRef]
29. Prkno, A.; Hoffmann, D.; Goerigk, D.; Kaiser, M.; van Maanen, A.C.F.; Jeske, K.; Jenckel, M.; Pfaff, F.; Vahlenkamp, T.W.; Beer, M.; et al. Epidemiological Investigations of Four Cowpox Virus Outbreaks in Alpaca Herds, Germany. *Viruses* **2017**, *9*, 344. [CrossRef]
30. Willemse, A.; Egberink, H.F. Transmission of Cowpox Virus Infection from Domestic Cat to Man. *Lancet* **1985**, *1*, 1515. [CrossRef]
31. Tryland, M.; Sandvik, T.; Hansen, H.; Haukenes, G.; Holtet, L.; Bennett, M.; Mehl, R.; Moens, U.; Olsvik; Traavik, T. Characteristics of Four Cowpox Virus Isolates from Norway and Sweden. *APMIS* **1998**, *106*, 623–635. [CrossRef]
32. Cronqvist, J.; Ekdahl, K.; Kjartansdottir, A.; Bauer, B.; Klinker, M. Cowpox—A Cat Disease in Man. *Lakartidningen* **1991**, *88*, 2605–2606.
33. Hansen, H.; Okeke, M.I.; Nilssen, Ø.; Traavik, T. Comparison and Phylogenetic Analysis of Cowpox Viruses Isolated from Cats and Humans in Fennoscandia. *Arch. Virol.* **2009**, *154*, 1293–1302. [CrossRef]
34. Okeke, M.I.; Hansen, H.; Traavik, T. A Naturally Occurring Cowpox Virus with an Ectromelia Virus A-Type Inclusion Protein Gene Displays Atypical A-Type Inclusions. *Infect. Genet. Evol.* **2012**, *12*, 160–168. [CrossRef]
35. Okeke, M.I.; Okoli, A.S.; Nilssen, Ø.; Moens, U.; Tryland, M.; Bøhn, T.; Traavik, T. Molecular Characterization and Phylogenetics of Fennoscandian Cowpox Virus Isolates Based on the P4c and Atip Genes. *Virol. J.* **2014**, *11*, 119. [CrossRef]
36. Carroll, D.S.; Emerson, G.L.; Li, Y.; Sammons, S.; Olson, V.; Frace, M.; Nakazawa, Y.; Czerny, C.P.; Tryland, M.; Kolodziejek, J.; et al. Chasing Jenner's Vaccine: Revisiting Cowpox Virus Classification. *PLoS ONE* **2011**, *6*, 4–9. [CrossRef]
37. Dabrowski, P.W.; Radonić, A.; Kurth, A.; Nitsche, A. Genome-Wide Comparison of Cowpox Viruses Reveals a New Clade Related to Variola Virus. *PLoS ONE* **2013**, *8*, e79953. [CrossRef] [PubMed]
38. Mauldin, M.R.; Antwerpen, M.; Emerson, G.L.; Li, Y.; Zoeller, G.; Carroll, D.S.; Meyer, H. Cowpox Virus: What's in a Name? *Viruses* **2017**, *9*, 101. [CrossRef]
39. Babkin, I.V.; Babkina, I.N.; Tikunova, N.V. An Update of Orthopoxvirus Molecular Evolution. *Viruses* **2022**, *14*, 388. [CrossRef]
40. Diaz-Cánova, D.; Moens, U.L.; Brinkmann, A.; Nitsche, A.; Okeke, M.I. Genomic Sequencing and Analysis of a Novel Human Cowpox Virus With Mosaic Sequences From North America and Old World Orthopoxvirus. *Front. Microbiol.* **2022**, *13*, 868887. [CrossRef]
41. Franke, A.; Pfaff, F.; Jenckel, M.; Hoffmann, B.; Höper, D.; Antwerpen, M.; Meyer, H.; Beer, M.; Hoffmann, D. Classification of Cowpox Viruses into Several Distinct Clades and Identification of a Novel Lineage. *Viruses* **2017**, *9*, 142. [CrossRef] [PubMed]
42. Senkevich, T.G.; Yutin, N.; Wolf, Y.I.; Koonin, E.V.; Moss, B. Ancient Gene Capture and Recent Gene Loss Shape the Evolution of Orthopoxvirus-Host Interaction Genes. *mBio* **2021**, *12*, e01495-21. [CrossRef] [PubMed]
43. Gubser, C.; Hué, S.; Kellam, P.; Smith, G.L. Poxvirus Genomes: A Phylogenetic Analysis. *J. Gen. Virol.* **2004**, *85*, 105–117. [CrossRef] [PubMed]
44. Hendrickson, R.C.; Wang, C.; Hatcher, E.L.; Lefkowitz, E.J. Orthopoxvirus Genome Evolution: The Role of Gene Loss. *Viruses* **2010**, *2*, 1933–1967. [CrossRef] [PubMed]
45. Zehender, G.; Lai, A.; Veo, C.; Bergna, A.; Ciccozzi, M.; Galli, M. Bayesian Reconstruction of the Evolutionary History and Cross-Species Transition of Variola Virus and Orthopoxviruses. *J. Med. Virol.* **2018**, *90*, 1134–1141. [CrossRef]
46. Babkin, I.V.; Babkina, I.N. A Retrospective Study of the Orthopoxvirus Molecular Evolution. *Infect. Genet. Evol.* **2012**, *12*, 1597–1604. [CrossRef]
47. Babkin, I.V.; Shchelkunov, S.N. Molecular Evolution of Poxviruses. *Russ. J. Genet.* **2008**, *44*, 895–908. [CrossRef]

48. Babkin, I.V.; Shchelkunov, S.N. Time Scale of Poxvirus Evolution. *Mol. Biol.* **2006**, *40*, 16–19. [CrossRef]
49. Babkin, I.V.; Babkina, I.N. Molecular Dating in the Evolution of Vertebrate Poxviruses. *Intervirology* **2011**, *54*, 253–260. [CrossRef] [PubMed]
50. Bankevich, A.; Nurk, S.; Antipov, D.; Gurevich, A.A.; Dvorkin, M.; Kulikov, A.S.; Lesin, V.M.; Nikolenko, S.I.; Pham, S.; Prjibelski, A.D.; et al. SPAdes: A New Genome Assembly Algorithm and Its Applications to Single-Cell Sequencing. *J. Comput. Biol.* **2012**, *19*, 477. [CrossRef]
51. Tcherepanov, V.; Ehlers, A.; Upton, C. Genome Annotation Transfer Utility (GATU): Rapid Annotation of Viral Genomes Using a Closely Related Reference Genome. *BMC Genom.* **2006**, *7*, 150. [CrossRef]
52. Camacho, C.; Coulouris, G.; Avagyan, V.; Ma, N.; Papadopoulos, J.; Bealer, K.; Madden, T.L. BLAST+: Architecture and Applications. *BMC Bioinform.* **2009**, *10*, 421. [CrossRef] [PubMed]
53. Ehlers, A.; Osborne, J.; Slack, S.; Roper, R.L.; Upton, C. Poxvirus Orthologous Clusters (POCs). *Bioinformatics* **2002**, *18*, 1544–1545. [CrossRef] [PubMed]
54. Katoh, K.; Standley, D.M. MAFFT Multiple Sequence Alignment Software Version 7: Improvements in Performance and Usability. *Mol. Biol. Evol.* **2013**, *30*, 772–780. [CrossRef]
55. Martin, D.P.; Murrell, B.; Golden, M.; Khoosal, A.; Muhire, B. RDP4: Detection and Analysis of Recombination Patterns in Virus Genomes. *Virus Evol.* **2015**, *1*, vev003. [CrossRef]
56. Martin, D.; Rybicki, E. RDP: Detection of Recombination amongst Aligned Sequences. *Bioinformatics* **2000**, *16*, 562–563. [CrossRef]
57. Padidam, M.; Sawyer, S.; Fauquet, C.M. Possible Emergence of New Geminiviruses by Frequent Recombination. *Virology* **1999**, *265*, 218–225. [CrossRef]
58. Martin, D.P.; Posada, D.; Crandall, K.A.; Williamson, C. A Modified Bootscan Algorithm for Automated Identification of Recombinant Sequences and Recombination Breakpoints. *AIDS Res. Hum. Retrovir.* **2005**, *21*, 98–102. [CrossRef] [PubMed]
59. Smith, J.M. Analyzing the Mosaic Structure of Genes. *J. Mol. Evol.* **1992**, *34*, 126–129. [CrossRef]
60. Posada, D.; Crandall, K.A. Evaluation of Methods for Detecting Recombination from DNA Sequences: Computer Simulations. *Proc. Natl. Acad. Sci. USA* **2001**, *98*, 13757–13762. [CrossRef] [PubMed]
61. Gibbs, M.J.; Armstrong, J.S.; Gibbs, A.J. Sister-Scanning: A Monte Carlo Procedure for Assessing Signals in Recombinant Sequences. *Bioinformatics* **2000**, *16*, 573–582. [CrossRef] [PubMed]
62. Boni, M.F.; Posada, D.; Feldman, M.W. An Exact Nonparametric Method for Inferring Mosaic Structure in Sequence Triplets. *Genetics* **2007**, *176*, 1035–1047. [CrossRef] [PubMed]
63. Talavera, G.; Castresana, J. Improvement of Phylogenies after Removing Divergent and Ambiguously Aligned Blocks from Protein Sequence Alignments. *Syst. Biol.* **2007**, *56*, 564–577. [CrossRef] [PubMed]
64. Minh, B.Q.; Schmidt, H.A.; Chernomor, O.; Schrempf, D.; Woodhams, M.D.; Von Haeseler, A.; Lanfear, R.; Teeling, E. IQ-TREE 2: New Models and Efficient Methods for Phylogenetic Inference in the Genomic Era. *Mol. Biol. Evol.* **2020**, *37*, 1530–1534. [CrossRef]
65. Darriba, D.; Posada, D.; Kozlov, A.M.; Stamatakis, A.; Morel, B.; Flouri, T. ModelTest-NG: A New and Scalable Tool for the Selection of DNA and Protein Evolutionary Models. *Mol. Biol. Evol.* **2020**, *37*, 294. [CrossRef] [PubMed]
66. Stamatakis, A. RAxML Version 8: A Tool for Phylogenetic Analysis and Post-Analysis of Large Phylogenies. *Bioinformatics* **2014**, *30*, 1313. [CrossRef] [PubMed]
67. Stamatakis, A.; Hoover, P.; Rougemont, J. A Rapid Bootstrap Algorithm for the RAxML Web Servers. *Syst. Biol.* **2008**, *57*, 758–771. [CrossRef]
68. Ronquist, F.; Teslenko, M.; Van Der Mark, P.; Ayres, D.L.; Darling, A.; Höhna, S.; Larget, B.; Liu, L.; Suchard, M.A.; Huelsenbeck, J.P. MrBayes 3.2: Efficient Bayesian Phylogenetic Inference and Model Choice Across a Large Model Space. *Syst. Biol.* **2012**, *61*, 539–542. [CrossRef]
69. Fourment, M.; Gibbs, M.J. PATRISTIC: A Program for Calculating Patristic Distances and Graphically Comparing the Components of Genetic Change. *BMC Evol. Biol.* **2006**, *6*, 1. [CrossRef] [PubMed]
70. Tamura, K.; Stecher, G.; Kumar, S. MEGA11: Molecular Evolutionary Genetics Analysis Version 11. *Mol. Biol. Evol.* **2021**, *38*, 3022–3027. [CrossRef]
71. Suchard, M.A.; Lemey, P.; Baele, G.; Ayres, D.L.; Drummond, A.J.; Rambaut, A. Bayesian Phylogenetic and Phylodynamic Data Integration Using BEAST 1.10. *Virus Evol.* **2018**, *4*, vey016. [CrossRef] [PubMed]
72. Rambaut, A.; Lam, T.T.; Carvalho, L.M.; Pybus, O.G. Exploring the Temporal Structure of Heterochronous Sequences Using TempEst (Formerly Path-O-Gen). *Virus Evol.* **2016**, *2*, vew007. [CrossRef]
73. Rambaut, A.; Drummond, A.J.; Xie, D.; Baele, G.; Suchard, M.A. Posterior Summarization in Bayesian Phylogenetics Using Tracer 1.7. *Syst. Biol.* **2018**, *67*, 901. [CrossRef]
74. Yu, G.; Smith, D.K.; Zhu, H.; Guan, Y.; Lam, T.T.Y. Ggtree: An r Package for Visualization and Annotation of Phylogenetic Trees with Their Covariates and Other Associated Data. *Methods Ecol. Evol.* **2017**, *8*, 28–36. [CrossRef]
75. Coulson, D.; Upton, C. Characterization of Indels in Poxvirus Genomes. *Virus Genes* **2011**, *42*, 171–177. [CrossRef]
76. Qin, L.; Upton, C.; Hazes, B.; Evans, D.H. Genomic Analysis of the Vaccinia Virus Strain Variants Found in Dryvax Vaccine. *J. Virol.* **2011**, *85*, 13049. [CrossRef] [PubMed]
77. Qin, L.; Favis, N.; Famulski, J.; Evans, D.H. Evolution of and Evolutionary Relationships between Extant Vaccinia Virus Strains. *J. Virol.* **2015**, *89*, 1809. [CrossRef] [PubMed]

78. Smithson, C.; Purdy, A.; Verster, A.J.; Upton, C. Prediction of Steps in the Evolution of Variola Virus Host Range. *PLoS ONE* **2014**, *9*, e91520. [CrossRef] [PubMed]
79. Smithson, C.; Meyer, H.; Gigante, C.M.; Gao, J.; Zhao, H.; Batra, D.; Damon, I.; Upton, C.; Li, Y. Two Novel Poxviruses with Unusual Genome Rearrangements: NY_014 and Murmansk. *Virus Genes* **2017**, *53*, 883–897. [CrossRef]
80. Smithson, C.; Kampman, S.; Hetman, B.M.; Upton, C. Incongruencies in Vaccinia Virus Phylogenetic Trees. *Computation* **2014**, *2*, 182–198. [CrossRef]
81. Jeske, K.; Weber, S.; Pfaff, F.; Imholt, C.; Jacob, J.; Beer, M.; Ulrich, R.G.; Hoffmann, D. Molecular Detection and Characterization of the First Cowpox Virus Isolate Derived from a Bank Vole. *Viruses* **2019**, *11*, 1075. [CrossRef]
82. Becker, C.; Kurth, A.; Hessler, F.; Kramp, H.; Gokel, M.; Hoffmann, R.; Kuczka, A.; Nitsche, A. Cowpox Virus Infection in Pet Rat Owners: Not Always Immediately Recognized. *Dtsch. Ärzteblatt Int.* **2009**, *106*, 329. [CrossRef]
83. Shchelkunov, S.N.; Safronov, P.F.; Totmenin, A.V.; Petrov, N.A.; Ryazankina, O.I.; Gutorov, V.V.; Kotwal, G.J. The Genomic Sequence Analysis of the Left and Right Species-Specific Terminal Region of a Cowpox Virus Strain Reveals Unique Sequences and a Cluster of Intact ORFs for Immunomodulatory and Host Range Proteins. *Virology* **1998**, *243*, 432–460. [CrossRef]
84. Hendrickson, R.C.; Wang, C.; Hatcher, E.L.; Lefkowitz, E.J. Orthopoxvirus Genome Evolution: The Role of Gene Loss. *Viruses* **2010**, *2*, 1933. [CrossRef]

Supplementary information

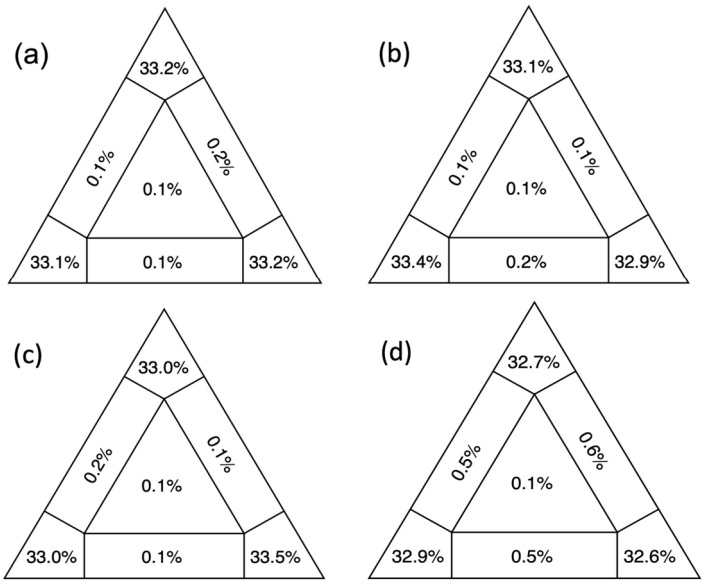

Figure S1. Presence of phylogenetic signal was evaluated by likelihood mapping checking for alternative topologies (tips), unresolved quartets (center) and partly resolved quartets (edges) for 87 OPXV whole genome (a), core genome (b), OPXV orthologous genes (c) and 62 conserved genes.

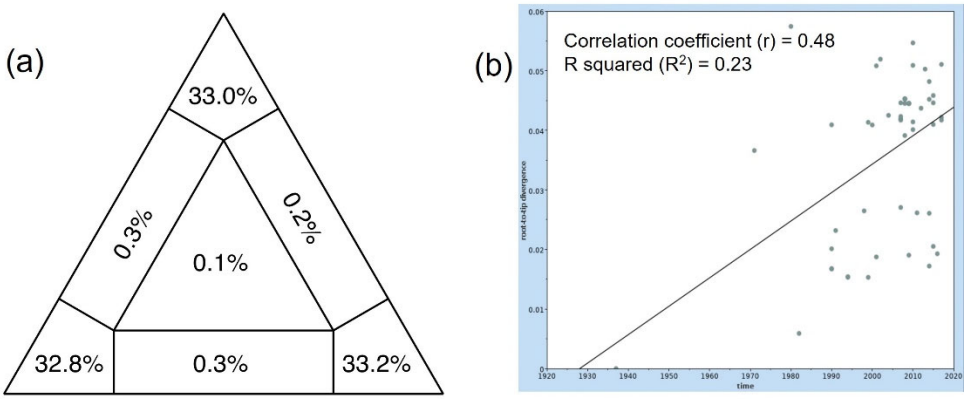

Figure S2. Phylogenetic and temporal signal analyses. (a) Presence of phylogenetic signal was evaluated by likelihood mapping checking for alternative topologies (tips), unresolved quartets (centre) and partly resolved quartets (edges) for 62 conserved genes of 55 CPXV strains. (b) Linear regression of root-to-tip genetic distance in a maximum likelihood phylogeny against sampling time for 62 conserved genes of 55 CPXV strains.

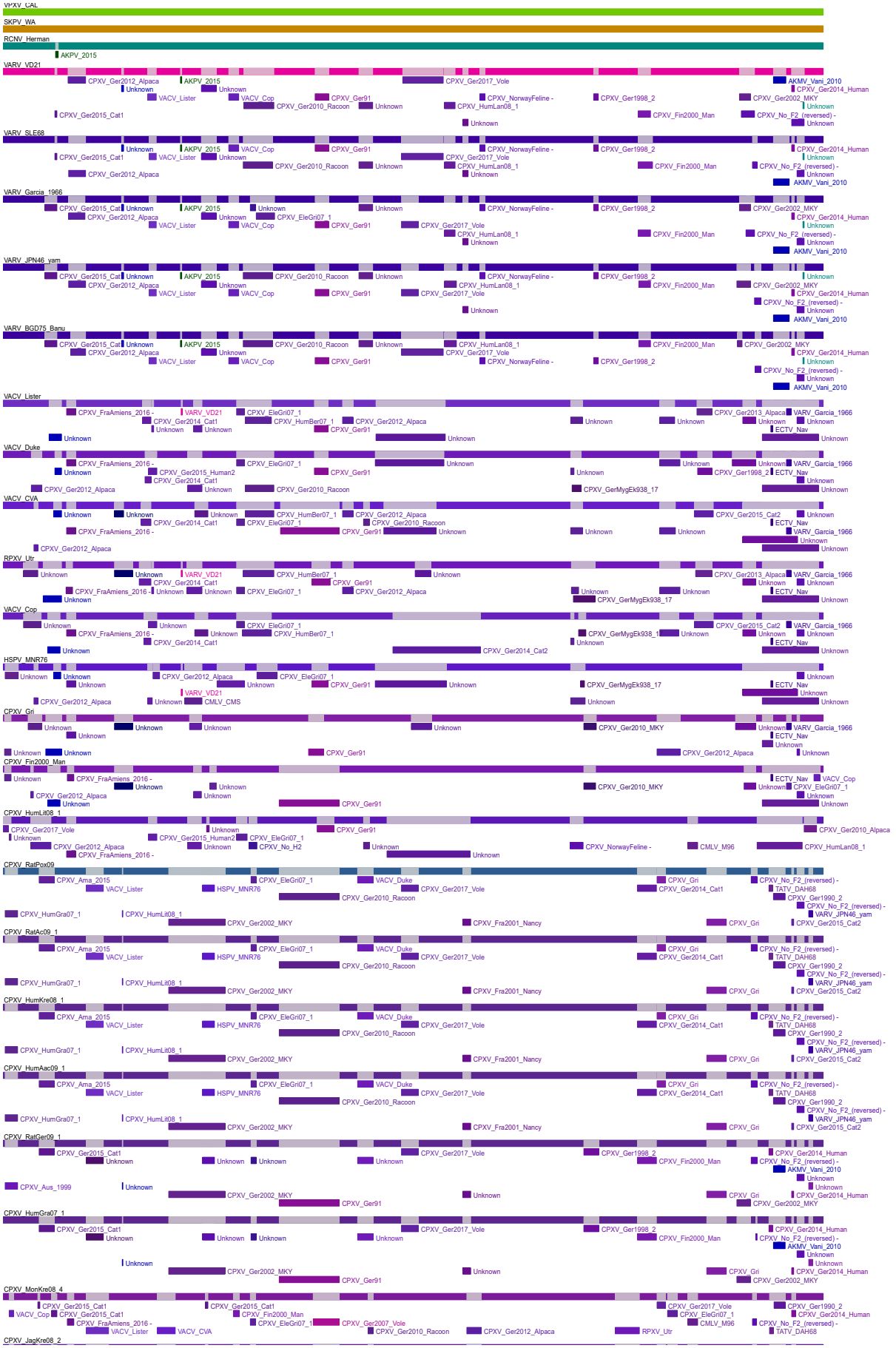
VPXV_CAL
SKPV_WA
RCNV_Herman
AKPV_2015
VARV_VD21
VARV_SLE68
VARV_Garcia_1966
VARV_JPN46_yam
VARV_BGD75_Banu
VACV_Lister
VACV_Duke
VACV_CVA
RPXV_Utr
VACV_Cop
HSPV_MNR76
CPXV_Gri
CPXV_Fin2000_Man
CPXV_HumLit08_1
CPXV_RatPox09
CPXV_RatAc09_1
CPXV_HumKre08_1
CPXV_HumAac09_1
CPXV_RatGer09_1
CPXV_HumGra07_1
CPXV_MonKre08_4
CPXV_JagKre08_2

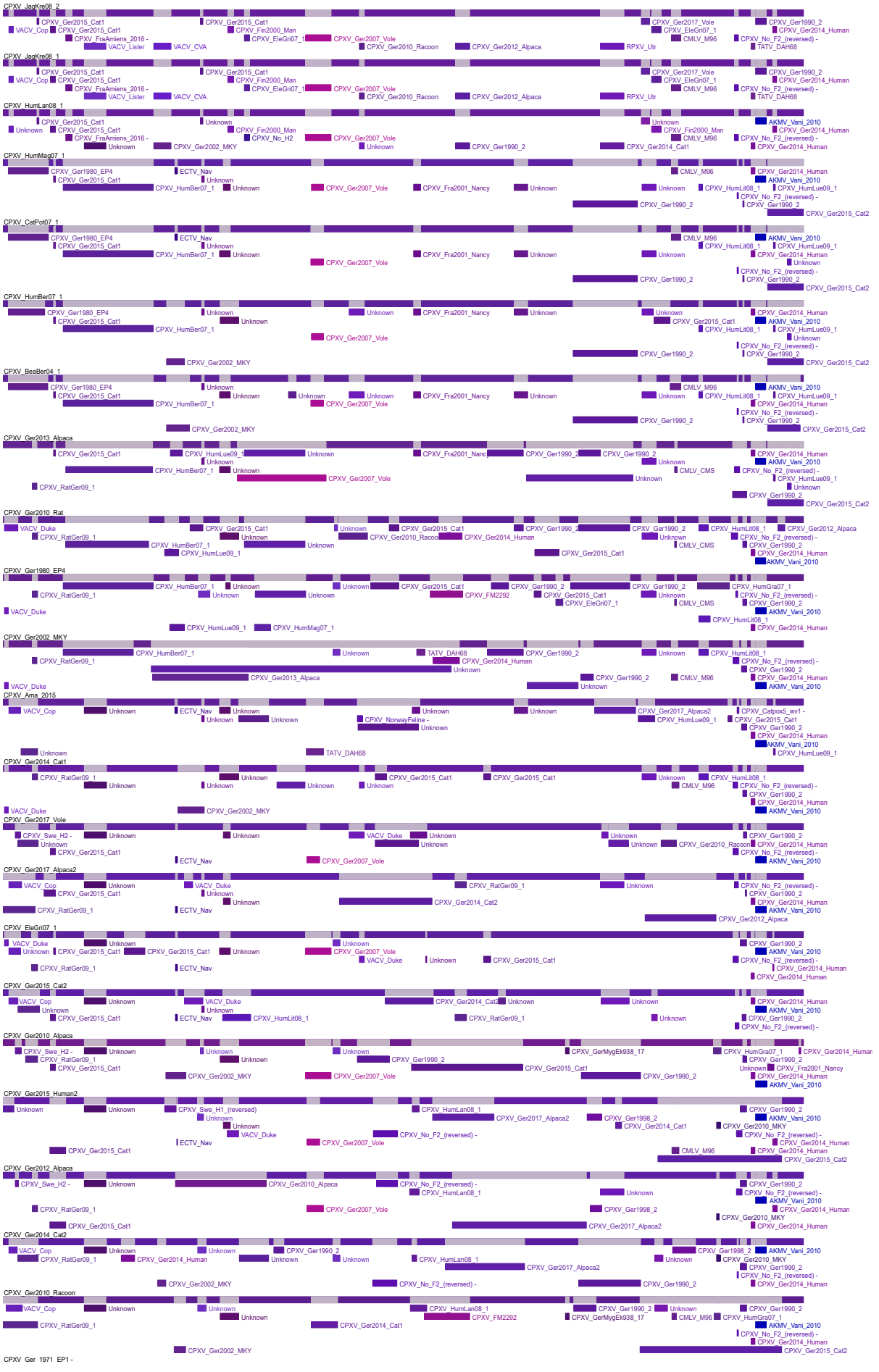
CPXV_JaqKre08_2
CPXV_Ger2015_Cat1
CPXV_Ger2015_Cat1
CPXV_Ger2017_Vole
CPXV_Ger1990_2
VACV_Cop
CPXV_Ger2015_Cat1
CPXV_Fin2000_Man
CPXV_Ger2014_Human
CPXV_FraAmiens_2016 -
CPXV_EleGri07_1
CPXV_Ger2007_Vole
CMLV_M96
CPXV_No_F2_(reversed) -
VACV_Lister
VACV_CVA
CPXV_Ger2010_Racoon
CPXV_Ger2012_Alpaca
RPXV_Utr
TATV_DAH68
CPXV_JaqKre08_1
CPXV_Ger2015_Cat1
CPXV_Ger2015_Cat1
CPXV_Ger2017_Vole
CPXV_Ger1990_2
VACV_Cop
CPXV_Ger2015_Cat1
CPXV_Fin2000_Man
CPXV_EleGri07_1
CPXV_Ger2014_Human
CPXV_FraAmiens_2016 -
CPXV_Ger2007_Vole
CMLV_M96
CPXV_No_F2_(reversed) -
VACV_Lister
VACV_CVA
CPXV_Ger2010_Racoon
CPXV_Ger2012_Alpaca
RPXV_Utr
TATV_DAH68
CPXV_HumLan08_1
CPXV_Ger2015_Cat1
Unknown
Unknown
AKMV_Vani_2010
Unknown
CPXV_Ger2015_Cat1
CPXV_Fin2000_Man
CPXV_Ger2014_Human
CPXV_FraAmiens_2016 -
CPXV_No_H2
CPXV_Ger2007_Vole
CMLV_M96
CPXV_No_F2_(reversed) -
Unknown
CPXV_Ger2002_MKY
Unknown
CPXV_Ger1990_2
CPXV_Ger2014_Cat1
CPXV_Ger2014_Human
CPXV_HumMag07_1
CPXV_Ger1980_EP4
ECTV_Nav
CMLV_M96
CPXV_Ger2014_Human
CPXV_Ger2015_Cat1
Unknown
AKMV_Vani_2010
CPXV_HumBer07_1
Unknown
CPXV_Ger2007_Vole
CPXV_Fra2001_Nancy
Unknown
Unknown
CPXV_HumLit08_1
CPXV_HumLue09_1
CPXV_No_F2_(reversed) -
CPXV_Ger1990_2
CPXV_Ger1990_2
CPXV_Ger2015_Cat2
CPXV_CatPot07_1
CPXV_Ger1980_EP4
ECTV_Nav
CMLV_M96
AKMV_Vani_2010
CPXV_Ger2015_Cat1
Unknown
CPXV_HumLit08_1
CPXV_HumLue09_1
CPXV_HumBer07_1
Unknown
CPXV_Fra2001_Nancy
Unknown
Unknown
CPXV_Ger2014_Human
CPXV_Ger2007_Vole
Unknown
CPXV_No_F2_(reversed) -
CPXV_Ger1990_2
CPXV_Ger1990_2
CPXV_Ger2015_Cat2
CPXV_HumBer07_1
CPXV_Ger1980_EP4
Unknown
Unknown
CPXV_Fra2001_Nancy
Unknown
Unknown
CPXV_Ger2014_Human
CPXV_Ger2015_Cat1
AKMV_Vani_2010
CPXV_HumBer07_1
Unknown
CPXV_HumLit08_1
CPXV_HumLue09_1
CPXV_Ger2007_Vole
Unknown
CPXV_No_F2_(reversed) -
CPXV_Ger1990_2
CPXV_Ger1990_2
CPXV_Ger2015_Cat2
CPXV_Ger2002_MKY
CPXV_BeaBer04_1
CPXV_Ger1980_EP4
Unknown
CMLV_M96
AKMV_Vani_2010
CPXV_Ger2015_Cat1
Unknown
Unknown
Unknown
CPXV_Fra2001_Nancy
Unknown
Unknown
CPXV_HumLit08_1
CPXV_HumLue09_1
CPXV_HumBer07_1
CPXV_Ger2007_Vole
CPXV_Ger2014_Human
CPXV_No_F2_(reversed) -
CPXV_Ger1990_2
CPXV_Ger1990_2
CPXV_Ger2015_Cat2
CPXV_Ger2002_MKY
CPXV_Ger2013_Alpaca
CPXV_Ger2015_Cat1
CPXV_HumLue09_1
Unknown
CPXV_Fra2001_Nanc
CPXV_Ger1990_2
CPXV_Ger1990_2
CPXV_Ger2014_Human
Unknown
Unknown
AKMV_Vani_2010
CPXV_HumBer07_1
Unknown
CMLV_CMS
CPXV_No_F2_(reversed) -
CPXV_Ger2007_Vole
Unknown
CPXV_HumLue09_1
CPXV_RatGer09_1
Unknown
CPXV_Ger1990_2
CPXV_Ger2015_Cat2
CPXV_Ger2010_Rat
VACV_Duke
CPXV_Ger2015_Cat1
Unknown
CPXV_Ger2015_Cat1
CPXV_Ger1990_2
CPXV_Ger1990_2
CPXV_HumLit08_1
CPXV_Ger2012_Alpaca
CPXV_RatGer09_1
Unknown
CPXV_Ger2010_Racoon
CPXV_Ger2014_Human
Unknown
CPXV_No_F2_(reversed) -
CPXV_HumBer07_1
Unknown
CMLV_CMS
CPXV_Ger1990_2
CPXV_HumLue09_1
CPXV_Ger2015_Cat1
CPXV_Ger2014_Human
AKMV_Vani_2010
CPXV_Ger1980_EP4
CPXV_HumBer07_1
Unknown
Unknown
CPXV_Ger2015_Cat1
CPXV_Ger1990_2
CPXV_Ger1990_2
CPXV_HumGra07_1
CPXV_RatGer09_1
Unknown
Unknown
CPXV_FM2292
CPXV_Ger2015_Cat1
Unknown
CPXV_No_F2_(reversed) -
CPXV_EleGri07_1
CMLV_CMS
CPXV_Ger1990_2
VACV_Duke
AKMV_Vani_2010
CPXV_HumLit08_1
CPXV_HumLue09_1
CPXV_HumMag07_1
CPXV_Ger2014_Human
CPXV_Ger2002_MKY
CPXV_HumBer07_1
Unknown
TATV_DAH68
CPXV_Ger1990_2
Unknown
CPXV_HumLit08_1
CPXV_RatGer09_1
CPXV_Ger2014_Human
CPXV_No_F2_(reversed) -
Unknown
CPXV_Ger1990_2
CPXV_Ger2013_Alpaca
CPXV_Ger1990_2
CMLV_M96
CPXV_Ger2014_Human
VACV_Duke
Unknown
AKMV_Vani_2010
CPXV_Ama_2015
VACV_Cop
Unknown
ECTV_Nav
Unknown
Unknown
Unknown
Unknown
CPXV_Ger2017_Alpaca2
CPXV_Catpox5_wv1 -
Unknown
Unknown
Unknown
CPXV_NorwayFeline -
CPXV_HumLue09_1
CPXV_Ger2015_Cat1
Unknown
CPXV_Ger1990_2
CPXV_Ger2014_Human
AKMV_Vani_2010
Unknown
TATV_DAH68
CPXV_HumLue09_1
CPXV_Ger2014_Cat1
CPXV_RatGer09_1
Unknown
CPXV_Ger2015_Cat1
CPXV_Ger2015_Cat1
Unknown
CPXV_HumLit08_1
Unknown
Unknown
Unknown
Unknown
CMLV_M96
CPXV_No_F2_(reversed) -
CPXV_Ger1990_2
CPXV_Ger2014_Human
AKMV_Vani_2010
VACV_Duke
CPXV_Ger2002_MKY
CPXV_Ger2017_Vole
CPXV_Swe_H2 -
Unknown
Unknown
VACV_Duke
Unknown
Unknown
CPXV_Ger1990_2
Unknown
Unknown
Unknown
CPXV_Ger2010_Racoon
CPXV_Ger2014_Human
CPXV_Ger2015_Cat1
CPXV_No_F2_(reversed) -
ECTV_Nav
CPXV_Ger2007_Vole
AKMV_Vani_2010
CPXV_Ger2017_Alpaca2
VACV_Cop
Unknown
VACV_Duke
CPXV_RatGer09_1
Unknown
CPXV_No_F2_(reversed) -
CPXV_Ger2015_Cat1
Unknown
CPXV_Ger1990_2
Unknown
CPXV_Ger2014_Cat2
CPXV_Ger2014_Human
CPXV_RatGer09_1
ECTV_Nav
AKMV_Vani_2010
CPXV_Ger2012_Alpaca
CPXV_EleGri07_1
VACV_Duke
Unknown
Unknown
CPXV_Ger1990_2
Unknown
Unknown
Unknown
CPXV_Ger2007_Vole
AKMV_Vani_2010
VACV_Duke
Unknown
CPXV_Ger2015_Cat1
CPXV_Ger2015_Cat1
Unknown
CPXV_No_F2_(reversed) -
CPXV_RatGer09_1
ECTV_Nav
CPXV_Ger2014_Human
CPXV_Ger2014_Human
CPXV_Ger2015_Cat2
VACV_Cop
Unknown
VACV_Duke
CPXV_Ger2014_Cat2
Unknown
Unknown
CPXV_Ger2014_Human
Unknown
Unknown
AKMV_Vani_2010
CPXV_Ger2015_Cat1
ECTV_Nav
CPXV_HumLit08_1
CPXV_RatGer09_1
Unknown
CPXV_Ger1990_2
CPXV_No_F2_(reversed) -
CPXV_Ger2010_Alpaca
CPXV_Swe_H2 -
Unknown
Unknown
Unknown
CPXV_GerMygEk938_17
CPXV_HumGra07_1
CPXV_Ger2014_Human
CPXV_RatGer09_1
Unknown
CPXV_Ger1990_2
CPXV_Ger1990_2
CPXV_Ger2015_Cat1
CPXV_Ger2015_Cat1
Unknown
CPXV_Fra2001_Nancy
CPXV_Ger2002_MKY
CPXV_Ger2007_Vole
CPXV_Ger1990_2
CPXV_Ger2014_Human
AKMV_Vani_2010
CPXV_Ger2015_Human2
Unknown
Unknown
CPXV_Swe_H1_(reversed)
Unknown
CPXV_HumLan08_1
CPXV_Ger1990_2
CPXV_Ger2017_Alpaca2
CPXV_Ger1998_2
AKMV_Vani_2010
Unknown
CPXV_Ger2014_Cat1
CPXV_Ger2010_MKY
Unknown
VACV_Duke
CPXV_No_F2_(reversed) -
CPXV_No_F2_(reversed) -
ECTV_Nav
CPXV_Ger2007_Vole
CPXV_Ger2014_Human
CPXV_Ger2015_Cat1
CMLV_M96
CPXV_Ger2014_Human
CPXV_Ger2015_Cat2
CPXV_Ger2012_Alpaca
CPXV_Swe_H2 -
Unknown
CPXV_Ger2010_Alpaca
CPXV_No_F2_(reversed) -
CPXV_Ger1990_2
CPXV_HumLan08_1
Unknown
CPXV_No_F2_(reversed) -
AKMV_Vani_2010
CPXV_RatGer09_1
CPXV_Ger2007_Vole
CPXV_Ger1998_2
CPXV_Ger2014_Human
CPXV_Ger2010_MKY
CPXV_Ger2015_Cat1
CPXV_Ger2017_Alpaca2
CPXV_Ger2014_Human
CPXV_Ger2014_Cat2
VACV_Cop
Unknown
Unknown
CPXV_Ger1990_2
CPXV_Ger1998_2
AKMV_Vani_2010
CPXV_RatGer09_1
CPXV_Ger2014_Human
Unknown
Unknown
CPXV_HumLan08_1
Unknown
CPXV_Ger2010_MKY
CPXV_Ger2017_Alpaca2
CPXV_Ger1990_2
CPXV_No_F2_(reversed) -
CPXV_Ger2002_MKY
CPXV_No_F2_(reversed) -
CPXV_Ger1990_2
CPXV_Ger2014_Human
CPXV_Ger2010_Racoon
VACV_Cop
Unknown
Unknown
CPXV_HumLan08_1
CPXV_Ger1990_2
Unknown
CPXV_Ger1990_2
Unknown
CPXV_FM2292
CPXV_GerMygEk938_17
CMLV_M96
CPXV_HumGra07_1
CPXV_RatGer09_1
CPXV_Ger2014_Cat1
AKMV_Vani_2010
CPXV_No_F2_(reversed) -
CPXV_Ger2014_Human
CPXV_Ger2002_MKY
CPXV_Ger2015_Cat2
CPXV_Ger 1971 EP1 -

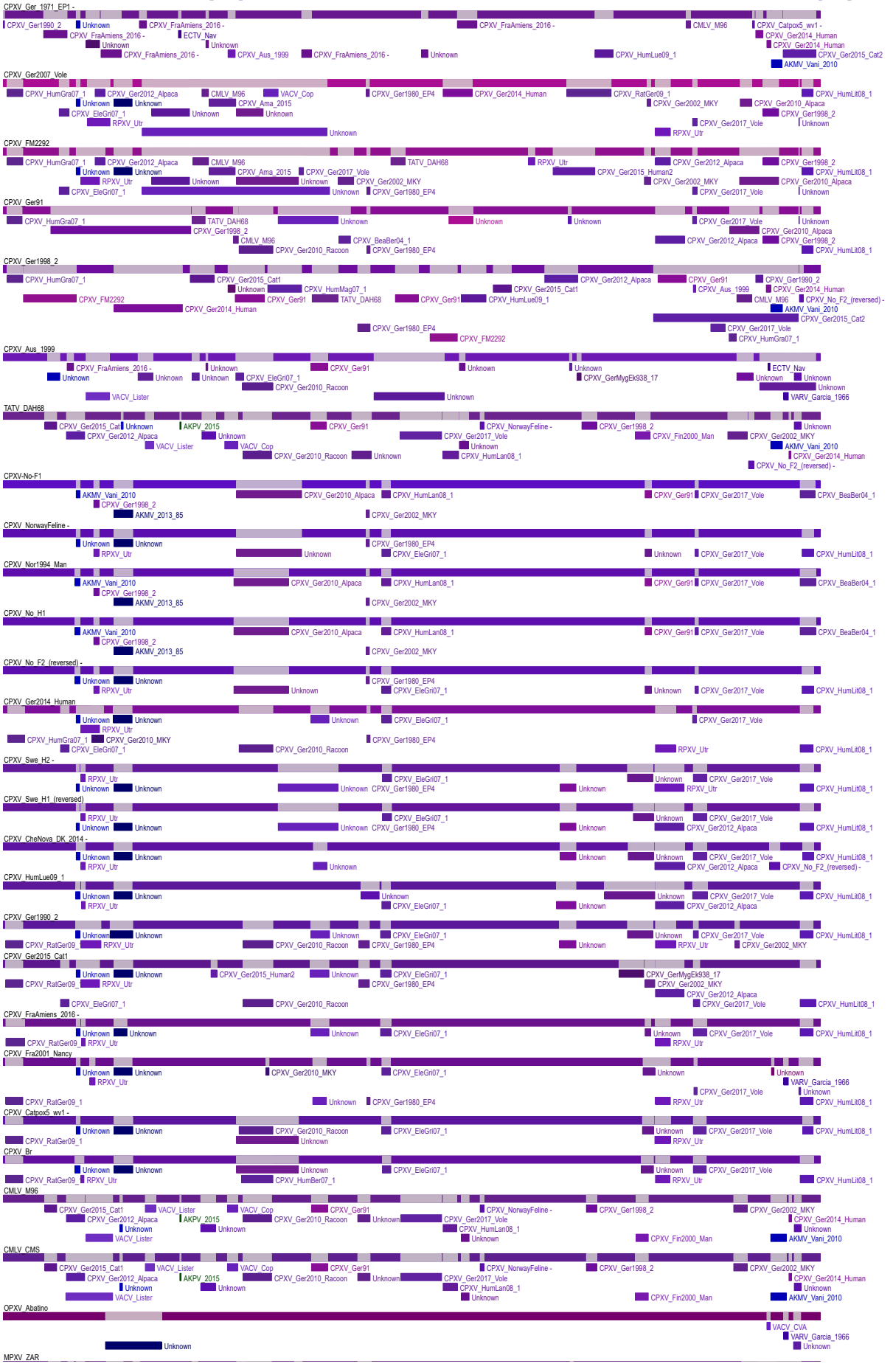
CPXV_Ger_1971_EP1 -
CPXV_Ger1990_2
Unknown
CPXV_FraAmiens_2016 -
CPXV_FraAmiens_2016 -
CMLV_M96
CPXV_Catpox5_wv1 -
CPXV_FraAmiens_2016 -
ECTV_Nav
CPXV_Ger2014_Human
Unknown
Unknown
CPXV_Ger2014_Human
CPXV_FraAmiens_2016 -
CPXV_Aus_1999
CPXV_FraAmiens_2016 -
Unknown
CPXV_HumLue09_1
CPXV_Ger2015_Cat2
AKMV_Vani_2010
CPXV_Ger2007_Vole
CPXV_HumGra07_1
CPXV_Ger2012_Alpaca
CMLV_M96
VACV_Cop
CPXV_Ger1980_EP4
CPXV_Ger2014_Human
CPXV_RatGer09_1
CPXV_HumLit08_1
Unknown
Unknown
CPXV_Ama_2015
CPXV_Ger2002_MKY
CPXV_Ger2010_Alpaca
CPXV_EleGri07_1
Unknown
Unknown
CPXV_Ger1998_2
RPXV_Utr
CPXV_Ger2017_Vole
Unknown
Unknown
RPXV_Utr
CPXV_FM2292
CPXV_HumGra07_1
CPXV_Ger2012_Alpaca
CMLV_M96
TATV_DAH68
RPXV_Utr
CPXV_Ger2012_Alpaca
CPXV_Ger1998_2
Unknown
Unknown
CPXV_Ama_2015
CPXV_Ger2017_Vole
CPXV_Ger2015_Human2
CPXV_HumLit08_1
RPXV_Utr
Unknown
Unknown
CPXV_Ger2002_MKY
CPXV_Ger2002_MKY
CPXV_Ger2010_Alpaca
CPXV_EleGri07_1
Unknown
CPXV_Ger1980_EP4
CPXV_Ger2017_Vole
Unknown
CPXV_Ger91
CPXV_HumGra07_1
CPXV_Ger2015_Cat1
CPXV_Ger91
CPXV_Ger1990_2
Unknown
CPXV_HumMag07_1
CPXV_Ger2015_Cat1
CPXV_Aus_1999
CPXV_Ger2014_Human
CPXV_FM2292
CPXV_Ger91
TATV_DAH68
CPXV_Ger91
CPXV_HumLue09_1
CMLV_M96
CPXV_No_F2_(reversed) -
CPXV_Ger2014_Human
AKMV_Vani_2010
CPXV_Ger2015_Cat2
CPXV_Ger1980_EP4
CPXV_Ger2017_Vole
CPXV_FM2292
CPXV_HumGra07_1
CPXV_Aus_1999
CPXV_FraAmiens_2016 -
Unknown
CPXV_Ger91
Unknown
Unknown
ECTV_Nav
Unknown
Unknown
Unknown
CPXV_EleGri07_1
CPXV_GerMygEk938_17
Unknown
Unknown
Unknown
CPXV_Ger2010_Racoon
VACV_Lister
Unknown
VARV_Garcia_1966
TATV_DAH68
CPXV_Ger2015_Cat1
Unknown
AKPV_2015
CPXV_Ger91
CPXV_NorwayFeline -
CPXV_Ger1998_2
Unknown
CPXV_Ger2012_Alpaca
Unknown
CPXV_Ger2017_Vole
CPXV_Fin2000_Man
CPXV_Ger2002_MKY
VACV_Lister
VACV_Cop
Unknown
AKMV_Vani_2010
CPXV_Ger2010_Racoon
Unknown
CPXV_HumLan08_1
CPXV_Ger2014_Human
CPXV_No_F2_(reversed) -
CPXV-No-F1
AKMV_Vani_2010
CPXV_Ger2010_Alpaca
CPXV_HumLan08_1
CPXV_Ger91
CPXV_Ger2017_Vole
CPXV_BeaBer04_1
CPXV_Ger1998_2
AKMV_2013_85
CPXV_Ger2002_MKY
CPXV_NorwayFeline -
Unknown
Unknown
CPXV_Ger1980_EP4
RPXV_Utr
Unknown
CPXV_EleGri07_1
Unknown
CPXV_Ger2017_Vole
CPXV_HumLit08_1
CPXV_Nor1994_Man
AKMV_Vani_2010
CPXV_Ger2010_Alpaca
CPXV_HumLan08_1
CPXV_Ger91
CPXV_Ger2017_Vole
CPXV_BeaBer04_1
CPXV_Ger1998_2
AKMV_2013_85
CPXV_Ger2002_MKY
CPXV_No_H1
AKMV_Vani_2010
CPXV_Ger2010_Alpaca
CPXV_HumLan08_1
CPXV_Ger91
CPXV_Ger2017_Vole
CPXV_BeaBer04_1
CPXV_Ger1998_2
AKMV_2013_85
CPXV_Ger2002_MKY
CPXV_No_F2_(reversed) -
Unknown
Unknown
CPXV_Ger1980_EP4
RPXV_Utr
Unknown
CPXV_EleGri07_1
Unknown
CPXV_Ger2017_Vole
CPXV_HumLit08_1
CPXV_Ger2014_Human
Unknown
Unknown
Unknown
CPXV_EleGri07_1
CPXV_Ger2017_Vole
RPXV_Utr
CPXV_HumGra07_1
CPXV_Ger2010_MKY
CPXV_Ger1980_EP4
CPXV_EleGri07_1
CPXV_Ger2010_Racoon
RPXV_Utr
CPXV_HumLit08_1
CPXV_Swe_H2 -
RPXV_Utr
CPXV_EleGri07_1
Unknown
CPXV_Ger2017_Vole
Unknown
Unknown
Unknown
Unknown
CPXV_Ger1980_EP4
Unknown
RPXV_Utr
CPXV_HumLit08_1
CPXV_Swe_H1_(reversed)
RPXV_Utr
CPXV_EleGri07_1
Unknown
CPXV_Ger2017_Vole
Unknown
Unknown
Unknown
CPXV_Ger1980_EP4
Unknown
CPXV_Ger2012_Alpaca
CPXV_HumLit08_1
CPXV_CheNova_DK_2014 -
Unknown
Unknown
Unknown
Unknown
CPXV_Ger2017_Vole
CPXV_HumLit08_1
RPXV_Utr
Unknown
CPXV_Ger2012_Alpaca
CPXV_No_F2_(reversed) -
CPXV_HumLue09_1
Unknown
Unknown
Unknown
Unknown
CPXV_Ger2017_Vole
CPXV_HumLit08_1
RPXV_Utr
CPXV_EleGri07_1
Unknown
CPXV_Ger2012_Alpaca
CPXV_Ger1990_2
Unknown
Unknown
Unknown
CPXV_EleGri07_1
Unknown
CPXV_Ger2017_Vole
CPXV_HumLit08_1
CPXV_RatGer09_1
RPXV_Utr
CPXV_Ger2010_Racoon
CPXV_Ger1980_EP4
Unknown
RPXV_Utr
CPXV_Ger2002_MKY
CPXV_Ger2015_Cat1
Unknown
Unknown
Unknown
CPXV_Ger2015_Human2
Unknown
CPXV_EleGri07_1
CPXV_GerMygEk938_17
CPXV_RatGer09_1
RPXV_Utr
CPXV_Ger1980_EP4
CPXV_Ger2002_MKY
CPXV_Ger2012_Alpaca
CPXV_EleGri07_1
CPXV_Ger2010_Racoon
CPXV_Ger2017_Vole
CPXV_HumLit08_1
CPXV_FraAmiens_2016 -
Unknown
Unknown
Unknown
CPXV_EleGri07_1
Unknown
CPXV_Ger2017_Vole
CPXV_HumLit08_1
CPXV_RatGer09_1
RPXV_Utr
RPXV_Utr
CPXV_Fra2001_Nancy
Unknown
Unknown
Unknown
CPXV_Ger2010_MKY
CPXV_EleGri07_1
Unknown
Unknown
RPXV_Utr
VARV_Garcia_1966
CPXV_Ger2017_Vole
Unknown
CPXV_RatGer09_1
Unknown
CPXV_Ger1980_EP4
RPXV_Utr
CPXV_HumLit08_1
CPXV_Catpox5_wv1 -
Unknown
Unknown
CPXV_Ger2010_Racoon
CPXV_EleGri07_1
Unknown
CPXV_Ger2017_Vole
CPXV_HumLit08_1
CPXV_RatGer09_1
Unknown
RPXV_Utr
CPXV_Br
Unknown
Unknown
Unknown
CPXV_EleGri07_1
Unknown
CPXV_Ger2017_Vole
CPXV_RatGer09_1
RPXV_Utr
CPXV_HumBer07_1
RPXV_Utr
CPXV_HumLit08_1
CMLV_M96
CPXV_Ger2015_Cat1
VACV_Lister
VACV_Cop
CPXV_Ger91
CPXV_NorwayFeline -
CPXV_Ger1998_2
CPXV_Ger2002_MKY
CPXV_Ger2012_Alpaca
AKPV_2015
CPXV_Ger2010_Racoon
Unknown
CPXV_Ger2017_Vole
CPXV_Ger2014_Human
Unknown
Unknown
CPXV_HumLan08_1
Unknown
VACV_Lister
Unknown
CPXV_Fin2000_Man
AKMV_Vani_2010
CMLV_CMS
CPXV_Ger2015_Cat1
VACV_Lister
VACV_Cop
CPXV_Ger91
CPXV_NorwayFeline -
CPXV_Ger1998_2
CPXV_Ger2002_MKY
CPXV_Ger2012_Alpaca
AKPV_2015
CPXV_Ger2010_Racoon
Unknown
CPXV_Ger2017_Vole
CPXV_Ger2014_Human
Unknown
Unknown
CPXV_HumLan08_1
Unknown
VACV_Lister
Unknown
CPXV_Fin2000_Man
AKMV_Vani_2010
OPXV_Abatino
VACV_CVA
VARV_Garcia_1966
Unknown
Unknown
MPXV_ZAR

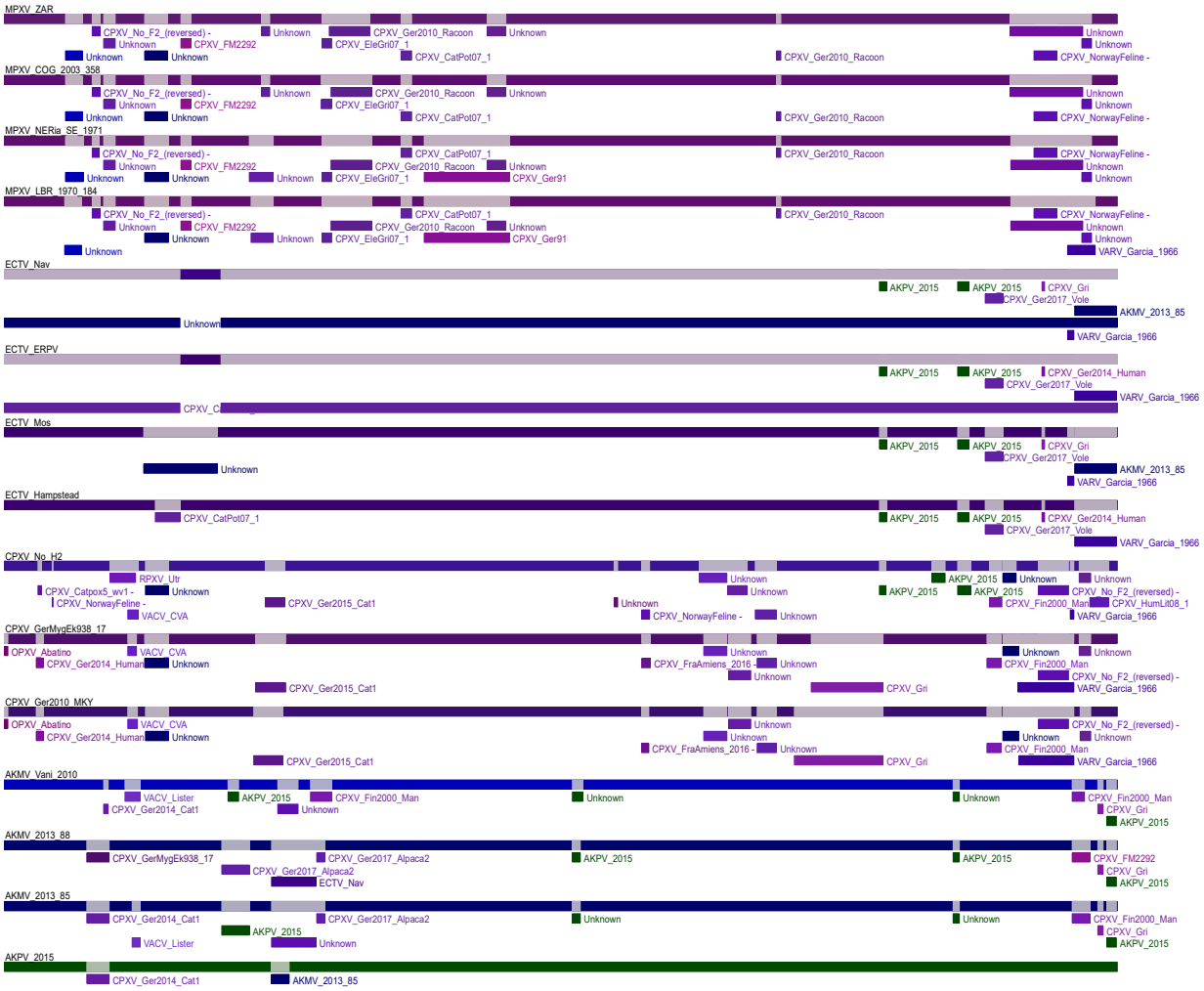

Figure S3. Recombination analysis of 87 orthopoxvirus (OPXV) core genomes with RPD4. Schematic sequence display depicting colour-coded representations of the analyzed sequences and the locations of detected recombination events in the 87 OPXV core genomes. The detected recombination events were detected for at least 5 of 7 methods (RDP, GENECONV, Bootscan, MaxChi, Chimaera, SiScan, and 3Seq) with significant p-values ($p \leq 0.01$).

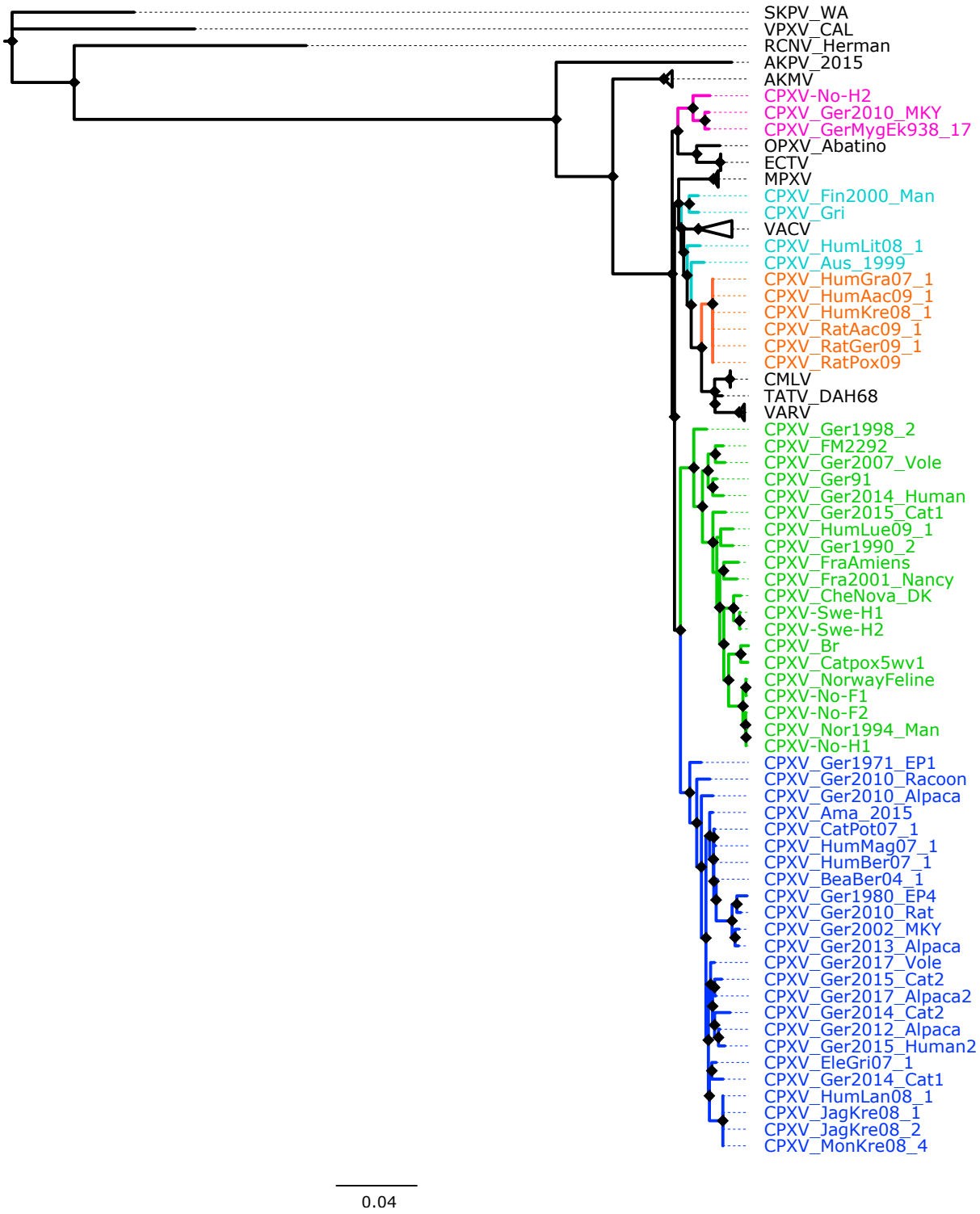

Figure S4. Bayesian inference phylogenetic tree of 62 conserved genes from 87 orthopoxviruses. Diamonds at the nodes indicate posterior probabilities >0.9. The scale bar represents expected substitutions per site. The main five cowpox virus (CPXV) clusters were highlighted in different colors: pink (Ectromelia-Abatino-like CPXV), blue (CPXV-like 1), green (CPXV-like 2), turquoise blue (Vaccinia-like CPXV) and orange (Variola-like CPXV).

Figure S5. Bayesian inference phylogenetic tree of 87 OPXV core genomes. Posterior probabilities are shown on the right side of each node and only posterior probabilities above 0.9. are shown. The scale bar represents expected substitutions per site. The main five cowpox virus (CPXV) clusters were highlighted in different colors: pink (Ectromelia-Abatino-like CPXV), blue (CPXV-like 1), green (CPXV-like 2), turquoise blue (Vaccinia-like CPXV) and orange (Variola-like CPXV).

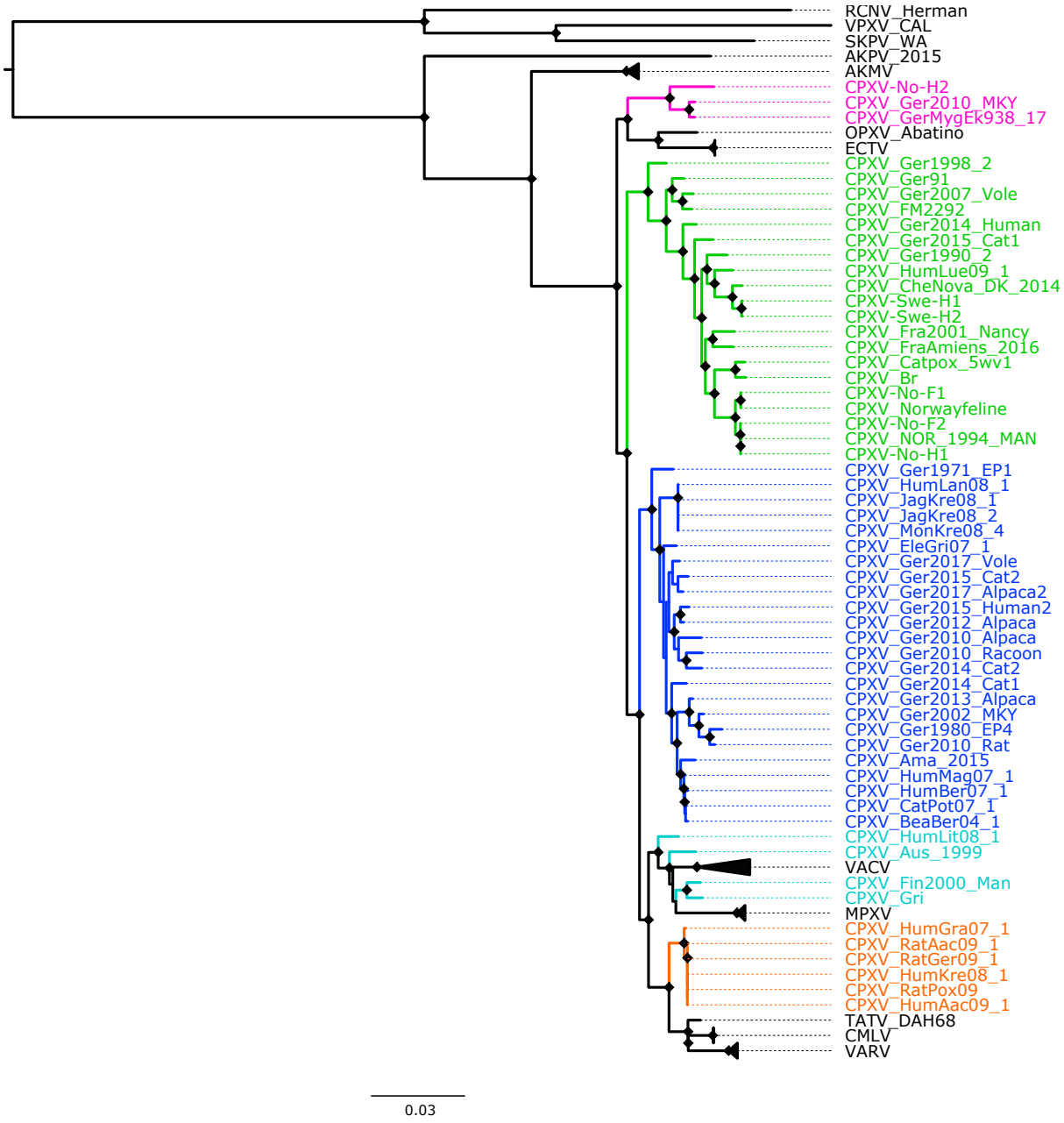

Figure S6. Maximum Likelihood phylogenetic tree of 87 orthopoxvirus whole genomes. Bootstrap values were inferred from 1000 rapid bootstrap replicates. Diamonds at the nodes indicate bootstrap values >80%. The scale bar indicates substitution per site. The main five cowpox virus (CPXV) clusters were highlighted in different colors: pink (Ectromelia-Abatino-like CPXV), blue (CPXV-like 1), green (CPXV-like 2), turquoise blue (Vaccinia-like CPXV) and orange (Variola-like CPXV).

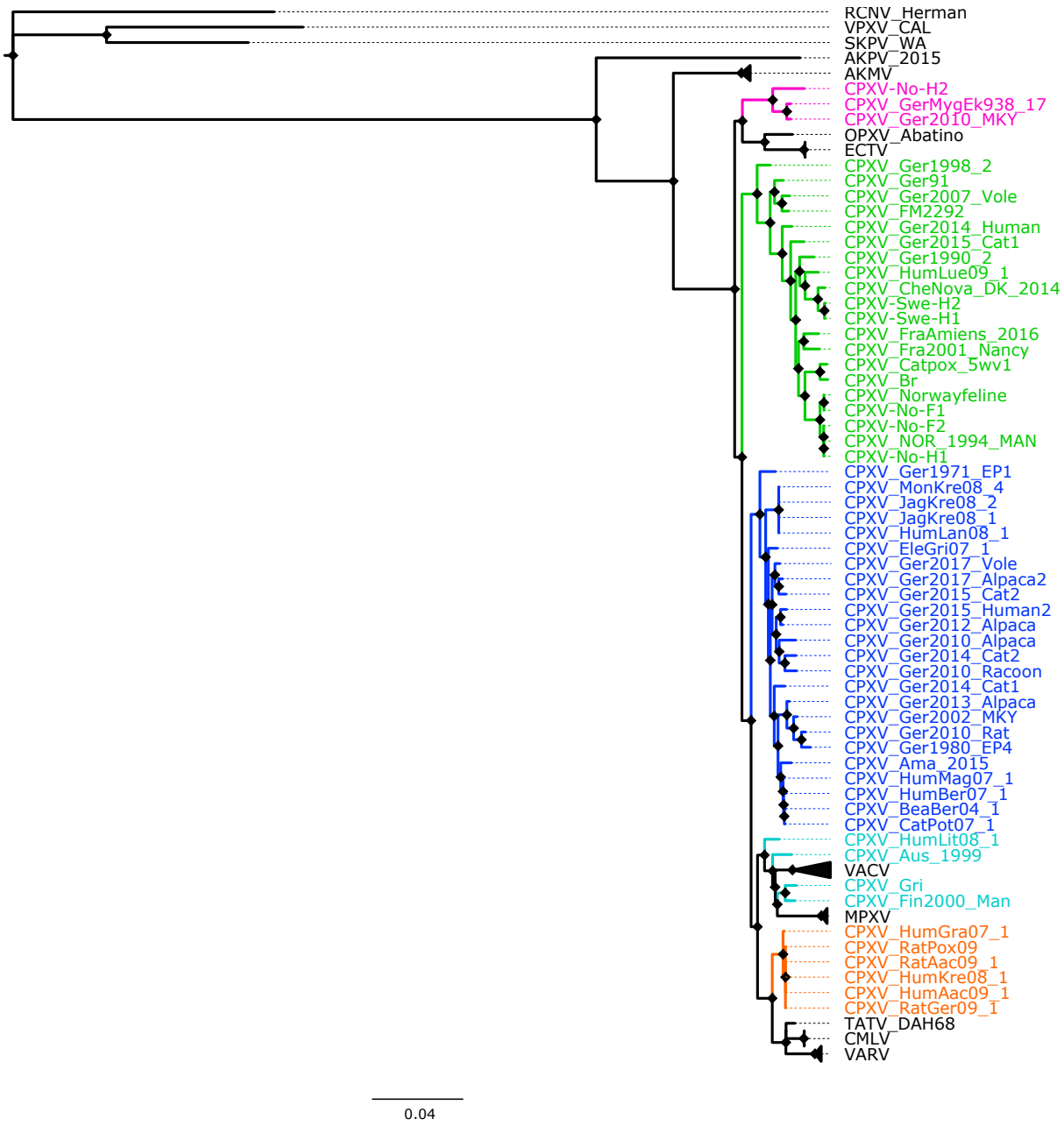

Figure S7. Bayesian inference phylogenetic tree of 87 OPXV whole genomes. Diamonds at the nodes indicate posterior probabilities > 0.9. The scale bar represents expected substitutions per site. The main five cowpox virus (CPXV) clusters were highlighted in different colors: pink (Ectromelia-Abatino-like CPXV), blue (CPXV-like 1), green (CPXV-like 2), turquoise blue (Vaccinia-like CPXV) and orange (Variola-like CPXV).

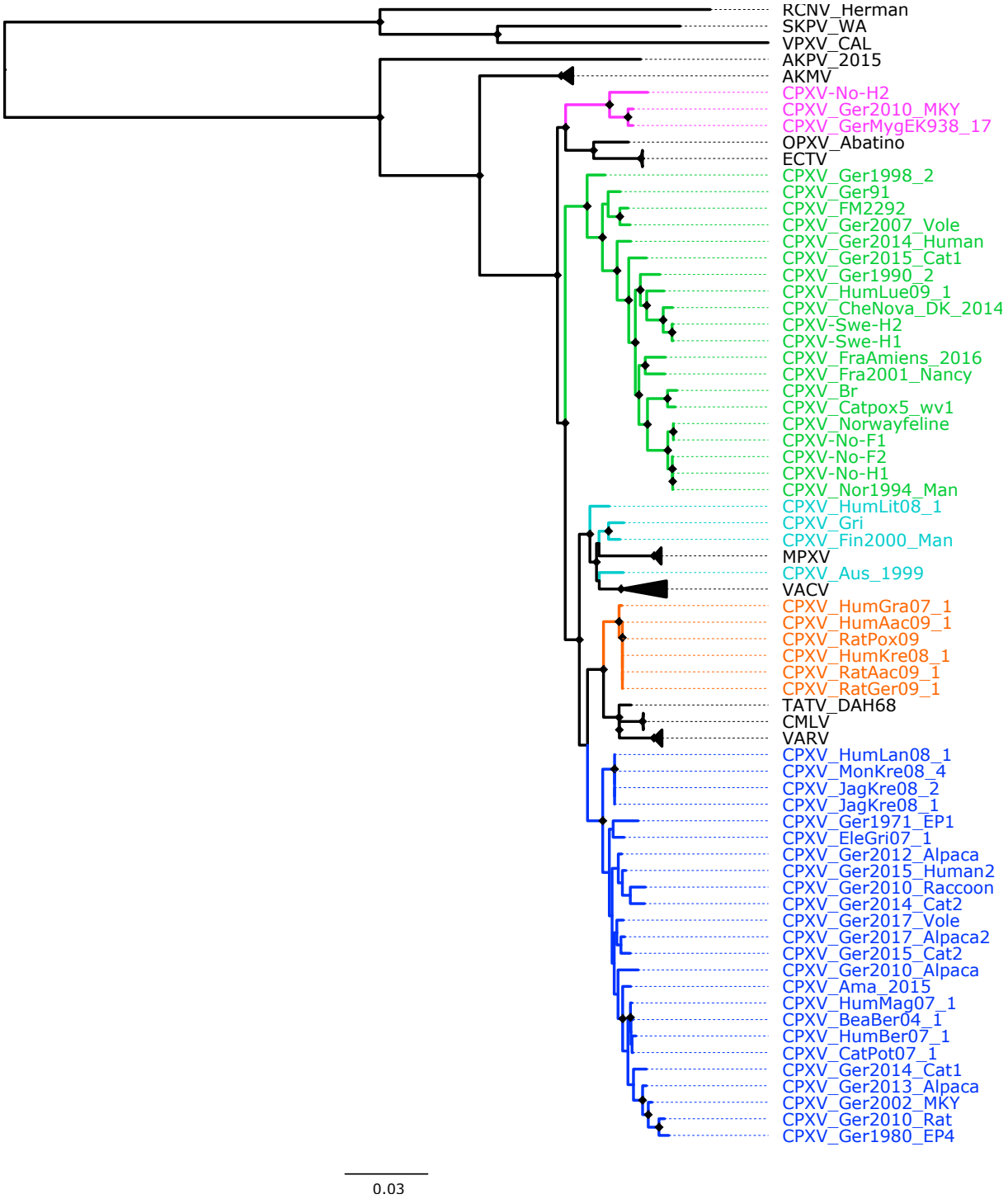

Figure S8. Maximum Likelihood phylogenetic tree based on orthopoxvirus orthologous genes. Bootstrap values were inferred from 1000 rapid bootstrap replicates. Diamonds at the nodes indicate bootstrap values >80%. The scale indicates substitution per site. The main five cowpox virus (CPXV) clusters were highlighted in different colors: pink (Ectromelia-Abatino-like CPXV), blue (CPXV-like 1), green (CPXV-like 2), turquoise blue (Vaccinia-like CPXV) and orange (Variola-like CPXV).

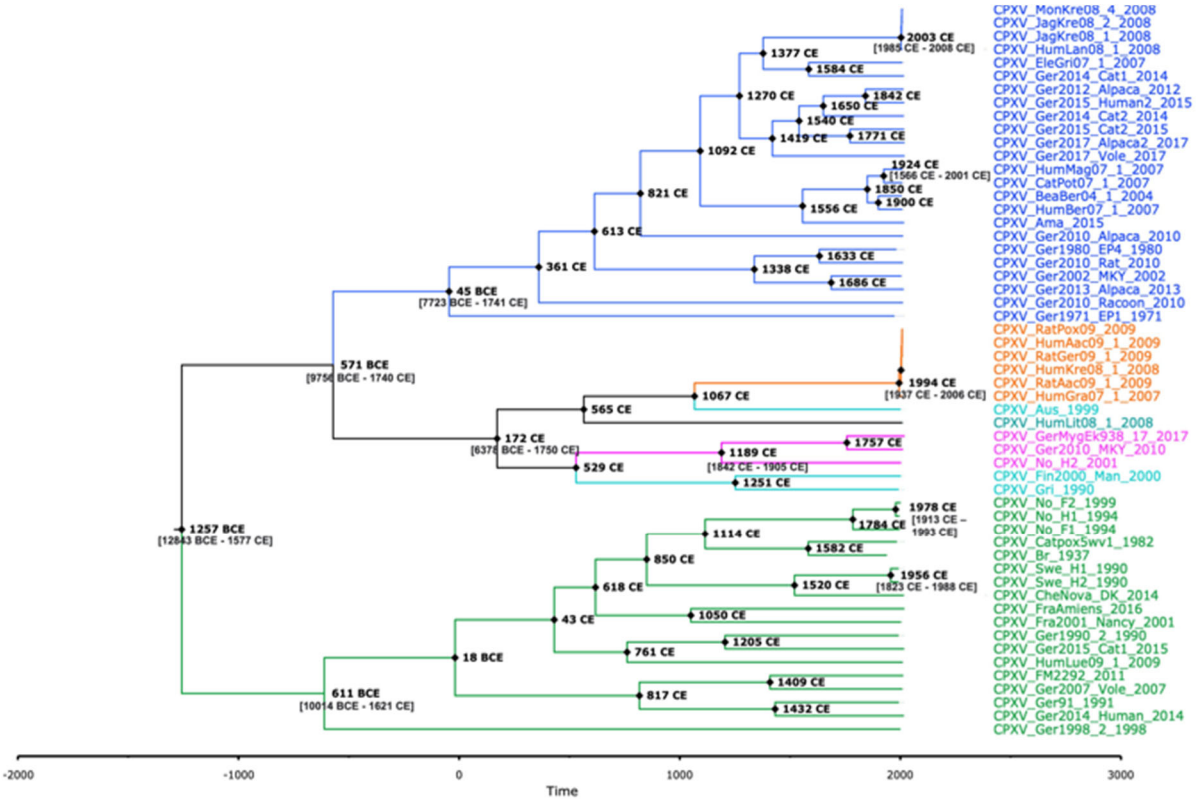

Figure S9. Bayesian maximum clade credibility (MCC) tree of 62 non-recombinant conserved genes of 55 CPXV genomes. The MCC tree was generated using BEAST 1, using a log-normal relaxed clock, coalescent Bayesian skyline population, HKY substitution model and four gamma categories. The numbers on the nodes indicate the time of the most recent common ancestor of the clades. Diamonds at the nodes indicate posterior probability values >0.9. The main five CPXV clusters were highlighted in different colors: pink (Ectromelia-Abatino-like CPXV), blue (CPXV-like 1), green (CPXV-like 2), turquoise blue (Vaccinia-like CPXV) and orange (Variola-like CPXV).

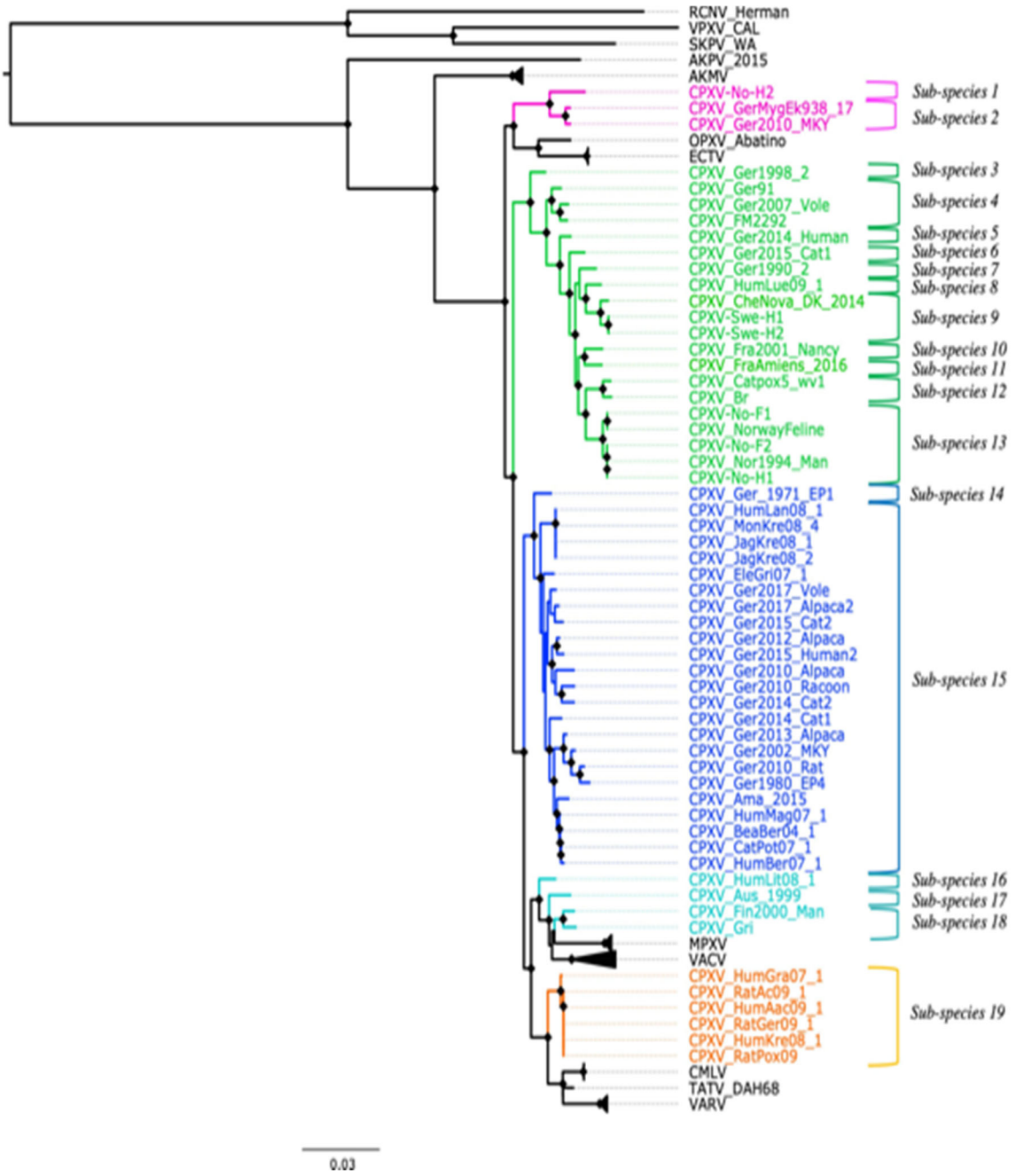

Figure S10. New classification of cowpox virus (CPXV) based on phylogenetic inference (from 87 OPXV whole genomes, core genomes and orthologous genes), patristic and genetic distances. Diamonds at the nodes indicate bootstrap values >80%. The main five CPXV clusters were highlighted in different colors: pink (Ectromelia-Abatino-like CPXV), blue (CPXV-like 1), green (CPXV-like 2), turquoise blue (Vaccinia-like CPXV) and orange (Variola-like CPXV).

Table S1. List of strains used in the phylogenetic analysis

GenBank number accession	Virus species	Strain
MH816996	*Abatino macacapox virus*	-
MH607142	*Akhmeta virus*	2013-85
MH607141	*Akhmeta virus*	2013-88
MH607143	*Akhmeta virus*	Vani_2010
MN240300	*Alaskapox virus*	2015
AY009089	*Camelpox virus*	CMS
NC_003391	*Camelpox virus*	M-96
LN879483	*Cowpox virus*	Amadeus 2015
HQ407377	*Cowpox virus*	Austria 1999
KC813491	*Cowpox virus*	BeaBer04/1
NC_003663	*Cowpox virus*	Brighton Red
KC813506	*Cowpox virus*	CatPot07/1
KY549144	*Cowpox virus*	CatPox5_wv1
KY569019	*Cowpox virus*	CheNova_DK_2014
KC813507	*Cowpox virus*	EleGri07/1
HQ420893	*Cowpox virus*	Finland_2000_MAN
LN864566	*Cowpox virus*	FM2292
HQ420894	*Cowpox virus*	France_2001_Nancy
LT883663	*Cowpox virus*	France Amiens 2016
DQ437593	*Cowpox virus*	Germany 91-3
HQ420895	*Cowpox virus*	Germany_1980_EP4
HQ420896	*Cowpox virus*	Germany_1990_2
HQ420897	*Cowpox virus*	Germany_1998_2
HQ420898	*Cowpox virus*	Germany_2002_MKY
LT896722	*Cowpox virus*	Ger/2007/Vole
LT896718	*Cowpox virus*	Ger/2010/Alpaca
LT896721	*Cowpox virus*	Ger 2010 MKY
LT896730	*Cowpox virus*	Ger/2010/Racoon
LT896728	*Cowpox virus*	Ger/2010/Rat
LT896726	*Cowpox virus*	Ger/2012/Alpaca
LT896719	*Cowpox virus*	Ger/2013/Alpaca
LT896723	*Cowpox virus*	Ger/2014/Cat1
LT896725	*Cowpox virus*	Ger/2014/Cat2
LT993226	*Cowpox virus*	Ger/2014/Human
LT896724	*Cowpox virus*	Ger/2015/Cat1
LT896727	*Cowpox virus*	Ger/2015/Cat2
LT993232	*Cowpox virus*	Ger/2015/Human2
LT896732	*Cowpox virus*	Ger/2017/Alpaca2
LT993228	*Cowpox virus*	Ger/2017/common vole FMEimka
KY463519	*Cowpox virus*	Ger/1971_EP1
LR812035	*Cowpox virus*	GerMygEK 938/17
X94355	*Cowpox virus*	GRI-90
KC813508	*Cowpox virus*	HumAac09/1
KC813509	*Cowpox virus*	HumBer07/1
KC813510	*Cowpox virus*	HumGra07/1
KC813512	*Cowpox virus*	HumKre08/1
KC813492	*Cowpox virus*	HumLan08/1
KC813493	*Cowpox virus*	HumLit08/1
KC813494	*Cowpox virus*	HumLue09/1
KC813495	*Cowpox virus*	HumMag07/1
KC813497	*Cowpox virus*	JagKre08/1
KC813498	*Cowpox virus*	JagKre08/2
KC813500	*Cowpox virus*	MonKre08/4
HQ420899	*Cowpox virus*	Norway_1994_MAN
KY549151	*Cowpox virus*	NorwayFeline
KC813501	*Cowpox virus*	RatAac09/1
KC813503	*Cowpox virus*	RatGer09/1
LN864565	*Cowpox virus*	RatPox09
OP125541	*Cowpox virus*	No-F1
OP125540	*Cowpox virus*	No-F2
OP125539	*Cowpox virus*	No-H1
OM460002	*Cowpox virus*	No-H2
OP125538	*Cowpox virus*	Swe-H1
OP125537	*Cowpox virus*	Swe-H2
KY554976	*Ectromelia virus*	Hampstead
NC_004105	*Ectromelia virus*	Moscow
JQ410350	*Ectromelia virus*	ERPV
KJ563295	*Ectromelia virus*	Naval
DQ011154	*Monkeypox virus*	Congo_2003_358
DQ011156	*Monkeypox virus*	Liberia_1970_184
KJ642617	*Monkeypox virus*	Nigeria-SE-1971
NC_003310	*Monkeypox virus*	Zaire-96-I-16
NC_008291	*Taterapox virus*	Dahomey 1968
AY484669	*Vaccinia virus*	Rabbitpox virus Utrecht
DQ792504	*Vaccinia virus*	MNR-76
M35027	*Vaccinia virus*	Copenhagen
AM501482	*Vaccinia virus*	chorioallantois vaccinia virus Ankara (CVA)
DQ439815	*Vaccinia virus*	Duke
AY678276	*Vaccinia virus*	Lister
Y16780	*Variola virus*	Garcia-1966
DQ437581	*Variola virus*	Bangladesh 1975 v75-550 Banu
DQ441429	*Variola virus*	Japan 1946 (Yamada MS-2(A) Tokyo)
DQ441437	*Variola virus*	Sierra Leone 1969 (V68-258)
KY358055	*Variola virus*	VD21
NC_031033.1	*Volepox virus*	CA
KP143769	*Raccoonpox virus*	Herman
NC_031038	*Skunkpox virus*	WA

Table S2. List of orthologous genes from 87 orthopoxviruses used in this study

Orthogroup	VACV_Cop	AKMV_2013_85	AKMV_2013_88	AKMV_Vani_2010	AKPV_2015	CMLV_CMS	CMLV_M96	CPXV_AMA_2015	CPXV_AUS_1999	CPXV_BR	CPXV_BeaBer04:1	CPXV_CatPot07:1	CPXV_CatpoxS_wv1	CPXV_ChoNova_DK_2014	CPXV_EleGri07:1	CPXV_FIN_2000_MAN	CPXV_FM2292	CPXV_FRA2001_Nancy	CPXV_FraAmiens2016	CPXV_GER91	CPXV_GER_1980EP4	CPXV_GER_1990_2	CPXV_GER_1998_2	CPXV_GER2002_MKY	CPXV_GRI	CPXV_Ger1971_EP11	CPXV_Ger:2007:Vole	CPXV_Ger:2010:Alpaca	CPXV_Ger:2010:MKY	CPXV_Ger:2010:Raccon	CPXV_Ger:2010:Rat	CPXV_Ger:2012:Alpaca	CPXV_Ger:2013:Alpaca	CPXV_Ger:2014:Cat1	CPXV_Ger:2014:Cat2	CPXV_Ger:2014:Human	CPXV_Ger:2015:Cat1	CPXV_Ger:2015:Cat2	CPXV_Ger:2015:Human2	CPXV_Ger:2017:Alpaca2	CPXV_Ger:2017:Vole	CPXV_GerMygEK_938:17	CPXV_HumAsc09:1	CPXV_HumBer07:1	CPXV_HumGra07:1	CPXV_HumKre08:1	CPXV_HumLan08:1	CPXV_HumLit08:1
OG0000027	VACV-Cop-024;Type	1	1	1	1	1	1	1	1	1	1	1	1	1	1	1	1	1	1	1	1	1	1	1	1	1	1	1	1	1	1	1	1	1	1	1	1	1	1	1	1	1	1	1	1	1
OG0000028	VACV-Cop-025;Bcl-2-like	1	1	1	1	1	1	1	1	1	1	1	1	1	1	1	1	1	1	1	1	1	1	1	1	1	1	1	1	1	1	1	1	1	1	1	1	1	1	1	1	1	1	1	1	1
OG0000029	VACV-Cop-032;Anti-apoptotic	1	1	1	1	1	1	1	1	1	1	1	1	1	1	1	1	1	1	1	1	1	1	1	1	1	1	1	1	1	1	1	1	1	1	1	1	1	1	1	1	1	1	1	1	1
OG0000030	VACV-Cop-034;ANK-containing	1	1	1	1	1	1	1	1	1	1	1	1	1	1	1	1	1	1	1	1	1	1	1	1	1	1	1	1	1	1	1	1	1	1	1	1	1	1	1	1	1	1	1	1	1
OG0000031	VACV-Cop-037;Serpin	1	1	1	1	1	1	1	1	1	1	1	1	1	1	1	1	1	1	1	1	1	1	1	1	1	1	1	1	1	1	1	1	1	1	1	1	1	1	1	1	1	1	1	1	1
OG0000032	VACV-Cop-046;dUTPase	1	1	1	1	1	1	1	1	1	1	1	1	1	1	1	1	1	1	1	1	1	1	1	1	1	1	1	1	1	1	1	1	1	1	1	1	1	1	1	1	1	1	1	1	1
OG0000033	VACV-Cop-047;Kelch-like	1	1	1	1	1	1	1	1	1	1	1	1	1	1	1	1	1	1	1	1	1	1	1	1	1	1	1	1	1	1	1	1	1	1	1	1	1	1	1	1	1	1	1	1	1
OG0000034	VACV-Cop-053;Hypothetical	1	1	1	1	1	1	1	1	1	1	1	1	1	1	1	1	1	1	1	1	1	1	1	1	1	1	1	1	1	1	1	1	1	1	1	1	1	1	1	1	1	1	1	1	1
OG0000035	VACV-Cop-054;Hypothetical	1	1	1	1	1	1	1	1	1	1	1	1	1	1	1	1	1	1	1	1	1	1	1	1	1	1	1	1	1	1	1	1	1	1	1	1	1	1	1	1	1	1	1	1	1
OG0000036	VACV-Cop-056;S-S	1	1	1	1	1	1	1	1	1	1	1	1	1	1	1	1	1	1	1	1	1	1	1	1	1	1	1	1	1	1	1	1	1	1	1	1	1	1	1	1	1	1	1	1	1
OG0000037	VACV-Cop-057;Essential	1	1	1	1	1	1	1	1	1	1	1	1	1	1	1	1	1	1	1	1	1	1	1	1	1	1	1	1	1	1	1	1	1	1	1	1	1	1	1	1	1	1	1	1	1
OG0000038	VACV-Cop-059;RhoA	1	1	1	1	1	1	1	1	1	1	1	1	1	1	1	1	1	1	1	1	1	1	1	1	1	1	1	1	1	1	1	1	1	1	1	1	1	1	1	1	1	1	1	1	1
OG0000039	VACV-Cop-060;EEV	1	1	1	1	1	1	1	1	1	1	1	1	1	1	1	1	1	1	1	1	1	1	1	1	1	1	1	1	1	1	1	1	1	1	1	1	1	1	1	1	1	1	1	1	1
OG0000040	VACV-Cop-062;Palmitylated	1	1	1	1	1	1	1	1	1	1	1	1	1	1	1	1	1	1	1	1	1	1	1	1	1	1	1	1	1	1	1	1	1	1	1	1	1	1	1	1	1	1	1	1	1
OG0000041	VACV-Cop-063;Unknown	1	1	1	1	1	1	1	1	1	1	1	1	1	1	1	1	1	1	1	1	1	1	1	1	1	1	1	1	1	1	1	1	1	1	1	1	1	1	1	1	1	1	1	1	1
OG0000042	VACV-Cop-066;Unknown	1	1	1	1	1	1	1	1	1	1	1	1	1	1	1	1	1	1	1	1	1	1	1	1	1	1	1	1	1	1	1	1	1	1	1	1	1	1	1	1	1	1	1	1	1
OG0000043	VACV-Cop-068;DNA-binding	1	1	1	1	1	1	1	1	1	1	1	1	1	1	1	1	1	1	1	1	1	1	1	1	1	1	1	1	1	1	1	1	1	1	1	1	1	1	1	1	1	1	1	1	1
OG0000044	VACV-Cop-070;Poly	1	1	1	1	1	1	1	1	1	1	1	1	1	1	1	1	1	1	1	1	1	1	1	1	1	1	1	1	1	1	1	1	1	1	1	1	1	1	1	1	1	1	1	1	1
OG0000045	VACV-Cop-071;IEV	1	1	1	1	1	1	1	1	1	1	1	1	1	1	1	1	1	1	1	1	1	1	1	1	1	1	1	1	1	1	1	1	1	1	1	1	1	1	1	1	1	1	1	1	1
OG0000046	VACV-Cop-073;RNA	1	1	1	1	1	1	1	1	1	1	1	1	1	1	1	1	1	1	1	1	1	1	1	1	1	1	1	1	1	1	1	1	1	1	1	1	1	1	1	1	1	1	1	1	1
OG0000047	VACV-Cop-076;Virion	1	1	1	1	1	1	1	1	1	1	1	1	1	1	1	1	1	1	1	1	1	1	1	1	1	1	1	1	1	1	1	1	1	1	1	1	1	1	1	1	1	1	1	1	1
OG0000048	VACV-Cop-079;ER-localized	1	1	1	1	1	1	1	1	1	1	1	1	1	1	1	1	1	1	1	1	1	1	1	1	1	1	1	1	1	1	1	1	1	1	1	1	1	1	1	1	1	1	1	1	1
OG0000049	VACV-Cop-081;DNA	1	1	1	1	1	1	1	1	1	1	1	1	1	1	1	1	1	1	1	1	1	1	1	1	1	1	1	1	1	1	1	1	1	1	1	1	1	1	1	1	1	1	1	1	1
OG0000050	VACV-Cop-083;Sulfhydryl	1	1	1	1	1	1	1	1	1	1	1	1	1	1	1	1	1	1	1	1	1	1	1	1	1	1	1	1	1	1	1	1	1	1	1	1	1	1	1	1	1	1	1	1	1
OG0000051	VACV-Cop-087;Glutaredoxin	1	1	1	1	1	1	1	1	1	1	1	1	1	1	1	1	1	1	1	1	1	1	1	1	1	1	1	1	1	1	1	1	1	1	1	1	1	1	1	1	1	1	1	1	1
OG0000052	VACV-Cop-088;DNA-binding	1	1	1	1	1	1	1	1	1	1	1	1	1	1	1	1	1	1	1	1	1	1	1	1	1	1	1	1	1	1	1	1	1	1	1	1	1	1	1	1	1	1	1	1	1
OG0000053	VACV-Cop-089;IMV	1	1	1	1	1	1	1	1	1	1	1	1	1	1	1	1	1	1	1	1	1	1	1	1	1	1	1	1	1	1	1	1	1	1	1	1	1	1	1	1	1	1	1	1	1
OG0000054	VACV-Cop-090;ssDNA-binding	1	1	1	1	1	1	1	1	1	1	1	1	1	1	1	1	1	1	1	1	1	1	1	1	1	1	1	1	1	1	1	1	1	1	1	1	1	1	1	1	1	1	1	1	1
OG0000055	VACV-Cop-091;Ribonucleotide	1	1	1	1	1	1	1	1	1	1	1	1	1	1	1	1	1	1	1	1	1	1	1	1	1	1	1	1	1	1	1	1	1	1	1	1	1	1	1	1	1	1	1	1	1
OG0000056	VACV-Cop-093;IMV	1	1	1	1	1	1	1	1	1	1	1	1	1	1	1	1	1	1	1	1	1	1	1	1	1	1	1	1	1	1	1	1	1	1	1	1	1	1	1	1	1	1	1	1	1
OG0000057	VACV-Cop-094;Telomere-binding	1	1	1	1	1	1	1	1	1	1	1	1	1	1	1	1	1	1	1	1	1	1	1	1	1	1	1	1	1	1	1	1	1	1	1	1	1	1	1	1	1	1	1	1	1
OG0000058	VACV-Cop-095;Virion	1	1	1	1	1	1	1	1	1	1	1	1	1	1	1	1	1	1	1	1	1	1	1	1	1	1	1	1	1	1	1	1	1	1	1	1	1	1	1	1	1	1	1	1	1
OG0000059	VACV-Cop-096;RNA	1	1	1	1	1	1	1	1	1	1	1	1	1	1	1	1	1	1	1	1	1	1	1	1	1	1	1	1	1	1	1	1	1	1	1	1	1	1	1	1	1	1	1	1	1
OG0000060	VACV-Cop-097;Metalloprotease	1	1	1	1	1	1	1	1	1	1	1	1	1	1	1	1	1	1	1	1	1	1	1	1	1	1	1	1	1	1	1	1	1	1	1	1	1	1	1	1	1	1	1	1	1
OG0000061	VACV-Cop-099;VLTF	1	1	1	1	1	1	1	1	1	1	1	1	1	1	1	1	1	1	1	1	1	1	1	1	1	1	1	1	1	1	1	1	1	1	1	1	1	1	1	1	1	1	1	1	1
OG0000062	VACV-Cop-100;Glutaredoxin-like	1	1	1	1	1	1	1	1	1	1	1	1	1	1	1	1	1	1	1	1	1	1	1	1	1	1	1	1	1	1	1	1	1	1	1	1	1	1	1	1	1	1	1	1	1
OG0000063	VACV-Cop-101;FEN1-like	1	1	1	1	1	1	1	1	1	1	1	1	1	1	1	1	1	1	1	1	1	1	1	1	1	1	1	1	1	1	1	1	1	1	1	1	1	1	1	1	1	1	1	1	1
OG0000064	VACV-Cop-102;RNA	1	1	1	1	1	1	1	1	1	1	1	1	1	1	1	1	1	1	1	1	1	1	1	1	1	1	1	1	1	1	1	1	1	1	1	1	1	1	1	1	1	1	1	1	1
OG0000065	VACV-Cop-104;Virion	1	1	1	1	1	1	1	1	1	1	1	1	1	1	1	1	1	1	1	1	1	1	1	1	1	1	1	1	1	1	1	1	1	1	1	1	1	1	1	1	1	1	1	1	1
OG0000066	VACV-Cop-107;VLTF-1	1	1	1	1	1	1	1	1	1	1	1	1	1	1	1	1	1	1	1	1	1	1	1	1	1	1	1	1	1	1	1	1	1	1	1	1	1	1	1	1	1	1	1	1	1
OG0000067	VACV-Cop-108;Entry/fusion	1	1	1	1	1	1	1	1	1	1	1	1	1	1	1	1	1	1	1	1	1	1	1	1	1	1	1	1	1	1	1	1	1	1	1	1	1	1	1	1	1	1	1	1	1
OG0000068	VACV-Cop-109;IMV	1	1	1	1	1	1	1	1	1	1	1	1	1	1	1	1	1	1	1	1	1	1	1	1	1	1	1	1	1	1	1	1	1	1	1	1	1	1	1	1	1	1	1	1	1
OG0000069	VACV-Cop-110;Viral	1	1	1	1	1	1	1	1	1	1	1	1	1	1	1	1	1	1	1	1	1	1	1	1	1	1	1	1	1	1	1	1	1	1	1	1	1	1	1	1	1	1	1	1	1
OG0000070	VACV-Cop-112;ss/dsDNA	1	1	1	1	1	1	1	1	1	1	1	1	1	1	1	1	1	1	1	1	1	1	1	1	1	1	1	1	1	1	1	1	1	1	1	1	1	1	1	1	1	1	1	1	1
OG0000071	VACV-Cop-113;Entry	1	1	1	1	1	1	1	1	1	1	1	1	1	1	1	1	1	1	1	1	1	1	1	1	1	1	1	1	1	1	1	1	1	1	1	1	1	1	1	1	1	1	1	1	1
OG0000072	VACV-Cop-115;Thymidine	1	1	1	1	1	1	1	1	1	1	1	1	1	1	1	1	1	1	1	1	1	1	1	1	1	1	1	1	1	1	1	1	1	1	1	1	1	1	1	1	1	1	1	1	1
OG0000073	VACV-Cop-116;Poly	1	1	1	1	1	1	1	1	1	1	1	1	1	1	1	1	1	1	1	1	1	1	1	1	1	1	1	1	1	1	1	1	1	1	1	1	1	1	1	1	1	1	1	1	1
OG0000074	VACV-Cop-118;IMV	1	1	1	1	1	1	1	1	1	1	1	1	1	1	1	1	1	1	1	1	1	1	1	1	1	1	1	1	1	1	1	1	1	1	1	1	1	1	1	1	1	1	1	1	1
OG0000075	VACV-Cop-121;Tyr/Ser	1	1	1	1	1	1	1	1	1	1	1	1	1	1	1	1	1	1	1	1	1	1	1	1	1	1	1	1	1	1	1	1	1	1	1	1	1	1	1	1	1	1	1	1	1
OG0000076	VACV-Cop-122;IMV	1	1	1	1	1	1	1	1	1	1	1	1	1	1	1	1	1	1	1	1	1	1	1	1	1	1	1	1	1	1	1	1	1	1	1	1	1	1	1	1	1	1	1	1	1
OG0000077	VACV-Cop-123;IMV	1	1	1	1	1	1	1	1	1	1	1	1	1	1	1	1	1	1	1	1	1	1	1	1	1	1	1	1	1	1	1	1	1	1	1	1	1	1	1	1	1	1	1	1	1
OG0000078	VACV-Cop-126;DNA	1	1	1	1	1	1	1	1	1	1	1	1	1	1	1	1	1	1	1	1	1	1	1	1	1	1	1	1	1	1	1	1	1	1	1	1	1	1	1	1	1	1	1	1	1
OG0000079	VACV-Cop-127;Viral	1	1	1	1	1	1	1	1	1	1	1	1	1	1	1	1	1	1	1	1	1	1	1	1	1	1	1	1	1	1	1	1	1	1	1	1	1	1	1	1	1	1	1	1	1
OG0000080	VACV-Cop-128;mRNA	1	1	1	1	1	1	1	1	1	1	1	1	1	1	1	1	1	1	1	1	1	1	1	1	1	1	1	1	1	1	1	1	1	1	1	1	1	1	1	1	1	1	1	1	1
OG0000081	VACV-Cop-130;Virion	1	1	1	1	1	1	1	1	1	1	1	1	1	1	1	1	1	1	1	1	1	1	1	1	1	1	1	1	1	1	1	1	1	1	1	1	1	1	1	1	1	1	1	1	1
OG0000082	VACV-Cop-132;Virion	1	1	1	1	1	1	1	1	1	1	1	1	1	1	1	1	1	1	1	1	1	1	1	1	1	1	1	1	1	1	1	1	1	1	1	1	1	1	1	1	1	1	1	1	1
OG0000083	VACV-Cop-135;NTPase_	1	1	1	1	1	1	1	1	1	1	1	1	1	1	1	1	1	1	1	1	1	1	1	1	1	1	1	1	1	1	1	1	1	1	1	1	1	1	1	1	1	1	1	1	1
OG0000084	VACV-Cop-139;RNA	1	1	1	1	1	1	1	1	1	1	1	1	1	1	1	1	1	1	1	1	1	1	1	1	1	1	1	1	1	1	1	1	1	1	1	1	1	1	1	1	1	1	1	1	1
OG0000085	VACV-Cop-140;Carbonic	1	1	1	1	1	1	1	1	1	1	1	1	1	1	1	1	1	1	1	1	1	1	1	1	1	1	1	1	1	1	1	1	1	1	1	1	1	1	1	1	1	1	1	1	1
OG0000086	VACV-Cop-141;mRNA	1	1	1	1	1	1	1	1	1	1	1	1	1	1	1	1	1	1	1	1	1	1	1	1	1	1	1	1	1	1	1	1	1	1	1	1	1	1	1	1	1	1	1	1	1
OG0000087	VACV-Cop-142;mRNA	1	1	1	1	1	1	1	1	1	1	1	1	1	1	1	1	1	1	1	1	1	1	1	1	1	1	1	1	1	1	1	1	1	1	1	1	1	1	1	1	1	1	1	1	1
OG0000088	VACV-Cop-143;ATPase_	1	1	1	1	1	1	1	1	1	1	1	1	1	1	1	1	1	1	1	1	1	1	1	1	1	1	1	1	1	1	1	1	1	1	1	1	1	1	1	1	1	1	1	1	1
OG0000089	VACV-Cop-146;mRNA	1	1	1	1	1	1	1	1	1	1	1	1	1	1	1	1	1	1	1	1	1	1	1	1	1	1	1	1	1	1	1	1	1	1	1	1	1	1	1	1	1	1	1	1	1
OG0000090	VACV-Cop-147;Trimeric	1	1	1	1	1	1	1	1	1	1	1	1	1	1	1	1	1	1	1	1	1	1	1	1	1	1	1	1	1	1	1	1	1	1	1	1	1	1	1	1	1	1	1	1	1
OG0000091	VACV-Cop-149;VLTF-2	1	1	1	1	1	1	1	1	1	1	1	1	1	1	1	1	1	1	1	1	1	1	1	1	1	1	1	1	1	1	1	1	1	1	1	1	1	1	1	1	1	1	1	1	1
OG0000092	VACV-Cop-150;VLTF-3	1	1	1	1	1	1	1	1	1	1	1	1	1	1	1	1	1	1	1	1	1	1	1	1	1	1	1	1	1	1	1	1	1	1	1	1	1	1	1	1	1	1	1	1	1

Orthogroup	VACV_Cop	AKMV_2013_85	AKMV_2013_88	AKMV_Vani_2010	AKPV_2015	CMLV_CMS	CMLV_M96	CPXV_AMA_2015	CPXV_AUS_1999	CPXV_BR	CPXV_BeaBer04:1	CPXV_CatPot07:1	CPXV_CatpoxS_wv1	CPXV_ChoNova_DK_2014	CPXV_EleGri07:1	CPXV_FIN_2000_MAN	CPXV_FM2292	CPXV_FRA2001_Nancy	CPXV_FraAmiens2016	CPXV_GER91	CPXV_GER_1980EP4	CPXV_GER_1990_2	CPXV_GER_1998_2	CPXV_GER2002_MKY	CPXV_GRI	CPXV_Ger1971_EP11	CPXV_Ger:2007:Vole	CPXV_Ger:2010:Alpaca	CPXV_Ger:2010:MKY	CPXV_Ger:2010:Raccon	CPXV_Ger:2010:Rat	CPXV_Ger:2012:Alpaca	CPXV_Ger:2013:Alpaca	CPXV_Ger:2014:Cat1	CPXV_Ger:2014:Cat2	CPXV_Ger2014:Human	CPXV_Ger:2015:Cat1	CPXV_Ger:2015:Cat2	CPXV_Ger:2015:Human2	CPXV_Ger:2017:Alpaca2	CPXV_Ger:2017:Vole	CPXV_GerMygEK_938:17	CPXV_HumAac09:1	CPXV_HumBer07:1	CPXV_HumGra07:1	CPXV_HumKre08:1	CPXV_HumLan08:1	CPXV_HumLit08:1
OG0000093	VACV-Cop-152;P4b	1	1	1	1	1	1	1	1	1	1	1	1	1	1	1	1	1	1	1	1	1	1	1	1	1	1	1	1	1	1	1	1	1	1	1	1	1	1	1	1	1	1	1	1	1	1	1
OG0000095	VACV-Cop-156;RNA	1	1	1	1	1	1	1	1	1	1	1	1	1	1	1	1	1	1	1	1	1	1	1	1	1	1	1	1	1	1	1	1	1	1	1	1	1	1	1	1	1	1	1	1	1	1	1
OG0000096	VACV-Cop-157;Viral	1	1	1	1	1	1	1	1	1	1	1	1	1	1	1	1	1	1	1	1	1	1	1	1	1	1	1	1	1	1	1	1	1	1	1	1	1	1	1	1	1	1	1	1	1	1	1
OG0000097	VACV-Cop-158;VETF-L	1	1	1	1	1	1	1	1	1	1	1	1	1	1	1	1	1	1	1	1	1	1	1	1	1	1	1	1	1	1	1	1	1	1	1	1	1	1	1	1	1	1	1	1	1	1	1
OG0000098	VACV-Cop-161;VITF-3	1	1	1	1	1	1	1	1	1	1	1	1	1	1	1	1	1	1	1	1	1	1	1	1	1	1	1	1	1	1	1	1	1	1	1	1	1	1	1	1	1	1	1	1	1	1	1
OG0000099	VACV-Cop-163;P4a	1	1	1	1	1	1	1	1	1	1	1	1	1	1	1	1	1	1	1	1	1	1	1	1	1	1	1	1	1	1	1	1	1	1	1	1	1	1	1	1	1	1	1	1	1	1	1
OG0000100	VACV-Cop-167;Viral	1	1	1	1	1	1	1	1	1	1	1	1	1	1	1	1	1	1	1	1	1	1	1	1	1	1	1	1	1	1	1	1	1	1	1	1	1	1	1	1	1	1	1	1	1	1	1
OG0000101	VACV-Cop-168;Virion	1	1	1	1	1	1	1	1	1	1	1	1	1	1	1	1	1	1	1	1	1	1	1	1	1	1	1	1	1	1	1	1	1	1	1	1	1	1	1	1	1	1	1	1	1	1	1
OG0000102	VACV-Cop-169;IMV	1	1	1	1	1	1	1	1	1	1	1	1	1	1	1	1	1	1	1	1	1	1	1	1	1	1	1	1	1	1	1	1	1	1	1	1	1	1	1	1	1	1	1	1	1	1	1
OG0000103	VACV-Cop-170;Essential	1	1	1	1	1	1	1	1	1	1	1	1	1	1	1	1	1	1	1	1	1	1	1	1	1	1	1	1	1	1	1	1	1	1	1	1	1	1	1	1	1	1	1	1	1	1	1
OG0000104	VACV-Cop-172;Core	1	1	1	1	1	1	1	1	1	1	1	1	1	1	1	1	1	1	1	1	1	1	1	1	1	1	1	1	1	1	1	1	1	1	1	1	1	1	1	1	1	1	1	1	1	1	1
OG0000105	VACV-Cop-173;Myristylated	1	1	1	1	1	1	1	1	1	1	1	1	1	1	1	1	1	1	1	1	1	1	1	1	1	1	1	1	1	1	1	1	1	1	1	1	1	1	1	1	1	1	1	1	1	1	1
OG0000106	VACV-Cop-174;IMV	1	1	1	1	1	1	1	1	1	1	1	1	1	1	1	1	1	1	1	1	1	1	1	1	1	1	1	1	1	1	1	1	1	1	1	1	1	1	1	1	1	1	1	1	1	1	1
OG0000107	VACV-Cop-175;DNA	1	1	1	1	1	1	1	1	1	1	1	1	1	1	1	1	1	1	1	1	1	1	1	1	1	1	1	1	1	1	1	1	1	1	1	1	1	1	1	1	1	1	1	1	1	1	1
OG0000108	VACV-Cop-176;Zinc	1	1	1	1	1	1	1	1	1	1	1	1	1	1	1	1	1	1	1	1	1	1	1	1	1	1	1	1	1	1	1	1	1	1	1	1	1	1	1	1	1	1	1	1	1	1	1
OG0000109	VACV-Cop-177;IMV	1	1	1	1	1	1	1	1	1	1	1	1	1	1	1	1	1	1	1	1	1	1	1	1	1	1	1	1	1	1	1	1	1	1	1	1	1	1	1	1	1	1	1	1	1	1	1
OG0000110	VACV-Cop-178;DNA	1	1	1	1	1	1	1	1	1	1	1	1	1	1	1	1	1	1	1	1	1	1	1	1	1	1	1	1	1	1	1	1	1	1	1	1	1	1	1	1	1	1	1	1	1	1	1
OG0000111	VACV-Cop-181;Holliday	1	1	1	1	1	1	1	1	1	1	1	1	1	1	1	1	1	1	1	1	1	1	1	1	1	1	1	1	1	1	1	1	1	1	1	1	1	1	1	1	1	1	1	1	1	1	1
OG0000112	VACV-Cop-182;VITF-3	1	1	1	1	1	1	1	1	1	1	1	1	1	1	1	1	1	1	1	1	1	1	1	1	1	1	1	1	1	1	1	1	1	1	1	1	1	1	1	1	1	1	1	1	1	1	1
OG0000113	VACV-Cop-183;RNA	1	1	1	1	1	1	1	1	1	1	1	1	1	1	1	1	1	1	1	1	1	1	1	1	1	1	1	1	1	1	1	1	1	1	1	1	1	1	1	1	1	1	1	1	1	1	1
OG0000114	VACV-Cop-187;IMV	1	1	1	1	1	1	1	1	1	1	1	1	1	1	1	1	1	1	1	1	1	1	1	1	1	1	1	1	1	1	1	1	1	1	1	1	1	1	1	1	1	1	1	1	1	1	1
OG0000115	VACV-Cop-188;IMV	1	1	1	1	1	1	1	1	1	1	1	1	1	1	1	1	1	1	1	1	1	1	1	1	1	1	1	1	1	1	1	1	1	1	1	1	1	1	1	1	1	1	1	1	1	1	1
OG0000116	VACV-Cop-189;RNA	1	1	1	1	1	1	1	1	1	1	1	1	1	1	1	1	1	1	1	1	1	1	1	1	1	1	1	1	1	1	1	1	1	1	1	1	1	1	1	1	1	1	1	1	1	1	1
OG0000117	VACV-Cop-197;C-type	1	1	1	1	1	1	1	1	1	1	1	1	1	1	1	1	1	1	1	1	1	1	1	1	1	1	1	1	1	1	1	1	1	1	1	1	1	1	1	1	1	1	1	1	1	1	1
OG0000118	VACV-Cop-200;EV	1	1	1	1	1	1	1	1	1	1	1	1	1	1	1	1	1	1	1	1	1	1	1	1	1	1	1	1	1	1	1	1	1	1	1	1	1	1	1	1	1	1	1	1	1	1	1
OG0000119	VACV-Cop-204;CD47-like_	1	1	1	1	1	1	1	1	1	1	1	1	1	1	1	1	1	1	1	1	1	1	1	1	1	1	1	1	1	1	1	1	1	1	1	1	1	1	1	1	1	1	1	1	1	1	1
OG0000120	VACV-Cop-208;Chemokine	1	1	1	1	1	1	1	1	1	1	1	1	1	1	1	1	1	1	1	1	1	1	1	1	1	1	1	1	1	1	1	1	1	1	1	1	1	1	1	1	1	1	1	1	1	1	1
OG0000121	VACV-Cop-209;Profilin-like	1	1	1	1	1	1	1	1	1	1	1	1	1	1	1	1	1	1	1	1	1	1	1	1	1	1	1	1	1	1	1	1	1	1	1	1	1	1	1	1	1	1	1	1	1	1	1
OG0000122	VACV-Cop-211;3	1	1	1	1	1	1	1	1	1	1	1	1	1	1	1	1	1	1	1	1	1	1	1	1	1	1	1	1	1	1	1	1	1	1	1	1	1	1	1	1	1	1	1	1	1	1	1
OG0000124	VACV-Cop-218;ATP-dependent	1	1	1	1	1	1	1	1	1	1	1	1	1	1	1	1	1	1	1	1	1	1	1	1	1	1	1	1	1	1	1	1	1	1	1	1	1	1	1	1	1	1	1	1	1	1	1
OG0000126	VACV-Cop-230;Ser/Thr	1	1	1	1	1	1	1	1	1	1	1	1	1	1	1	1	1	1	1	1	1	1	1	1	1	1	1	1	1	1	1	1	1	1	1	1	1	1	1	1	1	1	1	1	1	1	1
OG0000127	VACV-Cop-236;Ankyrin	1	1	1	1	1	1	1	1	1	1	1	1	1	1	1	1	1	1	1	1	1	1	1	1	1	1	1	1	1	1	1	1	1	1	1	1	1	1	1	1	1	1	1	1	1	1	1
OG0000128	VACV-Cop-237;EEV	1	1	1	1	1	1	1	1	1	1	1	1	1	1	1	1	1	1	1	1	1	1	1	1	1	1	1	1	1	1	1	1	1	1	1	1	1	1	1	1	1	1	1	1	1	1	1
OG0000130	VACV-Cop-241;Soluble	1	1	1	1	1	1	1	1	1	1	1	1	1	1	1	1	1	1	1	1	1	1	1	1	1	1	1	1	1	1	1	1	1	1	1	1	1	1	1	1	1	1	1	1	1	1	1
OG0000133	VACV-Cop-033;Alpha	1	1	1	1	1	1	1	1	1	1	1	1	1	1	1	1	1	1	1	1	1	1	1	1	1	1	1	1	1	1	1	1	1	1	1	1	1	1	1	1	1	1	1	1	1	1	1
OG0000136	VACV-Cop-049;Ribonucleotide	1	1	1	1	1	1	1	1	1	1	1	0	1	1	1	1	1	1	1	1	1	1	1	1	1	1	1	1	1	1	1	1	1	1	1	1	1	1	1	1	1	1	1	1	1	1	1
OG0000137	VACV-Cop-067;Non-functional	1	1	1	1	1	1	1	1	1	1	1	1	1	1	1	1	1	1	1	1	1	1	1	1	1	1	1	1	1	1	1	1	1	1	1	1	1	1	1	1	1	1	1	1	1	1	1
OG0000138	VACV-Cop-072;dsRNA-binding	1	1	1	1	1	1	1	1	1	1	1	0	1	1	1	1	1	1	1	1	1	1	1	1	1	1	1	1	1	1	1	1	1	1	1	1	1	1	1	1	1	1	1	1	1	1	1
OG0000139	VACV-Cop-084;Virion	1	1	1	1	1	1	1	1	1	1	1	1	1	1	1	1	1	1	1	1	1	1	1	1	1	1	1	1	1	1	1	1	1	1	1	1	1	1	1	1	1	1	1	1	1	1	1
OG0000140	VACV-Cop-098;Entry/fusion	1	1	1	1	1	1	1	1	1	1	1	1	1	1	1	1	1	1	1	1	1	1	1	1	1	1	1	1	1	1	1	1	1	1	1	1	1	1	1	1	1	1	1	1	1	1	1
OG0000141	VACV-Cop-103;NLPc/P60	1	1	1	1	1	1	1	1	1	1	1	1	1	1	1	1	1	1	1	1	1	1	1	1	1	1	1	1	1	1	1	1	1	1	1	1	1	1	1	1	1	1	1	1	1	1	1
OG0000142	VACV-Cop-114;Virion	1	1	1	1	1	1	1	1	1	1	1	1	1	1	1	1	1	1	1	1	1	1	1	1	1	1	1	1	1	1	1	1	1	1	1	1	1	1	1	1	1	1	1	1	1	1	1
OG0000143	VACV-Cop-117;RNA	1	1	1	1	1	1	1	1	1	1	1	1	1	1	1	1	1	1	1	1	1	1	1	1	1	1	1	1	1	1	1	1	1	1	1	1	1	1	1	1	1	1	1	1	1	1	1
OG0000144	VACV-Cop-125;VLTF-4	1	1	1	1	1	1	1	1	1	1	1	1	1	1	1	1	1	1	1	1	1	1	1	1	1	1	1	1	1	1	1	1	1	1	1	1	1	1	1	1	1	1	1	1	1	1	1
OG0000145	VACV-Cop-138;Morphogenesis_	1	1	1	1	1	1	1	1	1	1	1	1	1	1	1	1	1	1	1	1	1	1	1	1	1	1	1	1	1	1	1	1	1	1	1	1	1	1	1	1	1	1	1	1	1	1	1
OG0000146	VACV-Cop-151;S-S	1	1	1	1	1	1	1	1	1	1	1	1	1	1	1	1	1	1	1	1	1	1	1	1	1	1	1	1	1	1	1	1	1	1	1	1	1	1	1	1	1	1	1	1	1	1	1
OG0000147	VACV-Cop-191;IMV	1	1	1	1	1	1	1	1	1	1	1	1	1	1	1	1	1	1	1	1	1	1	1	1	1	1	1	1	1	1	1	1	1	1	1	1	1	1	1	1	1	1	1	1	1	1	1
OG0000148	VACV-Cop-193;Hypothetical	1	1	1	1	1	1	1	1	1	1	1	1	1	1	1	1	1	1	1	1	1	1	1	1	1	1	1	1	1	1	1	1	1	1	1	1	1	1	1	1	1	1	1	1	1	1	1
OG0000149	VACV-Cop-196;EEV	1	1	1	1	1	1	1	1	1	1	1	1	1	1	1	1	1	1	1	1	1	1	1	1	1	1	1	1	1	1	1	1	1	1	1	1	1	1	1	1	1	1	1	1	1	1	1
OG0000150	VACV-Cop-199;MHC	1	1	1	1	1	1	1	1	1	1	1	1	1	1	1	1	1	1	1	1	1	1	1	1	1	1	1	1	1	1	1	1	1	1	1	1	1	1	1	1	1	1	1	1	1	1	1
OG0000151	VACV-Cop-213;IL-1/TLR	1	1	1	1	1	1	1	1	1	1	1	1	1	1	1	1	1	1	1	1	1	1	1	1	1	1	1	1	1	1	1	1	1	1	1	1	1	1	1	1	1	1	1	1	1	1	1
OG0000152	VACV-Cop-227;Hemagglutinin	1	1	1	1	1	1	1	1	1	1	1	1	1	1	1	1	1	1	1	1	1	1	1	1	1	1	1	1	1	1	1	1	1	1	1	1	1	1	1	1	1	1	1	1	1	1	1
OG0000153	VACV-Cop-247;Serpin	1	1	1	1	1	1	1	1	1	1	1	1	1	1	1	1	1	1	1	1	1	1	1	1	0	1	1	1	1	1	1	1	1	1	1	1	1	1	1	1	1	1	1	1	1	1	1
OG0000154	VACV-Cop-248;Hypothetical	1	1	1	1	1	1	1	1	1	1	1	1	1	1	1	1	1	1	1	1	1	1	1	1	0	1	1	1	1	1	1	1	1	1	1	1	1	1	1	1	1	1	1	1	1	1	1
OG0000157	VACV-Cop-074;Virosome	1	1	1	1	1	1	1	1	1	1	1	1	1	1	1	1	1	1	1	1	1	1	1	1	1	1	1	1	1	1	1	1	1	1	1	1	1	1	1	1	1	1	1	1	1	1	1
OG0000158	VACV-Cop-077;Myristylated	1	1	1	1	1	1	1	1	1	1	1	1	1	1	1	1	1	1	1	1	1	1	1	1	1	1	1	1	1	1	1	1	1	1	1	1	1	1	1	1	1	1	1	1	1	1	1
OG0000159	VACV-Cop-133;Uracil-DNA	1	1	1	1	1	1	1	1	1	1	1	0	1	1	1	1	1	1	1	1	1	1	1	1	1	1	1	1	1	1	1	1	1	1	1	1	1	1	1	1	1	1	1	1	1	1	1
OG0000160	VACV-Cop-162;Viral	1	1	1	1	1	1	1	1	1	1	1	0	1	1	1	1	1	1	1	1	1	1	1	1	1	1	1	1	1	1	1	1	1	1	1	1	1	1	1	1	1	1	1	1	1	1	1
OG0000161	VACV-Cop-194;ATPase/DNA	1	1	1	1	1	1	1	1	1	1	1	1	0	1	1	1	1	1	1	1	1	1	1	1	1	1	1	1	1	1	1	1	1	1	1	1	1	1	1	1	1	1	1	1	1	1	1
OG0000162	VACV-Cop-210;Type	1	1	1	1	1	1	1	1	1	1	1	1	1	1	1	1	0	1	1	1	1	1	1	1	1	1	1	1	1	1	1	1	1	1	1	1	1	1	1	1	1	0	1	1	1	1	1
OG0000163	VACV-Cop-212;Inactive	1	1	1	1	1	1	1	1	1	1	1	1	1	1	1	1	1	1	1	1	1	1	1	1	1	1	1	1	1	1	1	1	1	1	1	1	1	1	1	1	1	1	1	1	1	1	1
OG0000164	VACV-Cop-216;Thymidylate	1	1	1	1	1	1	1	1	1	1	1	0	1	1	1	1	1	1	1	1	1	1	1	1	1	1	1	1	1	1	1	1	1	1	1	1	1	1	1	1	1	1	1	1	1	1	1
OG0000166	VACV-Cop-028;Complement	1	1	1	1	1	1	1	1	1	1	1	1	1	1	1	1	1	1	1	1	1	1	1	1	1	1	1	1	1	1	1	1	1	1	1	1	1	1	1	1	1	1	1	1	1	1	1
OG0000167	VACV-Cop-055;Cytoplasmic	1	1	1	1	1	1	1	1	1	1	1	1	1	1	1	1	1	1	1	1	1	1	1	1	1	1	0	1	1	1	1	1	1	1	1	1	1	1	1	1	1	1	0	1	1	1	1
OG0000170	VACV-Cop-035;NFkB	1	1	1	1	1	1	1	1	1	1	1	1	1	1	1	1	1	1	1	1	1	1	1	1	1	1	1	1	1	1	1	1	1	1	1	1	1	1	1	1	1	1	1	1	1	1	1
OG0000171	VACV-Cop-044;Host	1	1	1	1	1	1	1	1	1	1	1	1	1	1	1	1	1	1	1	1	1	1	1	1	1	1	1	1	1	1	1	1	1	1	1	1	1	1	1	1	1	1	1	1	1	1	1
OG0000172	VACV-Cop-052;36kDa	1	1	1	1	1	1	1	1	1	1	1	1	1	1	1	1	1	1	1	1	1	1	1	1	1	1	1	1	1	1	1	1	1	1	1	1	1	1	1	1	1	1	1	1	1	1	1
OG0000174	VACV-Cop-254;IFN-alpha/beta	1	1	1	1	1	1	1	1	1	1	1	1	0	1	1	1	1	1	1	1	1	1	1	1	0	1	1	1	1	1	1	1	1	1	1	1	1	1	1	1	1	1	1	1	1	1	1

Orthogroup	VACV_Cop	CPXV_HumLue09_1	CPXV_HumMag07:1	CPXV_JagKre08:1	CPXV_JagKre08:2	CPXV_MonKre08:4	CPXV_NOR_1994_MAN	CPXV_NoF1	CPXV_NoF2	CPXV_NoH1	CPXV_NorwayFeline	CPXV_RatAac09:1	CPXV_RatGer09:1	CPXV_RatPox09	CPXV_SweH1	CPXV_SweH2	ECTV_ERPV	ECTV_Hamptead	ECTV_Moss	ECTV_Nav	HSPV_MNR76	MPXV_COG_2003_358	MPXV_LBR_1970_184	MPXV_NERia_SE_1971	MPXV_ZAR	No_H2	OPXV_Abatino	RCNV_Herman	RPXV_Utr	SKPV_WA	TATV_DAH68	VACV_CVA	VACV_Cop	VACV_DUKE	VACV_Lister	VARV_BGD75_Banu	VARV_GAR_1966	VARV_JPN46_yam	VARV_SLE68	VARV_VD21	VPXV_CAL
OG0000027	VACV-Cop-024;Type	1	1	1	1	1	1	1	1	1	1	1	1	1	1	1	1	1	1	1	1	1	1	1	1	1	1	1	1	1	1	1	1	1	1	1	1	1	1	1
OG0000028	VACV-Cop-025;Bcl-2-like	1	1	1	1	1	1	1	1	1	1	1	1	1	1	1	1	1	1	1	1	1	1	1	1	1	1	1	1	1	1	1	1	1	1	1	1	1	1	1
OG0000029	VACV-Cop-032;Anti-apoptotic	1	1	1	1	1	1	1	1	1	1	1	1	1	1	1	1	1	1	1	1	1	1	1	1	1	1	1	1	1	1	1	1	1	1	1	1	1	1	1
OG0000030	VACV-Cop-034;ANK-containing	1	1	1	1	1	1	1	1	1	1	1	1	1	1	1	1	1	1	1	1	1	1	1	1	1	1	1	1	1	1	1	1	1	1	1	1	1	1	1
OG0000031	VACV-Cop-037;Serpin	1	1	1	1	1	1	1	1	1	1	1	1	1	1	1	1	1	1	1	1	1	1	1	1	1	1	1	1	1	1	1	1	1	1	1	1	1	1	1
OG0000032	VACV-Cop-046;dUTPase	1	1	1	1	1	1	1	1	1	1	1	1	1	1	1	1	1	1	1	1	1	1	1	1	1	1	1	1	1	1	1	1	1	1	1	1	1	1	1
OG0000033	VACV-Cop-047;Kelch-like	1	1	1	1	1	1	1	1	1	1	1	1	1	1	1	1	1	1	1	1	1	1	1	1	1	1	1	1	1	1	1	1	1	1	1	1	1	1	1
OG0000034	VACV-Cop-053;Hypothetical	1	1	1	1	1	1	1	1	1	1	1	1	1	1	1	1	1	1	1	1	1	1	1	1	1	1	1	1	1	1	1	1	1	1	1	1	1	1	1
OG0000035	VACV-Cop-054;Hypothetical	1	1	1	1	1	1	1	1	1	1	1	1	1	1	1	1	1	1	1	1	1	1	1	1	1	1	1	1	1	1	1	1	1	1	1	1	1	1	1
OG0000036	VACV-Cop-056;S-S	1	1	1	1	1	1	1	1	1	1	1	1	1	1	1	1	1	1	1	1	1	1	1	1	1	1	1	1	1	1	1	1	1	1	1	1	1	1	1
OG0000037	VACV-Cop-057;Essential	1	1	1	1	1	1	1	1	1	1	1	1	1	1	1	1	1	1	1	1	1	1	1	1	1	1	1	1	1	1	1	1	1	1	1	1	1	1	1
OG0000038	VACV-Cop-059;RhoA	1	1	1	1	1	1	1	1	1	1	1	1	1	1	1	1	1	1	1	1	1	1	1	1	1	1	1	1	1	1	1	1	1	1	1	1	1	1	1
OG0000039	VACV-Cop-060;EEV	1	1	1	1	1	1	1	1	1	1	1	1	1	1	1	1	1	1	1	1	1	1	1	1	1	1	1	1	1	1	1	1	1	1	1	1	1	1	1
OG0000040	VACV-Cop-062;Palmitylated	1	1	1	1	1	1	1	1	1	1	1	1	1	1	1	1	1	1	1	1	1	1	1	1	1	1	1	1	1	1	1	1	1	1	1	1	1	1	1
OG0000041	VACV-Cop-063;Unknown	1	1	1	1	1	1	1	1	1	1	1	1	1	1	1	1	1	1	1	1	1	1	1	1	1	1	1	1	1	1	1	1	1	1	1	1	1	1	1
OG0000042	VACV-Cop-066;Unknown	1	1	1	1	1	1	1	1	1	1	1	1	1	1	1	1	1	1	1	1	1	1	1	1	1	1	1	1	1	1	1	1	1	1	1	1	1	1	1
OG0000043	VACV-Cop-068;DNA-binding	1	1	1	1	1	1	1	1	1	1	1	1	1	1	1	1	1	1	1	1	1	1	1	1	1	1	1	1	1	1	1	1	1	1	1	1	1	1	1
OG0000044	VACV-Cop-070;Poly	1	1	1	1	1	1	1	1	1	1	1	1	1	1	1	1	1	1	1	1	1	1	1	1	1	1	1	1	1	1	1	1	1	1	1	1	1	1	1
OG0000045	VACV-Cop-071;IEV	1	1	1	1	1	1	1	1	1	1	1	1	1	1	1	1	1	1	1	1	1	1	1	1	1	1	1	1	1	1	1	1	1	1	1	1	1	1	1
OG0000046	VACV-Cop-073;RNA	1	1	1	1	1	1	1	1	1	1	1	1	1	1	1	1	1	1	1	1	1	1	1	1	1	1	1	1	1	1	1	1	1	1	1	1	1	1	1
OG0000047	VACV-Cop-076;Virion	1	1	1	1	1	1	1	1	1	1	1	1	1	1	1	1	1	1	1	1	1	1	1	1	1	1	1	1	1	1	1	1	1	1	1	1	1	1	1
OG0000048	VACV-Cop-079;ER-localized	1	1	1	1	1	1	1	1	1	1	1	1	1	1	1	1	1	1	1	1	1	1	1	1	1	1	1	1	1	1	1	1	1	1	1	1	1	1	1
OG0000049	VACV-Cop-081;DNA	1	1	1	1	1	1	1	1	1	1	1	1	1	1	1	1	1	1	1	1	1	1	1	1	1	1	1	1	1	1	1	1	1	1	1	1	1	1	1
OG0000050	VACV-Cop-083;Sulfhydryl	1	1	1	1	1	1	1	1	1	1	1	1	1	1	1	1	1	1	1	1	1	1	1	1	1	1	1	1	1	1	1	1	1	1	1	1	1	1	1
OG0000051	VACV-Cop-087;Glutaredoxin	1	1	1	1	1	1	1	1	1	1	1	1	1	1	1	1	1	1	1	1	1	1	1	1	1	1	1	1	1	1	1	1	1	1	1	1	1	1	1
OG0000052	VACV-Cop-088;DNA-binding	1	1	1	1	1	1	1	1	1	1	1	1	1	1	1	1	1	1	1	1	1	1	1	1	1	1	1	1	1	1	1	1	1	1	1	1	1	1	1
OG0000053	VACV-Cop-089;IMV	1	1	1	1	1	1	1	1	1	1	1	1	1	1	1	1	1	1	1	1	1	1	1	1	1	1	1	1	1	1	1	1	1	1	1	1	1	1	1
OG0000054	VACV-Cop-090;ssDNA-binding	1	1	1	1	1	1	1	1	1	1	1	1	1	1	1	1	1	1	1	1	1	1	1	1	1	1	1	1	1	1	1	1	1	1	1	1	1	1	1
OG0000055	VACV-Cop-091;Ribonucleotide	1	1	1	1	1	1	1	1	1	1	1	1	1	1	1	1	1	1	1	1	1	1	1	1	1	1	1	1	1	1	1	1	1	1	1	1	1	1	1
OG0000056	VACV-Cop-093;IMV	1	1	1	1	1	1	1	1	1	1	1	1	1	1	1	1	1	1	1	1	1	1	1	1	1	1	1	1	1	1	1	1	1	1	1	1	1	1	1
OG0000057	VACV-Cop-094;Telomere-binding	1	1	1	1	1	1	1	1	1	1	1	1	1	1	1	1	1	1	1	1	1	1	1	1	1	1	1	1	1	1	1	1	1	1	1	1	1	1	1
OG0000058	VACV-Cop-095;Virion	1	1	1	1	1	1	1	1	1	1	1	1	1	1	1	1	1	1	1	1	1	1	1	1	1	1	1	1	1	1	1	1	1	1	1	1	1	1	1
OG0000059	VACV-Cop-096;RNA	1	1	1	1	1	1	1	1	1	1	1	1	1	1	1	1	1	1	1	1	1	1	1	1	1	1	1	1	1	1	1	1	1	1	1	1	1	1	1
OG0000060	VACV-Cop-097;Metalloprotease	1	1	1	1	1	1	1	1	1	1	1	1	1	1	1	1	1	1	1	1	1	1	1	1	1	1	1	1	1	1	1	1	1	1	1	1	1	1	1
OG0000061	VACV-Cop-099;VLTF	1	1	1	1	1	1	1	1	1	1	1	1	1	1	1	1	1	1	1	1	1	1	1	1	1	1	1	1	1	1	1	1	1	1	1	1	1	1	1
OG0000062	VACV-Cop-100;Glutaredoxin-like	1	1	1	1	1	1	1	1	1	1	1	1	1	1	1	1	1	1	1	1	1	1	1	1	1	1	1	1	1	1	1	1	1	1	1	1	1	1	1
OG0000063	VACV-Cop-101;FEN1-like	1	1	1	1	1	1	1	1	1	1	1	1	1	1	1	1	1	1	1	1	1	1	1	1	1	1	1	1	1	1	1	1	1	1	1	1	1	1	1
OG0000064	VACV-Cop-102;RNA	1	1	1	1	1	1	1	1	1	1	1	1	1	1	1	1	1	1	1	1	1	1	1	1	1	1	1	1	1	1	1	1	1	1	1	1	1	1	1
OG0000065	VACV-Cop-104;Virion	1	1	1	1	1	1	1	1	1	1	1	1	1	1	1	1	1	1	1	1	1	1	1	1	1	1	1	1	1	1	1	1	1	1	1	1	1	1	1
OG0000066	VACV-Cop-107;VLTF-1	1	1	1	1	1	1	1	1	1	1	1	1	1	1	1	1	1	1	1	1	1	1	1	1	1	1	1	1	1	1	1	1	1	1	1	1	1	1	1
OG0000067	VACV-Cop-108;Entry/fusion	1	1	1	1	1	1	1	1	1	1	1	1	1	1	1	1	1	1	1	1	1	1	1	1	1	1	1	1	1	1	1	1	1	1	1	1	1	1	1
OG0000068	VACV-Cop-109;IMV	1	1	1	1	1	1	1	1	1	1	1	1	1	1	1	1	1	1	1	1	1	1	1	1	1	1	1	1	1	1	1	1	1	1	1	1	1	1	1
OG0000069	VACV-Cop-110;Viral	1	1	1	1	1	1	1	1	1	1	1	1	1	1	1	1	1	1	1	1	1	1	1	1	1	1	1	1	1	1	1	1	1	1	1	1	1	1	1
OG0000070	VACV-Cop-112;ss/dsDNA	1	1	1	1	1	1	1	1	1	1	1	1	1	1	1	1	1	1	1	1	1	1	1	1	1	1	1	1	1	1	1	1	1	1	1	1	1	1	1
OG0000071	VACV-Cop-113;Entry	1	1	1	1	1	1	1	1	1	1	1	1	1	1	1	1	1	1	1	1	1	1	1	1	1	1	1	1	1	1	1	1	1	1	1	1	1	1	1
OG0000072	VACV-Cop-115;Thymidine	1	1	1	1	1	1	1	1	1	1	1	1	1	1	1	1	1	1	1	1	1	1	1	1	1	1	1	1	1	1	1	1	1	1	1	1	1	1	1
OG0000073	VACV-Cop-116;Poly	1	1	1	1	1	1	1	1	1	1	1	1	1	1	1	1	1	1	1	1	1	1	1	1	1	1	1	1	1	1	1	1	1	1	1	1	1	1	1
OG0000074	VACV-Cop-118;IMV	1	1	1	1	1	1	1	1	1	1	1	1	1	1	1	1	1	1	1	1	1	1	1	1	1	1	1	1	1	1	1	1	1	1	1	1	1	1	1
OG0000075	VACV-Cop-121;Tyr/Ser	1	1	1	1	1	1	1	1	1	1	1	1	1	1	1	1	1	1	1	1	1	1	1	1	1	1	1	1	1	1	1	1	1	1	1	1	1	1	1
OG0000076	VACV-Cop-122;IMV	1	1	1	1	1	1	1	1	1	1	1	1	1	1	1	1	1	1	1	1	1	1	1	1	1	1	1	1	1	1	1	1	1	1	1	1	1	1	1
OG0000077	VACV-Cop-123;IMV	1	1	1	1	1	1	1	1	1	1	1	1	1	1	1	1	1	1	1	1	1	1	1	1	1	1	1	1	1	1	1	1	1	1	1	1	1	1	1
OG0000078	VACV-Cop-126;DNA	1	1	1	1	1	1	1	1	1	1	1	1	1	1	1	1	1	1	1	1	1	1	1	1	1	1	1	1	1	1	1	1	1	1	1	1	1	1	1
OG0000079	VACV-Cop-127;Viral	1	1	1	1	1	1	1	1	1	1	1	1	1	1	1	1	1	1	1	1	1	1	1	1	1	1	1	1	1	1	1	1	1	1	1	1	1	1	1
OG0000080	VACV-Cop-128;mRNA	1	1	1	1	1	1	1	1	1	1	1	1	1	1	1	1	1	1	1	1	1	1	1	1	1	1	1	1	1	1	1	1	1	1	1	1	1	1	1
OG0000081	VACV-Cop-130;Virion	1	1	1	1	1	1	1	1	1	1	1	1	1	1	1	1	1	1	1	1	1	1	1	1	1	1	1	1	1	1	1	1	1	1	1	1	1	1	1
OG0000082	VACV-Cop-132;Virion	1	1	1	1	1	1	1	1	1	1	1	1	1	1	1	1	1	1	1	1	1	1	1	1	1	1	1	1	1	1	1	1	1	1	1	1	1	1	1
OG0000083	VACV-Cop-135;NTPase_	1	1	1	1	1	1	1	1	1	1	1	1	1	1	1	1	1	1	1	1	1	1	1	1	1	1	1	1	1	1	1	1	1	1	1	1	1	1	1
OG0000084	VACV-Cop-139;RNA	1	1	1	1	1	1	1	1	1	1	1	1	1	1	1	1	1	1	1	1	1	1	1	1	1	1	1	1	1	1	1	1	1	1	1	1	1	1	1
OG0000085	VACV-Cop-140;Carbonic	1	1	1	1	1	1	1	1	1	1	1	1	1	1	1	1	1	1	1	1	1	1	1	1	1	1	1	1	1	1	1	1	1	1	1	1	1	1	1
OG0000086	VACV-Cop-141;mRNA	1	1	1	1	1	1	1	1	1	1	1	1	1	1	1	1	1	1	1	1	1	1	1	1	1	1	1	1	1	1	1	1	1	1	1	1	1	1	1
OG0000087	VACV-Cop-142;mRNA	1	1	1	1	1	1	1	1	1	1	1	1	1	1	1	1	1	1	1	1	1	1	1	1	1	1	1	1	1	1	1	1	1	1	1	1	1	1	1
OG0000088	VACV-Cop-143;ATPase_	1	1	1	1	1	1	1	1	1	1	1	1	1	1	1	1	1	1	1	1	1	1	1	1	1	1	1	1	1	1	1	1	1	1	1	1	1	1	1
OG0000089	VACV-Cop-146;mRNA	1	1	1	1	1	1	1	1	1	1	1	1	1	1	1	1	1	1	1	1	1	1	1	1	1	1	1	1	1	1	1	1	1	1	1	1	1	1	1
OG0000090	VACV-Cop-147;Trimeric	1	1	1	1	1	1	1	1	1	1	1	1	1	1	1	1	1	1	1	1	1	1	1	1	1	1	1	1	1	1	1	1	1	1	1	1	1	1	1
OG0000091	VACV-Cop-149;VLTF-2	1	1	1	1	1	1	1	1	1	1	1	1	1	1	1	1	1	1	1	1	1	1	1	1	1	1	1	1	1	1	1	1	1	1	1	1	1	1	1
OG0000092	VACV-Cop-150;VLTF-3	1	1	1	1	1	1	1	1	1	1	1	1	1	1	1	1	1	1	1	1	1	1	1	1	1	1	1	1	1	1	1	1	1	1	1	1	1	1	1

Orthogroup	VACV_Cop	CPXV_HumLue09_1	CPXV_HuMag07:1	CPXV_JagKre08:1	CPXV_JagKre08:2	CPXV_MonKre08:4	CPXV_NOR_1994_MAN	CPXV_NoF1	CPXV_NoF2	CPXV_NoH1	CPXV_NorwayFeline	CPXV_RatAac09:1	CPXV_RatGer09:1	CPXV_RatPox09	CPXV_SweH1	CPXV_SweH2	ECTV_ERPV	ECTV_Hamptead	ECTV_Moss	ECTV_Nav	HSPV_MNR76	MPXV_COG_2003_358	MPXV_LBR_1970_184	MPXV_NERia_SE_1971	MPXV_ZAR	No_H2	OPXV_Abatino	RCNV_Herman	RPXV_Utr	SKPV_WA	TATV_DAH68	VACV_CVA	VACV_Cop	VACV_DUKE	VACV_Lister	VARV_BGD75_Banu	VARV_GAR_1966	VARV_JPN46_yam	VARV_SLE68	VARV_VD21	VPXV_CAL
OG0000093	VACV-Cop-152;P4b	1	1	1	1	1	1	1	1	1	1	1	1	1	1	1	1	1	1	1	1	1	1	1	1	1	1	1	1	1	1	1	1	1	1	1	1	1	1	1
OG0000095	VACV-Cop-156;RNA	1	1	1	1	1	1	1	1	1	1	1	1	1	1	1	1	1	1	1	1	1	1	1	1	1	1	1	1	1	1	1	1	1	1	1	1	1	1	1
OG0000096	VACV-Cop-157;Viral	1	1	1	1	1	1	1	1	1	1	1	1	1	1	1	1	1	1	1	1	1	1	1	1	1	1	1	1	1	1	1	1	1	1	1	1	1	1	1
OG0000097	VACV-Cop-158;VETF-L	1	1	1	1	1	1	1	1	1	1	1	1	1	1	1	1	1	1	1	1	1	1	1	1	1	1	1	1	1	1	1	1	1	1	1	1	1	1	1
OG0000098	VACV-Cop-161;VITF-3	1	1	1	1	1	1	1	1	1	1	1	1	1	1	1	1	1	1	1	1	1	1	1	1	1	1	1	1	1	1	1	1	1	1	1	1	1	1	1
OG0000099	VACV-Cop-163;P4a	1	1	1	1	1	1	1	1	1	1	1	1	1	1	1	1	1	1	1	1	1	1	1	1	1	1	1	1	1	1	1	1	1	1	1	1	1	1	1
OG0000100	VACV-Cop-167;Viral	1	1	1	1	1	1	1	1	1	1	1	1	1	1	1	1	1	1	1	1	1	1	1	1	1	1	1	1	1	1	1	1	1	1	1	1	1	1	1
OG0000101	VACV-Cop-168;Virion	1	1	1	1	1	1	1	1	1	1	1	1	1	1	1	1	1	1	1	1	1	1	1	1	1	1	1	1	1	1	1	1	1	1	1	1	1	1	1
OG0000102	VACV-Cop-169;IMV	1	1	1	1	1	1	1	1	1	1	1	1	1	1	1	1	1	1	1	1	1	1	1	1	1	1	1	1	1	1	1	1	1	1	1	1	1	1	1
OG0000103	VACV-Cop-170;Essential	1	1	1	1	1	1	1	1	1	1	1	1	1	1	1	1	1	1	1	1	1	1	1	1	1	1	1	1	1	1	1	1	1	1	1	1	1	1	1
OG0000104	VACV-Cop-172;Core	1	1	1	1	1	1	1	1	1	1	1	1	1	1	1	1	1	1	1	1	1	1	1	1	1	1	1	1	1	1	1	1	1	1	1	1	1	1	1
OG0000105	VACV-Cop-173;Myristylated	1	1	1	1	1	1	1	1	1	1	1	1	1	1	1	1	1	1	1	1	1	1	1	1	1	1	1	1	1	1	1	1	1	1	1	1	1	1	1
OG0000106	VACV-Cop-174;IMV	1	1	1	1	1	1	1	1	1	1	1	1	1	1	1	1	1	1	1	1	1	1	1	1	1	1	1	1	1	1	1	1	1	1	1	1	1	1	1
OG0000107	VACV-Cop-175;DNA	1	1	1	1	1	1	1	1	1	1	1	1	1	1	1	1	1	1	1	1	1	1	1	1	1	1	1	1	1	1	1	1	1	1	1	1	1	1	1
OG0000108	VACV-Cop-176;Zinc	1	1	1	1	1	1	1	1	1	1	1	1	1	1	1	1	1	1	1	1	1	1	1	1	1	1	1	1	1	1	1	1	1	1	1	1	1	1	1
OG0000109	VACV-Cop-177;IMV	1	1	1	1	1	1	1	1	1	1	1	1	1	1	1	1	1	1	1	1	1	1	1	1	1	1	1	1	1	1	1	1	1	1	1	1	1	1	1
OG0000110	VACV-Cop-178;DNA	1	1	1	1	1	1	1	1	1	1	1	1	1	1	1	1	1	1	1	1	1	1	1	1	1	1	1	1	1	1	1	1	1	1	1	1	1	1	1
OG0000111	VACV-Cop-181;Holliday	1	1	1	1	1	1	1	1	1	1	1	1	1	1	1	1	1	1	1	1	1	1	1	1	1	1	1	1	1	1	1	1	1	1	1	1	1	1	1
OG0000112	VACV-Cop-182;VITF-3	1	1	1	1	1	1	1	1	1	1	1	1	1	1	1	1	1	1	1	1	1	1	1	1	1	1	1	1	1	1	1	1	1	1	1	1	1	1	1
OG0000113	VACV-Cop-183;RNA	1	1	1	1	1	1	1	1	1	1	1	1	1	1	1	1	1	1	1	1	1	1	1	1	1	1	1	1	1	1	1	1	1	1	1	1	1	1	1
OG0000114	VACV-Cop-187;IMV	1	1	1	1	1	1	1	1	1	1	1	1	1	1	1	1	1	1	1	1	1	1	1	1	1	1	1	1	1	1	1	1	1	1	1	1	1	1	1
OG0000115	VACV-Cop-188;IMV	1	1	1	1	1	1	1	1	1	1	1	1	1	1	1	1	1	1	1	1	1	1	1	1	1	1	1	1	1	1	1	1	1	1	1	1	1	1	1
OG0000116	VACV-Cop-189;RNA	1	1	1	1	1	1	1	1	1	1	1	1	1	1	1	1	1	1	1	1	1	1	1	1	1	1	1	1	1	1	1	1	1	1	1	1	1	1	1
OG0000117	VACV-Cop-197;C-type	1	1	1	1	1	1	1	1	1	1	1	1	1	1	1	1	1	1	1	1	1	1	1	1	1	1	1	1	1	1	1	1	1	1	1	1	1	1	1
OG0000118	VACV-Cop-200;IEV	1	1	1	1	1	1	1	1	1	1	1	1	1	1	1	1	1	1	1	1	1	1	1	1	1	1	1	1	1	1	1	1	1	1	1	1	1	1	1
OG0000119	VACV-Cop-204;CD47-like_	1	1	1	1	1	1	1	1	1	1	1	1	1	1	1	1	1	1	1	1	1	1	1	1	1	1	1	1	1	1	1	1	1	1	1	1	1	1	1
OG0000120	VACV-Cop-208;Chemokine	1	1	1	1	1	1	1	1	1	1	1	1	1	1	1	1	1	1	1	1	1	1	1	1	1	1	1	1	1	1	1	1	1	1	1	1	1	1	1
OG0000121	VACV-Cop-209;Profilin-like	1	1	1	1	1	1	1	1	1	1	1	1	1	1	1	1	1	1	1	1	1	1	1	1	1	1	1	1	1	1	1	1	1	1	1	1	1	1	1
OG0000122	VACV-Cop-211;3	1	1	1	1	1	1	1	1	1	1	1	1	1	1	1	1	1	1	1	1	1	1	1	1	1	1	1	1	1	1	1	1	1	1	1	1	1	1	1
OG0000124	VACV-Cop-218;ATP-dependent	1	1	1	1	1	1	1	1	1	1	1	1	1	1	1	1	1	1	1	1	1	1	1	1	1	1	1	1	1	1	1	1	1	1	1	1	1	1	1
OG0000126	VACV-Cop-230;Ser/Thr	1	1	1	1	1	1	1	1	1	1	1	1	1	1	1	1	1	1	1	1	1	1	1	1	1	1	1	1	1	1	1	1	1	1	1	1	1	1	1
OG0000127	VACV-Cop-236;Ankyrin	1	1	1	1	1	1	1	1	1	1	1	1	1	1	1	1	1	1	1	1	1	1	1	1	1	1	1	1	1	1	1	1	1	1	1	1	1	1	1
OG0000128	VACV-Cop-237;EEV	1	1	1	1	1	1	1	1	1	1	1	1	1	1	1	1	1	1	1	1	1	1	1	1	1	1	1	1	1	1	1	1	1	1	1	1	1	1	1
OG0000130	VACV-Cop-241;Soluble	1	1	1	1	1	1	1	1	1	1	1	1	1	1	1	1	1	1	1	1	1	1	1	1	1	1	1	1	1	1	1	1	1	1	1	1	1	1	1
OG0000133	VACV-Cop-033;Alpha	1	1	1	1	1	1	1	1	1	0	1	1	1	1	1	1	1	1	1	1	1	1	1	1	1	1	1	1	1	1	1	1	1	1	1	1	1	1	1
OG0000136	VACV-Cop-049;Ribonucleotide	1	1	1	1	1	1	1	1	1	1	1	1	1	1	1	1	1	1	1	1	1	1	1	1	1	1	1	1	1	1	1	1	1	1	1	1	1	1	1
OG0000137	VACV-Cop-067;Non-functional	1	1	1	1	1	1	1	1	1	0	1	1	1	1	1	1	1	1	1	1	1	1	1	1	1	1	1	1	1	1	1	1	1	1	1	1	1	1	1
OG0000138	VACV-Cop-072;dsRNA-binding	1	1	1	1	1	1	1	1	1	1	1	1	1	1	1	1	1	1	1	1	1	1	1	1	1	1	1	1	1	1	1	1	1	1	1	1	1	1	1
OG0000139	VACV-Cop-084;Virion	1	1	1	1	1	1	1	1	1	1	1	1	1	1	1	1	1	1	1	1	1	1	1	1	1	1	1	1	1	1	1	1	1	1	1	1	1	1	1
OG0000140	VACV-Cop-098;Entry/fusion	1	1	1	1	1	1	1	1	1	1	1	1	1	1	1	1	1	1	1	1	1	1	1	1	1	1	1	0	1	1	1	1	1	1	1	1	1	1	1
OG0000141	VACV-Cop-103;NLPc/P60	1	1	1	1	1	1	1	1	1	0	1	1	1	1	1	1	1	1	1	1	1	1	1	1	1	1	1	1	1	1	1	1	1	1	1	1	1	1	1
OG0000142	VACV-Cop-114;Virion	1	1	1	1	1	1	1	1	1	0	1	1	1	1	1	1	1	1	1	1	1	1	1	1	1	1	1	1	1	1	1	1	1	1	1	1	1	1	1
OG0000143	VACV-Cop-117;RNA	1	1	1	1	1	1	1	1	1	1	1	1	1	1	1	1	1	1	1	1	1	1	1	1	1	1	1	1	0	1	1	1	1	1	1	1	1	1	1
OG0000144	VACV-Cop-125;VLTF-4	1	1	1	1	1	1	1	1	1	0	1	1	1	1	1	1	1	1	1	1	1	1	1	1	1	1	1	1	1	1	1	1	1	1	1	1	1	1	1
OG0000145	VACV-Cop-138;Morphogenesis_	1	1	1	1	1	1	1	1	1	1	1	1	1	1	1	1	1	1	1	1	1	1	1	0	1	1	1	1	1	1	1	1	1	1	1	1	1	1	1
OG0000146	VACV-Cop-151;S-S	1	1	1	1	1	1	1	1	1	0	1	1	1	1	1	1	1	1	1	1	1	1	1	1	1	1	1	1	1	1	1	1	1	1	1	1	1	1	1
OG0000147	VACV-Cop-191;IMV	1	1	1	1	1	1	1	1	1	1	1	1	1	1	1	1	1	1	1	1	1	1	1	1	1	1	1	1	1	1	1	1	1	1	1	1	1	1	1
OG0000148	VACV-Cop-193;Hypothetical	1	1	1	1	1	1	1	1	1	0	1	1	1	1	1	1	1	1	1	1	1	1	1	1	1	1	1	1	1	1	1	1	1	1	1	1	1	1	1
OG0000149	VACV-Cop-196;EEV	1	1	1	1	1	1	1	1	1	0	1	1	1	1	1	1	1	1	1	1	1	1	1	1	1	1	1	1	1	1	1	1	1	1	1	1	1	1	1
OG0000150	VACV-Cop-199;MHC	1	1	1	1	1	1	1	1	1	1	1	1	1	1	1	1	1	1	1	1	1	1	1	1	1	1	1	1	1	1	1	1	1	1	1	1	1	0	1	1
OG0000151	VACV-Cop-213;IL-1/TLR	1	1	1	1	1	1	1	1	1	0	1	1	1	1	1	1	1	1	1	1	1	1	1	1	1	1	1	1	1	1	1	1	1	1	1	1	1	1	1
OG0000152	VACV-Cop-227;Hemagglutinin	1	1	1	1	1	1	1	1	1	0	1	1	1	1	1	1	1	1	1	1	1	1	1	1	1	1	1	1	1	1	1	1	1	1	1	1	1	1	1
OG0000153	VACV-Cop-247;Serpin	1	1	1	1	1	1	1	1	1	1	1	1	1	1	1	1	1	1	1	1	1	1	1	1	1	1	1	1	1	1	1	1	1	1	1	1	1	1	1
OG0000154	VACV-Cop-248;Hypothetical	1	1	1	1	1	1	1	1	1	1	1	1	1	1	1	1	1	1	1	1	1	1	1	1	1	1	1	1	1	1	1	1	1	1	1	1	1	1	1
OG0000157	VACV-Cop-074;Virosome	1	1	1	1	1	1	1	1	1	0	1	1	1	1	1	1	1	1	1	1	1	1	1	1	0	1	1	1	1	1	1	1	1	1	1	1	1	1	1
OG0000158	VACV-Cop-077;Myristylated	1	1	1	1	1	1	1	1	1	0	1	1	1	1	1	1	1	1	1	1	1	1	1	1	1	1	1	1	1	1	1	1	1	1	1	1	0	1	1
OG0000159	VACV-Cop-133;Uracil-DNA	1	1	1	1	1	1	1	1	1	0	1	1	1	1	1	1	1	1	1	1	1	1	1	1	1	1	1	1	1	1	1	1	1	1	1	1	1	1	1
OG0000160	VACV-Cop-162;Viral	1	1	1	1	1	1	1	1	1	0	1	1	1	1	1	1	1	1	1	1	1	1	1	1	1	1	1	1	1	1	1	1	1	1	1	1	1	1	1
OG0000161	VACV-Cop-194;ATPase/DNA	1	1	1	1	1	1	1	1	1	0	1	1	1	1	1	1	1	1	1	1	1	1	1	1	1	1	1	1	1	1	1	1	1	1	1	1	1	1	1
OG0000162	VACV-Cop-210;Type	1	1	1	1	1	1	1	1	1	1	1	1	1	1	1	1	1	1	1	1	1	1	1	1	1	1	1	1	1	1	1	1	1	1	1	1	1	1	1
OG0000163	VACV-Cop-212;Inactive	1	1	1	1	1	1	1	1	1	1	1	1	1	1	1	1	0	1	1	1	1	1	1	1	1	1	1	1	0	1	1	1	1	1	1	1	1	1	1
OG0000164	VACV-Cop-216;Thymidylate	1	1	1	1	1	1	1	1	1	0	1	1	1	1	1	1	1	1	1	1	1	1	1	1	1	1	1	1	1	1	1	1	1	1	1	1	1	1	1
OG0000166	VACV-Cop-028;Complement	1	1	1	1	1	1	1	1	1	0	1	1	1	1	1	1	1	1	1	1	1	0	0	1	1	1	1	1	1	1	1	1	1	1	1	1	1	1	1
OG0000167	VACV-Cop-055;Cytoplasmic	1	1	1	1	0	1	1	1	1	1	1	1	1	1	1	1	1	1	1	1	1	1	1	1	1	1	1	1	1	1	1	1	1	1	1	1	1	1	1
OG0000170	VACV-Cop-035;NFkB	1	1	1	1	1	1	1	1	1	1	1	1	1	1	1	0	0	0	0	1	1	1	1	1	1	1	1	1	1	1	1	1	1	1	1	1	1	1	1
OG0000171	VACV-Cop-044;Host	1	1	1	1	1	1	1	1	1	1	1	1	1	1	1	0	0	0	0	1	1	1	1	1	1	1	1	1	1	1	1	1	1	1	1	1	1	1	1
OG0000172	VACV-Cop-052;36kDa	1	1	1	1	1	1	1	1	1	1	1	1	1	1	1	0	0	0	0	1	1	1	1	1	1	1	1	1	1	1	1	1	1	1	1	1	1	1	1
OG0000174	VACV-Cop-254;IFN-alpha/beta	1	1	1	1	1	1	1	1	1	0	1	1	1	1	1	1	1	1	1	1	1	1	1	1	1	1	1	1	1	1	1	1	1	0	1	1	1	1	1

Table S3. List of 62 conserved genes from 87 orthopoxviruses used in this study

	VACV_Cop
1	A11R
2	A16L
3	A18R
4	A1L
5	A21L
6	A22R
7	A23R
8	A28L
9	A29L
10	A2L
11	A5R
12	A7L
13	D10R
14	D12L
15	D7R
16	E10R
17	E6R
18	F10L
19	F9L
20	G5R
21	G9R
22	H2R
23	H3L
24	H6R
25	J3R
26	J5L
27	L1R
28	L4R
29	L5R
30	A12L
31	A13L
32	A14L
33	A15L
34	A19L
35	A20E
36	A34R
37	A6L
38	A8R
39	D3R
40	D9R
41	E4L
42	E8R
43	F12L
44	F13L
45	F15L
46	F17R
47	G2R
48	G4L
49	G5.5.R
50	G7L
51	G8R
52	H1L
53	H7R
54	I1L
55	I2L
56	I3L
57	I5L
58	I6L
59	A2.5L
60	G6R
61	H5R
62	J1R

Table S4. List of strains used in the evolution molecular analysis.

GenBank number accession	Virus species	Strain	Country	Year
LN879483	*Cowpox virus*	Amadeus 2015	Germany	2015
HQ407377	*Cowpox virus*	Austria 1999	Austria	1999
KC813491	*Cowpox virus*	BeaBer04/1	Germany	2004
NC_003663	*Cowpox virus*	Brighton Red	UK	1937
KC813506	*Cowpox virus*	CatPot07/1	Germany	2007
KY549144	*Cowpox virus*	CatPox5_wv1	UK	1982
KY569019	*Cowpox virus*	CheNova_DK_2014	Denmark	2014
KC813507	*Cowpox virus*	EleGri07/1	Germany	2007
HQ420893	*Cowpox virus*	Finland_2000_MAN	Finland	2000
LN864566	*Cowpox virus*	FM2292	Germany	2011
HQ420894	*Cowpox virus*	France_2001_Nancy	France	2001
LT883663	*Cowpox virus*	France Amiens 2016	France	2016
DQ437593	*Cowpox virus*	Germany 91-3	Germany	1991
HQ420895	*Cowpox virus*	Germany_1980_EP4	Germany	1980
HQ420896	*Cowpox virus*	Germany_1990_2	Germany	1990
HQ420897	*Cowpox virus*	Germany_1998_2	Germany	1998
HQ420898	*Cowpox virus*	Germany_2002_MKY	Germany	2002
LT896722	*Cowpox virus*	Ger/2007/Vole	Germany	2007
LT896718	*Cowpox virus*	Ger/2010/Alpaca	Germany	2010
LT896721	*Cowpox virus*	Ger 2010 MKY	Germany	2010
LT896730	*Cowpox virus*	Ger/2010/Racoon	Germany	2010
LT896728	*Cowpox virus*	Ger/2010/Rat	Germany	2010
LT896726	*Cowpox virus*	Ger/2012/Alpaca	Germany	2012
LT896719	*Cowpox virus*	Ger/2013/Alpaca	Germany	2013
LT896723	*Cowpox virus*	Ger/2014/Cat1	Germany	2014
LT896725	*Cowpox virus*	Ger/2014/Cat2	Germany	2014
LT993226	*Cowpox virus*	Ger/2014/Human	Germany	2014
LT896724	*Cowpox virus*	Ger/2015/Cat1	Germany	2015
LT896727	*Cowpox virus*	Ger/2015/Cat2	Germany	2015
LT993232	*Cowpox virus*	Ger/2015/Human2	Germany	2015
LT896732	*Cowpox virus*	Ger/2017/Alpaca2	Germany	2017
LT993228	*Cowpox virus*	Ger/2017/common vole FMEimka	Germany	2017
KY463519	*Cowpox virus*	Ger/1971_EP1	Germany	1971
LR812035	*Cowpox virus*	GerMygEK 938/17	Germany	2017
X94355	*Cowpox virus*	GRI-90	Russia	1990
KC813508	*Cowpox virus*	HumAac09/1	Germany	2009
KC813509	*Cowpox virus*	HumBer07/1	Germany	2007
KC813510	*Cowpox virus*	HumGra07/1	Germany	2007
KC813512	*Cowpox virus*	HumKre08/1	Germany	2008
KC813492	*Cowpox virus*	HumLan08/1	Germany	2008
KC813493	*Cowpox virus*	HumLit08/1	Lithunia	2008
KC813494	*Cowpox virus*	HumLue09/1	Germany	2009
KC813495	*Cowpox virus*	HumMag07/1	Germany	2007
KC813497	*Cowpox virus*	JagKre08/1	Germany	2008
KC813498	*Cowpox virus*	JagKre08/2	Germany	2008
KC813500	*Cowpox virus*	MonKre08/4	Germany	2008
HQ420899	*Cowpox virus*	Norway_1994_MAN	Norway	1994
KY549151	*Cowpox virus*	NorwayFeline	Norway	1994
KC813501	*Cowpox virus*	RatAac09/1	Germany	2009
KC813503	*Cowpox virus*	RatGer09/1	Germany	2009
LN864565	*Cowpox virus*	RatPox09	Germany	2009
OP125541	*Cowpox virus*	No-F1	Norway	1994
OP125540	*Cowpox virus*	No-F2	Norway	1999
OP125539	*Cowpox virus*	No-H1	Norway	1994
OM460002	*Cowpox virus*	No-H2	Norway	2001
OP125538	*Cowpox virus*	Swe-H1	Sweden	1990
OP125537	*Cowpox virus*	Swe-H2	Sweden	1990

Table S5. Predicted genes in CPXV-No-F1, CPXv-No-F2, CPXV-No-H1, CPXv-Swe-H1 and CPXV-Swe-H2 compared to reference genomes CPXV-Brighton (CPXV_BR)

			CPXV-No-F1						CPXV-No-F2						CPXV-No-H1						CPXV-Swe-H1						CPXV-Swe-H2					
Function	VACV_Cop	CPXV_Br	CDS	Start	Stop	Length	Direction	Similarity (%)	CDS	Start	Stop	Length	Direction	Similarity (%)	CDS	Start	Stop	Length	Direction	Similarity (%)	CDS	Start	Stop	Length	Direction	Similarity (%)	CDS	Start	Stop	Length	Direction	Similarity (%)
CPV-B-002	-	CPXV002	NoF1-001	894	1121	228	(-)	85.135	NoF2-001	1246	1473	228	(-)	85.135	-	-	-	-	-	-	SweH1-001	795	1034	240	(-)	83.333	SweH2-001	768	1001	234	(-)	85.526
Chemokine binding protein (Cop-C23L)	B29R/C23L	vCCI/CPXV003	NoF1-002	1150	1887	738	(-)	91.129	NoF2-002	1502	2239	738	(-)	91.935	NoH1-001	1235	1972	738	(-)	92.339	SweH1-002	1063	1812	750	(-)	91.968	SweH2-002	1030	1779	750	(-)	93.574
CPV-B-004	-	CXPV004	overlap																													
TNF receptor (CrmB) (Cop-C22L)	B28R/C22L	crmB/CPXV005	NoF1-003	1961	3034	1074	(-)	91.808	NoF2-003	2313	3386	1074	(-)	92.09	NoH1-002	2046	3119	1074	(-)	92.09	SweH1-003	1912	2967	1056	(-)	92.537	SweH2-003	1879	2934	1056	(-)	92.537
Ankyrin (Cop-C19L)	B25R/C19L	CPXV006	NoF1-004	3112	4878	1767	(-)	95.748	NoF2-004	3464	5230	1767	(-)	95.748	NoH1-003	3197	4963	1767	(-)	95.748	SweH1-004	3053	4819	1767	(-)	94.898	SweH2-004	3020	4786	1767	(-)	94.898
Ankyrin-like repeat containing protein	-	CPXV007	NoF1-005	4960	5049	90	(-)	100	NoF2-005	5312	5401	90	(-)	93.1	NoH1-004	5045	5134	90	(-)	100	SweH1-005	4844	4975	132	(-)	82.927	SweH2-005	4811	4942	132	(-)	82.927
Ankyrin (Cop-C17L)	B23R/C17L	CPXV008	NoF1-006	5089	7095	2007	(-)	96.731	NoF2-006	5441	7447	2007	(-)	97.177	NoH1-005	5174	7180	2007	(-)	97.028	SweH1-006	5015	7036	2022	(-)	96.154	SweH2-006	4982	7003	2022	(-)	96.006
Hypothetical protein (Cop-C16L)	C16L	CPXV009/CPXV222	NoF1-007	7310	7771	462	(-)	96.732	NoF2-007	7640	8101	462	(-)	96.732	NoH1-006	7350	7811	462	(-)	96.732	SweH1-007	7238	7699	462	(-)	97.386	SweH2-007	7189	7650	462	(-)	97.386
Alpha amanatin target protein (Cop-N2L)	N2L	CPXV010	NoF1-008	7942	8595	654	(-)	95.392	NoF2-008	8271	8924	654	(-)	95.392	NoH1-007	7981	8634	654	(-)	95.392	SweH1-008	7866	8513	648	(-)	95.814	SweH2-008	7818	8465	648	(-)	95.814
BTB Kelch-domain containing protein; CRL complex (Cop-A55R)	-	-	NOF1-009	8908	9501	594	(-)	-	NoF2-009	9327	9920	594	(-)		NoH1-008	8937	9593	657	(-)	-	-	-	-	-	-	-	-	-	-	-	-	-
Ankyrin (Cop-B20R)	B20R	CPXV011	NoF1-010	9828	11843	2016	(-)	95.745	NoF2-010	10247	12268	2022	(-)	96.049	NoH1-009	9920	11935	2016	(-)	95.745	SweH1-009	8962	10926	1965	(-)	95.745	SweH2-009	8913	10877	1965	(-)	95.745
C-type lectin domain containing protein	-	CPXV012	NoF1-011	12070	12279	210	(-)	97.101	NoF2-011	12495	12704	210	(-)	98.551	NoH1-010	12162	12371	210	(-)	98.551	SweH1-010	10958	11440	483	(-)	55.224	SweH2-010	10909	11391	483	(-)	55.224
BTB Kelch-domain containing protein; CRL comple x (Cop-A55R)	A55R	CPXV013	NoF1-012	12707	13318	612	(-)	92.611	NoF2-012	13467	13742	276	(-)	97.619	NoH1-011	13135	13410	276	(-)	97.62	SweH1-011	11505	13082	1578	(-)	96.571	SweH2-011	11456	13039	1584	(-)	96.205
TNF receptor (CrmB) (Cop-C22L)	C22L	CPXV014	NoF1-013	13393	14001	609	(-)	97.03	NoF2-013	13817	14425	609	(-)	98.02	NoH1-012	13485	14093	609	(-)	98.02	SweH1-012	13156	13758	603	(-)	97.99	SweH2-012	13113	13715	603	(-)	97.99
TNF-alpha receptor like protein	-	vCD30/CPXV015	NoF1-014	13998	14330	333	(-)	98.182	NoF2-014	14422	14754	333	(-)	98.182	NoH1-013	14090	14422	333	(-)	98.182	SweH1-013	13755	14120	366	(-)	97.273	SweH2-013	13712	14077	366	(-)	96.364
Ankyrin (Cop-B18R)	B18R	CPXV016	NoF1-015	14405	16708	2304	(-)	97.772	NoF2-015	14828	17131	2304	(-)	98.034	NoH1-014	14496	16799	2304	(-)	98.034	SweH1-014	14181	16475	2295	(-)	98.168	SweH2-014	14138	16432	2295	(-)	98.168
Ankyrin (CPXV-017)	-	CPXV017	NoF1-016	16984	18291	1308	(-)	96.092	NoF2-016	17606	18913	1308	(-)	96.322	NoH1-015	17210	18517	1308	(-)	96.322	SweH1-015	16874	18181	1308	(-)	95.862	SweH2-015	16738	18045	1308	(-)	95.862
MPV-Z-N3R	-	CPXV018	NoF1-017	18390	18905	516	(-)	91.813	NoF2-017	19012	19527	516	(-)	91.813	NoH1-016	18616	19131	516	(-)	91.813	SweH1-016	18280	18804	525	(-)	91.954	SweH2-016	18144	18659	516	(-)	92.982
Ankyrin (Cop-B18R)	B18R	CPXV019	NoF1-018	18968	21583	2616	(-)	77.855	NoF2-018	19590	22304	2715	(-)	86.916	NoH1-017	19194	21908	2715	(-)	86.916	SweH1-017	18867	21278	2412	(-)	92.04	SweH2-017	18722	21142	2421	(-)	91.574
Host range protein	-	CPXV020	NoF1-019	21631	22149	519	(-)	97.674	NoF2-019	22246	22752	507	(-)	97.647	NoH1-018	21850	22356	507	(-)	97.647	SweH1-018	21374	21892	519	(-)	97.674	SweH2-018	21238	21756	519	(-)	97.674
Secreted EGF-like protein (Cop-C11R)	C11R	VGF/CPXV021	NoF1-020	22316	22741	426	(+)	94.326	NoF2-020	22917	23339	423	(+)	94.286	NoH1-019	22521	22943	423	(+)	94.286	SweH1-019	22058	22477	420	(+)	95	SweH2-019	21922	22341	420	(+)	95
IL-1 receptor antagonist (Cop-C10L)	C10L	CPXV022	NoF1-021	22894	23889	996	(-)	96.375	NoF2-021	23501	24496	996	(-)	96.073	NoH1-020	23105	24100	996	(-)	96.073	SweH1-020	22617	23606	990	(-)	93.656	SweH2-020	22481	23470	990	(-)	93.656
Zinc finger-like protein	-	CPXV023	NoF1-022	24404	25132	729	(+)	99.174	NoF2-022	25033	25761	729	(+)	98.76	NoH1-021	24630	25358	729	(+)	98.76	SweH1-021	24115	24843	729	(+)	95.868	SweH2-021	23979	24707	729	(+)	95.868
Soluble IL-18 binding protein (Bsh-D7L)	D7L	CPXV024	NoF1-023	25281	25661	381	(-)	96.825	NoF2-023	25910	26290	381	(-)	98.413	NoH1-022	25507	25887	381	(-)	98.413	SweH1-022	24995	25375	381	(-)	98.413	SweH2-022	24859	25239	381	(-)	98.413
Ankyrin(Host Range (Bang-D8L)	D8L	VHR1/CPXV025	NoF1-024	25720	27735	2016	(-)	95.827	NoF2-024	26350	28359	2010	(-)	95.815	NoH1-023	25947	27956	2010	(-)	95.815	SweH1-023	25434	27449	2016	(-)	95.529	SweH2-023	25298	27313	2016	(-)	95.38
ANK-containing protein	-	CPXV026	NoF1-025	27849	28040	192	(-)	95	NoF2-025	28473	28664	192	(-)	95	NoH1-024	28070	28261	192	(-)	95	SweH1-024	27564	27761	198	(-)	95	SweH2-024	27428	27625	198	(-)	95
Ankyrin; Type 1 IFN resistance (Cop-C9L)	C9L	CPXV027	NoF1-026	28214	30118	1905	(-)	95.11	NoF2-026	28841	30751	1911	(-)	92.296	NoH1-025	28438	30354	1917	(-)	92.476	SweH1-025	27932	29836	1905	(-)	93.543	SweH2-025	27796	29709	1914	(-)	93.093
Unknown (Cop-C8L)	C8L	CPXV028	NoF1-027	30160	30717	558	(-)	98.919	NoF2-027	30794	31351	558	(-)	100	NoH1-026	30397	30954	558	(-)	100	SweH1-026	29879	30436	558	(-)	100	SweH2-026	29751	30308	558	(-)	100
Type 1 IFN inhibitor (Cop-C7L)	C7L	CPXV029	NoF1-028	30789	31241	453	(-)	100	NoF2-028	31420	31872	453	(-)	100	NoH1-027	31023	31475	453	(-)	100	SweH1-027	30505	30957	453	(-)	100	SweH2-027	30377	30829	453	(-)	100
Bcl-2-like protein, IFN-beta inhibitor (Cop-C6L)	C6L	CPXV030	NoF1-029	31472	31939	468	(-)	98.71	NoF2-029	32103	32570	468	(-)	98.71	NoH1-028	31706	32173	468	(-)	98.71	SweH1-028	31186	31653	468	(-)	98.71	SweH2-028	31058	31525	468	(-)	98.71
Kelch-like protein (Cop-C5L)	C5L	CPXV031	overlap																													
Kelch-like protein (Cop-C5L)	C5L	CPXV032	NoF1-030	32272	32649	378	(-)	98.4	NoF2-030	32903	33280	378	(-)	98.4	NoH1-029	32506	32883	378	(-)	98.4	SweH1-029	31986	32348	363	(-)	93.6	SweH2-029	31858	32220	363	(-)	93.6
IL-1 receptor antagonist (Cop-C10L)	C4L	CPXV033	NoF1-031	32710	33657	948	(-)	95.886	NoF2-031	33341	34291	951	(-)	96.835	NoH1-030	32944	33894	951	(-)	97.152	SweH1-030	32409	33359	951	(-)	95.886	SweH2-030	32281	33231	951	(-)	95.886
Complement binding (secreted) (Cop-C3L)	C3L	CPXV034	NoF1-032	33724	34518	795	(-)	96.198	NoF2-032	34358	35152	795	(-)	97.338	NoH1-031	33961	34755	795	(-)	97.338	SweH1-031	33433	34227	795	(-)	95.437	SweH2-031	33305	34099	795	(-)	95.437
PO/ZBTB Kelch domain protein (Cop-C2L)	C2L	CPXV035	NoF1-033	34581	36119	1539	(-)	98.828	NoF2-033	35215	36753	1539	(-)	99.219	NoH1-032	34818	36356	1539	(-)	99.219	SweH1-032	34290	35828	1539	(-)	98.242	SweH2-032	34162	35700	1539	(-)	98.242
Putative TLR signalling inhibitor (Cop-C1L)	C1L	CPXV036	NoF1-034	36188	36826	639	(-)	99.528	NoF2-034	36822	37517	696	(-)	99.567	NoH1-033	36425	37120	696	(-)	99.567	SweH1-033	35899	36594	696	(-)	99.134	SweH2-033	35771	36466	696	(-)	99.134
Anti-apoptotic Bcl-2-like protein (Cop-N1L)	N1L	CPXV037	NoF1-035	36868	37221	354	(-)	99.145	NoF2-035	37504	37857	354	(-)	99.145	NoH1-034	37107	37460	354	(-)	99.145	SweH1-034	36578	36934	357	(-)	96.581	SweH2-034	36450	36806	357	(-)	96.581
Alpha amanatin target protein (Cop-N2L)	N2L	CPXV038	NoF1-036	37343	37873	531	(-)	93.22	NoF2-036	37980	38510	531	(-)	93.785	NoH1-035	37583	38113	531	(-)	93.785	SweH1-035	37061	37597	537	(-)	97.191	SweH2-035	36933	37469	537	(-)	97.191
ANK-containing protein; apoptosis inhibitor (C op-M1L)	M1L	CPXV039	NoF1-037	37916	39331	1416	(-)	97.674	NoF2-037	38552	39967	1416	(-)	97.674	NoH1-036	38155	39570	1416	(-)	97.674	SweH1-036	37638	39059	1422	(-)	98.097	SweH2-036	37510	38931	1422	(-)	98.097
NFkB inhibitor (Cop-M2L)	M2L	CPXV040	NoF1-038	39309	39971	663	(-)	98.182	NoF2-038	39945	40607	663	(-)	97.727	NoH1-037	39548	40210	663	(-)	97.727	SweH1-037	39037	39699	663	(-)	96.818	SweH2-037	38909	39571	663	(-)	96.818
Ankyrin(NFkB inhibitor (Cop-K1L)	K1L	CPXV041	NoF1-039	40095	40952	858	(-)	98.587	NoF2-039	40731	41588	858	(-)	97.173	NoH1-038	40334	41191	858	(-)	97.173	SweH1-038	39826	40680	855	(-)	97.535	SweH2-038	39698	40552	855	(-)	97.535
Serpin 1,2,3 (Cop-K2L)	K2L	SPI3/CPXV042	NoF1-040	41310	42431	1122	(-)	98.123	NoF2-040	41908	43029	1122	(-)	98.391	NoH1-039	41863	42984	1122	(-)	98.391	SweH1-039	41023	42141	1119	(-)	97.319	SweH2-039	40854	41972	1119	(-)	97.051
IFN resistance, PKR/eIF-alpha inhibitor (Cop-K3 L)	K3L	CPXV043	NoF1-041	42482	42748	267	(-)	97.727	NoF2-041	43080	43346	267	(-)	97.727	NoH1-040	43035	43301	267	(-)	97.727	SweH1-040	42193	42459	267	(-)	97.727	SweH2-040	42024	42290	267	(-)	97.727
Phospholipase-D-like protein (Cop-K4L)	K4L	CPXV044	NoF1-042	42808	44082	1275	(-)	98.585	NoF2-042	43406	44680	1275	(-)	98.821	NoH1-041	43361	44635	1275	(-)	98.821	SweH1-041	42519	43793	1275	(-)	99.057	SweH2-041	42350	43624	1275	(-)	99.057
Monoglyceride lipase (Cop-K5L)	K5L	CPXV045	NoF1-043	44110	44940	831	(-)	98.551	NoF2-043	44708	45538	831	(-)	98.188	NoH1-042	44663	45493	831	(-)	98.188	SweH1-042	43821	44651	831	(-)	98.551	SweH2-042	43652	44482	831	(-)	98.551
Host immune response repressor (Cop-K7R)	K7R	CPXV046	NoF1-044	45078	45527	450	(+)	100	NoF2-044	45677	46126	450	(+)	100	NoH1-043	45632	46081	450	(+)	100	SweH1-043	44790	45239	450	(+)	100	SweH2-043	44621	45070	450	(+)	100
CPV-B-047	-	CPXV047	overlap																													
Caspase-9 (apoptosis) inhibitor (mitochondrial- associated) (Cop-F1L)	F1L	CPXV048	NoF1-045	45601	46344	744	(-)	95.618	NoF2-045	46200	46955	756	(-)	94.422	NoH1-044	46155	46919	765	(-)	92.913	SweH1-044	45310	46095	786	(-)	93.103	SweH2-044	45141	45920	780	(-)	91.12
dUTPase (Cop-F2L)	F2L	CPXV049	NoF1-046	46344	46787	444	(-)	98.639	NoF2-046	46955	47398	444	(-)	97.959	NoH1-045	46919	47362	444	(-)	97.959	SweH1-045	46095	46538	444	(-)	97.959	SweH2-045	45920	46363	444	(-)	97.959
Kelch-like protein (Cop-F3L)	F3L	CPXV050	NoF1-047	46811	48253	1443	(-)	97.708	NoF2-047	47422	48864	1443	(-)	97.708	NoH1-046	47386	48828	1443	(-)	97.708	SweH1-046	46562	48004	1443	(-)	98.958	SweH2-046	46387	47829	1443	(-)	98.958
Ribonucleotide reductase small subunit (Cop-F4L)	F4L	CPXV051	NoF1-048	48264	49265	1002	(-)	99.099	NoF2-048	48875	49834	960	(-)	99.06	NoH1-047	48839	49798	960	(-)	99.06	SweH1-047	48015	49016	1002	(-)	98.198	SweH2-047	47840	48841	1002	(-)	98.198
36kDa major membrane protein (Cop-F5L)	F5L	CPXV052	NoF1-049	49255	50220	966	(-)	96.904	NoF2-049	49867	50832	966	(-)	98.142	NoH1-048	49831	50796	966	(-)	98.142	SweH1-048	49006	49974	969	(-)	94.427	SweH2-048	48831	49799	969	(-)	94.427
Hypothetical protein (Cop-F6L)	F6L	CPXV053	NoF1-050	50250	50465	216	(-)	98.592	NoF2-050	50862	51077	216	(-)	98.592	NoH1-049	50826	51041	216	(-)	98.592	SweH1-049	50004	50219	216	(-)	98.592	SweH2-049	49829	50044	216	(-)	98.592
Hypothetical protein (Cop-F7L)	F7L	CPXV054	NoF1-051	50481	50726	246	(-)	97.531	NoF2-051	51093	51344	252	(-)	96.386	NoH1-050	51057	51302	246	(-)	98.765	SweH1-050	50235	50480	246	(-)	98.765	SweH2-050	50060	50305	246	(-)	98.765
Cytoplasmic protein (Cop-F8L)	F8L	CPXV055	NoF1-052	51003	51200	198	(-)	100	NoF2-052	51491	51688	198	(-)	100	NoH1-051	51449	51646	198	(-)	100	SweH1-051	50635	50832	198	(-)	98.462	SweH2-051	50456	50653	198	(-)	98.462
S-S bond formation pathway protein substrate (C op-F9L)	F9L	CPXV056	NoF1-053	51261	51899	639	(-)	99.057	NoF2-053	51749	52387	639	(-)	99.057	NoH1-052	51707	52345	639	(-)	99.057	SweH1-052	50893	51531	639	(-)	99.057	SweH2-052	50714	51352	639	(-)	99.057
Essential Ser/Thr kinase morph (Cop-F10L)	F10L	CPXV057	NoF1-054	51886	53205	1320	(-)	99.772	NoF2-054	52374	53693	1320	(-)	99.772	NoH1-053	52332	53651	1320	(-)	99.772	SweH1-053	51518	52837	1320	(-)	100	SweH2-053	51339	52658	1320	(-)	100
VV_Cop-F ORF D	-	CPXV058	overlap																													
RhoA signalling inhibitor, virus release protei n (Cop-F11L)	F11L	CPXV059	NoF1-055	53228	54292	1065	(-)	98.305	NoF2-055	53716	54780	1065	(-)	98.023	NoH1-054	53674	54738	1065	(-)	98.023	SweH1-054	52860	53924	1065	(-)	98.87	SweH2-054	52681	53745	1065	(-)	99.153
EEV maturation protein (Cop-F12L)	F12L	CPXV060	NoF1-056	54335	56239	1905	(-)	99.369	NoF2-056	54823	56727	1905	(-)	99.211	NoH1-055	54781	56685	1905	(-)	99.211	SweH1-055	53982	55886	1905	(-)	99.211	SweH2-055	53803	55707	1905	(-)	99.211
Palmitylated EEV membrane glycoprotein (Cop-F13 L)	F13L	CPXV061	NoF1-057	56273	57391	1119	(-)	99.731	NoF2-057	56761	57879	1119	(-)	99.462	NoH1-056	56719	57837	1119	(-)	99.194	SweH1-056	55932	57050	1119	(-)	99.731	SweH2-056	55753	56871	1119	(-)	99.731
Unknown (Cop-F14L)	F14L	CPXV062	NoF1-058	57409	57630	222	(-)	98.63	NoF2-058	57897	58118	222	(-)	98.63	NoH1-057	57855	58076	222	(-)	98.63	SweH1-057	57068	57295	228	(-)	97.333	SweH2-057	56889	57116	228	(-)	97.333
CPV-B-063	-	CPXV063	NoF1-059	57677	57835	159	(+)	98.077	NoF2-059	58165	58323	159	(+)	98.077	NoH1-058	58123	58281	159	(+)	98.077	SweH1-058	57342	57500	159	(+)	100	SweH2-058	57163	57321	159	(+)	100
Unknown conserved protein (Cop-F15L)	F15L	CPXV064	NoF1-060	57903	58379	477	(-)	98.101	NoF2-060	58389	58865	477	(-)	98.101	NoH1-059	58347	58823	477	(-)	98.101	SweH1-059	57568	58044	477	(-)	98.101	SweH2-059	57389	57865	477	(-)	98.101
Non-functional Serine Recombinase (Cop-F16L)	F16L	CPXV065	NoF1-061	58379	59080	702	(-)	98.696	NoF2-061	58872	59567	696	(-)	99.134	NoH1-060	58830	59525	696	(-)	99.134	SweH1-060	58051	58746	696	(-)	97.835	SweH2-060	57872	58567	696	(-)	97.835
DNA-binding phosphoprotein (VP11); mTOR antagon ist (Cop-F17R)	F17R	CPXV066	NoF1-062	59143	59448	306	(+)	99.01	NoF2-062	59630	59935	306	(+)	98.02	NoH1-061	59588	59893	306	(+)	98.02	SweH1-061	58809	59114	306	(+)	99.01	SweH2-061	58630	58935	306	(+)	99.01
Poly (A) polymerase catalytic subunit (VP55) (C op-E1L)	E1L	CPXV067	NoF1-063	59445	60084	1440	(-)	99.582	NoF2-063	59932	61371	1440	(-)	99.582	NoH1-062	59890	61329	1440	(-)	99.582	SweH1-062	59111	60550	1440	(-)	99.791	SweH2-062	58932	60371	1440	(-)	99.791
IEV morphogenesis (Cop-E2L)	E2L	CPXV068	NoF1-064	60881	63094	2214	(-)	99.186	NoF2-064	61368	63581	2214	(-)	99.186	NoH1-063	61326	63539	2214	(-)	99.186	SweH1-063	60547	62760	2214	(-)	99.729	SweH2-063	60368	62581	2214	(-)	99.729
dsRNA-binding protein, IFN resistance/PKR inhib itor (Z-DNA binding) (Cop-E3L)	E3L	CPXV069	NoF1-065	63225	63797	573	(-)	98.421	NoF2-065	63711	64283	573	(-)	98.421	NoH1-064	63669	64241	573	(-)	98.421	SweH1-064	62896	63468	573	(-)	94.737	SweH2-064	62717	63289	573	(-)	94.737
RNA polymerase subunit (RPO30) (Cop-E4L)	E4L	CPXV070	NoF1-066	63852	64637	786	(-)	100	NoF2-066	64336	65123	786	(-)	100	NoH1-065	64296	65081	786	(-)	100	SweH1-065	63525	64310	786	(-)	99.617	SweH2-065	63346	64131	786	(-)	99.617
Virosome component (Cop-E5R)	E5R	CPXV071	NoF1-067	64757	65710	954	(+)	92.79	NoF2-067	65243	66196	954	(+)	93.417	NoH1-066	65201	66154	954	(+)	93.417	SweH1-066	64430	65389	960	(+)	94.357	SweH2-066	64251	65210	960	(+)	94.357
Virion protein (Cop-E6R)	E6R	CPXV072	NoF1-068	65830	67533	1704	(+)	99.647	NoF2-068	66308	68011	1704	(+)	99.471	NoH1-067	66266	67969	1704	(+)	99.471	SweH1-067	65581	67284	1704	(+)	99.471	SweH2-067	65431	67134	1704	(+)	99.471
Myristylated protein (Cop-E7R)	E7R	CPXV073	NoF1-069	67595	68092	498	(+)	93.939	NoF2-069	68073	68570	498	(+)	93.333	NoH1-068	68031	68528	498	(+)	93.939	SweH1-068	67349	67846	498	(+)	93.939	SweH2-068	67199	67696	498	(+)	93.939

ER-localized membrane protein, virion core prot ein (Cop-E8R)	E8R	CPXV074	NoF1-070	68203	69024	822	(+)	99.634	NoF2-070	68681	69502	822	(+)	99.634	NoH1-069	68639	69460	822	(+)	99.634	SweH1-069	67955	68776	822	(+)	99.634	SweH2-069	67805	68626	822	(+)	99.634
DNA polymerase (Cop-E9L)	E9L	CPXV075	NoF1-071	69031	72048	3018	(-)	99.502	NoF2-071	69509	72526	3018	(-)	99.801	NoH1-070	69467	72484	3018	(-)	99.801	SweH1-070	68783	71800	3018	(-)	99.602	SweH2-070	68633	71650	3018	(-)	99.602
Sulfhydryl oxidase (FAD-linked) (Cop-E10R)	E10R	CPXV076	NoF1-072	72080	72367	288	(+)	98.947	NoF2-072	72558	72845	288	(+)	97.895	NoH1-071	72516	72803	288	(+)	97.895	SweH1-071	71832	72119	288	(+)	97.895	SweH2-071	71682	71969	288	(+)	97.895
Virion core protein (Cop-E11L)	E11L	CPXV077	NoF1-073	72362	72751	390	(-)	99.225	NoF2-073	72840	73229	390	(-)	99.225	NoH1-072	72798	73187	390	(-)	99.225	SweH1-072	72114	72503	390	(-)	99.225	SweH2-072	71964	72353	390	(-)	99.225
Membrane protein (Cop-O1L)	O1L	CPXV078	NoF1-074	72738	74738	2001	(-)	98.498	NoF2-074	73216	75216	2001	(-)	98.799	NoH1-073	73174	75174	2001	(-)	98.799	SweH1-073	72490	74490	2001	(-)	98.498	SweH2-073	72340	74340	2001	(-)	98.498
Glutaredoxin 1 (Cop-O2L)	O2L	CPXV079	NoF1-075	74786	75112	327	(-)	98.148	NoF2-075	75264	75590	327	(-)	98.148	NoH1-074	75222	75548	327	(-)	98.148	SweH1-074	74537	74863	327	(-)	98.148	SweH2-074	74387	74713	327	(-)	98.148
Virus entry/fusion complex component (Cop-O3L)	O3L	-	NoF1-076	75136	75243	108	(-)	-	NoF2-076	75614	75721	108	(-)	-	NoH1-075	75572	75679	108	(-)	-	SweH1-075	74887	74994	108	(-)		SweH2-075	74737	74844	108	(-)	-
DNA-binding core protein (Cop-I1L)	I1L	CPXV080	NoF1-077	75258	76196	939	(-)	100	NoF2-077	75736	76674	939	(-)	100	NoH1-076	75694	76632	939	(-)	100	SweH1-076	75009	75947	939	(-)	99.359	SweH2-076	74859	75797	939	(-)	99.038
IMV membrane protein (Cop-I2L)	I2L	CPXV081	NoF1-078	76203	76424	222	(-)	98.63	NoF2-078	76681	76902	222	(-)	98.63	NoH1-077	76639	76860	222	(-)	98.63	SweH1-077	75954	76175	222	(-)	97.26	SweH2-077	75804	76025	222	(-)	97.26
ssDNA-binding phosphoprotein (Cop-I3L)	I3L	CPXV082	NoF1-079	76425	77234	810	(-)	98.141	NoF2-079	76903	77712	810	(-)	98.141	NoH1-078	76861	77670	810	(-)	98.141	SweH1-078	76176	76985	810	(-)	98.513	SweH2-078	76026	76835	810	(-)	98.141
Ribonucleotide reductase large subunit (Cop-I4L)	I4L	CPXV083	NoF1-080	77317	79632	2316	(-)	98.184	NoF2-080	77795	80110	2316	(-)	98.314	NoH1-079	77753	80068	2316	(-)	98.314	SweH1-079	77068	79383	2316	(-)	98.573	SweH2-079	76916	79231	2316	(-)	98.703
IMV protein VP13 (Cop-I5L)	I5L	CPXV084	NoF1-081	79659	79898	240	(-)	100	NoF2-081	80137	80376	240	(-)	100	NoH1-080	80095	80334	240	(-)	100	SweH1-080	79410	79649	240	(-)	100	SweH2-080	79258	79497	240	(-)	100
Telomere-binding protein (Cop-I6L)	I6L	CPXV085	NoF1-082	79917	81065	1149	(-)	99.476	NoF2-082	80395	81543	1149	(-)	99.476	NoH1-081	80353	81501	1149	(-)	99.476	SweH1-081	79668	80816	1149	(-)	99.215	SweH2-081	79516	80664	1149	(-)	99.215
Virion core cysteine protease (Cop-I7L)	I7L	CPXV086	NoF1-083	81058	82329	1272	(-)	99.291	NoF2-083	81536	82807	1272	(-)	99.291	NoH1-082	81494	82765	1272	(-)	99.291	SweH1-082	80809	82080	1272	(-)	99.291	SweH2-082	80657	81928	1272	(-)	99.291
RNA helicase, DExH-NPH-II domain (Cop-I8R)	I8R	CPXV087	NoF1-084	82335	84365	2031	(+)	99.26	NoF2-084	82813	84843	2031	(+)	99.26	NoH1-083	82771	84801	2031	(+)	99.26	SweH1-083	82086	84116	2031	(+)	99.26	SweH2-083	81934	83964	2031	(+)	99.408
Metalloprotease (Cop-G1L)	G1L	CPXV088	NoF1-085	84369	86144	1776	(-)	99.662	NoF2-085	84847	86622	1776	(-)	99.662	NoH1-084	84805	86580	1776	(-)	99.662	SweH1-084	84120	85895	1776	(-)	99.662	SweH2-084	83968	85743	1776	(-)	99.662
Entry/fusion complex component (Cop-G3L)	G3L	CPXV089	NoF1-086	86141	86476	336	(-)	99.099	NoF2-086	86619	86954	336	(-)	99.099	NoH1-085	86577	86912	336	(-)	99.099	SweH1-085	85892	86227	336	(-)	99.099	SweH2-085	85740	86075	336	(-)	99.099
VLTF (late transcription elongation factor) (Co p-G2R)	G2R	CPXV090	NoF1-087	86470	87132	663	(+)	98.636	NoF2-087	86948	87610	663	(+)	98.636	NoH1-086	86906	87568	663	(+)	98.636	SweH1-086	86221	86883	663	(+)	99.091	SweH2-086	86069	86731	663	(+)	99.091
Glutaredoxin-like protein (Cop-G4L)	G4L	CPXV091	NoF1-088	87102	87476	375	(-)	99.194	NoF2-088	87580	87954	375	(-)	99.194	NoH1-087	87538	87912	375	(-)	99.194	SweH1-087	86853	87227	375	(-)	98.387	SweH2-087	86701	87075	375	(-)	98.387
FEN1-like nuclease (Cop-G5R)	G5R	CPXV092	NoF1-089	87479	88786	1308	(+)	97.931	NoF2-089	87957	89264	1308	(+)	97.931	NoH1-088	87915	89222	1308	(+)	97.931	SweH1-088	87230	88534	1305	(+)	98.848	SweH2-088	87078	88382	1305	(+)	98.848
RNA polymerase subunit (RPO7) (Cop-G5.5R)	G5.5R	CPXV093	NoF1-090	88794	88985	192	(+)	100	NoF2-090	89272	89463	192	(+)	100	NoH1-089	89230	89421	192	(+)	100	SweH1-089	88542	88733	192	(+)	100	SweH2-089	88390	88581	192	(+)	100
NLPc/P60 superfamily protein (Cop-G6R)	G6R	CPXV094	NoF1-091	88987	89484	498	(+)	97.576	NoF2-091	89465	89962	498	(+)	97.576	NoH1-090	89423	89920	498	(+)	97.576	SweH1-090	88735	89232	498	(+)	97.576	SweH2-090	88583	89080	498	(+)	97.576
Virion phosphoprotein, early morphogenesis (Cop -G7L)	G7L	CPXV095	NoF1-092	89449	90564	1116	(-)	99.191	NoF2-092	89927	91042	1116	(-)	99.191	NoH1-091	89885	91000	1116	(-)	99.191	SweH1-091	89197	90312	1116	(-)	100	SweH2-091	89045	90160	1116	(-)	100
CC_Cop-G ORF B	-	CPXV096	overlap																													
VLTF-1 (late transcription factor 1) (Cop-G8R)	G8R	CPXV097	NoF1-093	90595	91377	783	(+)	99.615	NoF2-093	91073	91855	783	(+)	99.615	NoH1-092	91031	91813	783	(+)	99.615	SweH1-092	90343	91125	783	(+)	99.615	SweH2-092	90191	90973	783	(+)	99.615
Entry/fusion complex component, myristylprotein (Cop-G9R)	G9R	CPXV098	NoF1-094	91397	92419	1023	(+)	99.706	NoF2-094	91875	92897	1023	(+)	99.706	NoH1-093	91833	92855	1023	(+)	99.706	SweH1-093	91145	92167	1023	(+)	99.118	SweH2-093	90993	92015	1023	(+)	99.118
IMV membrane protein (Cop-L1R)	L1R	CPXV099	NoF1-095	92420	93172	753	(+)	99.2	NoF2-095	92898	93650	753	(+)	99.2	NoH1-094	92856	93608	753	(+)	99.2	SweH1-094	92168	92920	753	(+)	99.2	SweH2-094	92016	92768	753	(+)	99.2
Viral membrane assembly proteins (VMAP) (Cop-L2 R)	L2R	CPXV100	NoF1-096	93204	93470	267	(+)	97.727	NoF2-096	93682	93948	267	(+)	97.727	NoH1-095	93640	93906	267	(+)	97.727	SweH1-095	92959	93225	267	(+)	98.864	SweH2-095	92807	93073	267	(+)	98.864
Internal virion protein (Cop-L3L)	L3L	CPXV101	NoF1-097	93460	94512	1053	(-)	99.714	NoF2-097	93938	94990	1053	(-)	99.429	NoH1-096	93896	94948	1053	(-)	99.429	SweH1-096	93215	94249	1035	(-)	97.429	SweH2-096	93063	94115	1053	(-)	99.143
ssjdsDNA binding protein (VP8) (Cop-L4R)	L4R	CPXV102	NoF1-098	94537	95292	756	(+)	99.203	NoF2-098	95015	95770	756	(+)	99.203	NoH1-097	94973	95728	756	(+)	99.203	SweH1-097	94274	95029	756	(+)	100	SweH2-097	94140	94895	756	(+)	100
Entry and Fusion IMV protein (Cop-L5R)	L5R	CPXV103	NoF1-099	95302	95688	387	(+)	98.438	NoF2-099	95780	96166	387	(+)	99.219	NoH1-098	95738	96124	387	(+)	99.219	SweH1-098	95039	95425	387	(+)	99.219	SweH2-098	94905	95291	387	(+)	99.219
Virion morph (Cop-J1R)	J1R	CPXV104	NoF1-100	95645	96106	462	(+)	100	NoF2-100	96123	96584	462	(+)	99.338	NoH1-099	96081	96542	462	(+)	99.338	SweH1-099	95382	95843	462	(+)	100	SweH2-099	95248	95709	462	(+)	100
Thymidine kinase (Cop-J2R)	J2R	CPXV105	NoF1-101	96122	96655	534	(+)	97.74	NoF2-101	96600	97133	534	(+)	98.305	NoH1-100	96558	97091	534	(+)	98.305	SweH1-100	95859	96392	534	(+)	98.305	SweH2-100	95725	96258	534	(+)	98.305
Poly (A) polymerase small subunit (VP39) (Cop-J 3R)	J3R	CPXV106	NoF1-102	96723	97724	1002	(+)	99.7	NoF2-102	97200	98201	1002	(+)	99.7	NoH1-101	97158	98159	1002	(+)	99.7	SweH1-101	96459	97460	1002	(+)	99.7	SweH2-101	96325	97326	1002	(+)	99.7
RNA polymerase subunit (RPO22) (Cop-J4R)	J4R	CPXV107	NoF1-103	97639	98196	558	(+)	99.459	NoF2-103	98116	98673	558	(+)	98.919	NoH1-102	98074	98631	558	(+)	98.919	SweH1-102	97375	97932	558	(+)	100	SweH2-102	97241	97798	558	(+)	100
IMV membrane protein (Cop-J5L)	J5L	CPXV108	NoF1-104	98257	98658	402	(-)	100	NoF2-104	98734	99135	402	(-)	100	NoH1-103	98692	99093	402	(-)	100	SweH1-103	97987	98388	402	(-)	100	SweH2-103	97853	98254	402	(-)	100
RNA polymerase subunit (RPO147) (Cop-J6R)	J6R	CPXV109	NoF1-105	98765	102625	3861	(+)	99.844	NoF2-105	99242	103102	3861	(+)	99.844	NoH1-104	99200	103060	3861	(+)	99.844	SweH1-104	98495	102355	3861	(+)	99.689	SweH2-104	98361	102221	3861	(+)	99.689
TyrjSer phosphatase, IFN-gamma inhibitor (Cop-H 1L)	H1L	CPXV110	NoF1-106	102622	103137	516	(-)	98.83	NoF2-106	103099	103614	516	(-)	98.83	NoH1-105	103057	103572	516	(-)	98.83	SweH1-105	102352	102867	516	(-)	99.415	SweH2-105	102218	102733	516	(-)	99.415
IMV membrane protein (Cop-H2R)	H2R	CPXV111	NoF1-107	103151	103720	570	(+)	98.942	NoF2-107	103628	104197	570	(+)	98.942	NoH1-106	103586	104155	570	(+)	98.942	SweH1-106	102881	103450	570	(+)	100	SweH2-106	102747	103316	570	(+)	100
IMV heparin binding surface protein (Cop-H3L)	H3L	CPXV112	NoF1-108	103723	104700	978	(-)	99.385	NoF2-108	104200	105177	978	(-)	99.692	NoH1-107	104158	105135	978	(-)	99.692	SweH1-107	103452	104429	978	(-)	99.385	SweH2-107	103318	104295	978	(-)	99.385
RAP94 (RNA pol assoc protein) (Cop-H4L)	H4L	CPXV113	NoF1-109	104701	107088	2388	(-)	99.623	NoF2-109	105178	107565	2388	(-)	99.748	NoH1-108	105136	107523	2388	(-)	99.748	SweH1-108	104430	106817	2388	(-)	99.623	SweH2-108	104296	106683	2388	(-)	99.623
VLTF-4 (late transcription factor 4) (Cop-H5R)	H5R	CPXV114	NoF1-110	107274	107894	621	(+)	93.782	NoF2-110	107751	108374	624	(+)	96.135	NoH1-109	107709	108332	624	(+)	96.135	SweH1-109	107003	107623	621	(+)	98.544	SweH2-109	106869	107489	621	(+)	98.544
DNA topoisomerase type I (Cop-H6R)	H6R	CPXV115	NoF1-111	107895	108839	945	(+)	99.682	NoF2-111	108375	109319	945	(+)	99.682	NoH1-110	108333	109277	945	(+)	99.682	SweH1-110	107624	108568	945	(+)	99.682	SweH2-110	107490	108434	945	(+)	99.682
CPV-B-116	-	CPXV116	overlap																													
Viral membrane assembly proteins (VMAP) (Cop-H7 R)	H7R	CPXV117	NoF1-112	108877	109317	441	(+)	98.63	NoF2-112	109357	109797	441	(+)	97.945	NoH1-111	109315	109755	441	(+)	97.945	SweH1-111	108606	109046	441	(+)	97.945	SweH2-111	108472	108912	441	(+)	97.945
mRNA capping enzyme large subunit (Cop-D1R)	D1R	CPXV118	NoF1-113	109361	111895	2535	(+)	99.526	NoF2-113	109841	112375	2535	(+)	99.408	NoH1-112	109799	112333	2535	(+)	99.408	SweH1-112	109089	111623	2535	(+)	99.289	SweH2-112	108955	111489	2535	(+)	99.289
Virion core (Cop-D2L)	D2L	CPXV119	NoF1-114	111854	112294	441	(-)	99.315	NoF2-114	112334	112774	441	(-)	99.315	NoH1-113	112292	112732	441	(-)	99.315	SweH1-113	111582	112022	441	(-)	99.315	SweH2-113	111448	111888	441	(-)	99.315
Virion core (Cop-D3R)	D3R	CPXV120	NoF1-115	112287	113000	714	(+)	99.156	NoF2-115	112767	113480	714	(+)	99.156	NoH1-114	112725	113438	714	(+)	99.156	SweH1-114	112015	112728	714	(+)	99.156	SweH2-114	111881	112594	714	(+)	99.156
Uracil-DNA glycosylase, DNA polymerase processi vity factor (Cop-D4R)	D4R	CPXV121	NoF1-116	113000	113656	657	(+)	98.165	NoF2-116	113480	114136	657	(+)	98.165	NoH1-115	113438	114094	657	(+)	98.165	SweH1-115	112728	113384	657	(+)	97.706	SweH2-115	112594	113250	657	(+)	97.706
NTPase, DNA primase (Cop-D5R)	D5R	CPXV122	NoF1-117	113688	116045	2358	(+)	98.599	NoF2-117	114168	116525	2358	(+)	98.599	NoH1-116	114126	116483	2358	(+)	98.599	SweH1-116	113416	115773	2358	(+)	99.236	SweH2-116	113282	115639	2358	(+)	99.236
Morphogenesis, VETF-s (early transcription fact or small) (Cop-D6R)	D6R	CPXV123	NoF1-118	116086	117999	1914	(+)	100	NoF2-118	116566	118479	1914	(+)	100	NoH1-117	116524	118437	1914	(+)	100	SweH1-117	115814	117727	1914	(+)	100	SweH2-117	115680	117593	1914	(+)	100
RNA polymerase subunit (RPO18) (Cop-D7R)	D7R	CPXV124	NoF1-119	118026	118511	486	(+)	99.379	NoF2-119	118506	118991	486	(+)	99.379	NoH1-118	118464	118949	486	(+)	99.379	SweH1-118	117754	118239	486	(+)	99.379	SweH2-118	117620	118105	486	(+)	99.379
Carbonic anhydrase, GAG-binding IMV membrane pr otein (Cop-D8L)	D8L	CPXV125	NoF1-120	118474	119388	915	(-)	97.368	NoF2-120	118954	119868	915	(-)	98.355	NoH1-119	118912	119826	915	(-)	98.355	SweH1-119	118202	119116	915	(-)	99.013	SweH2-119	118068	118982	915	(-)	99.013
mRNA decapping enzyme (Cop-D9R)	D9R	CPXV126	NoF1-121	119430	120071	642	(+)	100	NoF2-121	119910	120551	642	(+)	100	NoH1-120	119868	120509	642	(+)	100	SweH1-120	119158	119799	642	(+)	100	SweH2-120	119024	119665	642	(+)	100
mRNA decapping enzyme (Cop-D10R)	D10R	CPXV127	NoF1-122	120068	120814	747	(+)	99.194	NoF2-122	120548	121294	747	(+)	99.194	NoH1-121	120506	121252	747	(+)	99.194	SweH1-121	119796	120542	747	(+)	99.597	SweH2-121	119662	120408	747	(+)	99.597
ATPase, NPH1 (Cop-D11L)	D11L	CPXV128	NoF1-123	120815	122710	1896	(-)	99.842	NoF2-123	121295	123190	1896	(-)	99.842	NoH1-122	121253	123148	1896	(-)	99.842	SweH1-122	120543	122438	1896	(-)	99.842	SweH2-122	120409	122304	1896	(-)	99.842
mRNA capping enzyme small subunit (Cop-D12L)	D12L	CPXV129	NoF1-124	122744	123607	864	(-)	99.652	NoF2-124	123224	124087	864	(-)	99.652	NoH1-123	123182	124045	864	(-)	99.652	SweH1-123	122472	123335	864	(-)	100	SweH2-123	122338	123201	864	(-)	100
VV_Tan-unkown-16	-	CPXV130	overlap																													
Trimeric virion coat protein (rifampicin res) (Cop-D13L)	D13L	CPXV131	NoF1-125	123638	125293	1656	(-)	99.637	NoF2-125	124118	125773	1656	(-)	99.456	NoH1-124	124076	125731	1656	(-)	99.637	SweH1-124	123366	125021	1656	(-)	99.819	SweH2-124	123232	124887	1656	(-)	99.819
VLTF-2 (late transcription factor 2) (Cop-A1L)	A1L	CPXV132	NoF1-126	125317	125769	453	(-)	100	NoF2-126	125797	126249	453	(-)	100	NoH1-125	125755	126207	453	(-)	100	SweH1-125	125045	125497	453	(-)	98.667	SweH2-125	124911	125363	453	(-)	98.667
VLTF-3 (late transcription factor 3) (Cop-A2L)	A2L	CPXV133	NoF1-127	125790	126464	675	(-)	100	NoF2-127	126270	126944	675	(-)	100	NoH1-126	126228	126902	675	(-)	100	SweH1-126	125518	126192	675	(-)	100	SweH2-126	125384	126058	675	(-)	100
S-S bond formation pathway protein (Cop-A2.5L)	A2.5L	CPXV134	NoF1-128	126461	126694	234	(-)	89.61	NoF2-128	126941	127174	234	(-)	89.61	NoH1-127	126899	127132	234	(-)	89.61	SweH1-127	126189	126419	231	(-)	100	SweH2-127	126055	126285	231	(-)	100
P4b precursor (Cop-A3L)	A3L	CPXV135	NoF1-129	126709	128643	1935	(-)	99.224	NoF2-129	127189	129123	1935	(-)	99.224	NoH1-128	127147	129081	1935	(-)	99.224	SweH1-128	126434	128371	1938	(-)	99.07	SweH2-128	126300	128237	1938	(-)	99.07
39kDa virion core protein (Cop-A4L)	A4L	CPXV136	NoF1-130	128696	129577	882	(-)	92.617	NoF2-130	129176	130084	909	(-)	92.384	NoH1-129	129134	130015	882	(-)	92.617	SweH1-129	128424	129272	849	(-)	93.559	SweH2-129	128290	129138	849	(-)	93.559
RNA polymerase subunit (RPO19) (Cop-A5R)	A5R	CPXV137	NoF1-131	129615	130109	495	(+)	99.39	NoF2-131	130122	130616	495	(+)	100	NoH1-130	130053	130547	495	(+)	100	SweH1-130	129310	129804	495	(+)	100	SweH2-130	129176	129670	495	(+)	100
Viral membrane assembly proteins (VMAP), core p rotein (Cop-A6L)	A6L	CPXV138	NoF1-132	130106	131224	1119	(-)	98.925	NoF2-132	130613	131731	1119	(-)	98.925	NoH1-131	130544	131662	1119	(-)	98.925	SweH1-131	129801	130919	1119	(-)	99.462	SweH2-131	129667	130785	1119	(-)	99.462
VETF-L (early transcription factor large) (Cop- A7L)	A7L	CPXV139	NoF1-133	131248	133380	2133	(-)	99.718	NoF2-133	131755	133887	2133	(-)	99.718	NoH1-132	131686	133818	2133	(-)	99.577	SweH1-132	130943	133075	2133	(-)	99.718	SweH2-132	130809	132941	2133	(-)	99.718
VITF-3 34kda subunit (Cop-A8R)	A8R	CPXV140	NoF1-134	133434	134300	867	(+)	100	NoF2-134	133941	134807	867	(+)	100	NoH1-133	133872	134738	867	(+)	100	SweH1-133	133129	133995	867	(+)	99.653	SweH2-133	132995	133861	867	(+)	99.653
Viral membrane associated, early morphogenesis protein (Cop-A9L)	A9L	CPXV141	NoF1-135	134293	134640	348	(-)	98.667	NoF2-135	134800	135159	360	(-)	98.667	NoH1-134	134731	135093	363	(-)	98.667	SweH1-134	133988	134335	348	(-)	98.667	SweH2-134	133854	134201	348	(-)	98.667
P4a precursor (Cop-A10L)	A10L	CPXV142	NoF1-136	134641	137322	2682	(-)	98.658	NoF2-136	135160	137841	2682	(-)	98.658	NoH1-135	135094	137775	2682	(-)	98.658	SweH1-135	134336	137017	2682	(-)	96.98	SweH2-135	134202	136883	2682	(-)	96.98
Viral membrane assembly proteins (VMAP) (Cop-A1 1R)	A11R	CPXV143	NoF1-137	137337	138293	957	(+)	100	NoF2-137	137856	138812	957	(+)	100	NoH1-136	137790	138746	957	(+)	100	SweH1-136	137032	137988	957	(+)	100	SweH2-136	136898	137854	957	(+)	99.686
Virion core and cleavage processing protein (Co p-A12L)	A12L	CPXV144	NoF1-138	138295	138873	579	(-)	92.708	NoF2-138	138814	139389	576	(-)	97.382	NoH1-137	138748	139323	576	(-)	97.382	SweH1-137	137990	138565	576	(-)	98.429	SweH2-137	137856	138431	576	(-)	98.429
IMV membrane protein, virion maturation (Cop-A1 3L)	A13L	CPXV145	NoF1-139	138897	139109	213	(-)	100	NoF2-139	139413	139625	213	(-)	100	NoH1-138	139347	139559	213	(-)	100	SweH1-138	138589	138801	213	(-)	100	SweH2-138	138455	138667	213	(-)	100
Essential IMV membrane protein (Cop-A14L)	A14L	CPXV146	NoF1-140	139217	139489	273	(-)	98.889	NoF2-140	139733	140005	273	(-)	98.889	NoH1-139	139667	139939	273	(-)	98.889	SweH1-139	138911	139183	273	(-)	98.889	SweH2-139	138777	139049	273	(-)	98.889
Non-essential IMV membrane protein (Cop-A14.5L)	A14.5L	CPXV147	NoF1-141	139506	139667	162	(-)	100	NoF2-141	140022	140183	162	(-)	100	NoH1-140	139956	140117	162	(-)	100	SweH1-140	139200	139361	162	(-)	100	SweH2-140	139066	139227	162	(-)	100
Core protein (Cop-A15L)	A15L	CPXV148	NoF1-142	139657	139941	285	(-)	97.872	NoF2-142	140173	140457	285	(-)	97.872	NoH1-141	140107	140391	285	(-)	97.872	SweH1-141	139351	139635	285	(-)	97.872	SweH2-141	139217	139501	285	(-)	97.872
Myristylated protein, essential for entry/fusio n (Cop-A16L)	A16L	CPXV149	NoF1-143	139925	141058	1134	(-)	99.469	NoF2-143	140441	141574	1134	(-)	99.469	NoH1-142	140375	141508	1134	(-)	99.469	SweH1-142	139619	140752	1134	(-)	99.204	SweH2-142	139485	140618	1134	(-)	99.469
IMV membrane protein (Cop-A17L)	A17L	CPXV150	NoF1-144	141061	141669	609	(-)	100	NoF2-144	141577	142185	609	(-)	100	NoH1-143	141511	142119	609	(-)	100	SweH1-143	140755	141363	609	(-)	99.01	SweH2-143	140621	141229	609	(-)	99.01

DNA helicase, transcript release factor (Cop-A1 8R)	**A18R**	**CPXV151**	NoF1-145	141684	143165	1482	(+)	97.769	NoF2-145	142200	143681	1482	(+)	98.377	NoH1-144	142134	143615	1482	(+)	98.377	SweH1-144	141378	142856	1479	(+)	98.577	SweH2-144	141244	142722	1479	(+)	98.577
Zinc finger-like protein (Cop-A19L)	**A19L**	**CPXV152**	NoF1-146	143146	143379	234	(-)	100	NoF2-146	143662	143895	234	(-)	98.701	NoH1-145	143596	143829	234	(-)	98.701	SweH1-145	142837	143070	234	(-)	100	SweH2-145	142703	142936	234	(-)	100
IMV membrane protein, entry/fusion complex comp onent (Cop-A21L)	**A21L**	**CPXV153**	NoF1-147	143380	143733	354	(-)	100	NoF2-147	143896	144249	354	(-)	100	NoH1-146	143830	144183	354	(-)	100	SweH1-146	143071	143424	354	(-)	100	SweH2-146	142937	143290	354	(-)	100
DNA polymerase processivity factor (Cop-A20R)	**A20R**	**CPXV154**	NoF1-148	143732	145012	1281	(+)	99.296	NoF2-148	144248	145528	1281	(+)	99.061	NoH1-147	144182	145462	1281	(+)	99.061	SweH1-147	143423	144703	1281	(+)	99.765	SweH2-147	143289	144569	1281	(+)	99.765
Holliday junction resolvase (Cop-A22R)	**A22R**	**CPXV155**	NoF1-149	144942	145505	564	(+)	100	NoF2-149	145458	146021	564	(+)	100	NoH1-148	145392	145955	564	(+)	100	SweH1-148	144633	145196	564	(+)	100	SweH2-148	144499	145062	564	(+)	100
VITF-3 45kda subunit (Cop-A23R)	**A23R**	**CPXV156**	NoF1-150	145525	146673	1149	(+)	99.738	NoF2-150	146041	147189	1149	(+)	99.738	NoH1-149	145975	147123	1149	(+)	99.738	SweH1-149	145216	146364	1149	(+)	99.738	SweH2-149	145082	146230	1149	(+)	99.738
RNA polymerase subunit (RPO132) (Cop-A24R)	**A24R**	**rpo132/CPXV157**	NoF1-151	146670	150164	3495	(+)	99.742	NoF2-151	147186	150680	3495	(+)	99.828	NoH1-150	147120	150614	3495	(+)	99.828	SweH1-150	146361	149855	3495	(+)	99.914	SweH2-150	146227	149721	3495	(+)	99.914
A-type inclusion protein (Cop-A25L)	**A25L**	**CPXV158**	NoF1-152	150142	153918	3777	(-)	94.319	NoF2-152	150658	154434	3777	(-)	94.397	NoH1-151	150592	154368	3777	(-)	94.397	SweH1-151	149833	153621	3789	(-)	94.88	SweH2-151	149699	153487	3789	(-)	94.88
Unknown (CPV-B-160)	-	**CPXV160**	overlap																												
Pic precursor (Cop-A26L)	**A26L**	**CPXV161**	NoF1-153	153964	155532	1569	(-)	97.255	NoF2-153	154480	156033	1554	(-)	97.255	NoH1-152	154414	155985	1572	(-)	97.255	SweH1-152	153666	155255	1590	(-)	98.039	SweH2-152	153532	155121	1590	(-)	98.039
IMV surface protein, fusion protein (Cop-A27L)	**A27L**	**CPXV162**	NoF1-154	155584	155916	333	(-)	100	NoF2-154	156085	156417	333	(-)	100	NoH1-153	156037	156369	333	(-)	100	SweH1-153	155307	155639	333	(-)	100	SweH2-153	155173	155505	333	(-)	100
IMV MP|Virus entry (Cop-A28L)	**A28L**	**CPXV163**	NoF1-155	155917	156357	441	(-)	98.63	NoF2-155	156418	156858	441	(-)	98.63	NoH1-154	156370	156810	441	(-)	98.63	SweH1-154	155640	156080	441	(-)	98.63	SweH2-154	155506	155946	441	(-)	98.63
RNA polymerase subunit (RPO35) (Cop-A29L)	**A29L**	**CPXV164**	NoF1-156	156358	157275	918	(-)	99.344	NoF2-156	156859	157776	918	(-)	99.016	NoH1-155	156811	157728	918	(-)	99.344	SweH1-155	156081	156998	918	(-)	98.361	SweH2-155	155947	156864	918	(-)	98.361
IMV protein (Cop-A30L)	**A30L**	**CPXV165**	NoF1-157	157238	157468	231	(-)	98.684	NoF2-157	157739	157969	231	(-)	98.684	NoH1-156	157691	157921	231	(-)	98.684	SweH1-156	156961	157194	234	(-)	96.104	SweH2-156	156827	157060	234	(-)	96.104
Viral membrane assembly proteins (VMAP) (Cop-A 30.5L)	**A30.5L**	**165.5**	NoF1-158	157501	157629	129	(-)	100	NoF2-158	158002	158130	129	(-)	100	NoH1-157	157954	158082	129	(-)	100	SweH1-157	157227	157355	129	(-)	97.619	SweH2-157	157093	157221	129	(-)	97.619
Hypothetical protein (Cop-A31R)	**A31R**	**CPXV166**	NoF1-159	157628	158041	414	(+)	97.143	NoF2-159	158129	158536	408	(+)	95.714	NoH1-158	158081	158488	408	(+)	95.714	SweH1-158	157354	157764	411	(+)	95	SweH2-158	157220	157624	405	(+)	93.617
ATPase|DNA packaging protein (Cop-A32L)	**A32L**	**CPXV167**	NoF1-160	158011	158820	810	(-)	99.257	NoF2-160	158506	159315	810	(-)	99.257	NoH1-159	158458	159267	810	(-)	99.257	SweH1-159	157773	158543	771	(-)	100	SweH2-159	157594	158403	810	(-)	100
EEV membrane phosphoglycoprotein, C-type lectin -like domain (Cop-A33R)	**A33R**	**CPXV168**	NoF1-161	158938	159513	576	(+)	95.312	NoF2-161	159433	160023	591	(+)	89.848	NoH1-160	159385	159999	615	(+)	86.341	SweH1-160	158661	159221	561	(+)	98.396	SweH2-160	158521	159081	561	(+)	98.396
C-type lectin-like IEV|EEV glycoprotein (Cop-A34R)	**A34R**	**CPXV169**	NoF1-162	159537	160043	507	(+)	99.405	NoF2-162	160047	160553	507	(+)	99.405	NoH1-161	160023	160529	507	(+)	99.405	SweH1-161	159245	159751	507	(+)	100	SweH2-161	159105	159611	507	(+)	100
VV-Cop-A ORF M	-	**CPXV170**	overlap																												
MHC class II antigen presentation inhibitor (Co p-A35R)	**A35R**	**CPXV171**	NoF1-163	160089	160619	531	(+)	100	NoF2-163	160599	161129	531	(+)	100	NoH1-162	160575	161105	531	(+)	100	SweH1-162	159794	160324	531	(+)	99.432	SweH2-162	159654	160184	531	(+)	99.432
IEV transmembrane phosphoprotein (Cop-A36R)	**A36R**	**CPXV172**	NoF1-164	160683	161351	669	(+)	98.214	NoF2-164	161193	161861	669	(+)	97.768	NoH1-163	161169	161837	669	(+)	97.768	SweH1-163	160388	161050	663	(+)	97.768	SweH2-163	160248	160910	663	(+)	97.768
Hypothetical protein (Cop-A37R)	**A37R**	**CPXV173**	NoF1-165	161418	162209	792	(+)	99.24	NoF2-165	161928	162719	792	(+)	98.859	NoH1-164	161904	162695	792	(+)	98.859	SweH1-164	161117	161908	792	(+)	96.958	SweH2-164	160977	161768	792	(+)	96.958
Unknown (Gar-A43R)	-	**CPXV174**	NoF1-166	162317	162502	186	(+)	93.651	NoF2-166	162827	163006	180	(+)	90.476	NoH1-165	162803	162982	180	(+)	90.476	SweH1-165	162016	162204	189	(+)	96.61	SweH2-165	161876	162064	189	(+)	96.61
CD47-like, integral membrane protein (Cop-A38L)	**A38L**	**CPXV175**	NoF1-167	162499	163332	834	(-)	99.278	NoF2-167	163003	163836	834	(-)	98.917	NoH1-166	162979	163812	834	(-)	98.917	SweH1-166	162201	163034	834	(-)	96.751	SweH2-166	162061	162894	834	(-)	96.751
Semaphorin (Cop-A39R)	**A39R**	**CPXV176**	NoF1-168	163348	164559	1212	(+)	98.01	NoF2-168	163852	165057	1206	(+)	98.25	NoH1-167	163828	165033	1206	(+)	98.25	SweH1-167	163050	164288	1239	(+)	98.786	SweH2-167	162910	164148	1239	(+)	98.544
Lectin homolog (Cop-A40R)	**A40R**	**CPXV177**	NoF1-169	164581	165063	483	(+)	97.5	NoF2-169	165079	165561	483	(+)	97.5	NoH1-168	165055	165537	483	(+)	97.5	SweH1-168	164285	164767	483	(+)	96.875	SweH2-168	164145	164627	483	(+)	96.875
Chemokine binding protein (Cop-A41L)	**A41L**	**CPXV178**	NoF1-170	165161	165823	663	(-)	98.182	NoF2-170	165659	166321	663	(-)	97.727	NoH1-169	165635	166297	663	(-)	97.727	SweH1-169	164865	165524	660	(-)	98.174	SweH2-169	164725	165384	660	(-)	98.174
Profilin-like protein, ATI-localized (Cop-A42R)	**A42R**	**CPXV179**	NoF1-171	166002	166403	402	(+)	99.248	NoF2-171	166500	166901	402	(+)	99.248	NoH1-170	166476	166877	402	(+)	99.248	SweH1-170	165696	166097	402	(+)	100	SweH2-170	165556	165957	402	(+)	100
Type I membrane glycoprotein (Cop-A43R)	**A43R**	**CPXV180**	NoF1-172	166441	167022	582	(+)	98.964	NoF2-172	166939	167520	582	(+)	99.482	NoH1-171	166915	167496	582	(+)	99.482	SweH1-171	166135	166716	582	(+)	100	SweH2-171	165995	166576	582	(+)	100
Hypothetical protein (Cop-A43.5R)	**A43.5R**	**CPXV181**	NoF1-173	167025	167270	246	(+)	100	NoF2-173	167523	167768	246	(+)	100	NoH1-172	167499	167744	246	(+)	100	SweH1-172	166719	166964	246	(+)	98.765	SweH2-172	166579	166824	246	(+)	98.765
3 beta-hydroxysteroid dehydrogenase|delta 5->4 isomerase (Cop-A44L)	**A44L**	**CPXV182**	NoF1-174	167362	168402	1041	(-)	98.261	NoF2-174	167859	168899	1041	(-)	98.261	NoH1-173	167835	168875	1041	(-)	98.261	SweH1-173	167058	168095	1038	(-)	98.261	SweH2-173	166918	167955	1038	(-)	98.261
Inactive Cu-Zn superoxide dismutase-like virion protein (Cop-A45R)	**A45R**	**CPXV183**	NoF1-175	168449	168826	378	(+)	98.4	NoF2-175	168946	169323	378	(+)	98.4	NoH1-174	168922	169299	378	(+)	98.4	SweH1-174	168142	168519	378	(+)	98.4	SweH2-174	168002	168379	378	(+)	98.4
IL-1|TLR signaling inhibitor (Cop-A46R)	**A46R**	**CPXV184**	NoF1-176	168816	169538	723	(+)	98.75	NoF2-176	169313	170035	723	(+)	98.333	NoH1-175	169289	170011	723	(+)	98.333	SweH1-175	168509	169231	723	(+)	99.583	SweH2-175	168369	169091	723	(+)	99.167
Immunoprevalent protein (Cop-A47L)	**A47L**	**CPXV185**	NoF1-177	169674	170408	735	(-)	97.131	NoF2-177	170147	170881	735	(-)	97.131	NoH1-176	170123	171031	909	(-)	97.131	SweH1-176	169376	170110	735	(-)	97.541	SweH2-176	169249	169983	735	(-)	97.541
Thymidylate kinase (Cop-A48R)	**A48R**	**CPXV186**	NoF1-178	170281	171123	843	(+)	97.333	NoF2-178	170754	171596	843	(+)	97.333	NoH1-177	170730	171572	843	(+)	97.333	SweH1-177	170143	170826	684	(+)	97.797	SweH2-177	170016	170699	684	(+)	97.797
Putative phosphotransferase|anion transport pro tein (Cop-A49R)	**A49R**	**CPXV187**	NoF1-179	171172	171660	489	(+)	96.296	NoF2-179	171645	172133	489	(+)	96.296	NoH1-178	171621	172109	489	(+)	96.296	SweH1-178	170875	171387	513	(+)	96.296	SweH2-178	170748	171260	513	(+)	96.296
ATP-dependent DNA ligase (Cop-A50R)	**A50R**	**CPXV188**	NoF1-180	171693	173357	1665	(+)	99.638	NoF2-180	172168	173832	1665	(+)	99.639	NoH1-179	172144	173808	1665	(+)	99.639	SweH1-179	171384	173042	1659	(+)	99.097	SweH2-179	171257	172915	1659	(+)	99.097
Hypothetical protein (Cop-A51R)	**A51R**	**CPXV189**	NoF1-181	173410	174414	1005	(+)	99.102	NoF2-181	173885	174889	1005	(+)	98.802	NoH1-180	173861	174865	1005	(+)	99.102	SweH1-180	173095	174099	1005	(+)	98.802	SweH2-180	172968	173972	1005	(+)	98.802
Toll|IL-1 receptor-like protein, IL-1, NFkB sig nalling inhibitor (Cop-A52R)	**A52R**	**CPXV190**	NoF1-182	174483	175055	573	(+)	98.947	NoF2-182	174960	175532	573	(+)	98.947	NoH1-181	174935	175507	573	(+)	98.947	SweH1-181	174168	174743	576	(+)	98.429	SweH2-181	174041	174616	576	(+)	98.429
TNF receptor (CrmC) (Cop-A53R)	**A53R**	**CrmC/CPXV191**	-	-	-	-	-	-	NoF2-183	175854	176414	561	(+)	94.086	NoH1-182	175829	176389	561	(+)	94.086	SweH1-182	175055	175615	561	(+)	93.548	SweH2-182	174928	175488	561	(+)	93.548
CPV-B-192	-	**CPXV192**	NoF1-183	175819	175989	171	(+)	100	overlap																						
BTB Kelch-domain containing protein; CRL comple x (Cop-A55R)	**A55R**	**CPXV193**	NoF1-184	176193	177884	1692	(+)	98.224	NoF2-184	176679	178370	1692	(+)	98.579	NoH1-183	176654	178345	1692	(+)	98.579	SweH1-183	175884	177575	1692	(+)	98.579	SweH2-183	175757	177448	1692	(+)	98.579
Hemagglutinin (Cop-A56R)	**A56R**	**CPXV194**	NoF1-185	177936	178850	915	(+)	94.737	NoF2-185	178422	179336	915	(+)	95.066	NoH1-184	178397	179311	915	(+)	95.066	SweH1-184	177627	178526	900	(+)	92	SweH2-184	177500	178402	903	(+)	92.667
Guanylate kinase (Cop-A56.5R)	**A57R**	**CPXV195**	NoF1-186	178867	179460	594	(+)	98.985	NoF2-186	179353	179946	594	(+)	98.985	NoH1-185	179328	179921	594	(+)	98.985	SweH1-185	178543	179136	594	(+)	98.985	SweH2-185	178419	179012	594	(+)	98.985
Ser|Thr Kinase (Cop-B1R)	**B1R**	**CPXV196**	NoF1-187	179610	180509	900	(+)	97.324	NoF2-187	180096	180995	900	(+)	98.328	NoH1-186	180071	180970	900	(+)	98.328	SweH1-186	179286	180185	900	(+)	97.324	SweH2-186	179162	180061	900	(+)	97.324
Schlafen (Cop-B2R)	**B2R**	**CPXV197**	NoF1-188	180579	182096	1518	(+)	94.257	NoF2-188	181065	182582	1518	(+)	94.257	NoH1-187	181040	182557	1518	(+)	94.257	SweH1-187	180253	181770	1518	(+)	96.238	SweH2-187	180129	181646	1518	(+)	96.238
Ankyrin (Cop-B4R)	**B4R**	**CPXV198**	NoF1-189	182360	184045	1686	(+)	97.504	NoF2-189	182880	184490	1611	(+)	94.454	NoH1-188	182855	184528	1674	(+)	98.211	SweH1-188	182014	183690	1677	(+)	97.317	SweH2-188	181890	183566	1677	(+)	97.317
EEV type-1 membrane glycoprotein, protective an tigen (Cop-B5R)	**B5R**	**CPXV199**	NoF1-190	184149	185102	954	(+)	98.738	NoF2-190	184594	185547	954	(+)	98.738	NoH1-189	184632	185585	954	(+)	98.738	SweH1-189	183794	184747	954	(+)	98.738	SweH2-189	183670	184623	954	(+)	98.423
Ankyrin-like protein (Cop-B6R)	**B6R**	**CPXV200**	NoF1-191	185201	185500	300	(+)	100	NoF2-191	185646	186179	534	(+)	98.324	NoH1-190	185684	186217	534	(+)	98.324	SweH1-190	184833	185369	537	(+)	93.296	SweH2-190	184709	185245	537	(+)	93.296
Virulence, ER resident (Cop-B7R)	**B7R**	**CPXV201**	NoF1-192	185774	186319	546	(+)	97.79	NoF2-192	186218	186763	546	(+)	97.238	NoH1-191	186256	186801	546	(+)	97.238	SweH1-191	185408	185962	555	(+)	94.565	SweH2-191	185284	185838	555	(+)	94.565
Soluble IFN-g receptor-like protein (Cop-B8R)	**B8R**	**CPXV202**	NoF1-193	186371	187171	801	(+)	99.248	NoF2-193	186815	187615	801	(+)	99.248	NoH1-192	186853	187653	801	(+)	99.248	SweH1-192	186014	186814	801	(+)	98.872	SweH2-192	185890	186690	801	(+)	98.872
ER-localized apoptosis regulator (Cop-B9R)	**B9R**	**CPXV203**	NoF1-194	187192	187929	738	(+)	97.333	NoF2-194	187636	188373	738	(+)	97.333	NoH1-193	187674	188411	738	(+)	97.333	SweH1-193	186896	187573	678	(+)	96.889	SweH2-193	186772	187449	678	(+)	96.889
Kelch-like protein (Cop-B10R)	**B10R**	**CPXV204**	NoF1-195	188076	189581	1506	(+)	99.002	NoF2-195	188519	190024	1506	(+)	99.002	NoH1-194	188557	190062	1506	(+)	99.002	SweH1-194	187719	189224	1506	(+)	99.202	SweH2-194	187595	189100	1506	(+)	99.202
Hypothetical protein (Cop-B11R)	**B11R**	**CPXV205**	NoF1-196	189663	189887	225	(+)	94.03	NoF2-196	190106	190330	225	(+)	94.03	NoH1-195	190144	190368	225	(+)	94.03	SweH1-195	189306	189530	225	(+)	94.03	SweH2-195	189182	189406	225	(+)	94.03
Ser|Thr Kinase (Cop-B12R)	**B12R**	**CPXV206**	NoF1-197	189954	190817	864	(+)	98.258	NoF2-197	190397	191260	864	(+)	98.955	NoH1-196	190435	191298	864	(+)	98.955	SweH1-196	189597	190466	870	(+)	98.616	SweH2-196	189473	190342	870	(+)	98.616
Serpin 1,2,3 (Cop-K2L)	**B14R**	**CrmA/CPXV207**	NoF1-198	190914	191948	1035	(+)	97.674	NoF2-198	191356	192390	1035	(+)	97.093	NoH1-197	191394	192428	1035	(+)	97.093	SweH1-197	190563	191597	1035	(+)	97.093	SweH2-197	190439	191473	1035	(+)	97.093
Hypothetical protein (Cop-C16L)	**B15R**	**CPXV208**	NoF1-199	192079	192528	450	(+)	99.329	NoF2-199	192520	192969	450	(+)	99.329	NoH1-198	192558	193007	450	(+)	99.329	SweH1-198	191722	192171	450	(+)	99.329	SweH2-198	191597	192046	450	(+)	98.658
IL-1 beta receptor (Cop-B16R)	**B16R**	**CPXV209**	NoF1-200	192612	193589	978	(+)	96.933	NoF2-200	193053	194030	978	(+)	96.933	NoH1-199	193091	194068	978	(+)	96.933	SweH1-199	192256	193236	981	(+)	95.399	SweH2-199	192131	193111	981	(+)	95.399
IL-1 beta inhibitor (Cop-B17L)	**B17L**	**CPXV210**	NoF1-201	193637	194659	1023	(-)	98.235	NoF2-201	194078	195100	1023	(-)	98.824	NoH1-200	194116	195138	1023	(-)	98.824	SweH1-200	193284	194306	1023	(-)	98.235	SweH2-200	193159	194181	1023	(-)	98.235
Ankyrin (Cop-B18R)	**B18R**	**CPXV211**	NoF1-202	194801	196525	1725	(+)	97.387	NoF2-202	195242	196966	1725	(+)	97.213	NoH1-201	195280	197004	1725	(+)	97.213	SweH1-201	194447	196171	1725	(+)	97.909	SweH2-201	194322	196046	1725	(+)	97.909
IFN-alpha|beta receptor glycoprotein (Cop-B19R)	**B19R**	**CPXV212**	NoF1-203	196544	197641	1098	(+)	92.077	NoF2-203	196985	198082	1098	(+)	91.803	NoH1-202	197023	198120	1098	(+)	91.803	SweH1-202	196190	197287	1098	(+)	95.082	SweH2-202	196065	197162	1098	(+)	94.809
Ankyrin (Cop-B20R)	**B20R**	**CPXV213**	NoF1-204	197702	200059	2358	(+)	89.25	NoF2-204	198144	200525	2382	(+)	89.552	NoH1-203	198182	200563	2382	(+)	89.552	SweH1-203	197349	199751	2403	(+)	96.02	SweH2-203	197224	199626	2403	(+)	96.02
CPV-B-214	-	**CPXV214**	overlap																												
kelch-like protein (EV-M-167)	-	**CPXV215**	NoF1-205	200162	201835	1674	(+)	97.846	NoF2-205	200631	202304	1674	(+)	96.409	NoH1-204	200669	202342	1674	(+)	96.409	SweH1-204	199852	201525	1674	(+)	97.846	SweH2-204	199727	201400	1674	(+)	97.846
Hypothetical protein (Cop-C11.5R)	**C11.5R**	**CPXV216**	-	-	-	-	-	-	-	-	-	-	-	-	-	-	-	-	-	-	-	-	-	-	-	-	-	-	-	-	-
Serpin 1,2,3 (Cop-K2L)	**C12L**	**CPXV217**	NoF1-206	202015	203124	1110	(+)	95.81	NoF2-206	202484	203596	1113	(+)	95.014	NoH1-205	202522	203634	1113	(+)	95.014	SweH1-205	201705	202826	1122	(+)	96.774	SweH2-205	201580	202701	1122	(+)	96.505
Hypothetical protein (Cop-C14L)	**C14L**	**CPXV218**	NoF1-207	203301	203882	582	(+)	94.845	NoF2-207	203756	204337	582	(+)	94.845	NoH1-206	203794	204375	582	(+)	94.845	SweH1-206	202990	203571	582	(+)	96.373	SweH2-206	202865	203446	582	(+)	96.373
Surface glycoprotein	**B20.5R**	**CPXV219**	NoF1-208	204128	209893	5766	(+)	96.573	NoF2-208	204583	210348	5766	(+)	96.573	NoH1-207	204621	210386	5766	(+)	96.573	SweH1-207	203817	209591	5775	(+)	96.366	SweH2-207	203692	209466	5775	(+)	96.469
Ankyrin (Cop-C19L)	**C19L**	**CPXV220**	NoF1-209	210110	211915	1806	(+)	95.958	NoF2-209	210565	212370	1806	(+)	95.958	NoH1-208	210603	212408	1806	(+)	95.958	SweH1-208	209874	211613	1740	(+)	95.855	SweH2-208	209749	211488	1740	(+)	95.855
TNF receptor (CrmD)	-	**CPXV221**	NoF1-210	211922	212890	969	(+)	98.137	NoF2-210	212377	213345	969	(+)	98.447	NoH1-209	212415	213383	969	(+)	98.447	SweH1-209	211620	212588	969	(+)	98.758	SweH2-209	211495	212463	969	(+)	98.758
TNF-alpha receptor (CPXV-GRI-K3R)*	-	-	-	-	-	-	-	-	-	-	-	-	-	-	-	-	-	-	-	-	SweH1-210	212662	213087	426	(+)	-	SweH2-210	212537	212962	426	(+)	-
Hypothetical protein (Cop-C16L)	**C16L**	**CPXV222**	NoF1-211	213564	214025	462	(+)	96.732	NoF2-211	214078	214539	462	(+)	96.732	NoH1-210	214116	214577	462	(+)	96.732	SweH1-211	213283	213744	462	(+)	97.386	SweH2-211	213159	213620	462	(+)	97.386
Ankyrin (Cop-C17L)	**B23R/C17L**	**CPXV223**	NoF1-212	214240	216246	2007	(+)	96.731	NoF2-212	214732	216738	2007	(+)	97.177	NoH1-211	214747	216753	2007	(+)	97.028	SweH1-212	213946	215967	2022	(+)	96.154	SweH2-212	213806	215827	2022	(+)	96.006
Ankyrin-like repeat containing protein	-	**CPXV224**	NoF1-213	216286	216375	90	(+)	100	NoF2-213	216778	216867	90	(-)	93.1	NoH1-212	216793	216882	90	(-)	100	SweH1-213	216007	216138	132	(+)	82.927	SweH2-213	215867	215998	132	(+)	82.927
Ankyrin (Cop-C19L)	**B25R/C19L**	**CPXV225**	NoF1-214	216457	218223	1767	(+)	95.748	NoF2-214	216949	218715	1767	(+)	95.748	NoH1-213	216964	218730	1767	(+)	95.748	SweH1-214	216163	217929	1767	(+)	94.898	SweH2-214	216023	217789	1767	(+)	94.898
TNF receptor (CrmB) (Cop-C22L)	**B28R/C22L**	**crmB/CPXV226**	NoF1-215	218301	219374	1074	(+)	91.808	NoF2-215	218793	219866	1074	(+)	92.09	NoH1-214	218808	219881	1074	(+)	92.09	SweH1-215	218015	219070	1056	(+)	92.537	SweH2-215	217875	218930	1056	(+)	92.537
Chemokine binding protein (Cop-C23L)	**B29R/C23L**	**vCCI/CPXV227**	NoF1-216	219448	220185	738	(+)	91.129	NoF2-216	219940	220677	738	(+)	91.935	NoH1-215	219955	220692	738	(+)	92.339	SweH1-216	219170	219919	750	(+)	91.968	SweH2-216	219030	219779	750	(+)	93.574
CPV-B-002	-	**CPXV228**	NoF1-217	220214	220441	228	(+)	85.135	NoF2-217	220706	220933	228	(+)	85.135	-	-	-	-	-	-	SweH1-217	219948	220187	240	(+)	83.333	SweH2-217	219808	220041	234	(+)	85.526

Table S6. Patristic distances between CPXV clusters and OPXV species calculated from the Maximum likelihood (ML) and Bayesian inference (BI) trees of 62 conserved genes, 87 OPXV whole genomes, core genomes and orthologous genes.

ML tree of 62 conserved genes															
	VACV	VACV-like	CPXV-like1	CPXV-like2	VARV-like	TATV	CMLV	ABATINO	MPXV	ECTV	TV-Abatino-	VARV	AKMV	AKPV	New World
VACV															
VACV-like	0.026														
CPXV-like1	0.045	0.037													
CPXV-like2	0.050	0.042	0.048												
VARV-like	0.031	0.021	0.043	0.049											
TATV	0.036	0.026	0.048	0.053	0.016										
CMLV	0.040	0.030	0.052	0.058	0.020	0.011									
ABATINO	0.046	0.038	0.049	0.055	0.044	0.049	0.053								
MPXV	0.034	0.030	0.043	0.048	0.033	0.037	0.041	0.044							
ECTV	0.044	0.038	0.048	0.053	0.043	0.047	0.052	0.028	0.045						
ECTV-Abatino-like	0.041	0.033	0.044	0.049	0.039	0.044	0.048	0.037	0.041	0.037					
VARV	0.046	0.037	0.059	0.064	0.026	0.018	0.022	0.059	0.052	0.060	0.054				
AKMV	0.082	0.074	0.085	0.091	0.080	0.085	0.089	0.084	0.083	0.084	0.078	0.095			
AKPV	0.170	0.162	0.174	0.179	0.169	0.173	0.178	0.172	0.171	0.173	0.167	0.184	0.148		
New World	0.693	0.685	0.697	0.702	0.692	0.696	0.700	0.695	0.694	0.696	0.690	0.707	0.671	0.703	
BI tree of 62 conserved genes															
	VACV	VACV-like	CPXV-like1	CPXV-like2	VARV-like	TATV	CMLV	ABATINO	MPXV	ECTV	TV-Abatino-	VARV	AKMV	AKPV	New World
VACV															
VACV-like	0.026														
CPXV-like1	0.044	0.036													
CPXV-like2	0.051	0.043	0.048												
VARV-like	0.030	0.021	0.042	0.049											
TATV	0.035	0.026	0.047	0.054	0.016										
CMLV	0.039	0.030	0.051	0.058	0.020	0.011									
ABATINO	0.045	0.038	0.048	0.055	0.044	0.048	0.052								
MPXV	0.038	0.030	0.045	0.052	0.036	0.041	0.045	0.046							
ECTV	0.046	0.038	0.048	0.055	0.044	0.049	0.053	0.023	0.047						
ECTV-Abatino-like	0.040	0.032	0.043	0.050	0.038	0.043	0.047	0.036	0.041	0.037					
VARV	0.046	0.036	0.057	0.064	0.026	0.018	0.022	0.059	0.051	0.059	0.054				
AKMV	0.080	0.073	0.083	0.090	0.079	0.083	0.087	0.082	0.081	0.083	0.077	0.094			
AKPV	0.166	0.158	0.169	0.176	0.165	0.169	0.173	0.168	0.167	0.168	0.163	0.180	0.220		
New World	0.427	0.419	0.430	0.437	0.426	0.430	0.434	0.429	0.428	0.429	0.424	0.441	0.405	0.435	
ML tree of 87 OPXV whole genomes															
	VACV	VACV-like	CPXV-like1	CPXV-like2	VARV-like	TATV	CMLV	ABATINO	MPXV	ECTV	TV-Abatino-	VARV	AKMV	AKPV	New World
VACV															
VACV-like	0.026														
CPXV-like1	0.043	0.034													
CPXV-like2	0.063	0.053	0.052												
VARV-like	0.037	0.027	0.031	0.051											
TATV	0.041	0.031	0.036	0.055	0.016										
CMLV	0.045	0.036	0.040	0.059	0.020	0.012									
ABATINO	0.060	0.051	0.049	0.061	0.048	0.053	0.057								
MPXV	0.039	0.072	0.050	0.069	0.043	0.048	0.052	0.067							
ECTV	0.066	0.056	0.055	0.066	0.054	0.058	0.062	0.030	0.072						
ECTV-Abatino-like	0.062	0.052	0.051	0.062	0.050	0.054	0.058	0.046	0.068	0.052					
VARV	0.052	0.043	0.047	0.066	0.027	0.019	0.023	0.064	0.059	0.070	0.065				
AKMV	0.096	0.087	0.085	0.096	0.084	0.089	0.093	0.088	0.103	0.093	0.089	0.100			
AKPV	0.188	0.179	0.178	0.189	0.177	0.181	0.185	0.180	0.195	0.185	0.181	0.192	0.161		
New World	0.744	0.735	0.733	0.745	0.733	0.737	0.741	0.736	0.751	0.741	0.737	0.748	0.717	0.740	
BI tree of 87 OPXV whole genomes															
	VACV	VACV-like	CPXV-like1	CPXV-like2	VARV-like	TATV	CMLV	ABATINO	MPXV	ECTV	TV-Abatino-	VARV	AKMV	AKPV	New World
VACV															
VACV-like	0.026														
CPXV-like1	0.043	0.033													
CPXV-like2	0.069	0.053	0.058												
VARV-like	0.036	0.027	0.031	0.050											
TATV	0.041	0.031	0.035	0.055	0.016										
CMLV	0.045	0.035	0.040	0.059	0.020	0.012									
ABATINO	0.060	0.050	0.049	0.060	0.048	0.052	0.056								
MPXV	0.039	0.032	0.049	0.069	0.043	0.047	0.051	0.066							
ECTV	0.065	0.056	0.054	0.065	0.053	0.058	0.062	0.030	0.072						
ECTV-Abatino-like	0.061	0.052	0.050	0.061	0.049	0.054	0.058	0.046	0.068	0.051					
VARV	0.052	0.042	0.047	0.066	0.027	0.019	0.023	0.063	0.058	0.069	0.065				
AKMV	0.095	0.086	0.084	0.095	0.083	0.088	0.092	0.086	0.102	0.092	0.088	0.099			
AKPV	0.185	0.176	0.175	0.186	0.174	0.178	0.182	0.177	0.192	0.182	0.178	0.189	0.158		
New World	0.469	0.460	0.459	0.470	0.458	0.462	0.466	0.461	0.476	0.466	0.462	0.473	0.442	0.464	

ML tree of 87 OPXV core genomes															
	VACV	VACV-like	CPXV-like1	CPXV-like2	VARV-like	TATV	CMLV	ABATINO	MPXV	ECTV	TV-Abatino-	VARV	AKMV	AKPV	New World
VACV															
VACV-like	0.026														
CPXV-like1	0.042	0.033													
CPXV-like2	0.040	0.053	0.034												
VARV-like	0.037	0.027	0.031	0.051											
TATV	0.041	0.031	0.035	0.055	0.016										
CMLV	0.045	0.035	0.039	0.059	0.020	0.012									
ABATINO	0.060	0.051	0.049	0.060	0.048	0.052	0.056								
MPXV	0.039	0.032	0.050	0.070	0.044	0.048	0.052	0.067							
ECTV	0.067	0.057	0.055	0.067	0.055	0.059	0.063	0.032	0.074						
ECTV-Abatino-like	0.057	0.052	0.045	0.049	0.045	0.049	0.053	0.046	0.063	0.053					
VARV	0.054	0.044	0.048	0.068	0.029	0.021	0.025	0.065	0.060	0.072	0.067				
AKMV	0.096	0.086	0.085	0.096	0.084	0.088	0.092	0.087	0.103	0.094	0.089	0.101			
AKPV	0.187	0.177	0.175	0.187	0.175	0.179	0.183	0.178	0.194	0.184	0.180	0.191	0.159		
New World	0.739	0.729	0.728	0.739	0.727	0.731	0.735	0.730	0.746	0.737	0.732	0.744	0.711	0.734	
BI tree of 87 OPXV core genomes															
	VACV	VACV-like	CPXV-like1	CPXV-like2	VARV-like	TATV	CMLV	ABATINO	MPXV	ECTV	TV-Abatino-	VARV	AKMV	AKPV	New World
VACV															
VACV-like	0.026														
CPXV-like1	0.043	0.033													
CPXV-like2	0.062	0.053	0.051												
VARV-like	0.037	0.027	0.031	0.051											
TATV	0.040	0.031	0.035	0.054	0.016										
CMLV	0.044	0.035	0.039	0.058	0.020	0.012									
ABATINO	0.052	0.050	0.040	0.045	0.040	0.044	0.048								
MPXV	0.039	0.031	0.049	0.069	0.043	0.047	0.051	0.066							
ECTV	0.066	0.057	0.055	0.066	0.054	0.058	0.062	0.031	0.073						
ECTV-Abatino-like	0.061	0.052	0.050	0.061	0.050	0.053	0.057	0.046	0.068	0.052					
VARV	0.053	0.043	0.047	0.067	0.028	0.020	0.024	0.064	0.059	0.070	0.066				
AKMV	0.095	0.085	0.083	0.095	0.083	0.087	0.091	0.086	0.101	0.092	0.087	0.099			
AKPV	0.183	0.174	0.172	0.183	0.171	0.175	0.179	0.174	0.190	0.181	0.176	0.188	0.155		
New World	0.464	0.454	0.452	0.464	0.452	0.456	0.460	0.455	0.470	0.461	0.456	0.468	0.436	0.458	
ML tree of OPXV orthologous genes															
	VACV	VACV-like	CPXV-like1	CPXV-like2	VARV-like	TATV	CMLV	ABATINO	MPXV	ECTV	TV-Abatino-	VARV	AKMV	AKPV	New World
VACV															
VACV-like	0.024														
CPXV-like1	0.042	0.034													
CPXV-like2	0.061	0.053	0.058												
VARV-like	0.038	0.030	0.029	0.054											
TATV	0.041	0.033	0.033	0.057	0.017										
CMLV	0.045	0.038	0.037	0.062	0.021	0.013									
ABATINO	0.056	0.048	0.054	0.062	0.049	0.053	0.057								
MPXV	0.039	0.023	0.049	0.068	0.045	0.048	0.052	0.063							
ECTV	0.061	0.053	0.058	0.067	0.054	0.057	0.062	0.030	0.061						
ECTV-Abatino-like	0.059	0.052	0.057	0.066	0.053	0.056	0.060	0.049	0.060	0.054					
VARV	0.052	0.044	0.043	0.068	0.027	0.018	0.023	0.063	0.052	0.068	0.066				
AKMV	0.092	0.084	0.089	0.098	0.085	0.088	0.093	0.087	0.092	0.092	0.091	0.099			
AKPV	0.189	0.181	0.187	0.195	0.182	0.186	0.190	0.185	0.190	0.189	0.188	0.196	0.164		
New World	0.762	0.754	0.760	0.768	0.755	0.759	0.763	0.758	0.763	0.762	0.761	0.769	0.737	0.762	

Table S7. Genetic distances between CPXV clusters and OPXV species estimated by p-distances from the alignment of 62 conserved genes (A), 87 OPXV whole genomes (B), core genomes (C) and orthologous genes (D).

A															
	VACV	VACV-like	CPXV-like1	CPXV-like2	VARV-like	TATV	CMLV	ABATINO	MPXV	ECTV	TV-Abatino-	VARV	AKMV	AKPV	New World
VACV															
VACV-like	0.013														
CPXV-like1	0.016	0.014													
CPXV-like2	0.022	0.019	0.019												
VARV-like	0.015	0.013	0.014	0.021											
TATV	0.018	0.016	0.016	0.023	0.011										
CMLV	0.020	0.018	0.019	0.025	0.014	0.008									
ABATINO	0.025	0.022	0.023	0.023	0.023	0.026	0.028								
MPXV	0.021	0.018	0.021	0.024	0.020	0.023	0.025	0.027							
ECTV	0.024	0.021	0.023	0.025	0.022	0.025	0.028	0.016	0.026						
ECTV-Abatino-like	0.020	0.017	0.020	0.021	0.020	0.023	0.025	0.022	0.023	0.023					
VARV	0.024	0.022	0.022	0.029	0.017	0.012	0.015	0.032	0.028	0.031	0.029				
AKMV	0.042	0.040	0.039	0.043	0.039	0.041	0.043	0.044	0.045	0.044	0.044	0.046			
AKPV	0.075	0.073	0.073	0.075	0.074	0.075	0.076	0.075	0.077	0.077	0.074	0.079	0.068		
New World	0.127	0.125	0.126	0.126	0.125	0.126	0.127	0.127	0.128	0.128	0.126	0.128	0.126	0.130	

B															
	VACV	VACV-like	CPXV-like1	CPXV-like2	VARV-like	TATV	CMLV	ABATINO	MPXV	ECTV	TV-Abatino-	VARV	AKMV	AKPV	New World
VACV															
VACV-like	0.015														
CPXV-like1	0.019	0.017													
CPXV-like2	0.026	0.023	0.021												
VARV-like	0.019	0.016	0.015	0.024											
TATV	0.022	0.019	0.018	0.027	0.012										
CMLV	0.025	0.022	0.021	0.030	0.015	0.009									
ABATINO	0.030	0.026	0.028	0.028	0.028	0.031	0.034								
MPXV	0.024	0.021	0.025	0.029	0.025	0.028	0.031	0.032							
ECTV	0.031	0.028	0.030	0.031	0.030	0.034	0.036	0.021	0.034						
ECTV-Abatino-like	0.030	0.027	0.027	0.027	0.029	0.032	0.035	0.028	0.033	0.032					
VARV	0.030	0.027	0.025	0.034	0.019	0.014	0.017	0.038	0.035	0.040	0.039				
AKMV	0.049	0.046	0.045	0.050	0.045	0.046	0.049	0.050	0.054	0.050	0.053	0.053			
AKPV	0.088	0.085	0.085	0.086	0.085	0.087	0.089	0.087	0.090	0.087	0.087	0.092	0.081		
New World	0.150	0.148	0.148	0.148	0.148	0.149	0.150	0.149	0.151	0.150	0.149	0.152	0.150	0.153	

B															
	VACV	VACV-like	CPXV-like1	CPXV-like2	VARV-like	TATV	CMLV	ABATINO	MPXV	ECTV	TV-Abatino-	VARV	AKMV	AKPV	New World
VACV															
VACV-like	0.015														
CPXV-like1	0.019	0.017													
CPXV-like2	0.026	0.023	0.021												
VARV-like	0.019	0.016	0.015	0.024											
TATV	0.023	0.020	0.018	0.028	0.012										
CMLV	0.026	0.022	0.021	0.030	0.015	0.009									
ABATINO	0.030	0.026	0.027	0.028	0.028	0.031	0.034								
MPXV	0.024	0.021	0.026	0.030	0.026	0.029	0.031	0.032							
ECTV	0.032	0.029	0.030	0.032	0.031	0.034	0.037	0.022	0.035						
ECTV-Abatino-like	0.030	0.027	0.028	0.027	0.029	0.033	0.035	0.029	0.033	0.033					
VARV	0.031	0.028	0.026	0.036	0.021	0.015	0.018	0.039	0.036	0.042	0.040				
AKMV	0.049	0.047	0.045	0.050	0.045	0.047	0.049	0.050	0.054	0.049	0.053	0.054			
AKPV	0.088	0.086	0.086	0.086	0.086	0.087	0.089	0.087	0.090	0.087	0.087	0.093	0.081		
New World	0.151	0.149	0.149	0.150	0.149	0.151	0.152	0.150	0.152	0.152	0.151	0.154	0.151	0.154	

D															
	VACV	VACV-like	CPXV-like1	CPXV-like2	VARV-like	TATV	CMLV	ABATINO	MPXV	ECTV	TV-Abatino-	VARV	AKMV	AKPV	New World
VACV															
VACV-like	0.014														
CPXV-like1	0.019	0.017													
CPXV-like2	0.026	0.024	0.022												
VARV-like	0.019	0.016	0.015	0.025											
TATV	0.022	0.019	0.017	0.028	0.012										
CMLV	0.025	0.022	0.020	0.030	0.015	0.009									
ABATINO	0.030	0.027	0.028	0.028	0.029	0.031	0.033								
MPXV	0.023	0.021	0.025	0.029	0.026	0.028	0.031	0.032							
ECTV	0.031	0.028	0.030	0.031	0.030	0.033	0.035	0.021	0.033						
ECTV-Abatino-like	0.031	0.028	0.029	0.027	0.030	0.033	0.036	0.030	0.033	0.032					
VARV	0.028	0.026	0.024	0.034	0.019	0.014	0.016	0.037	0.034	0.039	0.039				
AKMV	0.049	0.046	0.044	0.050	0.045	0.046	0.048	0.050	0.053	0.049	0.052	0.052			
AKPV	0.088	0.086	0.086	0.087	0.086	0.087	0.090	0.088	0.090	0.086	0.088	0.091	0.081		
New World	0.149	0.149	0.148	0.148	0.148	0.148	0.150	0.150	0.150	0.149	0.149	0.150	0.150	0.153	

Table S8. Patristic and genetic distances within CPXV clusters calculated from the Maximum likelihood (ML) and Bayesian inference (BI) trees of 62 conserved genes, 87 OPXV core genomes, whole genomes and orthologous genes and their alignments, respectively.

	Patristic distances						
Cluster	**ML tree of 62 conserved genes**	**BI tree of 62 conserved genes**	**ML tree of 87 OPXV whole genomes**	**BI tree of 87 OPXV whole genomes**	**ML tree of 87 OPXV core genomes**	**BI tree of 87 OPXV core genomes**	**ML tree of OPXV orthologous genes**
VACV-like	0.018	0.017	0.018	0.018	0.018	0.017	0.017
CPXV-like1	0.016	0.016	0.015	0.015	0.015	0.015	0.015
CPXV-like2	0.022	0.022	0.023	0.023	0.023	0.023	0.025
VARV-like	0.000	0.000	0.001	0.001	0.001	0.001	0.001
ECTV-Abatino like	0.012	0.012	0.016	0.016	0.016	0.016	0.016
TATV - CMLV	0.011	0.011	0.012	0.012	0.012	0.012	0.013
TATV-VARV	0.018	0.018	0.019	0.019	0.021	0.020	0.018

TATV: Taterapox virus, CMLV:Camelpox virus, VARV: Variola virus

	Genetic distances			
Cluster	**62 conserved genes**	**87 OPXV whole genomes**	**87 OPXV core genomes**	**OPXV orthologous genes**
VACV-like	0.010	0.012	0.012	0.011
CPXV-like1	0.008	0.008	0.008	0.008
CPXV-like2	0.012	0.013	0.013	0.014
VARV-like	0.000	0.000	0.000	0.001
ECTV-Abatino like	0.008	0.012	0.011	0.011
TATV - CMLV	0.008	0.009	0.009	0.009
TATV-VARV	0.012	0.014	0.015	0.014

TATV: Taterapox virus, CMLV:Camelpox virus, VARV: Variola virus

Table S9. Patristic distances within CPXV-like 2 calculated from the Maximum likelihood (ML) and Bayesian inference (BI) trees of 62 conserved genes, 87 OPXV whole genomes, core genomes and orthologous genes.

ML tree of 62 conserved genes

		1	8	9	10		11					7			5	4	6	3	2		
		CPXV_Ger1998_2_1998	CPXV_Fra2001_Nancy_2001	CPXV_FraAmiens_2016	CPXV_Br_1937	CPXV_Catpox5wv1_1982	CPXV_No_F2_1999	CPXV_Nor1994_Man_1994	CPXV_No_H1_1994	CPXV_No_F1_1994	CPXV_NorwayFeline_1994	CPXV_CheNova_DK_2014	CPXV_Swe_H2_1990	CPXV_Swe_H1_1990	CPXV_Ger1990_2_1990	CPXV_Ger2015_Cat1_2015	CPXV_HumLue09_1_2009	CPXV_Ger2014_Human_2014	CPXV_Ger91_1991	CPXV_Ger2007_Vole_2007	CPXV_FM2292_2011
1	CPXV_Ger1998_2_1998																				
8	CPXV_Fra2001_Nancy_2001	0.026																			
9	CPXV_FraAmiens_2016	0.027	0.014																		
10	CPXV_Br_1937	0.032	0.023	0.024																	
	CPXV_Catpox5wv1_1982	0.032	0.023	0.024	0.007																
11	CPXV_No_F2_1999	0.031	0.022	0.022	0.018	0.018															
	CPXV_Nor1994_Man_1994	0.031	0.022	0.023	0.019	0.018	0.000														
	CPXV_No_H1_1994	0.031	0.022	0.023	0.019	0.018	0.000	0.000													
	CPXV_No_F1_1994	0.031	0.022	0.022	0.019	0.018	0.003	0.003	0.003												
	CPXV_NorwayFeline_1994	0.031	0.022	0.022	0.019	0.018	0.003	0.003	0.003	0.000											
	CPXV_CheNova_DK_2014	0.028	0.019	0.020	0.021	0.021	0.020	0.020	0.020	0.020	0.020										
	CPXV_Swe_H2_1990	0.028	0.019	0.020	0.021	0.020	0.019	0.019	0.019	0.019	0.019	0.007									
7	CPXV_Swe_H1_1990	0.028	0.019	0.020	0.020	0.020	0.019	0.019	0.019	0.019	0.019	0.007	0.000								
5	CPXV_Ger1990_2_1990	0.026	0.019	0.020	0.025	0.025	0.024	0.024	0.024	0.024	0.024	0.022	0.021	0.021							
4	CPXV_Ger2015_Cat1_2015	0.026	0.020	0.021	0.026	0.025	0.024	0.024	0.024	0.024	0.024	0.022	0.022	0.021	0.012						
6	CPXV_HumLue09_1_2009	0.024	0.018	0.019	0.024	0.023	0.022	0.022	0.022	0.022	0.022	0.020	0.019	0.019	0.014	0.015					
3	CPXV_Ger2014_Human_2014	0.021	0.026	0.027	0.032	0.032	0.030	0.031	0.031	0.031	0.031	0.028	0.028	0.028	0.026	0.026	0.024				
	CPXV_Ger91_1991	0.018	0.023	0.024	0.029	0.028	0.027	0.027	0.027	0.027	0.027	0.025	0.024	0.024	0.022	0.023	0.021	0.007			
	CPXV_Ger2007_Vole_2007	0.022	0.027	0.028	0.033	0.032	0.031	0.031	0.031	0.031	0.031	0.029	0.029	0.029	0.026	0.027	0.025	0.016	0.013		
2	CPXV_FM2292_2011	0.021	0.026	0.027	0.032	0.032	0.030	0.031	0.031	0.030	0.030	0.028	0.028	0.028	0.026	0.026	0.024	0.015	0.012	0.009	

BI tree of 62 conserved genes

		2			3	6	5	10		11					7			9	8	4	1
		CPXV_FM2292_2011	CPXV_Ger2007_Vole_2007	CPXV_Ger91_1991	CPXV_Ger2014_Human_2014	CPXV_HumLue09_1_2009	CPXV_Ger1990_2_1990	CPXV_Br_1937	CPXV_Catpox5wv1_1982	CPXV_Nor1994_Man_1994	CPXV_No_H1_1994	CPXV_No_F2_1999	CPXV_NorwayFeline_1994	CPXV_No_F1_1994	CPXV_CheNova_DK_2014	CPXV_Swe_H1_1990	CPXV_Swe_H2_1990	CPXV_FraAmiens_2016	CPXV_Fra2001_Nancy_2001	CPXV_Ger2015_Cat1_2015	CPXV_Ger1998_2_1998
2	CPXV_FM2292_2011																				
	CPXV_Ger2007_Vole_2007	0.0086																			
	CPXV_Ger91_1991	0.0118	0.0127																		
3	CPXV_Ger2014_Human_2014	0.0150	0.0159	0.0071																	
6	CPXV_HumLue09_1_2009	0.0254	0.0263	0.0222	0.0254																
5	CPXV_Ger1990_2_1990	0.0253	0.0262	0.0222	0.0254	0.0121															
10	CPXV_Br_1937	0.0331	0.0340	0.0299	0.0331	0.0237	0.0236														
	CPXV_Catpox5wv1_1982	0.0328	0.0337	0.0296	0.0328	0.0234	0.0233	0.0073													
11	CPXV_Nor1994_Man_1994	0.0319	0.0328	0.0287	0.0319	0.0225	0.0224	0.0185	0.0182												
	CPXV_No_H1_1994	0.0319	0.0328	0.0287	0.0319	0.0225	0.0224	0.0185	0.0182	0.0000											
	CPXV_No_F2_1999	0.0317	0.0326	0.0285	0.0318	0.0223	0.0223	0.0183	0.0180	0.0003	0.0003										
	CPXV_NorwayFeline_1994	0.0318	0.0327	0.0286	0.0318	0.0224	0.0223	0.0184	0.0181	0.0030	0.0030	0.0028									
	CPXV_No_F1_1994	0.0318	0.0327	0.0286	0.0318	0.0224	0.0223	0.0184	0.0181	0.0030	0.0030	0.0028	0.0000								
7	CPXV_CheNova_DK_2014	0.0294	0.0303	0.0262	0.0294	0.0200	0.0199	0.0207	0.0204	0.0195	0.0195	0.0194	0.0194	0.0194							
	CPXV_Swe_H1_1990	0.0288	0.0297	0.0257	0.0289	0.0194	0.0194	0.0202	0.0199	0.0190	0.0190	0.0188	0.0189	0.0189	0.0068						
	CPXV_Swe_H2_1990	0.0289	0.0298	0.0258	0.0290	0.0195	0.0195	0.0203	0.0200	0.0191	0.0191	0.0189	0.0190	0.0190	0.0069	0.0004					
9	CPXV_FraAmiens_2016	0.0281	0.0290	0.0249	0.0281	0.0187	0.0186	0.0235	0.0232	0.0223	0.0223	0.0222	0.0222	0.0222	0.0198	0.0193	0.0194				
8	CPXV_Fra2001_Nancy_2001	0.0274	0.0283	0.0242	0.0274	0.0180	0.0179	0.0229	0.0226	0.0217	0.0217	0.0215	0.0216	0.0216	0.0191	0.0186	0.0187	0.0140			
4	CPXV_Ger2015_Cat1_2015	0.0217	0.0226	0.0185	0.0217	0.0161	0.0160	0.0238	0.0235	0.0226	0.0226	0.0224	0.0225	0.0225	0.0201	0.0195	0.0196	0.0188	0.0181		
1	CPXV_Ger1998_2_1998	0.0208	0.0217	0.0177	0.0209	0.0257	0.0256	0.0334	0.0331	0.0322	0.0322	0.0320	0.0321	0.0321	0.0296	0.0291	0.0292	0.0284	0.0277	0.0220	

ML tree of 87 OPXV whole genomes

		1	2			3	4	5	6	7			8	9	10		11				
		CPXV_Ger1998_2	CPXV_Ger91	CPXV_Ger2007_Vole	CPXV_FM2292	CPXV_Ger2014_Human	CPXV_Ger2015_Cat1	CPXV_Ger1990_2	CPXV_HumLue09_1	CPXV_CheNova_DK_2014	CPXV_Swe_H1	CPXV_Swe_H2	CPXV_Fra2001_Nancy	CPXV_FraAmiens_2016	CPXV_Catpox_5wv1	CPXV_Br	CPXV_No_F2	CPXV_NOR_1994_MAN	CPXV_No_H1	CPXV_No_F1	CPXV_Norwayfeline
1	CPXV_Ger1998_2																				
2	CPXV_Ger91	0.0175																			
	CPXV_Ger2007_Vole	0.0203	0.0106																		
	CPXV_FM2292	0.0199	0.0102	0.0064																	
3	CPXV_Ger2014_Human	0.0214	0.0155	0.0183	0.0179																
4	CPXV_Ger2015_Cat1	0.0268	0.0209	0.0237	0.0233	0.0140															
5	CPXV_Ger1990_2	0.0313	0.0254	0.0283	0.0278	0.0185	0.0164														
6	CPXV_HumLue09_1	0.0332	0.0273	0.0301	0.0297	0.0204	0.0183	0.0149													
7	CPXV_CheNova_DK_2014	0.0361	0.0303	0.0331	0.0327	0.0234	0.0212	0.0178	0.0148												
	CPXV_Swe_H1	0.0361	0.0303	0.0331	0.0327	0.0234	0.0213	0.0178	0.0148	0.0063											
	CPXV_Swe_H2	0.0362	0.0303	0.0331	0.0327	0.0234	0.0213	0.0179	0.0148	0.0063	0.0005										
8	CPXV_Fra2001_Nancy	0.0336	0.0278	0.0306	0.0302	0.0209	0.0187	0.0187	0.0206	0.0235	0.0235	0.0236									
9	CPXV_FraAmiens_2016	0.0333	0.0275	0.0303	0.0299	0.0206	0.0185	0.0184	0.0203	0.0232	0.0233	0.0233	0.0136								
10	CPXV_Catpox_5wv1	0.0370	0.0311	0.0340	0.0335	0.0242	0.0221	0.0221	0.0239	0.0269	0.0269	0.0269	0.0220	0.0218							
	CPXV_Br	0.0373	0.0315	0.0343	0.0339	0.0246	0.0224	0.0224	0.0243	0.0272	0.0272	0.0273	0.0224	0.0221	0.0064						
11	CPXV_No_F2	0.0356	0.0297	0.0326	0.0321	0.0228	0.0207	0.0207	0.0226	0.0255	0.0255	0.0255	0.0206	0.0204	0.0182	0.0185					
	CPXV_NOR_1994_MAN	0.0356	0.0298	0.0326	0.0322	0.0229	0.0208	0.0207	0.0226	0.0255	0.0255	0.0256	0.0207	0.0204	0.0182	0.0185	0.0001				
	CPXV_No_H1	0.0356	0.0298	0.0326	0.0322	0.0229	0.0208	0.0207	0.0226	0.0255	0.0255	0.0256	0.0207	0.0204	0.0182	0.0185	0.0001	0.0000			
	CPXV_No_F1	0.0357	0.0298	0.0326	0.0322	0.0229	0.0208	0.0207	0.0226	0.0255	0.0256	0.0256	0.0207	0.0204	0.0182	0.0185	0.0034	0.0034	0.0034		
	CPXV_Norwayfeline	0.0357	0.0298	0.0326	0.0322	0.0229	0.0208	0.0207	0.0226	0.0255	0.0256	0.0256	0.0207	0.0204	0.0182	0.0185	0.0034	0.0034	0.0034	0.0000	

BI tree of 87 OPXV whole genomes

		1	2			7			6	5	9	8	11					10		4	3
		CPXV_Ger1998_2	CPXV_Ger2007_Vole	CPXV_FM2292	CPXV_Ger91	CPXV_Swe_H2	CPXV_Swe_H1	CPXV_CheNova_DK_2014	CPXV_HumLue09_1	CPXV_Ger1990_2	CPXV_FraAmiens_2016	CPXV_Fra2001_Nancy	CPXV_Norwayfeline	CPXV_No_F1	CPXV_NOR_1994_MAN	CPXV_No_H1	CPXV_No_F2	CPXV_Catpox_5wv1	CPXV_Br	CPXV_Ger2015_Cat1	CPXV_Ger2014_Human
1	CPXV_Ger1998_2																				
	CPXV_Ger2007_Vole	0.0201																			
	CPXV_FM2292	0.0197	0.0063																		
2	CPXV_Ger91	0.0173	0.0105	0.0101																	
	CPXV_Swe_H2	0.0358	0.0328	0.0324	0.0300																
	CPXV_Swe_H1	0.0358	0.0328	0.0324	0.0300	0.0005															
7	CPXV_CheNova_DK_2014	0.0358	0.0327	0.0323	0.0300	0.0063	0.0062														
6	CPXV_HumLue09_1	0.0329	0.0298	0.0294	0.0271	0.0147	0.0146	0.0146													
5	CPXV_Ger1990_2	0.0310	0.0280	0.0276	0.0252	0.0177	0.0177	0.0176	0.0148												
9	CPXV_FraAmiens_2016	0.0330	0.0300	0.0296	0.0272	0.0231	0.0230	0.0230	0.0201	0.0182											
8	CPXV_Fra2001_Nancy	0.0333	0.0303	0.0299	0.0275	0.0233	0.0233	0.0233	0.0204	0.0185	0.0135										
	CPXV_Norwayfeline	0.0353	0.0323	0.0319	0.0295	0.0254	0.0253	0.0253	0.0224	0.0205	0.0202	0.0205									
	CPXV_No_F1	0.0353	0.0323	0.0319	0.0295	0.0254	0.0253	0.0253	0.0224	0.0205	0.0202	0.0205	0.0000								
	CPXV_NOR_1994_MAN	0.0353	0.0323	0.0319	0.0295	0.0253	0.0253	0.0253	0.0224	0.0205	0.0202	0.0205	0.0034	0.0034							
	CPXV_No_H1	0.0353	0.0323	0.0319	0.0295	0.0253	0.0253	0.0253	0.0224	0.0205	0.0202	0.0205	0.0034	0.0034	0.0000						
11	CPXV_No_F2	0.0352	0.0322	0.0318	0.0294	0.0253	0.0253	0.0252	0.0223	0.0205	0.0202	0.0204	0.0034	0.0034	0.0001	0.0001					
	CPXV_Catpox_5wv1	0.0366	0.0336	0.0332	0.0308	0.0267	0.0266	0.0266	0.0237	0.0218	0.0215	0.0218	0.0180	0.0180	0.0180	0.0180	0.0180				
10	CPXV_Br	0.0369	0.0339	0.0335	0.0311	0.0270	0.0270	0.0269	0.0240	0.0222	0.0219	0.0221	0.0184	0.0184	0.0183	0.0183	0.0183	0.0063			
4	CPXV_Ger2015_Cat1	0.0265	0.0235	0.0231	0.0207	0.0211	0.0211	0.0210	0.0181	0.0163	0.0183	0.0186	0.0206	0.0206	0.0206	0.0206	0.0205	0.0219	0.0222		
3	CPXV_Ger2014_Human	0.0211	0.0181	0.0177	0.0153	0.0232	0.0231	0.0231	0.0202	0.0183	0.0204	0.0206	0.0227	0.0227	0.0226	0.0226	0.0226	0.0240	0.0243	0.0139	

ML tree of 87 OPXV core genomes

		1	2			3	4	5	6	7			8	9	10		11				
		CPXV_Ger1998_2	CPXV_Ger2007_Vole	CPXV_FM2292	CPXV_Ger91	CPXV_Ger2014_Human	CPXV_Ger2015_Cat1	CPXV_Ger1990_2	CPXV_HumLue09_1	CPXV_CheNova_DK_2014	CPXV_Swe_H1	CPXV_Swe_H2	CPXV_Fra2001_Nancy	CPXV_FraAmiens_2016	CPXV_Catpox5_wv1	CPXV_Br	CPXV_No_F1	CPXV_NorwayFeline	CPXV_No_F2	CPXV_Nor1994_Man	CPXV_No_H1
1	CPXV_Ger1998_2																				
2	CPXV_Ger2007_Vole	0.0207																			
	CPXV_FM2292	0.0203	0.0061																		
	CPXV_Ger91	0.0179	0.0102	0.0098																	
3	CPXV_Ger2014_Human	0.0217	0.0181	0.0177	0.0153																
4	CPXV_Ger2015_Cat1	0.0271	0.0235	0.0231	0.0207	0.0140															
5	CPXV_Ger1990_2	0.0316	0.0279	0.0275	0.0251	0.0184	0.0163														
6	CPXV_HumLue09_1	0.0335	0.0299	0.0295	0.0270	0.0203	0.0183	0.0149													
7	CPXV_CheNova_DK_2014	0.0363	0.0327	0.0323	0.0299	0.0231	0.0211	0.0177	0.0147												
	CPXV_Swe_H1	0.0365	0.0329	0.0325	0.0301	0.0234	0.0213	0.0180	0.0149	0.0062											
	CPXV_Swe_H2	0.0366	0.0330	0.0326	0.0301	0.0234	0.0214	0.0180	0.0150	0.0063	0.0005										
8	CPXV_Fra2001_Nancy	0.0340	0.0304	0.0300	0.0276	0.0209	0.0188	0.0187	0.0207	0.0235	0.0237	0.0238									
9	CPXV_FraAmiens_2016	0.0338	0.0302	0.0298	0.0274	0.0207	0.0186	0.0185	0.0205	0.0233	0.0235	0.0236	0.0137								
10	CPXV_Catpox5_wv1	0.0373	0.0336	0.0332	0.0308	0.0241	0.0220	0.0220	0.0239	0.0267	0.0269	0.0270	0.0221	0.0218							
	CPXV_Br	0.0376	0.0340	0.0336	0.0311	0.0244	0.0223	0.0223	0.0242	0.0270	0.0273	0.0273	0.0224	0.0222	0.0064						
11	CPXV_No_F1	0.0359	0.0323	0.0319	0.0295	0.0228	0.0207	0.0206	0.0226	0.0254	0.0256	0.0257	0.0207	0.0205	0.0182	0.0185					
	CPXV_NorwayFeline	0.0359	0.0323	0.0319	0.0295	0.0228	0.0207	0.0206	0.0226	0.0254	0.0256	0.0257	0.0207	0.0205	0.0182	0.0185	0.0000				
	CPXV_No_F2	0.0358	0.0322	0.0318	0.0294	0.0227	0.0206	0.0206	0.0225	0.0253	0.0255	0.0256	0.0207	0.0204	0.0181	0.0184	0.0034	0.0034			
	CPXV_Nor1994_Man	0.0359	0.0323	0.0319	0.0294	0.0227	0.0206	0.0206	0.0225	0.0253	0.0256	0.0256	0.0207	0.0205	0.0181	0.0184	0.0034	0.0034	0.0001		
	CPXV_No_H1	0.0359	0.0323	0.0319	0.0294	0.0227	0.0206	0.0206	0.0225	0.0253	0.0256	0.0256	0.0207	0.0205	0.0181	0.0184	0.0034	0.0034	0.0001	0.0000	

BI tree of 87 OPXV core genomes

		2			11					10		9	8	7			6	5	4	3	1
		CPXV_Ger2007_Vole	CPXV_FM2292	CPXV_Ger91	CPXV_No_F1	CPXV_NorwayFeline	CPXV_Nor1994_Man	CPXV_No_H1	CPXV_No_F2__reversed_	CPXV_Catpox5_wv1	CPXV_Br	CPXV_FraAmiens_2016	CPXV_Fra2001_Nancy	CPXV_Swe_H2	CPXV_Swe_H1__reversed_	CPXV_CheNova_DK_2014	CPXV_HumLue09_1	CPXV_Ger1990_2	CPXV_Ger2015_Cat1	CPXV_Ger2014_Human	CPXV_Ger1998_2
2	CPXV_Ger2007_Vole																				
	CPXV_FM2292	0.0061																			
	CPXV_Ger91	0.0101	0.0097																		
11	CPXV_No_F1	0.0319	0.0315	0.0291																	
	CPXV_NorwayFeline	0.0319	0.0315	0.0291	0.0000																
	CPXV_Nor1994_Man	0.0319	0.0315	0.0291	0.0034	0.0034															
	CPXV_No_H1	0.0319	0.0315	0.0291	0.0034	0.0034	0.0000														
	CPXV_No_F2__reversed_	0.0318	0.0314	0.0290	0.0034	0.0034	0.0001	0.0001													
10	CPXV_Catpox5_wv1	0.0332	0.0328	0.0304	0.0179	0.0179	0.0179	0.0179	0.0178												
	CPXV_Br	0.0335	0.0332	0.0308	0.0182	0.0182	0.0182	0.0182	0.0182	0.0063											
9	CPXV_FraAmiens_2016	0.0298	0.0294	0.0270	0.0202	0.0202	0.0202	0.0202	0.0202	0.0216	0.0219										
8	CPXV_Fra2001_Nancy	0.0300	0.0296	0.0272	0.0205	0.0205	0.0204	0.0204	0.0204	0.0218	0.0221	0.0135									
7	CPXV_Swe_H2	0.0326	0.0322	0.0298	0.0254	0.0254	0.0253	0.0253	0.0253	0.0267	0.0270	0.0233	0.0235								
	CPXV_Swe_H1__reversed_	0.0326	0.0322	0.0298	0.0253	0.0253	0.0253	0.0253	0.0253	0.0267	0.0270	0.0232	0.0235	0.0005							
	CPXV_CheNova_DK_2014	0.0323	0.0319	0.0295	0.0251	0.0251	0.0251	0.0251	0.0250	0.0264	0.0267	0.0230	0.0232	0.0062	0.0062						
6	CPXV_HumLue09_1	0.0295	0.0291	0.0267	0.0223	0.0223	0.0223	0.0223	0.0222	0.0236	0.0239	0.0202	0.0204	0.0148	0.0148	0.0145					
5	CPXV_Ger1990_2	0.0276	0.0272	0.0248	0.0204	0.0204	0.0203	0.0203	0.0203	0.0217	0.0220	0.0183	0.0185	0.0178	0.0178	0.0175	0.0147				
4	CPXV_Ger2015_Cat1	0.0232	0.0228	0.0204	0.0204	0.0204	0.0204	0.0204	0.0203	0.0217	0.0221	0.0183	0.0186	0.0211	0.0211	0.0208	0.0180	0.0161			
3	CPXV_Ger2014_Human	0.0179	0.0175	0.0151	0.0225	0.0225	0.0224	0.0224	0.0224	0.0238	0.0241	0.0204	0.0206	0.0232	0.0231	0.0229	0.0201	0.0182	0.0138		
1	CPXV_Ger1998_2	0.0205	0.0201	0.0177	0.0355	0.0355	0.0354	0.0354	0.0354	0.0368	0.0371	0.0334	0.0336	0.0362	0.0361	0.0359	0.0331	0.0311	0.0268	0.0214	

ML tree of OPXV orthologous genes																					
		1	3	4	6	7			5	9	8	10		11					2		
		CPXV_Ger1998_2	CPXV_Ger2014_Human	CPXV_Ger2015_Cat1	CPXV_HumLue09_1	CPXV_CheNova_DK_2014	CPXV_SweH2	CPXV_SweH1	CPXV_Ger1990_2	CPXV_FraAmiens_2016	CPXV_Fra2001_Nancy	CPXV_Br	CPXV_Catpox5_wv1	CPXV_Norwayfeline	CPXV_NoF1	CPXV_NoF2	CPXV_NoH1	CPXV_Nor1994_Man	CPXV_FM2292	CPXV_Ger2007_Vole	CPXV_Ger91
1	CPXV_Ger1998_2																				
3	CPXV_Ger2014_Human	0.0223																			
4	CPXV_Ger2015_Cat1	0.0280	0.0156																		
6	CPXV_HumLue09_1	0.0344	0.0219	0.0193																	
7	CPXV_CheNova_DK_2014	0.0374	0.0250	0.0223	0.0156																
	CPXV_SweH2	0.0376	0.0252	0.0225	0.0158	0.0069															
	CPXV_SweH1	0.0376	0.0251	0.0225	0.0157	0.0069	0.0006														
5	CPXV_Ger1990_2	0.0329	0.0204	0.0178	0.0157	0.0188	0.0190	0.0189													
9	CPXV_FraAmiens_2016	0.0349	0.0224	0.0198	0.0213	0.0244	0.0246	0.0245	0.0198												
8	CPXV_Fra2001_Nancy	0.0347	0.0222	0.0195	0.0211	0.0242	0.0244	0.0243	0.0196	0.0144											
10	CPXV_Br	0.0390	0.0266	0.0239	0.0255	0.0286	0.0287	0.0287	0.0240	0.0234	0.0232										
	CPXV_Catpox5_wv1	0.0384	0.0260	0.0233	0.0249	0.0280	0.0281	0.0281	0.0234	0.0228	0.0226	0.0062									
11	CPXV_Norwayfeline	0.0377	0.0253	0.0226	0.0242	0.0273	0.0274	0.0274	0.0227	0.0221	0.0219	0.0201	0.0195								
	CPXV_NoF1	0.0377	0.0253	0.0226	0.0242	0.0273	0.0274	0.0274	0.0227	0.0221	0.0219	0.0201	0.0195	0.0000							
	CPXV_NoF2	0.0375	0.0250	0.0223	0.0239	0.0270	0.0272	0.0271	0.0224	0.0218	0.0216	0.0198	0.0192	0.0037	0.0037						
	CPXV_NoH1	0.0375	0.0250	0.0224	0.0239	0.0270	0.0272	0.0271	0.0225	0.0218	0.0216	0.0198	0.0192	0.0037	0.0037	0.0001					
	CPXV_Nor1994_Man	0.0375	0.0250	0.0224	0.0239	0.0270	0.0272	0.0271	0.0225	0.0218	0.0216	0.0198	0.0192	0.0037	0.0037	0.0001	0.0000				
2	CPXV_FM2292	0.0213	0.0195	0.0252	0.0316	0.0347	0.0348	0.0348	0.0301	0.0321	0.0319	0.0362	0.0356	0.0349	0.0349	0.0347	0.0347	0.0347			
	CPXV_Ger2007_Vole	0.0220	0.0202	0.0259	0.0323	0.0353	0.0355	0.0355	0.0308	0.0328	0.0326	0.0369	0.0363	0.0356	0.0356	0.0354	0.0354	0.0354	0.0066		
	CPXV_Ger91	0.0185	0.0167	0.0224	0.0288	0.0318	0.0320	0.0320	0.0273	0.0293	0.0291	0.0334	0.0328	0.0321	0.0321	0.0319	0.0319	0.0319	0.0116	0.0123	

Table S10. Genetic distances within CPXV-like 2 estimated by p-distances from the alignment of 62 conserved genes (A), 87 OPXV whole genomes (B), core genomes (C) and orthologous genes (D).

A																					
		1	2				3	9		4	5	10					8			7	6
		CPXV_Ger1998_2	CPXV_FM2292	CPXV_Ger91	CPXV_Ger2007_Vole	CPXV_Ger2014_Human	CPXV_HumLue09_1	CPXV_Br	CPXV_Catpox5wv1	CPXV_Ger1990_2	CPXV_Ger2015_Cat1	CPXV_Nor1994_Man	CPXV_No_F2	CPXV_No_H1	CPXV_NorwayFeline	CPXV_No_F1	CPXV_CheNova_DK	CPXV_Swe_H1	CPXV_Swe_H2	CPXV_FraAmiens	CPXV_Fra2001_Nancy
1	CPXV_Ger1998_2																				
2	CPXV_FM2292	0.0103																			
	CPXV_Ger91	0.0102	0.0071																		
	CPXV_Ger2007_Vole	0.0124	0.0061	0.0080																	
	CPXV_Ger2014_Human	0.0124	0.0099	0.0051	0.0101																
3	CPXV_HumLue09_1	0.0130	0.0136	0.0118	0.0133	0.0118															
9	CPXV_Br	0.0163	0.0157	0.0143	0.0150	0.0137	0.0126														
	CPXV_Catpox5wv1	0.0165	0.0159	0.0143	0.0154	0.0139	0.0123	0.0053													
4	CPXV_Ger1990_2	0.0137	0.0148	0.0125	0.0142	0.0119	0.0086	0.0141	0.0140												
5	CPXV_Ger2015_Cat1	0.0133	0.0133	0.0111	0.0127	0.0105	0.0094	0.0129	0.0129	0.0083											
10	CPXV_Nor1994_Man	0.0161	0.0152	0.0135	0.0152	0.0132	0.0119	0.0117	0.0117	0.0133	0.0127										
	CPXV_No_F2	0.0160	0.0151	0.0134	0.0151	0.0131	0.0119	0.0116	0.0116	0.0132	0.0126	0.0002									
	CPXV_No_H1	0.0161	0.0152	0.0135	0.0152	0.0132	0.0119	0.0117	0.0117	0.0133	0.0127	0.0000	0.0002								
	CPXV_NorwayFeline	0.0158	0.0149	0.0130	0.0149	0.0129	0.0118	0.0116	0.0116	0.0127	0.0124	0.0021	0.0020	0.0021							
	CPXV_No_F1	0.0158	0.0149	0.0130	0.0149	0.0129	0.0118	0.0116	0.0116	0.0127	0.0124	0.0021	0.0020	0.0021	0.0000						
8	CPXV_CheNova_DK	0.0148	0.0150	0.0138	0.0150	0.0133	0.0100	0.0119	0.0119	0.0113	0.0116	0.0117	0.0117	0.0117	0.0120	0.0120					
	CPXV_Swe_H1	0.0145	0.0147	0.0132	0.0142	0.0127	0.0097	0.0117	0.0116	0.0107	0.0112	0.0119	0.0119	0.0119	0.0121	0.0121	0.0049				
	CPXV_Swe_H2	0.0145	0.0148	0.0132	0.0143	0.0128	0.0098	0.0119	0.0117	0.0108	0.0112	0.0120	0.0120	0.0120	0.0122	0.0122	0.0049	0.0003			
7	CPXV_FraAmiens	0.0151	0.0146	0.0128	0.0147	0.0126	0.0106	0.0121	0.0121	0.0109	0.0115	0.0119	0.0119	0.0119	0.0119	0.0119	0.0117	0.0115	0.0114		
6	CPXV_Fra2001_Nancy	0.0134	0.0139	0.0123	0.0136	0.0120	0.0103	0.0132	0.0130	0.0094	0.0105	0.0126	0.0125	0.0126	0.0122	0.0122	0.0112	0.0110	0.0110	0.0098	

B																					
		1	2			7			6	4	5	9	8	11					3	10	
		CPXV_Ger1998_2	CPXV_Ger2007_Vole	CPXV_FM2292	CPXV_Ger91	CPXV_Swe_H2	CPXV_Swe_H1	CPXV_CheNova_DK_2014	CPXV_HumLue09_1	CPXV_Ger2015_Cat1	CPXV_Ger1990_2	CPXV_FraAmiens_2016_-	CPXV_Fra2001_Nancy	CPXV_Norwayfeline_-	CPXV_NOR_1994_MAN	CPXV_No_H1	CPXV_No_F2	CPXV_No_F1	CPXV_Ger2014_Human	CPXV_Catpox_5wv1	CPXV_Br
1	CPXV_Ger1998_2																				
2	CPXV_Ger2007_Vole	0.0126																			
	CPXV_FM2292	0.0119	0.0048																		
	CPXV_Ger91	0.0109	0.0077	0.0070																	
7	CPXV_Swe_H2	0.0180	0.0170	0.0176	0.0173																
	CPXV_Swe_H1	0.0180	0.0169	0.0175	0.0172	0.0004															
	CPXV_CheNova_DK_2014	0.0180	0.0173	0.0177	0.0176	0.0047	0.0047														
6	CPXV_HumLue09_1	0.0170	0.0161	0.0164	0.0160	0.0106	0.0105	0.0106													
4	CPXV_Ger2015_Cat1	0.0157	0.0138	0.0145	0.0142	0.0126	0.0126	0.0129	0.0108												
5	CPXV_Ger1990_2	0.0165	0.0152	0.0154	0.0151	0.0118	0.0117	0.0120	0.0098	0.0094											
9	CPXV_FraAmiens_2016	0.0175	0.0163	0.0164	0.0159	0.0123	0.0123	0.0125	0.0119	0.0118	0.0119										
8	CPXV_Fra2001_Nancy	0.0169	0.0148	0.0153	0.0149	0.0130	0.0130	0.0129	0.0119	0.0113	0.0105	0.0101									
11	CPXV_Norwayfeline	0.0182	0.0166	0.0171	0.0168	0.0133	0.0132	0.0130	0.0133	0.0126	0.0131	0.0125	0.0134								
	CPXV_NOR_1994_MAN	0.0184	0.0169	0.0174	0.0171	0.0131	0.0130	0.0127	0.0133	0.0130	0.0133	0.0122	0.0135	0.0026							
	CPXV_No_H1	0.0184	0.0169	0.0174	0.0171	0.0131	0.0130	0.0127	0.0133	0.0130	0.0133	0.0122	0.0135	0.0026	0.0000						
	CPXV_No_F2	0.0183	0.0169	0.0174	0.0171	0.0131	0.0130	0.0127	0.0133	0.0130	0.0133	0.0122	0.0134	0.0026	0.0001	0.0001					
	CPXV_No_F1	0.0182	0.0166	0.0171	0.0168	0.0133	0.0132	0.0130	0.0133	0.0126	0.0131	0.0125	0.0134	0.0000	0.0026	0.0026	0.0026				
3	CPXV_Ger2014_Human	0.0150	0.0114	0.0116	0.0096	0.0138	0.0137	0.0139	0.0123	0.0097	0.0114	0.0125	0.0121	0.0129	0.0130	0.0130	0.0130	0.0129			
10	CPXV_Catpox_5wv1	0.0192	0.0173	0.0179	0.0176	0.0134	0.0132	0.0136	0.0140	0.0137	0.0143	0.0125	0.0140	0.0128	0.0126	0.0126	0.0125	0.0128	0.0143		
	CPXV_Br	0.0197	0.0175	0.0179	0.0179	0.0138	0.0136	0.0136	0.0144	0.0140	0.0145	0.0125	0.0141	0.0129	0.0126	0.0126	0.0125	0.0129	0.0147	0.0049	

C

		2			1	11					3	7			6	5	4	9	8	10	
		CPXV_Ger2007_Vole	CPXV_FM2292	CPXV_Ger91	CPXV_Ger1998_2	CPXV-No-F1	CPXV_NorwayFeline	CPXV_Nor1994_Man	CPXV_No_H1	CPXV_No_F2	CPXV_Ger2014_Human	CPXV_Swe_H2	CPXV_Swe_H1	CPXV_CheNova_DK_2014	CPXV_HumLue09_1	CPXV_Ger1990_2	CPXV_Ger2015_Cat1	CPXV_FraAmiens_2016	CPXV_Fra2001_Nancy	CPXV_Catpox5_wv1	CPXV_Br
2	CPXV_Ger2007_Vole																				
	CPXV_FM2292	0.0047																			
	CPXV_Ger91	0.0075	0.0068																		
1	CPXV_Ger1998_2	0.0130	0.0123	0.0113																	
11	CPXV-No-F1	0.0167	0.0171	0.0168	0.0185																
	CPXV_NorwayFeline	0.0167	0.0171	0.0168	0.0185	0.0000															
	CPXV_Nor1994_Man	0.0170	0.0174	0.0170	0.0186	0.0027	0.0027														
	CPXV_No_H1	0.0170	0.0174	0.0170	0.0186	0.0027	0.0027	0.0000													
	CPXV_No_F2	0.0170	0.0174	0.0170	0.0186	0.0026	0.0026	0.0001	0.0001												
3	CPXV_Ger2014_Human	0.0113	0.0115	0.0096	0.0153	0.0130	0.0130	0.0130	0.0130	0.0130											
7	CPXV_Swe_H2	0.0172	0.0177	0.0174	0.0183	0.0135	0.0135	0.0133	0.0133	0.0133	0.0139										
	CPXV_Swe_H1	0.0171	0.0176	0.0173	0.0183	0.0134	0.0134	0.0132	0.0132	0.0132	0.0139	0.0004									
	CPXV_CheNova_DK_2014	0.0175	0.0178	0.0177	0.0182	0.0131	0.0131	0.0127	0.0127	0.0127	0.0139	0.0048	0.0048								
6	CPXV_HumLue09_1	0.0162	0.0165	0.0160	0.0172	0.0135	0.0135	0.0134	0.0134	0.0134	0.0124	0.0108	0.0107	0.0106							
5	CPXV_Ger1990_2	0.0152	0.0154	0.0151	0.0167	0.0132	0.0132	0.0134	0.0134	0.0133	0.0114	0.0120	0.0119	0.0121	0.0099						
4	CPXV_Ger2015_Cat1	0.0138	0.0145	0.0141	0.0159	0.0126	0.0126	0.0130	0.0130	0.0130	0.0097	0.0128	0.0127	0.0129	0.0109	0.0094					
9	CPXV_FraAmiens_2016	0.0164	0.0164	0.0160	0.0179	0.0126	0.0126	0.0123	0.0123	0.0123	0.0126	0.0126	0.0126	0.0126	0.0121	0.0120	0.0120				
8	CPXV_Fra2001_Nancy	0.0150	0.0154	0.0150	0.0171	0.0135	0.0135	0.0136	0.0136	0.0136	0.0122	0.0132	0.0131	0.0130	0.0120	0.0106	0.0114	0.0102			
10	CPXV_Catpox5_wv1	0.0174	0.0179	0.0176	0.0195	0.0128	0.0128	0.0126	0.0126	0.0126	0.0144	0.0135	0.0134	0.0136	0.0141	0.0143	0.0137	0.0126	0.0142		
	CPXV_Br	0.0176	0.0180	0.0179	0.0200	0.0129	0.0129	0.0126	0.0126	0.0126	0.0148	0.0139	0.0138	0.0136	0.0145	0.0145	0.0141	0.0126	0.0142	0.0049	

D

		2			1	10		4	11			7			5	6	11		8	9	3
		CPXV_FM2292	CPXV_Ger2007_Vole	CPXV_Ger91	CPXV_Ger1998_2	CPXV_Br	CPXV_Catpox5_wv1	CPXV_Ger2015_Cat1	CPXV_Nor1994_Man	CPXV_NoF2	CPXV_NoH1	CPXV_SweH1	CPXV_SweH2	CPXV_CheNova_DK_2014	CPXV_Ger1990_2	CPXV_HumLue09_1	CPXV_NoF1	CPXV_Norwayfeline	CPXV_Fra2001_Nancy	CPXV_FraAmiens_2016	CPXV_Ger2014_Human
2	CPXV_FM2292																				
	CPXV_Ger2007_Vole	0.0049																			
	CPXV_Ger91	0.0079	0.0089																		
1	CPXV_Ger1998_2	0.0124	0.0131	0.0113																	
10	CPXV_Br	0.0185	0.0180	0.0186	0.0199																
	CPXV_Catpox5_wv1	0.0185	0.0179	0.0182	0.0195	0.0046															
4	CPXV_Ger2015_Cat1	0.0152	0.0145	0.0149	0.0165	0.0145	0.0139														
11	CPXV_Nor1994_Man	0.0183	0.0180	0.0181	0.0190	0.0133	0.0130	0.0137													
	CPXV_NoF2	0.0183	0.0179	0.0181	0.0189	0.0133	0.0129	0.0137	0.0001												
	CPXV_NoH1	0.0183	0.0180	0.0181	0.0190	0.0133	0.0130	0.0137	0.0000	0.0001											
7	CPXV_SweH1	0.0181	0.0178	0.0180	0.0187	0.0140	0.0133	0.0133	0.0138	0.0138	0.0138										
	CPXV_SweH2	0.0182	0.0179	0.0181	0.0187	0.0141	0.0134	0.0133	0.0138	0.0138	0.0138	0.0005									
	CPXV_CheNova_DK_2014	0.0178	0.0177	0.0181	0.0183	0.0138	0.0134	0.0133	0.0128	0.0128	0.0128	0.0051	0.0051								
5	CPXV_Ger1990_2	0.0162	0.0161	0.0159	0.0169	0.0152	0.0147	0.0101	0.0143	0.0143	0.0143	0.0124	0.0124	0.0125							
6	CPXV_HumLue09_1	0.0169	0.0168	0.0164	0.0174	0.0145	0.0140	0.0114	0.0135	0.0136	0.0135	0.0110	0.0112	0.0108	0.0101						
11	CPXV_NoF1	0.0181	0.0177	0.0179	0.0189	0.0136	0.0132	0.0135	0.0028	0.0028	0.0028	0.0139	0.0141	0.0133	0.0142	0.0137					
	CPXV_Norwayfeline	0.0160	0.0160	0.0165	0.0180	0.0123	0.0122	0.0127	0.0028	0.0027	0.0028	0.0132	0.0133	0.0128	0.0134	0.0130	0.0000				
8	CPXV_Fra2001_Nancy	0.0160	0.0156	0.0155	0.0174	0.0145	0.0140	0.0116	0.0139	0.0139	0.0139	0.0134	0.0134	0.0132	0.0110	0.0122	0.0140	0.0131			
9	CPXV_FraAmiens_2016	0.0166	0.0165	0.0161	0.0179	0.0131	0.0129	0.0123	0.0130	0.0130	0.0130	0.0129	0.0129	0.0129	0.0127	0.0125	0.0133	0.0121	0.0105		
3	CPXV_Ger2014_Human	0.0119	0.0118	0.0097	0.0155	0.0156	0.0150	0.0105	0.0140	0.0140	0.0140	0.0144	0.0145	0.0142	0.0122	0.0127	0.0141	0.0136	0.0129	0.0133	

Table S11. Patristic and genetic distances within ECTV-Abatino-like calculated from the Maximum likelihood (ML) and Bayesian inference (BI) trees of 62 conserved genes, 87 OPXV whole genomes, core genomes and orthologous genes and their alignments, respectively.

	Patristic distances						
	ML tree of 62 conserved genes	BI tree of 62 conserved genes	ML tree of 87 OPXV whole genomes	BI tree of 87 OPXV whole genomes	ML tree of 87 OPXV core genomes	BI tree of 87 OPXV core genomes	ML tree of OPXV orthologous genes
CPXV-No-H2 - CPXV_GerMygEK938_17	0.016	0.016	0.022	0.022	0.022	0.021	0.022
CPXV-No-H2 - CPXV_Ger2010_MKY	0.016	0.016	0.022	0.022	0.022	0.021	0.022
CPXV_GerMygEK938_17 - CPXV_Ger2010_MKY	0.004	0.004	0.004	0.004	0.004	0.004	0.004
TATV - CMLV	0.011	0.011	0.012	0.012	0.012	0.012	0.013
TATV-VARV	0.018	0.018	0.019	0.019	0.021	0.020	0.018

TATV: Taterapox virus, CMLV:Camelpox virus, VARV: Variola virus

	Genetic distances			
	62 conserved genes	87 OPXV whole genomes	87 OPXV core genomes	OPXV orthologous genes
CPXV-No-H2 - CPXV_GerMygEK938_17	0.011	0.016	0.016	0.015
CPXV-No-H2 - CPXV_Ger2010_MKY	0.011	0.016	0.016	0.016
CPXV_GerMygEK938_17 - CPXV_Ger2010_MKY	0.003	0.003	0.003	0.003
TATV - CMLV	0.008	0.009	0.009	0.009
TATV-VARV	0.012	0.014	0.015	0.014

TATV: Taterapox virus, CMLV:Camelpox virus, VARV: Variola virus

Table S12. Patristic distances within VACV-like calculated from the Maximum likelihood (ML) and Bayesian inference (BI) trees of 62 conserved genes, 87 OPXV whole genomes, core genomes and orthologous genes.

ML tree of 62 conserved genes				
	CPXV_Fin2000_Man_2000	CPXV_Gri_1990	CPXV_HumLit08_1_2008	CPXV_Aus_1999
CPXV_Fin2000_Man_2000				
CPXV_Gri_1990	0.0090			
CPXV_HumLit08_1_2008	0.0181	0.0182		
CPXV_Aus_1999	0.0201	0.0203	0.0150	
BI tree of 62 conserved genes				
	CPXV_Fin2000_Man_2000	CPXV_Gri_1990	CPXV_HumLit08_1_2008	CPXV_Aus_1999
CPXV_Fin2000_Man_2000				
CPXV_Gri_1990	0.0089			
CPXV_HumLit08_1_2008	0.0179	0.0180		
CPXV_Aus_1999	0.0199	0.0200	0.0148	
ML tree of 87 OPXV whole genomes				
	CPXV_HumLit08_1	CPXV_Aus_1999	CPXV_Fin2000_Man	CPXV_Gri
CPXV_HumLit08_1				
CPXV_Aus_1999	0.0185			
CPXV_Fin2000_Man	0.0201	0.0185		
CPXV_Gri	0.0207	0.0191	0.0094	
BI tree of 87 OPXV whole genomes				
	CPXV_Gri	CPXV_Fin2000_Man	CPXV_Aus_1999	CPXV_HumLit08_1
CPXV_Gri				
CPXV_Fin2000_Man	0.0092			
CPXV_Aus_1999	0.0189	0.0183		
CPXV_HumLit08_1	0.0205	0.0199	0.0184	
ML tree of 87 OPXV core genomes				
	CPXV_HumLit08_1	CPXV_Aus_1999	CPXV_Fin2000_Man	CPXV_Gri
CPXV_HumLit08_1				
CPXV_Aus_1999	0.0186			
CPXV_Fin2000_Man	0.0201	0.0182		
CPXV_Gri	0.0208	0.0189	0.0094	
BI tree of 87 OPXV core genomes				
	CPXV_Gri	CPXV_Fin2000_Man	CPXV_Aus_1999	CPXV_HumLit08_1
CPXV_Gri				
CPXV_Fin2000_Man	0.0092			
CPXV_Aus_1999	0.0187	0.0180		
CPXV_HumLit08_1	0.0205	0.0199	0.0184	
ML tree of OPXV orthologous genes				
	CPXV_HumLit08_1	CPXV_Gri	CPXV_Fin2000_Man	CPXV_Aus_1999
CPXV_HumLit08_1				
CPXV_Gri	0.0194			
CPXV_Fin2000_Man	0.0179	0.0097		
CPXV_Aus_1999	0.0192	0.0197	0.0182	

Table S13. Genetic distances within VACV-like clade estimated by p-distances from the alignment of 62 conserved genes (A), 87 OPXV whole genomes (B), core genomes(C), orthologous genes (D).

A				
	CPXV_Gri	CPXV_Fin2000_Man	CPXV_Aus_1999	CPXV_HumLit08_1
CPXV_Gri				
CPXV_Fin2000_Man	0.006			
CPXV_Aus_1999	0.012	0.012		
CPXV_HumLit08_1	0.010	0.010	0.010	
B				
	CPXV_Gri	CPXV_Fin2000_Man	CPXV_HumLit08_1	CPXV_Aus_1999
CPXV_Gri				
CPXV_Fin2000_Man	0.007			
CPXV_HumLit08_1	0.013	0.012		
CPXV_Aus_1999	0.012	0.012	0.013	
C				
	CPXV_Gri	CPXV_Fin2000_Man	CPXV_HumLit08_1	CPXV_Aus_1999
CPXV_Gri				
CPXV_Fin2000_Man	0.007			
CPXV_HumLit08_1	0.013	0.012		
CPXV_Aus_1999	0.012	0.012	0.013	
D				
	CPXV_Gri	CPXV_Fin2000_Man	CPXV_Aus_1999	CPXV_HumLit08_1
CPXV_Gri				
CPXV_Fin2000_Man	0.007			
CPXV_Aus_1999	0.012	0.012		
CPXV_HumLit08_1	0.013	0.011	0.013	

Table S14. Patristic and genetic distances within CPXV-like 1 calculated from the Maximum likelihood (ML) and Bayesian inference (BI) trees of 87 OPXV whole genomes, core genomes and orthologous genes and their alignments, respectively.

	Patristic distances						
	ML tree of 62 conserved genes	**BI tree of 62 conserved genes**	**ML tree of 87 OPXV whole genomes**	**BI tree of 87 OPXV whole genomes**	**ML tree of 87 OPXV core genomes**	**BI tree of 87 OPXV core genomes**	**ML tree of OPXV orthologous genes**
CPXV_Ger_1971_EP1 - CPXV-like 1*	0.0229	0.0219	0.0193	0.0191	0.0187	0.0185	0.0201
TATV - CMLV	0.0114	0.0113	0.0121	0.0120	0.0123	0.0121	0.0130
TATV-VARV	0.0179	0.0175	0.0193	0.0191	0.0207	0.0204	0.0182

* All CPXV-like1 strains without CPXV_Ger_1971_EP1

	Genetic distances			
	OPXV conserved genes	**87 OPXV whole genomes**	**87 OPXV core genomes**	**OPXV orthologous genes**
CPXV_Ger_1971_EP1 - CPXV-like 1*	0.0105	0.0102	0.0101	0.0105
TATV - CMLV	0.0080	0.0090	0.0092	0.0094
TATV-VARV	0.0121	0.0141	0.0152	0.0136

* All CPXV-like1 strains without CPXV_Ger_1971_EP1

Table S15. Patristic distances within CPXV-like 1 calculated from the Maximum likelihood (ML) and Bayesian inference (BI) trees of 62 conserved genes, 87 OPXV whole genomes, core genomes and orthologous genes.

ML tree of 62 conserved genes

	CPXV_Ger2010_Racoon_2010	CPXV_EleGri07_1_2007	CPXV_Ger2014_Cat1_2014	CPXV_Ger2017_Vole_2017	CPXV_Ger2017_Alpaca2_2017	CPXV_Ger2014_Cat2_2014	CPXV_HumLan08_1_2008	CPXV_JagKre08_1_2008	CPXV_MonKre08_4_2008	CPXV_JagKre08_2_2008	CPXV_Ger2015_Cat2_2015	CPXV_Ger2015_Human2_2015	CPXV_Ger2012_Alpaca_2012	CPXV_Ama_2015	CPXV_CatPot07_1_2007	CPXV_HumMag07_1_2007	CPXV_BeaBer04_1_2004	CPXV_Ger1980_EP4_1980	CPXV_Ger2010_Rat_2010	CPXV_Ger2002_MKY_2002	CPXV_Ger2013_Alpaca_2013	CPXV_HumBer07_1_2007	CPXV_Ger2010_Alpaca_2010	CPXV_Ger1971_EP1_1971
CPXV_Ger2010_Racoon_2010																								
CPXV_EleGri07_1_2007	0.016																							
CPXV_Ger2014_Cat1_2014	0.020	0.008																						
CPXV_Ger2017_Vole_2017	0.015	0.006	0.010																					
CPXV_Ger2017_Alpaca2_2017	0.016	0.007	0.011	0.005																				
CPXV_Ger2014_Cat2_2014	0.024	0.014	0.018	0.012	0.010																			
CPXV_HumLan08_1_2008	0.023	0.014	0.018	0.012	0.010	0.015																		
CPXV_JagKre08_1_2008	0.023	0.014	0.018	0.012	0.010	0.015	0.000																	
CPXV_MonKre08_4_2008	0.023	0.014	0.018	0.012	0.010	0.015	0.000	0.000																
CPXV_JagKre08_2_2008	0.023	0.014	0.018	0.012	0.010	0.015	0.000	0.000	0.000															
CPXV_Ger2015_Cat2_2015	0.019	0.010	0.014	0.008	0.006	0.011	0.009	0.008	0.008	0.008														
CPXV_Ger2015_Human2_2015	0.020	0.011	0.015	0.009	0.008	0.015	0.015	0.015	0.015	0.015	0.011													
CPXV_Ger2012_Alpaca_2012	0.018	0.009	0.012	0.006	0.005	0.012	0.012	0.012	0.012	0.012	0.008	0.004												
CPXV_Ama_2015	0.015	0.008	0.012	0.008	0.009	0.016	0.016	0.016	0.016	0.016	0.012	0.013	0.010											
CPXV_CatPot07_1_2007	0.015	0.009	0.013	0.008	0.009	0.017	0.017	0.017	0.017	0.017	0.013	0.014	0.011	0.004										
CPXV_HumMag07_1_2007	0.016	0.009	0.013	0.009	0.010	0.017	0.017	0.017	0.017	0.017	0.013	0.014	0.011	0.004	0.001									
CPXV_BeaBer04_1_2004	0.016	0.010	0.014	0.010	0.011	0.018	0.018	0.018	0.018	0.018	0.014	0.015	0.012	0.005	0.002	0.002								
CPXV_Ger1980_EP4_1980	0.032	0.025	0.029	0.025	0.026	0.033	0.033	0.033	0.033	0.033	0.029	0.030	0.027	0.020	0.017	0.018	0.016							
CPXV_Ger2010_Rat_2010	0.028	0.022	0.026	0.021	0.023	0.030	0.030	0.030	0.030	0.030	0.026	0.027	0.024	0.017	0.014	0.014	0.012	0.007						
CPXV_Ger2002_MKY_2002	0.028	0.021	0.025	0.021	0.022	0.029	0.029	0.029	0.029	0.029	0.025	0.026	0.023	0.016	0.013	0.014	0.012	0.011	0.008					
CPXV_Ger2013_Alpaca_2013	0.027	0.021	0.025	0.021	0.022	0.029	0.029	0.029	0.029	0.029	0.025	0.026	0.023	0.016	0.013	0.014	0.011	0.011	0.008	0.004				
CPXV_HumBer07_1_2007	0.016	0.009	0.013	0.009	0.010	0.017	0.017	0.017	0.017	0.017	0.013	0.014	0.011	0.004	0.001	0.002	0.002	0.017	0.014	0.013	0.013			
CPXV_Ger2010_Alpaca_2010	0.015	0.013	0.017	0.012	0.013	0.021	0.020	0.020	0.020	0.020	0.016	0.017	0.015	0.012	0.012	0.013	0.013	0.028	0.025	0.025	0.024	0.013		
CPXV_Ger1971_EP1_1971	0.016	0.019	0.022	0.018	0.019	0.026	0.026	0.026	0.026	0.026	0.022	0.023	0.021	0.017	0.018	0.019	0.019	0.034	0.031	0.030	0.030	0.018	0.017	

BI tree of 62 conserved genes

	CPXV_Ger2014_Cat2_2014	CPXV_Ger2012_Alpaca_2012	CPXV_Ger2015_Human2_2015	CPXV_Ger2015_Cat2_2015	CPXV_Ger2017_Alpaca2_2017	CPXV_Ger2017_Vole_2017	CPXV_HumLan08_1_2008	CPXV_JagKre08_1_2008	CPXV_JagKre08_2_2008	CPXV_MonKre08_4_2008	CPXV_EleGri07_1_2007	CPXV_Ger2014_Cat1_2014	CPXV_Ama_2015	CPXV_BeaBer04_1_2004	CPXV_Ger1980_EP4_1980	CPXV_Ger2010_Rat_2010	CPXV_Ger2002_MKY_2002	CPXV_Ger2013_Alpaca_2013	CPXV_HumBer07_1_2007	CPXV_CatPot07_1_2007	CPXV_HumMag07_1_2007	CPXV_Ger2010_Alpaca_2010	CPXV_Ger2010_Racoon_2010	CPXV_Ger1971_EP1_1971
CPXV_Ger2014_Cat2_2014																								
CPXV_Ger2012_Alpaca_2012	0.010																							
CPXV_Ger2015_Human2_2015	0.013	0.004																						
CPXV_Ger2015_Cat2_2015	0.013	0.008	0.011																					
CPXV_Ger2017_Alpaca2_2017	0.010	0.005	0.008	0.004																				
CPXV_Ger2017_Vole_2017	0.012	0.006	0.009	0.007	0.004																			
CPXV_HumLan08_1_2008	0.018	0.013	0.015	0.014	0.011	0.010																		
CPXV_JagKre08_1_2008	0.018	0.013	0.015	0.014	0.011	0.010	0.000																	
CPXV_JagKre08_2_2008	0.018	0.013	0.015	0.014	0.011	0.010	0.000	0.000																
CPXV_MonKre08_4_2008	0.018	0.013	0.015	0.014	0.011	0.010	0.000	0.000	0.000															
CPXV_EleGri07_1_2007	0.015	0.010	0.012	0.010	0.008	0.007	0.010	0.010	0.010	0.010														
CPXV_Ger2014_Cat1_2014	0.018	0.013	0.015	0.014	0.011	0.010	0.013	0.013	0.013	0.013	0.008													
CPXV_Ama_2015	0.015	0.010	0.013	0.011	0.008	0.008	0.012	0.012	0.012	0.012	0.008	0.012												
CPXV_BeaBer04_1_2004	0.017	0.012	0.015	0.013	0.010	0.010	0.014	0.014	0.014	0.014	0.010	0.014	0.005											
CPXV_Ger1980_EP4_1980	0.032	0.027	0.030	0.028	0.025	0.025	0.029	0.029	0.029	0.029	0.025	0.029	0.020	0.016										
CPXV_Ger2010_Rat_2010	0.029	0.024	0.027	0.025	0.022	0.021	0.026	0.026	0.026	0.026	0.022	0.026	0.017	0.012	0.007									
CPXV_Ger2002_MKY_2002	0.028	0.023	0.026	0.024	0.021	0.021	0.025	0.025	0.025	0.025	0.021	0.025	0.016	0.012	0.011	0.008								
CPXV_Ger2013_Alpaca_2013	0.028	0.023	0.026	0.024	0.021	0.020	0.025	0.025	0.025	0.025	0.021	0.025	0.016	0.011	0.011	0.008	0.004							
CPXV_HumBer07_1_2007	0.016	0.011	0.014	0.012	0.009	0.009	0.013	0.013	0.013	0.013	0.010	0.013	0.004	0.002	0.017	0.014	0.013	0.013						
CPXV_CatPot07_1_2007	0.016	0.011	0.014	0.012	0.009	0.009	0.013	0.013	0.013	0.013	0.009	0.013	0.004	0.002	0.017	0.014	0.013	0.013	0.001					
CPXV_HumMag07_1_2007	0.016	0.011	0.014	0.012	0.009	0.009	0.013	0.013	0.013	0.013	0.010	0.013	0.004	0.003	0.018	0.015	0.014	0.013	0.002	0.001				
CPXV_Ger2010_Alpaca_2010	0.020	0.015	0.017	0.016	0.013	0.012	0.016	0.016	0.016	0.016	0.013	0.016	0.011	0.013	0.028	0.025	0.024	0.024	0.012	0.012	0.013			
CPXV_Ger2010_Racoon_2010	0.023	0.018	0.020	0.019	0.016	0.015	0.019	0.019	0.019	0.019	0.016	0.019	0.014	0.016	0.031	0.028	0.027	0.027	0.016	0.015	0.016	0.014		
CPXV_Ger1971_EP1_1971	0.026	0.021	0.023	0.022	0.019	0.018	0.022	0.022	0.022	0.022	0.019	0.022	0.017	0.019	0.034	0.031	0.030	0.030	0.018	0.018	0.018	0.017	0.016	

ML tree of 87 OPXV whole genomes

	CPXV_Ger1971_EP1	CPXV_JagKre08_2	CPXV_MonKre08_4	CPXV_JagKre08_1	CPXV_HumLan08_1	CPXV_Ger2017_Vole	CPXV_Ger2015_Cat2	CPXV_Ger2017_Alpaca2	CPXV_Ger2010_Alpaca	CPXV_Ger2010_Racoon	CPXV_Ger2014_Cat2	CPXV_Ger2015_Human2	CPXV_Ger2012_Alpaca	CPXV_Ger2014_Cat1	CPXV_Ger2013_Alpaca	CPXV_Ger1980_EP4	CPXV_Ger2010_Rat	CPXV_Ger2002_MKY	CPXV_HumMag07_1	CPXV_HumBer07_1	CPXV_CatPot07_1	CPXV_BeaBer04_1	CPXV_Ama_2015	CPXV_EleGri07_1
CPXV_Ger1971_EP1																								
CPXV_JagKre08_2	0.015																							
CPXV_MonKre08_4	0.015	0.000																						
CPXV_JagKre08_1	0.015	0.000	0.000																					
CPXV_HumLan08_1	0.015	0.000	0.000	0.000																				
CPXV_Ger2017_Vole	0.016	0.012	0.012	0.012	0.012																			
CPXV_Ger2015_Cat2	0.019	0.015	0.015	0.015	0.015	0.007																		
CPXV_Ger2017_Alpaca2	0.017	0.013	0.013	0.013	0.013	0.006	0.005																	
CPXV_Ger2010_Alpaca	0.023	0.019	0.019	0.019	0.019	0.014	0.017	0.015																
CPXV_Ger2010_Racoon	0.023	0.020	0.020	0.020	0.020	0.014	0.017	0.015	0.015															
CPXV_Ger2014_Cat2	0.023	0.019	0.019	0.019	0.019	0.014	0.017	0.015	0.015	0.010														
CPXV_Ger2015_Human2	0.019	0.015	0.015	0.015	0.015	0.010	0.013	0.011	0.013	0.014	0.014													
CPXV_Ger2012_Alpaca	0.017	0.014	0.014	0.014	0.014	0.008	0.011	0.009	0.012	0.012	0.012	0.004												
CPXV_Ger2014_Cat1	0.018	0.014	0.014	0.014	0.014	0.011	0.014	0.012	0.018	0.018	0.018	0.014	0.012											
CPXV_Ger2013_Alpaca	0.020	0.016	0.016	0.016	0.016	0.013	0.016	0.014	0.020	0.020	0.020	0.016	0.014	0.012										
CPXV_Ger1980_EP4	0.029	0.026	0.026	0.026	0.026	0.022	0.025	0.023	0.029	0.030	0.029	0.025	0.023	0.021	0.012									
CPXV_Ger2010_Rat	0.027	0.024	0.024	0.024	0.024	0.020	0.023	0.021	0.027	0.027	0.027	0.023	0.021	0.019	0.009	0.006								
CPXV_Ger2002_MKY	0.024	0.020	0.020	0.020	0.020	0.016	0.019	0.017	0.023	0.024	0.023	0.019	0.018	0.015	0.006	0.009	0.007							
CPXV_HumMag07_1	0.018	0.014	0.014	0.014	0.014	0.010	0.013	0.011	0.017	0.018	0.017	0.013	0.012	0.009	0.008	0.017	0.015	0.011						
CPXV_HumBer07_1	0.018	0.015	0.015	0.015	0.015	0.011	0.014	0.012	0.018	0.019	0.018	0.014	0.013	0.010	0.008	0.018	0.016	0.012	0.002					
CPXV_CatPot07_1	0.018	0.014	0.014	0.014	0.014	0.011	0.013	0.012	0.018	0.018	0.018	0.014	0.012	0.010	0.008	0.017	0.015	0.011	0.001	0.002				
CPXV_BeaBer04_1	0.018	0.015	0.015	0.015	0.015	0.011	0.014	0.012	0.018	0.019	0.018	0.014	0.012	0.010	0.008	0.018	0.016	0.012	0.002	0.002	0.001			
CPXV_Ama_2015	0.021	0.017	0.017	0.017	0.017	0.014	0.016	0.015	0.021	0.021	0.021	0.017	0.015	0.012	0.011	0.020	0.018	0.014	0.006	0.007	0.006	0.007		
CPXV_EleGri07_1	0.015	0.011	0.011	0.011	0.011	0.009	0.012	0.010	0.016	0.017	0.016	0.012	0.011	0.012	0.014	0.023	0.021	0.017	0.011	0.012	0.011	0.012	0.014	

BI tree of 87 OPXV whole genomes

	CPXV_MonKre08_4	CPXV_JagKre08_2	CPXV_JagKre08_1	CPXV_HumLan08_1	CPXV_Ger2017_Vole	CPXV_Ger2017_Alpaca2	CPXV_Ger2015_Cat2	CPXV_Ger2015_Human2	CPXV_Ger2012_Alpaca	CPXV_Ger2014_Cat2	CPXV_Ger2010_Racoon	CPXV_Ger2010_Alpaca	CPXV_HumMag07_1	CPXV_HumBer07_1	CPXV_BeaBer04_1	CPXV_CatPot07_1	CPXV_Ama_2015	CPXV_Ger2013_Alpaca	CPXV_Ger2010_Rat	CPXV_Ger1980_EP4	CPXV_Ger2002_MKY	CPXV_Ger2014_Cat1	CPXV_EleGri07_1	CPXV_Ger1971_EP1
CPXV_MonKre08_4																								
CPXV_JagKre08_2	0.00001																							
CPXV_JagKre08_1	0.00001	0.00001																						
CPXV_HumLan08_1	0.00002	0.00002	0.00002																					
CPXV_Ger2017_Vole	0.012	0.012	0.012	0.012																				
CPXV_Ger2017_Alpaca2	0.013	0.013	0.013	0.013	0.005																			
CPXV_Ger2015_Cat2	0.015	0.015	0.015	0.015	0.007	0.005																		
CPXV_Ger2015_Human2	0.015	0.015	0.015	0.015	0.010	0.011	0.013																	
CPXV_Ger2012_Alpaca	0.013	0.013	0.013	0.013	0.008	0.009	0.011	0.004																
CPXV_Ger2014_Cat2	0.019	0.019	0.019	0.019	0.014	0.015	0.017	0.013	0.012															
CPXV_Ger2010_Racoon	0.019	0.019	0.019	0.019	0.014	0.015	0.017	0.014	0.012	0.010														
CPXV_Ger2010_Alpaca	0.019	0.019	0.019	0.019	0.014	0.015	0.016	0.013	0.012	0.015	0.015													
CPXV_HumMag07_1	0.014	0.014	0.014	0.014	0.010	0.011	0.013	0.013	0.012	0.017	0.018	0.017												
CPXV_HumBer07_1	0.015	0.015	0.015	0.015	0.011	0.012	0.014	0.014	0.012	0.018	0.019	0.018	0.002											
CPXV_BeaBer04_1	0.015	0.015	0.015	0.015	0.011	0.012	0.014	0.014	0.012	0.018	0.018	0.018	0.002	0.002										
CPXV_CatPot07_1	0.014	0.014	0.014	0.014	0.011	0.012	0.013	0.014	0.012	0.018	0.018	0.018	0.001	0.002	0.001									
CPXV_Ama_2015	0.017	0.017	0.017	0.017	0.013	0.015	0.016	0.017	0.015	0.021	0.021	0.020	0.006	0.007	0.007	0.006								
CPXV_Ger2013_Alpaca	0.016	0.016	0.016	0.016	0.013	0.014	0.015	0.016	0.014	0.020	0.020	0.020	0.007	0.008	0.008	0.008	0.011							
CPXV_Ger2010_Rat	0.023	0.023	0.023	0.023	0.020	0.021	0.023	0.023	0.021	0.027	0.027	0.027	0.015	0.016	0.015	0.015	0.018	0.009						
CPXV_Ger1980_EP4	0.026	0.026	0.026	0.026	0.022	0.023	0.025	0.025	0.023	0.029	0.029	0.029	0.017	0.018	0.018	0.017	0.020	0.011	0.006					
CPXV_Ger2002_MKY	0.020	0.020	0.020	0.020	0.016	0.017	0.019	0.019	0.017	0.023	0.023	0.023	0.011	0.012	0.012	0.011	0.014	0.006	0.007	0.009				
CPXV_Ger2014_Cat1	0.014	0.014	0.014	0.014	0.011	0.012	0.013	0.014	0.012	0.018	0.018	0.018	0.009	0.010	0.010	0.009	0.012	0.011	0.019	0.021	0.015			
CPXV_EleGri07_1	0.011	0.011	0.011	0.011	0.009	0.010	0.012	0.012	0.010	0.016	0.017	0.016	0.011	0.012	0.012	0.011	0.014	0.013	0.020	0.023	0.017	0.011		
CPXV_Ger1971_EP1	0.015	0.015	0.015	0.015	0.016	0.017	0.018	0.019	0.017	0.023	0.023	0.023	0.017	0.018	0.018	0.018	0.021	0.020	0.027	0.029	0.023	0.018	0.015	

ML tree of 87 OPXV core genomes

	CPXV_Ger_1971_EP1	CPXV_Ger2010_Alpaca	CPXV_Ger2010_Racoon	CPXV_Ger2014_Cat2	CPXV_Ger2015_Human2	CPXV_Ger2012_Alpaca	CPXV_Ger2017_Vole	CPXV_Ger2015_Cat2	CPXV_Ger2017_Alpaca2	CPXV_Ger2014_Cat1	CPXV_Ger2013_Alpaca	CPXV_Ger2002_MKY	CPXV_Ger2010_Rat	CPXV_Ger1980_EP4	CPXV_BeaBer04_1	CPXV_HumBer07_1	CPXV_CatPot07_1	CPXV_HumMag07_1	CPXV_Ama_2015	CPXV_EleGri07_1	CPXV_HumLan08_1	CPXV_JagKre08_1	CPXV_MonKre08_4	CPXV_JagKre08_2
CPXV_Ger_1971_EP1																								
CPXV_Ger2010_Alpaca	0.022																							
CPXV_Ger2010_Racoon	0.022	0.015																						
CPXV_Ger2014_Cat2	0.022	0.015	0.010																					
CPXV_Ger2015_Human2	0.018	0.013	0.013	0.013																				
CPXV_Ger2012_Alpaca	0.017	0.011	0.012	0.011	0.004																			
CPXV_Ger2017_Vole	0.015	0.014	0.014	0.014	0.010	0.008																		
CPXV_Ger2015_Cat2	0.018	0.016	0.017	0.016	0.012	0.011	0.007																	
CPXV_Ger2017_Alpaca2	0.016	0.015	0.015	0.015	0.011	0.009	0.005	0.005																
CPXV_Ger2014_Cat1	0.017	0.018	0.018	0.018	0.013	0.012	0.010	0.013	0.012															
CPXV_Ger2013_Alpaca	0.019	0.019	0.020	0.019	0.015	0.014	0.012	0.015	0.014	0.011														
CPXV_Ger2002_MKY	0.023	0.023	0.023	0.023	0.019	0.017	0.016	0.018	0.017	0.015	0.006													
CPXV_Ger2010_Rat	0.026	0.026	0.027	0.026	0.022	0.021	0.019	0.022	0.020	0.018	0.009	0.007												
CPXV_Ger1980_EP4	0.028	0.028	0.029	0.029	0.024	0.023	0.021	0.024	0.023	0.020	0.011	0.009	0.005											
CPXV_BeaBer04_1	0.018	0.018	0.018	0.018	0.013	0.012	0.010	0.013	0.012	0.009	0.008	0.011	0.015	0.017										
CPXV_HumBer07_1	0.018	0.018	0.019	0.018	0.014	0.013	0.011	0.014	0.012	0.010	0.009	0.012	0.016	0.018	0.002									
CPXV_CatPot07_1	0.017	0.017	0.018	0.018	0.013	0.012	0.010	0.013	0.012	0.009	0.008	0.011	0.015	0.017	0.001	0.001								
CPXV_HumMag07_1	0.017	0.017	0.017	0.017	0.013	0.011	0.010	0.013	0.011	0.009	0.007	0.011	0.014	0.016	0.001	0.002	0.001							
CPXV_Ama_2015	0.020	0.020	0.020	0.020	0.016	0.015	0.013	0.016	0.014	0.012	0.011	0.014	0.018	0.020	0.007	0.007	0.006	0.006						
CPXV_EleGri07_1	0.014	0.016	0.016	0.016	0.012	0.010	0.009	0.012	0.010	0.011	0.013	0.017	0.020	0.022	0.011	0.012	0.011	0.011	0.014					
CPXV_HumLan08_1	0.015	0.019	0.019	0.019	0.015	0.013	0.012	0.015	0.013	0.014	0.016	0.019	0.023	0.025	0.014	0.015	0.014	0.014	0.017	0.011				
CPXV_JagKre08_1	0.015	0.019	0.019	0.019	0.015	0.013	0.012	0.015	0.013	0.014	0.016	0.019	0.023	0.025	0.014	0.015	0.014	0.014	0.017	0.011	0.000			
CPXV_MonKre08_4	0.015	0.019	0.019	0.019	0.015	0.013	0.012	0.015	0.013	0.014	0.016	0.019	0.023	0.025	0.014	0.015	0.014	0.014	0.017	0.011	0.000	0.000		
CPXV_JagKre08_2	0.015	0.019	0.019	0.019	0.015	0.013	0.012	0.015	0.013	0.014	0.016	0.019	0.023	0.025	0.014	0.015	0.014	0.014	0.017	0.011	0.000	0.000	0.000	

BI tree of 87 OPXV core genomes

	CPXV_HumBer07_1	CPXV_CatPot07_1	CPXV_BeaBer04_1	CPXV_HumMag07_1	CPXV_Ama_2015	CPXV_Ger2013_Alpaca	CPXV_Ger2010_Rat	CPXV_Ger1980_EP4	CPXV_Ger2002_MKY	CPXV_Ger2014_Cat1	CPXV_Ger2017_Vole	CPXV_Ger2017_Alpaca2	CPXV_Ger2015_Cat2	CPXV_Ger2010_Alpaca	CPXV_Ger2014_Cat2	CPXV_Ger2010_Racoon	CPXV_Ger2015_Human2	CPXV_Ger2012_Alpaca	CPXV_EleGri07_1	CPXV_MonKre08_4	CPXV_JagKre08_1	CPXV_JagKre08_2	CPXV_HumLan08_1	CPXV_Ger_1971_EP1
CPXV_HumBer07_1																								
CPXV_CatPot07_1	0.001																							
CPXV_BeaBer04_1	0.002	0.001																						
CPXV_HumMag07_1	0.002	0.001	0.001																					
CPXV_Ama_2015	0.007	0.006	0.006	0.006																				
CPXV_Ger2013_Alpaca	0.009	0.008	0.008	0.007	0.011																			
CPXV_Ger2010_Rat	0.016	0.015	0.015	0.014	0.017	0.009																		
CPXV_Ger1980_EP4	0.018	0.017	0.017	0.016	0.019	0.011	0.005																	
CPXV_Ger2002_MKY	0.012	0.011	0.011	0.011	0.014	0.006	0.006	0.009																
CPXV_Ger2014_Cat1	0.010	0.009	0.009	0.009	0.012	0.011	0.018	0.020	0.015															
CPXV_Ger2017_Vole	0.011	0.010	0.010	0.010	0.013	0.012	0.019	0.021	0.016	0.010														
CPXV_Ger2017_Alpaca2	0.012	0.011	0.012	0.011	0.014	0.013	0.020	0.022	0.017	0.011	0.005													
CPXV_Ger2015_Cat2	0.014	0.013	0.013	0.013	0.016	0.015	0.022	0.024	0.018	0.013	0.007	0.005												
CPXV_Ger2010_Alpaca	0.018	0.017	0.017	0.017	0.020	0.019	0.026	0.028	0.022	0.017	0.014	0.015	0.016											
CPXV_Ger2014_Cat2	0.018	0.017	0.017	0.017	0.020	0.019	0.026	0.028	0.023	0.017	0.014	0.015	0.016	0.014										
CPXV_Ger2010_Racoon	0.018	0.018	0.018	0.017	0.020	0.019	0.026	0.028	0.023	0.017	0.014	0.015	0.016	0.015	0.010									
CPXV_Ger2015_Human2	0.014	0.013	0.013	0.013	0.016	0.015	0.022	0.024	0.018	0.013	0.009	0.011	0.012	0.013	0.013	0.013								
CPXV_Ger2012_Alpaca	0.013	0.012	0.012	0.011	0.014	0.014	0.020	0.022	0.017	0.012	0.008	0.009	0.011	0.011	0.011	0.012	0.004							
CPXV_EleGri07_1	0.012	0.011	0.011	0.011	0.014	0.013	0.020	0.022	0.016	0.011	0.009	0.010	0.012	0.016	0.016	0.016	0.012	0.010						
CPXV_MonKre08_4	0.015	0.014	0.014	0.014	0.017	0.016	0.023	0.025	0.019	0.014	0.012	0.013	0.015	0.019	0.019	0.019	0.015	0.013	0.011					
CPXV_JagKre08_1	0.015	0.014	0.014	0.014	0.017	0.016	0.023	0.025	0.019	0.014	0.012	0.013	0.015	0.019	0.019	0.019	0.015	0.013	0.011	0.000				
CPXV_JagKre08_2	0.015	0.014	0.014	0.014	0.017	0.016	0.023	0.025	0.019	0.014	0.012	0.013	0.015	0.019	0.019	0.019	0.015	0.013	0.011	0.000	0.000			
CPXV_HumLan08_1	0.015	0.014	0.014	0.014	0.017	0.016	0.023	0.025	0.019	0.014	0.012	0.013	0.015	0.019	0.019	0.019	0.015	0.013	0.011	0.000	0.000	0.000		
CPXV_Ger_1971_EP1	0.018	0.017	0.017	0.017	0.020	0.019	0.026	0.028	0.022	0.017	0.015	0.016	0.018	0.022	0.022	0.022	0.018	0.016	0.014	0.015	0.015	0.015	0.015	

ML tree of OPXV orthogolous genes

	CPXV_MonKre08_4	CPXV_JagKre08_2	CPXV_JagKre08_1	CPXV_HumLan08_1	CPXV_Ger1971_EP1	CPXV_EleGri07_1	CPXV_Ger2010_Racoon	CPXV_Ger2014_Cat2	CPXV_Ger2015_Human2	CPXV_Ger2012_Alpaca	CPXV_Ger2017_Vole	CPXV_Ger2017_Alpaca2	CPXV_Ger2015_Cat2	CPXV_Ama_2015	CPXV_BeaBer04_1	CPXV_HumBer07_1	CPXV_CatPot07_1	CPXV_HumMag07_1	CPXV_Ger2014_Cat1	CPXV_Ger2013_Alpaca	CPXV_Ger2002_MKY	CPXV_Ger2010_Rat	CPXV_Ger1980_EP4	CPXV_Ger2010_Alpaca
CPXV_MonKre08_4																								
CPXV_JagKre08_2	0.000																							
CPXV_JagKre08_1	0.000	0.000																						
CPXV_HumLan08_1	0.000	0.000	0.000																					
CPXV_Ger1971_EP1	0.017	0.017	0.017	0.017																				
CPXV_EleGri07_1	0.012	0.012	0.012	0.012	0.013																			
CPXV_Ger2010_Raccoon	0.020	0.020	0.020	0.020	0.023	0.018																		
CPXV_Ger2014_Cat2	0.019	0.019	0.019	0.019	0.023	0.018	0.011																	
CPXV_Ger2015_Human2	0.013	0.013	0.013	0.013	0.016	0.011	0.010	0.009																
CPXV_Ger2012_Alpaca	0.011	0.011	0.011	0.011	0.015	0.010	0.011	0.011	0.004															
CPXV_Ger2017_Vole	0.012	0.012	0.012	0.012	0.015	0.010	0.016	0.016	0.009	0.008														
CPXV_Ger2017_Alpaca2	0.012	0.012	0.012	0.012	0.016	0.011	0.017	0.016	0.010	0.008	0.005													
CPXV_Ger2015_Cat2	0.014	0.014	0.014	0.014	0.018	0.013	0.019	0.018	0.012	0.010	0.007	0.005												
CPXV_Ama_2015	0.014	0.014	0.014	0.014	0.018	0.013	0.019	0.019	0.012	0.010	0.009	0.010	0.012											
CPXV_BeaBer04_1	0.015	0.015	0.015	0.015	0.019	0.014	0.020	0.019	0.013	0.011	0.010	0.011	0.013	0.007										
CPXV_HumBer07_1	0.016	0.016	0.016	0.016	0.020	0.015	0.021	0.020	0.014	0.012	0.011	0.012	0.014	0.008	0.002									
CPXV_CatPot07_1	0.015	0.015	0.015	0.015	0.019	0.014	0.020	0.019	0.013	0.011	0.010	0.011	0.013	0.007	0.001	0.002								
CPXV_HumMag07_1	0.015	0.015	0.015	0.015	0.019	0.013	0.019	0.019	0.012	0.011	0.010	0.010	0.012	0.006	0.001	0.002	0.001							
CPXV_Ger2014_Cat1	0.020	0.020	0.020	0.020	0.024	0.019	0.025	0.024	0.017	0.016	0.015	0.015	0.018	0.012	0.009	0.010	0.009	0.008						
CPXV_Ger2013_Alpaca	0.020	0.020	0.020	0.020	0.024	0.019	0.025	0.024	0.017	0.016	0.015	0.015	0.018	0.011	0.009	0.010	0.009	0.008	0.009					
CPXV_Ger2002_MKY	0.022	0.022	0.022	0.022	0.026	0.021	0.027	0.026	0.019	0.018	0.017	0.018	0.020	0.014	0.011	0.012	0.011	0.010	0.012	0.005				
CPXV_Ger2010_Rat	0.027	0.027	0.027	0.027	0.030	0.025	0.031	0.031	0.024	0.023	0.022	0.022	0.024	0.018	0.015	0.016	0.015	0.015	0.016	0.009	0.007			
CPXV_Ger1980_EP4	0.028	0.028	0.028	0.028	0.032	0.027	0.033	0.032	0.026	0.024	0.023	0.024	0.026	0.020	0.017	0.018	0.017	0.016	0.018	0.011	0.009	0.006		
CPXV_Ger2010_Alpaca	0.017	0.017	0.017	0.017	0.021	0.016	0.022	0.021	0.015	0.013	0.012	0.013	0.015	0.012	0.013	0.014	0.013	0.012	0.018	0.018	0.020	0.024	0.026	

Table S16. Genetic distances within CPXV-like 1 estimated by p-distances from the alignment of the conserved genes (A), 87 OPXV whole genomes (B), core genomes (C) and orthologous genes (D).

A

	CPXV_Ger2014_Cat2_2014	CPXV_Ger2015_Cat2_2015	CPXV_HumLan08_1_2008	CPXV_JagKre08_1_2008	CPXV_JagKre08_2_2008	CPXV_MonKre08_4_2008	CPXV_Ama_2015	CPXV_Ger2010_Alpaca_2010	CPXV_Ger2012_Alpaca_2012	CPXV_Ger2017_Alpaca2_2017	CPXV_Ger2017_Vole_2017	CPXV_BeaBer04_1_2004	CPXV_CatPot07_1_2007	CPXV_EleGri07_1_2007	CPXV_Ger2015_Human2_2015	CPXV_Ger1971_EP1_1971	CPXV_HumBer07_1_2007	CPXV_HumMag07_1_2007	CPXV_Ger2014_Cat1_2014	CPXV_Ger1980_EP4_1980	CPXV_Ger2010_Racoon_2010	CPXV_Ger2002_MKY_2002	CPXV_Ger2013_Alpaca_2013	CPXV_Ger2010_Rat_2010
CPXV_Ger2014_Cat2_2014																								
CPXV_Ger2015_Cat2_2015	0.007																							
CPXV_HumLan08_1_2008	0.009	0.006																						
CPXV_JagKre08_1_2008	0.009	0.006	0.000																					
CPXV_JagKre08_2_2008	0.009	0.006	0.000	0.000																				
CPXV_MonKre08_4_2008	0.009	0.006	0.000	0.000	0.000																			
CPXV_Ama_2015	0.008	0.006	0.007	0.007	0.007	0.007																		
CPXV_Ger2010_Alpaca_2010	0.009	0.009	0.010	0.010	0.010	0.010	0.007																	
CPXV_Ger2012_Alpaca_2012	0.007	0.005	0.007	0.007	0.007	0.007	0.005	0.007																
CPXV_Ger2017_Alpaca2_2017	0.007	0.003	0.006	0.006	0.006	0.006	0.004	0.007	0.003															
CPXV_Ger2017_Vole_2017	0.008	0.005	0.006	0.006	0.006	0.006	0.005	0.008	0.004	0.003														
CPXV_BeaBer04_1_2004	0.008	0.008	0.009	0.009	0.009	0.009	0.003	0.008	0.007	0.007	0.006													
CPXV_CatPot07_1_2007	0.008	0.007	0.008	0.008	0.008	0.008	0.003	0.007	0.007	0.006	0.005	0.001												
CPXV_EleGri07_1_2007	0.008	0.006	0.007	0.007	0.007	0.007	0.006	0.007	0.005	0.005	0.004	0.006	0.005											
CPXV_Ger2015_Human2_2015	0.007	0.007	0.007	0.007	0.007	0.007	0.006	0.009	0.003	0.005	0.006	0.008	0.007	0.006										
CPXV_Ger1971_EP1_1971	0.012	0.010	0.011	0.011	0.011	0.011	0.010	0.010	0.009	0.009	0.010	0.010	0.010	0.009	0.010									
CPXV_HumBer07_1_2007	0.008	0.007	0.008	0.008	0.008	0.008	0.003	0.007	0.007	0.006	0.006	0.001	0.001	0.006	0.007	0.010								
CPXV_HumMag07_1_2007	0.008	0.008	0.008	0.008	0.008	0.008	0.003	0.007	0.007	0.006	0.006	0.002	0.001	0.006	0.007	0.010	0.001							
CPXV_Ger2014_Cat1_2014	0.010	0.009	0.009	0.009	0.009	0.009	0.007	0.009	0.008	0.007	0.006	0.007	0.006	0.005	0.008	0.010	0.007	0.006						
CPXV_Ger1980_EP4_1980	0.011	0.013	0.013	0.013	0.013	0.013	0.010	0.011	0.011	0.012	0.012	0.008	0.009	0.012	0.011	0.012	0.009	0.009	0.010					
CPXV_Ger2010_Racoon_2010	0.010	0.010	0.010	0.010	0.010	0.010	0.009	0.009	0.009	0.009	0.009	0.009	0.008	0.009	0.007	0.010	0.009	0.009	0.010	0.010				
CPXV_Ger2002_MKY_2002	0.011	0.011	0.011	0.011	0.011	0.011	0.009	0.010	0.010	0.011	0.010	0.007	0.008	0.010	0.010	0.011	0.008	0.008	0.009	0.006	0.010			
CPXV_Ger2013_Alpaca_2013	0.010	0.011	0.011	0.011	0.011	0.011	0.009	0.010	0.010	0.010	0.009	0.007	0.007	0.009	0.010	0.012	0.007	0.007	0.009	0.007	0.011	0.003		
CPXV_Ger2010_Rat_2010	0.010	0.012	0.012	0.012	0.012	0.012	0.010	0.010	0.011	0.011	0.011	0.008	0.009	0.011	0.011	0.013	0.009	0.009	0.010	0.005	0.011	0.005	0.005	

B

	CPXV_MonKre08_4	CPXV_JagKre08_2	CPXV_JagKre08_1	CPXV_HumLan08_1	CPXV_Ger2017_Vole	CPXV_EleGri07_1	CPXV_Ger2017_Alpaca2	CPXV_Ger2015_Cat2	CPXV_Ger2015_Human2	CPXV_Ger2012_Alpaca	CPXV_Ger2014_Cat2	CPXV_Ger2010_Racoon	CPXV_Ger2010_Alpaca	CPXV_HumMag07_1	CPXV_HumBer07_1	CPXV_BeaBer04_1	CPXV_Ama_2015	CPXV_Ger2013_Alpaca	CPXV_CatPot07_1	CPXV_Ger2010_Rat	CPXV_Ger1980_EP4	CPXV_Ger2002_MKY	CPXV_Ger2014_Cat1	CPXV_Ger1971_EP1
CPXV_MonKre08_4																								
CPXV_JagKre08_2	0.000																							
CPXV_JagKre08_1	0.000	0.000																						
CPXV_HumLan08_1	0.000	0.000	0.000																					
CPXV_Ger2017_Vole	0.007	0.007	0.007	0.007																				
CPXV_EleGri07_1	0.008	0.008	0.008	0.008	0.005																			
CPXV_Ger2017_Alpaca2	0.007	0.007	0.007	0.007	0.004	0.007																		
CPXV_Ger2015_Cat2	0.007	0.007	0.007	0.007	0.005	0.008	0.004																	
CPXV_Ger2015_Human2	0.008	0.008	0.008	0.008	0.007	0.007	0.006	0.007																
CPXV_Ger2012_Alpaca	0.008	0.008	0.008	0.008	0.005	0.007	0.005	0.006	0.003															
CPXV_Ger2014_Cat2	0.011	0.011	0.011	0.011	0.008	0.009	0.008	0.008	0.007	0.007														
CPXV_Ger2010_Racoon	0.011	0.011	0.011	0.011	0.009	0.010	0.009	0.010	0.007	0.008	0.008													
CPXV_Ger2010_Alpaca	0.011	0.011	0.011	0.011	0.008	0.010	0.008	0.010	0.010	0.008	0.010	0.009												
CPXV_HumMag07_1	0.009	0.009	0.009	0.009	0.006	0.007	0.007	0.008	0.008	0.007	0.009	0.009	0.009											
CPXV_HumBer07_1	0.009	0.009	0.009	0.009	0.006	0.007	0.007	0.008	0.008	0.007	0.009	0.009	0.009	0.001										
CPXV_BeaBer04_1	0.009	0.009	0.009	0.009	0.006	0.007	0.007	0.008	0.008	0.007	0.009	0.009	0.009	0.001	0.001									
CPXV_Ama_2015	0.009	0.009	0.009	0.009	0.007	0.008	0.007	0.008	0.008	0.007	0.009	0.010	0.009	0.005	0.005	0.005								
CPXV_Ger2013_Alpaca	0.010	0.010	0.010	0.010	0.008	0.009	0.009	0.009	0.009	0.008	0.010	0.010	0.009	0.005	0.005	0.005	0.008							
CPXV_CatPot07_1	0.009	0.009	0.009	0.009	0.006	0.007	0.007	0.008	0.008	0.007	0.009	0.009	0.009	0.001	0.001	0.001	0.005	0.005						
CPXV_Ger2010_Rat	0.012	0.012	0.012	0.012	0.011	0.011	0.011	0.012	0.011	0.011	0.010	0.010	0.010	0.009	0.009	0.009	0.010	0.007	0.009					
CPXV_Ger1980_EP4	0.013	0.013	0.013	0.013	0.011	0.012	0.011	0.012	0.011	0.011	0.010	0.009	0.010	0.009	0.010	0.009	0.011	0.008	0.009	0.004				
CPXV_Ger2002_MKY	0.011	0.011	0.011	0.011	0.009	0.009	0.010	0.010	0.010	0.009	0.010	0.009	0.010	0.007	0.008	0.007	0.009	0.004	0.007	0.005	0.007			
CPXV_Ger2014_Cat1	0.009	0.009	0.009	0.009	0.006	0.007	0.008	0.009	0.008	0.008	0.009	0.009	0.010	0.006	0.007	0.006	0.008	0.007	0.006	0.009	0.009	0.007		
CPXV_Ger1971_EP1	0.011	0.011	0.011	0.011	0.009	0.009	0.010	0.010	0.010	0.010	0.012	0.010	0.011	0.009	0.009	0.009	0.010	0.010	0.009	0.012	0.012	0.010	0.010	

C

	CPXV_HumBer07_1	CPXV_CatPot07_1	CPXV_HumMag07_1	CPXV_BeaBer04_1	CPXV_Ger2013_Alpaca	CPXV_Ger2010_Rat	CPXV_Ger1980_EP4	CPXV_Ger2002_MKY	CPXV_Ama_2015	CPXV_Ger2014_Cat1	CPXV_EleGri07_1	CPXV_Ger2017_Vole	CPXV_Ger2017_Alpaca2	CPXV_Ger2015_Cat2	CPXV_Ger2010_Alpaca	CPXV_Ger2015_Human2	CPXV_Ger2012_Alpaca	CPXV_Ger2014_Cat2	CPXV_Ger2010_Racoon	CPXV_MonKre08_4	CPXV_JagKre08_1	CPXV_JagKre08_2	CPXV_HumLan08_1	CPXV_Ger_1971_EP1_-
CPXV_HumBer07_1																								
CPXV_CatPot07_1	0.001																							
CPXV_HumMag07_1	0.001	0.001																						
CPXV_BeaBer04_1	0.001	0.001	0.001																					
CPXV_Ger2013_Alpaca	0.005	0.005	0.005	0.005																				
CPXV_Ger2010_Rat	0.009	0.009	0.009	0.009	0.007																			
CPXV_Ger1980_EP4	0.010	0.009	0.009	0.009	0.008	0.004																		
CPXV_Ger2002_MKY	0.008	0.007	0.007	0.007	0.004	0.005	0.006																	
CPXV_Ama_2015	0.005	0.005	0.004	0.005	0.008	0.010	0.010	0.009																
CPXV_Ger2014_Cat1	0.007	0.006	0.006	0.006	0.007	0.009	0.009	0.007	0.008															
CPXV_EleGri07_1	0.007	0.007	0.007	0.007	0.008	0.011	0.012	0.009	0.008	0.007														
CPXV_Ger2017_Vole	0.006	0.006	0.006	0.006	0.008	0.010	0.011	0.009	0.006	0.006	0.005													
CPXV_Ger2017_Alpaca2	0.007	0.007	0.007	0.007	0.008	0.011	0.011	0.010	0.006	0.008	0.007	0.004												
CPXV_Ger2015_Cat2	0.008	0.008	0.007	0.008	0.009	0.011	0.012	0.010	0.007	0.008	0.008	0.005	0.004											
CPXV_Ger2010_Alpaca	0.009	0.009	0.009	0.009	0.009	0.010	0.009	0.010	0.009	0.010	0.010	0.008	0.008	0.010										
CPXV_Ger2015_Human2	0.008	0.008	0.008	0.008	0.009	0.011	0.011	0.010	0.008	0.008	0.007	0.006	0.006	0.007	0.009									
CPXV_Ger2012_Alpaca	0.007	0.007	0.007	0.007	0.008	0.011	0.011	0.009	0.007	0.007	0.007	0.005	0.005	0.006	0.008	0.003								
CPXV_Ger2014_Cat2	0.009	0.009	0.009	0.009	0.010	0.010	0.010	0.009	0.009	0.009	0.009	0.008	0.007	0.008	0.010	0.007	0.007							
CPXV_Ger2010_Racoon	0.009	0.009	0.009	0.009	0.010	0.010	0.009	0.009	0.009	0.009	0.010	0.009	0.009	0.010	0.009	0.007	0.008	0.007						
CPXV_MonKre08_4	0.009	0.009	0.009	0.009	0.010	0.012	0.013	0.011	0.009	0.009	0.008	0.007	0.007	0.006	0.011	0.008	0.008	0.011	0.010					
CPXV_JagKre08_1	0.009	0.009	0.009	0.009	0.010	0.012	0.013	0.011	0.009	0.009	0.008	0.007	0.007	0.006	0.011	0.008	0.008	0.011	0.010	0.000				
CPXV_JagKre08_2	0.009	0.009	0.009	0.009	0.010	0.012	0.013	0.011	0.009	0.009	0.008	0.007	0.007	0.006	0.011	0.008	0.008	0.011	0.010	0.000	0.000			
CPXV_HumLan08_1	0.009	0.009	0.009	0.009	0.010	0.012	0.013	0.011	0.009	0.009	0.008	0.007	0.007	0.006	0.011	0.008	0.008	0.011	0.010	0.000	0.000	0.000		
CPXV_Ger_1971_EP1_-	0.009	0.009	0.009	0.009	0.010	0.012	0.012	0.010	0.010	0.010	0.009	0.009	0.009	0.010	0.011	0.009	0.010	0.011	0.010	0.011	0.011	0.011	0.011	

D

	CPXV_EleGri07_1	CPXV_Ger1980_EP4	CPXV_Ger2002_MKY	CPXV_Ger1971_EP1	CPXV_Ger2010_Raccoon	CPXV_Ger2010_Rat	CPXV_Ger2014_Cat1	CPXV_Ger2015_Human2	CPXV_HumLan08_1	CPXV_JagKre08_1	CPXV_JagKre08_2	CPXV_MonKre08_4	CPXV_Ama_2015	CPXV_Ger2010_Alpaca	CPXV_Ger2012_Alpaca	CPXV_Ger2014_Cat2	CPXV_Ger2015_Cat2	CPXV_Ger2017_Alpaca2	CPXV_Ger2017_Vole	CPXV_BeaBer04_1	CPXV_CatPot07_1	CPXV_Ger2013_Alpaca	CPXV_HumBer07_1	CPXV_HumMag07_1
CPXV_EleGri07_1																								
CPXV_Ger1980_EP4	0.012																							
CPXV_Ger2002_MKY	0.009	0.006																						
CPXV_Ger1971_EP1	0.009	0.012	0.011																					
CPXV_Ger2010_Raccoon	0.010	0.010	0.009	0.011																				
CPXV_Ger2010_Rat	0.011	0.004	0.005	0.012	0.010																			
CPXV_Ger2014_Cat1	0.007	0.009	0.007	0.010	0.010	0.009																		
CPXV_Ger2015_Human2	0.007	0.010	0.009	0.010	0.007	0.011	0.008																	
CPXV_HumLan08_1	0.008	0.012	0.011	0.011	0.010	0.012	0.009	0.007																
CPXV_JagKre08_1	0.008	0.012	0.011	0.011	0.010	0.012	0.009	0.007	0.000															
CPXV_JagKre08_2	0.008	0.012	0.011	0.011	0.010	0.012	0.009	0.007	0.000	0.000														
CPXV_MonKre08_4	0.008	0.012	0.011	0.011	0.010	0.012	0.009	0.007	0.000	0.000	0.000													
CPXV_Ama_2015	0.008	0.010	0.009	0.010	0.009	0.010	0.008	0.007	0.009	0.009	0.009	0.009												
CPXV_Ger2010_Alpaca	0.010	0.009	0.009	0.011	0.008	0.010	0.009	0.010	0.010	0.010	0.010	0.010	0.009											
CPXV_Ger2012_Alpaca	0.006	0.010	0.009	0.010	0.008	0.010	0.007	0.003	0.007	0.007	0.007	0.007	0.006	0.008										
CPXV_Ger2014_Cat2	0.009	0.010	0.010	0.012	0.008	0.010	0.010	0.007	0.010	0.010	0.010	0.011	0.009	0.010	0.007									
CPXV_Ger2015_Cat2	0.008	0.012	0.010	0.010	0.010	0.012	0.009	0.006	0.006	0.006	0.006	0.006	0.007	0.010	0.006	0.008								
CPXV_Ger2017_Alpaca2	0.007	0.011	0.009	0.010	0.009	0.011	0.008	0.006	0.007	0.007	0.007	0.007	0.006	0.008	0.004	0.008	0.004							
CPXV_Ger2017_Vole	0.005	0.011	0.009	0.010	0.009	0.011	0.006	0.006	0.007	0.007	0.007	0.007	0.006	0.008	0.005	0.008	0.005	0.004						
CPXV_BeaBer04_1	0.008	0.008	0.007	0.010	0.009	0.009	0.006	0.008	0.009	0.009	0.009	0.009	0.004	0.008	0.007	0.009	0.008	0.007	0.006					
CPXV_CatPot07_1	0.007	0.009	0.007	0.010	0.009	0.009	0.006	0.008	0.009	0.009	0.009	0.009	0.004	0.009	0.007	0.009	0.008	0.007	0.006	0.001				
CPXV_Ger2013_Alpaca	0.009	0.007	0.004	0.011	0.010	0.006	0.007	0.009	0.010	0.010	0.010	0.010	0.008	0.009	0.008	0.010	0.009	0.008	0.008	0.005	0.005			
CPXV_HumBer07_1	0.008	0.009	0.008	0.010	0.009	0.009	0.006	0.008	0.009	0.009	0.009	0.009	0.005	0.009	0.007	0.009	0.008	0.007	0.006	0.002	0.001	0.006		
CPXV_HumMag07_1	0.007	0.009	0.007	0.010	0.009	0.009	0.006	0.007	0.009	0.009	0.009	0.009	0.004	0.008	0.006	0.009	0.008	0.007	0.006	0.001	0.001	0.005	0.001	

Paper III